PROTEOMIC AND TRANSCRIPTOMIC INVESTIGATION OF THE MECHANISMS AND CONSEQUENCES OF p53 GAIN OF FUNCTION MUTATION IN LARYNGEAL SQUAMOUS CELL CARCINOMA

Thesis submitted in accordance with the requirements

of University of Liverpool for the degree

of Doctor of Philosophy

by

Anna Behrendt

August 2011

Acknowledgements

It is my great pleasure to thank all those who supported me throughout my PhD studies at University of Liverpool. First of all, I would like to thank my supervisors Dr Mark Boyd and Mr Terry Jones, for giving me the great opportunity of being a part of their research group, for giving me extraordinary opportunities of attending numerous scientific meetings and for their invaluable help and support in the writing of this thesis. I would also like to thank Dr Nikolina Vlatković, for her help and support throughout all my time in the Boyd lab. I would also like to express my gratitude to the School of Cancer Studies for funding my studentship.

I wish to thank Dr Carlos Rubbi for his support and tremendous help with the live imaging system on innumerable occasions, for valuable discussions and for always being there when I needed him. I am also extremely grateful to Dr Bryony Lloyd for all the help and support she has given me in my project and in the writing of this thesis. I would like to express my appreciation to all the past and current members of the Boyd lab for providing a friendly work environment, especially to Dr Radosław Polański, Dr Maria Maguire and Dr Karolina Krawczyńska, from whom I learnt a lot and who supported me during my time in Liverpool.

I would also like to thank Ms Kerryanne Crawford for being my dear and loving friend, and for all the fun times we had in and outside of the lab. I also wish to thank my long-time friend, Dr Anna Kopeć, for her friendship, support on both scientific and personal grounds and for always being there for me when I needed her.

Finally, I would like to express my deepest gratitude and appreciation to my parents, Krystyna and Roman, and boyfriend Krzysztof for their constant love and support, without which I would have never made it this far.

Declaration of originality

The studies described in this thesis are a result of my own work performed during the course of PhD studies in the School of Cancer Studies, Division of Surgery and Oncology, University of Liverpool between October 2007 and September 2010. All the experiments described were performed by me with the exception of:

- DNA sequencing (Appendices 2, 3, 4, 5, 6, 7 and 8), which was performed as a service by Eurofins MWG Operon,
- mass spectroscopy (Table 3.2), which was performed by Dr Rosalind Jenkins (University of Liverpool),
- exon microarrays, which were performed within the Cancer Research UK Affymetrix Genechip Microarray Service hosted by the Molecular Biology Core Facility (Patterson Institute for Cancer Research); data analysis (Figures 3.37 and 3.38; Appendices 13 and 14) was performed by Dr Bryony Lloyd (University of Liverpool),
- qRT-PCR (Tables 3.5, 3.7 and 3.9; Figures 3.39, 3.42 and 3.45; Appendices 15 and 16), which was performed by members of the Applied Biology team (led by Prof. D. Ross Sibson and Dr Bryony Lloyd, University of Liverpool); data analysis was performed by Dr Bryony Lloyd.

The thesis was written entirely by me under the valued guidance of my supervisors, Dr Mark Boyd and Mr Terry Jones.

Anna Behrendt

June 2011

Public presentation of this work

The work described in this thesis was presented at a number of national and international conferences, both clinical and scientific.

1) NCRI Conference, October 2008 (Birmingham, UK)

   Poster presentation: "The mechanisms and consequences of p53 inactivation in laryngeal squamous cell carcinoma"

2) BACO Conference, July 2009 (Liverpool, UK)

   Poster presentation: "The mechanisms and consequences of p53 inactivation in laryngeal squamous cell carcinomas of the head and neck (LSCC)"

3) NCRI Conference, October 2009 (Birmingham, UK)

   Poster presentation: "The mechanisms and consequences of p53 inactivation in laryngeal squamous cell carcinoma"

   Awarded the **BACR/Gordon Hamilton-Fairley Young Investigator Award** for the best poster

4) EHNS Conference, March 2010 (Athens, Greece)

   Poster presentation: "Proteomic and transcriptomic identification of the mechanisms and consequences of p53 gain of function mutation in laryngeal squamous cell carcinoma"

5) ORS Conference, March 2010 (Oxford, UK)

   Oral presentation: "Proteomic and transcriptomic identification of the mechanisms and consequences of p53 gain of function mutation in laryngeal squamous cell carcinoma"

6) NCRI Conference, November 2010 (Liverpool, UK)

   Poster presentation: "Proteomic and transcriptomic identification of the mechanisms and consequences of p53 gain of function mutation in laryngeal squamous cell carcinoma"

Abstract

Loss of p53 function is a critical event in tumour development. It has been well documented that p53 mutation can lead to an oncogenic gain of function (GOF) associated with poorer prognosis and therapeutic response. Such mutants exert their gain-of-function properties by modifying cells through altered transcriptional activity as well as novel protein-protein interactions, but the molecular details of the mechanisms involved are still not entirely understood. Recent reports indicate that mutant p53 increases TGFβ-dependent metastatic potential of cancer cells via inhibition of p63 function and also promotes invasion through increased integrin (α5β1) and EGFR recycling, which is also linked with suppression of transcriptionally active p63 in normal epithelial cells, lung cancer cells and invasive breast cancer cells.

The aim of this study was to investigate the mechanism of mutant p53 GOF in squamous cell carcinoma of the head and neck (SCCHN) cells. To avoid the potentially confounding impact of studying cells from biologically distinct anatomical sub-sites, the studies described here focused upon the most common sub-type of SCCHN – laryngeal squamous cell carcinoma (LSCC).

Two hot-spot p53 mutants representing two distinct mutational classes have been chosen for these studies: R175H (structural mutation) and R273H (contact mutation), both of which have been previously demonstrated to have GOF properties and have been documented to occur in laryngeal cancer. The mechanism of mutant p53 GOF was investigated by identifying protein interactions of mutant p53 and by studying gene expression changes in LSCC cells expressing these p53 mutants. In addition, the functional consequences of mutant p53 expression in LSCC cells were investigated in terms of response to radiation (a primary treatment modality for LSCC) and motility/invasiveness (key determinants of metastatic potential).

A number of proteins have been identified in the mutant p53 containing protein complexes in LSCC cells and one of these, HSP70, has been confirmed by immunoprecipitation to selectively interact with the p53-175H mutant.

p53-273H-expressing cells and to a smaller extent p53-175H-expressing cells display increased motility. A stable knock-down of the mutant p53 has been shown to reduce the motility of cells suggesting that p53-273H contributes to increased

migratory potential of these cells. Interestingly, exon-array analyses revealed a number of differentially regulated genes in the p53-273H expressing LSCC cells compared to parental p53-null cells. Importantly, the most significantly affected pathways included cell adhesion and extracellular matrix remodelling. Significantly, these cells appear to express predominantly the ΔNp63 and little (if any) TAp63 and thus p53 GOF mutant appears to act via an alternative pathway in LSCC cells. Analysis of the transcriptional networks generated on the basis of the expression data also suggests that this p53 mutant might modulate transcription through other transcription factors, such as Sp1 and NF-κB.

Unexpectedly, though in accordance with earlier studies from our group, mutant p53 expression seemed to sensitise laryngeal cancer cells to ionising radiation. The results presented here suggest that we have a system that can be used in further studies to gain insight into the mechanism of radiosensitivity of mutant p53-expressing LSCC cells.

In conclusion, the studies described here have identified several new lines of investigation connecting mutant p53 with critical pathways involved in the regulation of cell survival (HSP70), cell motility (FN1, TIMP2 and others) and in radiosensitivity. These results suggest that in LSCC cells p53 GOF mutants may act via different pathways than those previously identified in other cancers and moreover it appears there may be differences in the modes of action of structural and DNA-contact mutants. Functional analysis of these pathways should provide insights into the mechanisms of action of two classes of p53 GOF mutants in LSCC and may lead also to the identification of novel therapeutic targets.

LIST OF ABBREVIATIONS

ACN	Acetonitrile
Apaf-1	Apoptotic protease-activating factor 1
APC	Adenomatous polyposis coli
APS	Ammonium persulfate
ATM	Ataxia telangiectasia mutated
ATP	Adenosine 5'-triphosphate
ATR	Ataxia telangiectasia related
BAG2	Bcl-2-associated athanogene 2
BAI1	Brain-specific angiogenesis inhibitor 1
Bcl-2	B-cell lymphoma gene 2
bFGF	basic fibroblast growth factor
bFGF-BP	bFGF-binding protein
bla	Beta-lactamase
bp	Base pair
BSA	Bovine serum albumin
cAMP	Cyclic adenosine monophosphate
CBB	Calmodulin binding buffer
CBP	Calmodulin-binding peptide / CREB-binding protein
CDK	Cyclin-dependent kinase
CEB	Calmodulin elution buffer
Chk	Checkpoint kinase
CI	Confidence interval
CMV	Cytomegalovirus
COX-2	Cyclooxygenase-2
CRB	Calmodulin rinsing buffer
CREB	cAMP responsive element binding protein

CV	Coefficient of variation
DBD	DNA-binding domain
DD	Death domain
DDB2	Damage-specific DNA binding protein 2
DISC	Death-inducing signalling complex
DMEM	Dulbecco's Modified Eagle's Medium
DMF	Dimethylformamide
DMSO	Dimethyl sulfoxide
DNA	Deoxyribonucleic acid
dsDNA	Double-stranded DNA
DTT	Dithiothreitol
ECM	Extracellular matrix remodelling
EDTA	Ethylenediaminetetra-acetic acid
EGF	Epidermal growth factor
EGFR	Epidermal growth factor receptor
EGTA	Ethylene glycol-bis(β-aminoethyl ether)-N,N,N',N'-tetracetic acid
EMT	Epithelial-to-mesenchymal transition
ESI	Electrospray ionisation
EtBr	Ethidium bromide
FBS	Fetal bovine serum
FDR	False discovery rate
G1/2	Gap1/2
GADD45	Growth arrest and DNA-damage-inducible α
GAP	GTPase activating protein
GEF	Guanine nucleotide exchange factor
GGR	Global genomic repair
GOF	Gain of function

GR	Glucocorticoid receptor
GTG	Genetic Technology Grade
GTP	Guanosine triphosphate
HAT	Histone acetyltransferase
HCC	Hexamminecobalt(III) chloride
HDAC1	Histone deacetylases 1
HIF	Hypoxia inducible factor
HPV	Human papillomavirus
HRP	Horseradish peroxidase
HSC70	Heat shock cognate 71 kDa protein
HSP70	Heat shock 70 kDa protein
HSV	Herpes simplex virus
IAA	Iodoacetamide
IR	Ionising radiation
JMY	Junction-mediating and regulatory protein
KAc	Potassium acetate
LAR II	Luciferase Assay Reagent II
LC	Liquid chromatography
LOH	Loss of heterozygosity
LPS	Lipopolysaccharide
LSCC	Laryngeal squamous cell carcinoma
M	Mitosis
MAPK	Mitogen-activated protein kinase
MDM2	Murine double minute 2
MEF	Mouse embryonic fibroblast
MgAc	Magnesium acetate
MIAME	Minimum Information About a Microarray Experiment

min.	Minute
MLC	Myosin light chain
MMR	Mismatch repair
MRCK	Myotonic dystrophy kinase-related CDC42-binding protein kinase
mRNA	Messenger RNA
MS	Mass spectrometry
MTBP	MDM2-binding protein
NaAc	Sodium acetate
NaCl	Sodium chloride
NaF	Sodium fluoride
NaOH	Sodium hydroxide
NER	Nucleotide excision repair
NES	Nuclear export signal
NLS	Nuclear localization signal
NSCLC	Non-small cell lung carcinoma
OR	Odds ratio
p53AIP1	p53-regulated Apoptosis-Inducing Protein 1
PAGE	Polyacrylamide gel electrophoresis
PARC	Parkin-like ubiquitin ligase
PBS	Phosphate buffered saline
PCAF	p300/CBP-associated factor
PCNA	Proliferating cell nuclear antigen
PCR	Polymerase chain reaction
PGK	Phosphoglycerate kinase
PIDD	p53-induced protein with a death domain
PIP_3	Phosphatidylinositol 3,4,5-trisphosphate
PML	Promyelocytic leukaemia

PTEN	Phosphatase and tensin homolog
Pu	Purine
Py	Pyrimidine
qRT-PCR	Quantitative real-time PCR
Rb	Retinoblastoma
rc	Reverse complement
RGC	Ribosomal gene cluster
rNTP	Ribonucleotide triphosphate
ROCK	Rho kinase
ROI	Region of interest
ROS	Reactive oxygen species
RPE	Retinal pigment epithelium
RR	Relative risk (incidence rate ratio)
rRNA	Ribosomal RNA
S	Synthesis
SBB	Streptavidin binding buffer
SBP	Streptavidin-binding peptide
SCCHN	Squamous cell carcinoma of the head and neck
SEB	Streptavidin elution buffer
sec.	Second
SF	Serum-free
SNP	Single nucleotide polymorphism
STI	Soybean trypsin inhibitor
SUMO	Small ubiquitin-related modifier
SV40	Simian virus 40
TA	Transcriptional activation
TAF	TBP-associated factor

TAP	Tandem affinity purification
TBP	TATA box binding protein
TEMED	N,N,N',N'-tetramethylenediamine
TFA	Trifluoroacetic acid
Tmod3	Tropomodulin-3
TNF	Tumour necrosis factor
TRAIL	TNF-related apoptosis-inducing ligand
TSP-1	Thrombospondin-1
UV	Ultraviolet
VEGF	Vascular endothelial growth factor
VICE	Variations In Cellular Expression
wt	Wild-type
XP	Xeroderma pigmentosum
XPC	Xeroderma pigmentosum group C
XPE	Xeroderma pigmentosum group E
ZEB1	Zinc finger E-box binding homeobox 1
α(II)PH	α(II) collagen prolyl-4-hydroxylase

Table of contents

Chapter 1

Introduction

1. Introduction

The aim of this thesis was the study of the mechanisms and consequences of gain of oncogenic function by p53 mutants in laryngeal cancer. Therefore, the purpose of this section is to introduce the reader to background information and concepts of importance to this project.

First of all, a brief introduction on the nature of cancer is given in section 1.1. Since the studies within this thesis focus on laryngeal cancer, an overview of the disease is then given in section 1.2, including epidemiology, aetiology and risk factors, disease diagnosis and treatment as well as the underlying molecular mechanisms.

The rest of the introduction is focused upon the p53 pathway (section 1.3), which is the most frequently affected pathway in human cancer and the main subject of this thesis. p53 structure is first discussed (section 1.3.1) to allow understanding of how mutations in the *TP53* gene result in the inactivation of the protein. This is followed by a detailed discussion of the most important functions of p53 (section 1.3.2) to allow an insight into how loss of these functions leads to tumour development. The importance of p53 regulation (at the level of protein stability, activity and subcellular localization) is also discussed (section 1.3.3).

Finally, loss of p53 function through missense mutations of the *TP53* gene is discussed in detail (section 1.3.4). The types of p53 mutations are described (section 1.3.4.2) and their impact on wild-type p53 analysed (section 1.3.4.1). Further, the evidence for the existence of the oncogenic gain of function (GOF) of p53 mutants is closely examined in section 1.3.4.3. The mechanisms of the gain of oncogenic function are discussed in section 1.3.4.3.1. Finally, the section is concluded with an

analysis of the biological consequences and manifestations of GOF p53 mutations (section 1.3.4.3.2) and the aims of this project are described (section 1.4).

1.1. Introduction to cancer

Cancer is a genetic disease (1). It is caused by numerous cumulative changes of the genome, resulting from the action of exogenous factors, such as carcinogens (asbestos, tobacco smoke), infection with DNA viruses, UV and ionising radiation or errors in the endogenous cellular processes, such as DNA replication, cell division or DNA repair. The accumulation of such genomic alterations transforms normal cells into malignant ones, which can be characterised by uncontrolled proliferation and the ability to invade surrounding tissues and metastasise to distant parts of the body.

The genomic alterations in cancer include mutations in certain key genes as well as severe chromosomal abnormalities, in which entire chromosomes are duplicated or lost (aneuploidy), structurally rearranged or truncated (2). These processes are summarised in Figure 1.1. The most commonly mutated genes in cancer belong to two classes: proto-oncogenes and tumour suppressors (3). Proto-oncogenes are involved in the regulation of proliferation and differentiation. Upon mutation of only one allele, they become activated (dominant gain of function) and may promote uncontrolled growth, which is crucial for the development of cancer (3). Most tumour suppressor genes, on the other hand, typically have growth-suppressing properties and function by inhibiting cell division, induction of apoptosis, maintaining the integrity of the genome and inhibition of metastasis (4). In the event of cellular stress (such as DNA damage or oncogene activation) tumour suppressors induce cell cycle arrest or apoptosis, hence preventing the damaged cells from proliferating. It was believed for a long time that both tumour suppressor alleles have to be inactivated for the loss of

function. More recent data, however, suggesting a possible oncogenic gain of function of selected mutant tumour suppressors, provide evidence that this might not always be the case (5, 6, 7).

In addition to the canonical tumour suppressors, some genes exert their tumour suppressor function indirectly. The DNA repair genes, which are sometimes considered as a sub-group of tumour suppressor genes, are another type of genes frequently altered in cancer (3). Their main functions are sensing DNA damage and inducing many different types of DNA repair programmes, including mismatch repair (MMR), base-excision repair (BER), nucleotide-excision repair (NER), recombinational repair and error-prone translesion synthesis (8). Consequently, mutations inactivating DNA repair genes result in the occurrence of multiple random mutations, which are not repaired. This allows genome instability and variability, and leads to the generation of cancer cells with a selective advantage (1).

Carcinogenesis is a multistage process with genomic alterations usually accumulating over long periods of time (9). This explains why cancer is predominantly a disease of old age (childhood leukaemia is an exception with the highest incidence rate below 20 years of age) (10).

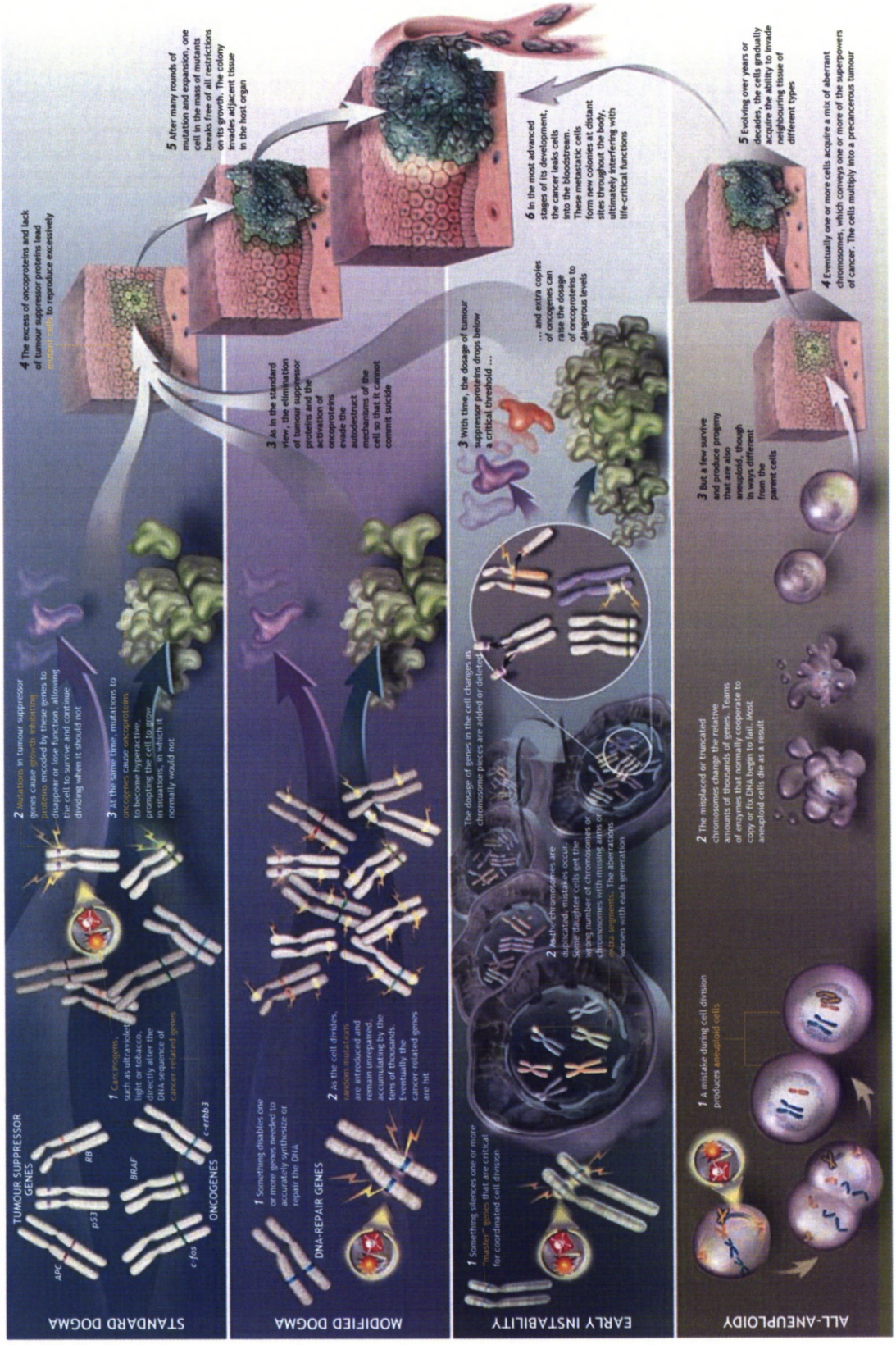

Figure 1.1: The genesis of cancer. A schematic representation of the multistep process of carcinogenesis. Figure reproduced from reference (2).

In the process of carcinogenesis normal cells undergo malignant transformation and acquire multiple capabilities, which allow for their unrestricted growth. These "superpowers" or "hallmarks" of cancer, described by Hanahan and Weinberg in their review (1), are summarised in Figure 1.2 and include: self-sufficiency in growth signals (autocrine signalling), insensitivity to growth-inhibitory signals, evasion of apoptosis (cell suicide), limitless replicative potential (immortality), sustained angiogenesis (formation of new blood vessels) and tissue invasion and metastasis (1). More recently additional hallmarks of evading immune destruction (11) and deregulating cellular energetics (12) have been proposed. It is believed that these traits are shared by most types of human cancer.

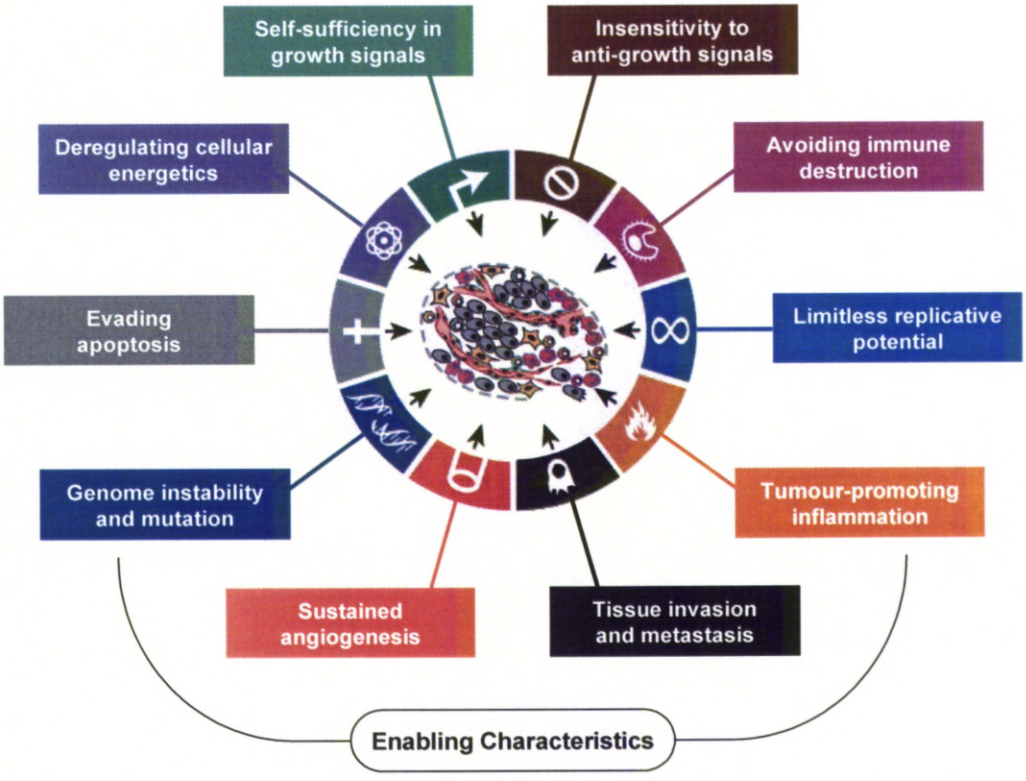

Figure 1.2: The hallmarks of cancer. Acquired functional capabilities of cancer cells, which establish their malignancy, and enabling characteristics crucial to the acquisition of these hallmarks. Figure adapted from reference (12).

The acquisition of the above described hallmarks of cancer is dependent on two enabling characteristics: genomic instability and tumour-promoting inflammation (12). Genomic instability and high mutability enable the selection of rare genetic changes that confer selective advantage on cancer cells and can drive tumour progression. The response of the immune system to tumour formation can have both tumour-antagonizing and tumour-promoting effects. Chronic inflammation not only predisposes to cancer but also plays a role in tumour progression (13). The persistent infiltration of many tumours by cells of the immune system (macrophages, neutrophils and other cells involved in wound healing) makes tumours comparable to non-healing wounds (14). The inflammatory cells secrete many signalling molecules, including growth factors fostering continuous proliferation, survival factors limiting cell death, pro-angiogenic factors, extracellular matrix-degrading enzymes and reactive oxygen species, which are highly mutagenic (15). Therefore, the inflammatory cells are recruited by the tumour to support many of its hallmark capabilities such as angiogenesis or invasiveness and metastatic potential.

In addition to the eight described hallmark capabilities, cancer cells have been proposed to share a number of characteristics, described collectively as the stress phenotypes of tumorigenesis (16). In order to form a tumour, cancer cells have to be able to survive and proliferate in adverse conditions (such as hypoxia) and hence must be capable of tolerating a number of cellular stresses, including metabolic stress, oxidative stress, proteotoxic stress, mitotic stress, DNA damage and replicative stress (16). The ability of cancer cells to tolerate these stresses through stress-support pathways is crucial for the acquisition of the key hallmarks of cancer.

1.2. Head and neck cancer

"Head and neck cancer" is a collective term used to describe the malignant tumours arising from the mucosa of the upper aerodigestive tract. This area includes the oral cavity, pharynx and larynx. Cancers of the brain and melanomas, although occurring in the head and neck region, are excluded from this group and will not be considered here. Moreover, the term "head and neck cancer" will be confined to squamous cell carcinomas, which account for 90% of all cancers in this anatomical region (17).

1.2.1. Overview

Squamous cell carcinoma of the head and neck (SCCHN) is the sixth most common cancer worldwide with over 560,000 new cases each year (18). In spite of advances in treatment and surgical reconstruction, there has been no significant improvement in survival over the past couple of decades (Figure 1.3A). Overall five-year survival is still only 50% (19), mostly due to tumour resistance to treatment, recurrence and high frequency of second primary tumours (20). The incidence of SCCHN increases with age (21) with 98% of patients in Europe being over 40 years old (22). The disease is significantly more frequent in men (Figure 1.3B), with male:female sex ratios in developed countries of about 10:1 (23). The incidence and mortality of head and neck cancer varies between different countries of the world (21, 24), which suggests that there may be geographical differences in the prevalence of the risk factors or that environmental factors may be important in the pathogenesis of this disease.

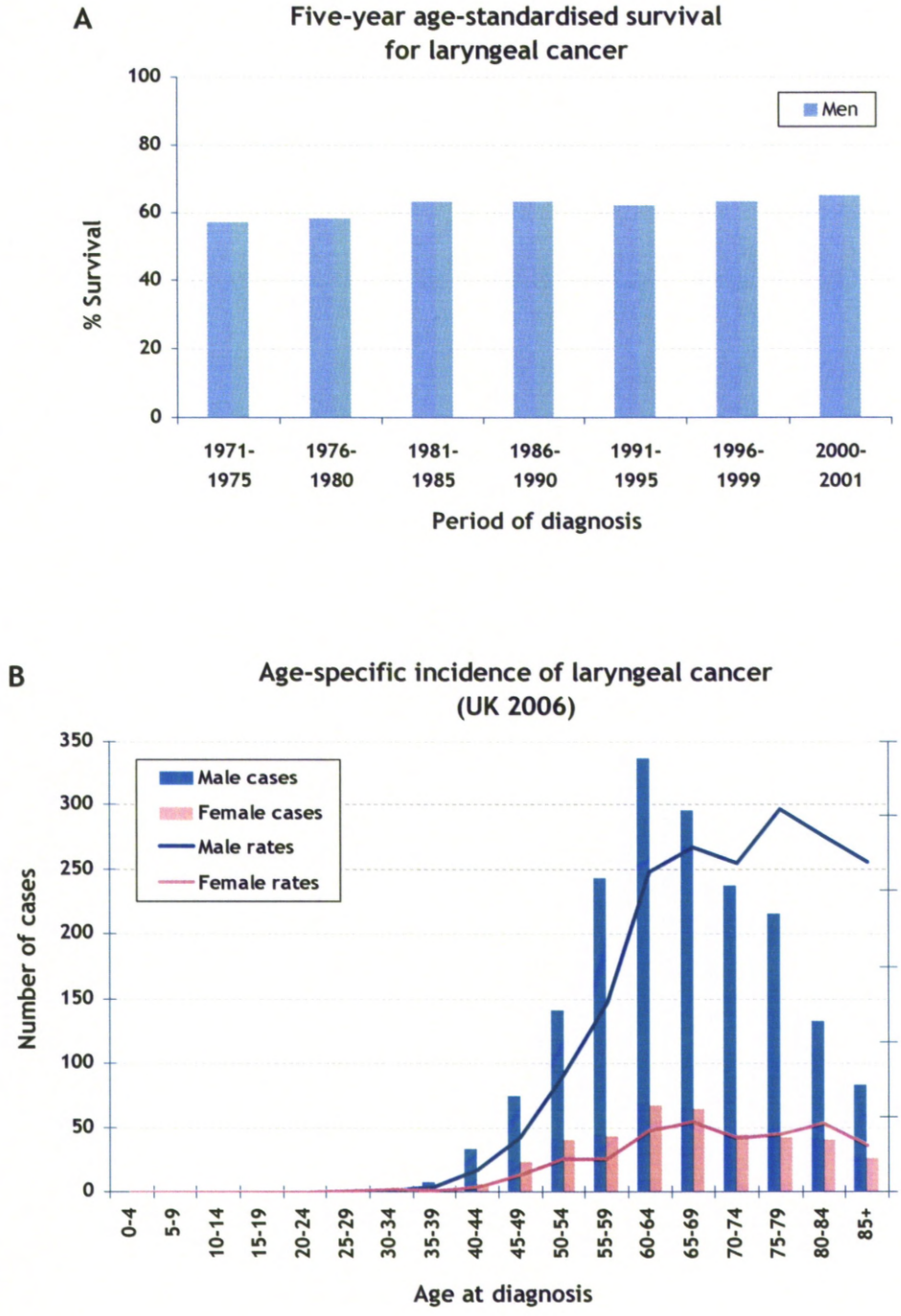

Figure 1.3: Laryngeal cancer statistics (adapted from the Cancer Research UK website (25)).

A. 5-year age-standardised survival in men between 1971 and 2001.

B. Age-specific incidence of laryngeal cancer in the UK in 2006, for men and women.

While the overall incidence of head and neck cancer is decreasing, the incidence of certain types of SCCHN is increasing (26), which is related to a changing prevalence of different risk factors. It is important to note that incidence, mortality and response to treatment depend on the actual sub-sites within the head and neck where the tumours arose. However, there is also marked clinical and molecular heterogeneity among tumours arising from the same anatomical sub-sites, emphasizing the need for a better understanding of the disease.

1.2.2. Head and neck sub-sites

Head and neck cancers can be divided into groups of tumours arising from different anatomical sub-sites (Figure 1.4). About 40% of head and neck cancers arise in the oral cavity (which is further divided into base of tongue, tongue, floor of mouth, gum, palate and lip), 25% in the larynx, 15% in the pharynx (comprising nasopharynx, oropharynx and hypopharynx) and the remaining 20% in sites like salivary glands and thyroid (27). Hence, laryngeal cancer is the largest homogenous group of tumours.

The individual prognosis is strongly influenced by the actual tumour site (28). Tumours arising in the larynx for instance have a significantly better prognosis than cancers in the oral cavity or in the hypopharynx, which have the worst prognosis of all SCCHN tumours (28).

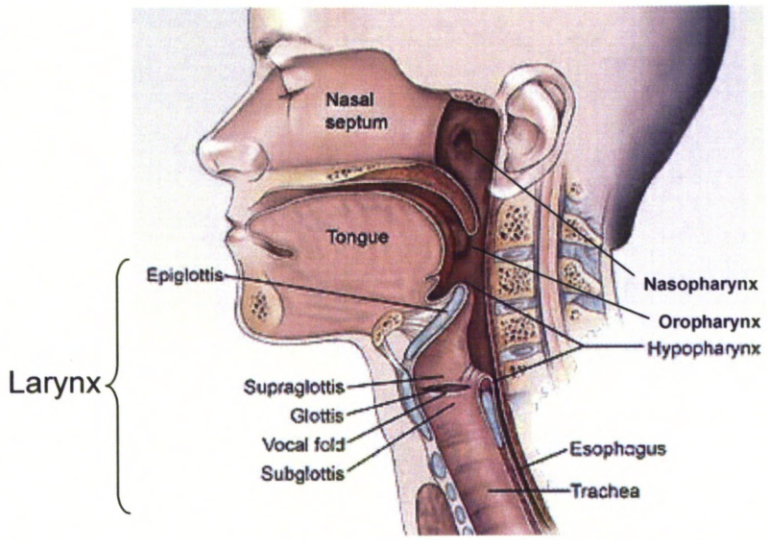

Figure 1.4: Head and neck cancer sub-sites. A diagrammatic representation of the different anatomical sub-sites within the head and neck. Figure adapted from the Radiation Medical Group, Inc. website (29).

1.2.3. Aetiology and risk factors

The pathogenesis of SCCHN is multifactorial and is linked to the use of tobacco (30) and alcohol (31) as well as infection with the human papillomavirus (HPV) (32). The importance of dietary factors (33), occupational exposures (34) and oral hygiene (35) has also been investigated. Multiple studies have demonstrated a link between head and neck cancer incidence and low socioeconomic status (36, 37). All these different factors are not necessarily causal agents but are associated with an increased probability of occurrence of head and neck cancers and are referred to as risk factors.

1.2.3.1. The use of tobacco and alcohol

The major risk factors in the development of head and neck cancer are the use of tobacco and alcohol (38). Distinguishing the individual effects of these agents has been difficult due to the fact that many tobacco users also tend to consume alcohol and vice versa. However, large epidemiological studies have made evaluation of the individual risk factors possible.

Since tobacco was traded from North America almost 500 years ago, it has been extensively used through smoking cigarettes, cigars and pipes, chewing or in oral snuff. Smoking is the single most common cause of cancer-related deaths (39). Presently, there are nearly 1.3 billion active smokers worldwide (40). In Europe approximately 60% of oral cancers in men and 30% in women could be attributable to smoking alone (24). Tobacco smoking has repeatedly been reported to increase the risk of cancer for all sites of the head and neck with RR = 8.4 for current smokers (95% CI = 5.8-12.2) (31). The use of filter cigarettes or exclusive use of blond tobacco is associated with lower risk (RR = 0.5; 95% CI = 0.3-0.8) compared to smokers of plain cigarettes or black tobacco, respectively (41). Moreover, smoking history is a critical factor influencing survival of cancer patients (42). The risk of developing head and neck cancer decreases gradually after smoking cessation (down to RR = 1.1; 95% CI = 0.6-2.0 after more than 20 years from quitting) (31, 43). It has also been suggested that giving up smoking may be a potential way of improving survival of head and neck cancer patients (42). While smoking tobacco is the major risk factor for head and neck cancers in developed countries, many forms of smokeless tobacco, such as moist chewing tobacco and oral snuff, pose a significant problem of increased cancer risk in the developing world (RR = 1.8; 95% CI = 1.1-2.9) (44, 45).

Alcohol intake has been found to increase the risk of head and neck cancer, with the strongest relative effect for pharyngeal cancer (RR = 8.5; 95% CI = 4.0-18.2) (31). Both tobacco and alcohol increase the risk of head and neck cancer in a dose-dependent manner (38). While each factor alone may be responsible for a 2- to 8-fold increase in risk (depending on intensity and duration of usage) (31), combined exposure to tobacco and alcohol results in up to 22-fold increase

(95% CI = 12.9-37.8) in the relative risk (31, 38). Therefore, it can be concluded that alcohol and tobacco act synergistically in increasing the risk of head and neck cancer.

In spite of the fact that the incidence of head and neck cancer in general is decreasing (attributed mainly to a decrease in smoking prevalence) (26), the incidence of oropharyngeal cancer is rising (46), which likely reflects the rising prevalence of another risk factor – infection with high-risk types of human papillomaviruses (HPVs).

1.2.3.2. HPV infection

Oncogenic HPVs are the major cause of cervical cancer (47). Nearly 30 years ago it was suggested that high-risk HPVs may also be involved in the pathogenesis of head and neck cancer (48). Epidemiological and clinical evidence suggests that high-risk HPV infection may account for the development of some head and neck cancers, especially in patients who do not have a history of alcohol and/or tobacco use (49).

So far, more than 200 different HPV types have been identified, which include the oncogenic HPV types 16, 18, 31, 33, 35 and 45 (48, 50). The HPV-16 subtype is most commonly involved in SCCHN and accounts for 87% of all HPV-positive tumours (51), including 86.7% of HPV-positive oropharyngeal and 69.2% of HPV-positive laryngeal cancers (52). HPV-18 is quite rare among the HPV-positive cancers of the oropharynx (2.8%) and larynx (17%) (52). The other most commonly detected types of HPV are HPV-31 and HPV-33 (51, 53). Other oncogenic HPV types are rarely found in cancers of the head and neck (52).

Viral DNA has been isolated from tumours arising within the upper aerodigestive tract with a high variation of prevalence between the individual anatomical sub-sites (50). In a large systematic review, 25% of SCCHN cancer specimens were found to

be HPV-positive (52). HPV prevalence was significantly higher in cancers of the oropharynx (35.6%) than in those of oral cavity (23.5%) or the larynx (24%) (52, 54). The biological reason for these differences between sub-sites remains unclear.

Since the incidence of oropharyngeal cancer has been rising over the past couple of years, likely due to HPV infections, most recent studies have reported much higher prevalence of HPV-positive oropharyngeal cancers, ranging from 50% (55) to 74% (56). The prevalence of high-risk HPV in laryngeal cancer varies significantly between individual studies, from as low as 1% (57) up to 37% (58, 59). This discrepancy in the reported prevalence rates may be due to selection bias, geographical differences, quality of the tissue material studied and methods used to determine the HPV infection status. The most commonly used screening method relies on PCR-based detection of viral DNA. Unfortunately, such assays are generally too sensitive, as they can detect only a few copies of the viral DNA (possibly yielding false-positive results), and they do not demonstrate the role of HPV in carcinogenesis (60). Therefore, this method cannot distinguish between the clinically relevant and irrelevant HPV infections. Detection of the E6 and E7 viral oncogene transcripts, on the other hand, is a more reliable technique for identifying the oncogenic HPV infections (61). Moreover, biologically relevant high-risk HPV infections are also associated with p16 expression (62) (discussed in detail in section 1.2.5.3) and hence immunohistochemical investigation of p16 levels could be used as a surrogate marker of clinically meaningful HPV infections (63).

The majority of HPV prevalence data in SCCHN is based on PCR amplification of HPV DNA (52) suggesting that these studies provide little information on the causal role of HPV in SCCHN. Only a few studies looked at the clinically-relevant HPV infections in individual sub-sites of head and neck by evaluating p16 expression

(64, 65, 66). As defined by a molecular profile with HPV-positivity and p16 expression, HPV was found to be causally associated with 23% of oropharyngeal cancers (66) and between 16% (64) and 58% (65) of laryngeal cancers. The small sample size of the above studies may be the source of high variability of the reported prevalence of clinically meaningful HPV infections in laryngeal cancer. On the other hand, a relatively recent systematic review looking at the association between HPV-16 infection and risk of head and neck cancer at individual anatomical sub-sites concluded that the association is strongest for tonsillar cancer (RR = 15.1; 95% CI = 6.8-33.7), intermediate for oropharyngeal cancer (RR = 4.3; 95% CI = 2.1-8.9) and weakest for oral (RR = 2.0; 95% CI = 1.2-3.4) and laryngeal (RR = 2.0; 95% CI =1.0-4.2) cancers (67). While this review clearly suggests that HPV infection is a risk factor for some head and neck cancers, larger series and case-control studies evaluating the oncogenic activity of HPV will be essential for reliable evaluation of the association between HPV infection and risk of head and neck cancer at different anatomical sub-sites.

In spite of the limited so far investigation of the clinically relevant HPV infections within the head and neck, HPV-positive tumours, predominantly of the oropharyngeal origin, seem to comprise a separate group with a distinct biological behaviour, which is generally associated with a better prognosis in terms of improved response to treatment as well as better overall and disease-specific survival in comparison with the HPV-negative tumours (49, 51, 68, 69). Recent reports suggest that patients with HPV-positive/p16-overexpressing tumours (class III, see Figure 1.5) have a significantly better 5-year overall survival (79%) versus patients with class I (20%) or class II (18%) tumours (66). Similarly, class III tumours have an improved 5-year disease-free survival of 75% compared to 15% and 13% for class I and class II

tumours, respectively (66). Class III tumours were also shown to have a lower recurrence rate (14%) than class I (45%) and class II (74%) tumours (66). Moreover, HPV infection has also been implicated in the treatment response of SCCHN (70, 71). HPV-positive tumours have an improved response to radiotherapy (OR = 4.07; 95% CI = 1.48-11.18; p = 0.006) and to concurrent chemo-radiation (OR = 2.87; 95% CI = 1.29-6.41; p = 0.01) compared to HPV-negative tumours (51).

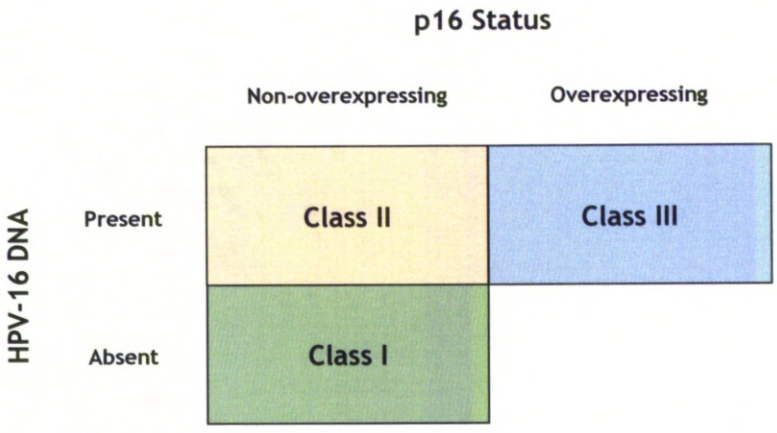

Figure 1.5: Classification of oropharyngeal tumours by p16 expression and HPV-16 DNA presence. Possible groups included: HPV-16-negative/p16 non-overexpressing (class I), HPV-16-positive/p16 non-overexpressing (class II) and HPV-16-positive/p16 overexpressing. HPV-negative/p16 overexpressing tumours were hardly ever found. Figure adapted from reference (66).

In summary, biologically relevant HPV infection is a risk factor for a sub-group of SCCHN, but is also associated with a favourable prognosis of HPV-positive tumours.

1.2.3.3. Dietary factors

In addition to the major risk factors for head and neck cancer discussed above, many epidemiological studies have implicated dietary and nutritional factors in the aetiology of this disease, although the effects observed could potentially be

confounded by the socioeconomic status of the patients. Nevertheless, many studies have consistently shown that high intake of fruit and vegetables was associated with reduced risk of cancer in many sites within the head and neck with RR = 0.55 (95% CI = 0.47-0.65) and RR = 0.52 (95% CI = 0.45-0.61), respectively (72). Carotene-rich vegetables were found to have the strongest protective effect against oral cancer (RR = 0.4; 95% CI = 0.2-1.0) (73). High intake of whole grain was also reported to have a protective effect against upper aerodigestive tract cancers (RR = 0.53; 95% CI = 0.34-0.81) (74).

While the evidence relating to other dietary components is not so strong, certain trends could still be observed. High consumption of some types of fish and seafood was suggested to have a protective effect against head and neck cancers, with most prominent effect observed for common carp (OR = 0.30; 95% CI = 0.13-0.67), hairtail (OR = 0.48; 95% CI = 0.25-0.91) and shrimp (OR = 0.54; 95% CI = 0.33-0.90) (75). However, frequent consumption of salted meat and fish was associated with increased risk of oral cancer (OR = 3.71; 95% CI = 1.05-13.03) (76). Consumption of liver had a significant protective effect (RR = 0.3; 95% CI = 0.2-0.6; $p < 0.0001$) (77). High intake of olive oil was associated with significantly lowered risk of oral and pharyngeal cancers (OR = 0.7; 95% CI = 0.4-0.9) while high butter intake was found to increase the risk of these cancers (OR = 2.4; 95% CI = 1.6-3.5) (78). High intake of milk was reported to reduce the risk of oral cancer (OR = 0.48; 95% CI = 0.23-1.01) (75), while coffee and tea drinking were associated with increased risk of oral cancer with RR = 1.5 (95% CI = 0.9-2.6) and RR = 1.3 (95% CI = 0.7-2.3), respectively (73). Elevated consumption of stew was associated with significantly increased risk of oral and pharyngeal cancers (OR = 3.95; 95% CI = 2.10-7.44, $p < 0.0001$) (77). Finally, consuming foods that have been charcoal-grilled or deep-fried was associated with

increased risk of oral cancer (RR = 5.3; 95% CI = 1.9-15.0 and OR = 2.15; 95% CI = 1.10-4.20, respectively) (73, 76).

1.2.3.4. Oral hygiene

Oral hygiene and dental status, which could be closely related to the socioeconomic status of the patients, have also been investigated in relation to cancers of the head and neck. Case-control studies suggested that poor general oral condition was significantly more common among oral and oropharyngeal cancer patients than in control subjects (OR = 4.5; 95% CI = 1.8-10.9, p = 0.001) (79). In particular, the factors associated with increased risk of oral and pharyngeal cancers included: frequent gum bleeding (OR = 3.1; 95% CI = 1.2-7.9), no dental check-ups (OR = 2.5; 95% CI = 1.3-4.8), no tooth brushing (OR = 1.3; 95% CI = 0.4-4.5) and frequent mouthwash use (OR = 3.3; 95% CI = 1.7-6.1) (80). Poor dentition (measured by the number of missing teeth) also proved to be a strong risk factor for oral cancer (OR = 5.3; 95% CI = 2.3-11.9 in males and OR = 7.3; 95% CI = 2.5-21.6 in females who lost 15-32 teeth) (35). Moreover, it has been suggested that poor oral hygiene may act synergistically with other risk factors like alcohol, as it increases production of acetaldehyde in the oral cavity (81), or on its own may be a reason of delayed diagnosis.

1.2.3.5. Occupational exposures

While considering the aetiology of head and neck cancer, specific occupational exposures should also be taken into account. It is estimated that in western countries approximately 4-10% of all head and neck cancers are due to occupational exposures (82). Firstly, exposure to asbestos was reported to increase the risk of laryngeal cancer

in a dose-dependent manner (RR = 1.82; 95% CI = 1.08-3.04, p = 0.02 for highest exposure) (34). Elevated risk of pharyngeal and laryngeal cancers was reported among welders, who are exposed to welding fumes (RR = 2.26; 95% CI = 1.09-4.68, p = 0.04 and RR = 1.95; 95% CI = 1.03-3.69, p = 0.04, respectively, for more than 8-year exposure) (34). Welding fumes consist of metal dust, irritant gasses and polycyclic aromatic hydrocarbons (PAHs), some of which are known carcinogens (34). Exposure to wood dust was also associated with a strongly increased risk of head and neck cancer of all sites in subjects who had never smoked (RR = 2.27; 95% CI = 1.1-3.9) (34).

In summary, head and neck cancer is a disease with a complex aetiology and multiple risk factors, and the increasing incidence of some types of SCCHN is of great concern. According to IARC estimates, reducing the prevalence of the discussed risk factors could prevent 60-80% of these cancers (83).

1.2.4. Diagnosis, staging and disease management

1.2.4.1. Diagnosis

Some head and neck cancers are preceded by the appearance of premalignant lesions, such as oral leukoplakia or erythroplakia. The rate of malignant transformation of these lesions varies between 5% and 15% and continued use of tobacco increases the risk of transformation (84). Since early-stage tumours are often asymptomatic, they are frequently overlooked by the patient and examiner and there is often a delay of up to a year between first professional visit and diagnosis (85).

Head and neck cancer patients are at a high risk of developing second primary tumours, which occur in 27% of cases and are often fatal (86). This suggests that these patients are in a cancer-prone group, which is most likely related to their continuous

exposure to tobacco smoke and alcohol. The term "field cancerization" was introduced to describe repeated exposure of the squamous epithelium of the upper respiratory tract to carcinogenic substances, resulting in multiple primary lesions (87). Therefore, these second primaries arise mostly in areas such as lung, oesophagus and other parts of the upper aerodigestive tract (87), which have been exposed to carcinogens. However, the molecular evidence that could determine whether the second tumour represents a second primary cancer or a recurrence of the original malignancy is very limited. In fact, studies, which analysed the molecular background of such multiple tumours, provide evidence that some of these cancers arise from one preneoplastic lesion (88, 89, 90), while others may have independent clonal origins (91).

Up to 36% of head and neck cancers metastasise to distant sites and the risk is higher for advanced stage at presentation, especially with nodal involvement (92). In the majority of cases these head and neck cancers metastasize to the cervical lymph nodes before colonising distant sites such as the bones, liver or lungs (93).

The primary screening method for detection of both precancerous lesions and early invasive tumours is physical examination. Suspected tumours are biopsied, usually with the patient anaesthetised, and the biopsies are subjected to histopathological examination (85). In addition to an obvious epithelial primary tumour, it is common for patients to present with enlarged cervical lymph nodes as a result of regional metastatic spread. Diagnosis of regional metastasis is commonly achieved by fine needle aspiration (FNA) and subsequent histological evaluation (85). Computed tomography (CT) and magnetic resonance imaging (MRI) of the head and neck are used for determination of invasion of nearby structures and detection of lymph node involvement. In addition, it is mandatory that patients have a CT scan of their thorax

and upper abdomen to exclude the presence of a second primary bronchogenic carcinoma or distant metastasis (94).

1.2.4.2. Disease staging and management

The conventional treatment modalities for advanced SCCHN include primary surgery and post-operative radiotherapy (85). In an attempt to preserve function, patients are frequently treated with radiation therapy in combination with cisplatin-based chemotherapy (with salvage surgery if other treatment fails), which yields similar survival rates as radical surgery and radiation therapy (95). The damage associated with any of the above mentioned treatments affects speech, swallowing, cosmesis and overall quality of life (95).

In clinical practice the treatment for SCCHN is selected based on the fitness of the patient as well as TNM (tumour, node, metastasis) stage and histological grade (96). Unfortunately, these parameters have limited predictive value for therapeutic response. This is frequently due to the fact that SCCHN is usually considered to be a homogenous group of tumours even though cancers arise from the surface epithelium of several different anatomical sub-sites within the upper aerodigestive tract (85). There is a notable variability in biological behaviour and therapeutic response both between and within the sub-sites (97). The actual tumour site, nodal involvement and extracapsular spread are the strongest prognostic factors (98).

The group of HPV-positive oropharyngeal cancers forms a distinct biological entity with a better prognosis than HPV-negative tumours (99). Although currently this distinction is not made when deciding on the type of treatment, it has been frequently suggested that less aggressive treatment modalities should be considered in an attempt to reduce the treatment-related morbidities. Moreover, the fact that the

majority of HPV-infections detected in head and neck cancer were of the HPV-16 or HPV-18 type suggests that the prophylactic vaccines for cervical cancer might also prove to be protective against SCCHN (100).

In conclusion, there is a constant need to identify novel prognostic markers that would enable determining how well the patient is going to respond to different modalities or combinations of therapy and to develop novel treatments that could be tailored to the individual tumours.

1.2.5. Molecular alterations

As stated above, head and neck cancers include a heterogeneous group of tumours. The established risk factors (described in section 1.2.3), e.g. smoking, alcohol consumption and infection with the HPVs, influence many of the genetic alteration observed in SCCHN.

1.2.5.1. p53 tumour suppressor alterations in SCCHN

Among the various molecular alterations found in human cancer (including SCCHN), the inactivation of the p53 tumour suppressor pathway, especially through p53 mutation, seems to be paramount in tumour development. Moreover, mutations in this tumour suppressor gene have been found to be associated with reduced survival in SCCHN patients (101). Most of this association was attributed to mutations disrupting the native structure of the p53 protein (101). The most frequent p53 mutations were G:C → A:T transitions and G:C → T:A transversions (102), which comes as no surprise given the high exposure of SCCHN patients to nitrosamines (and other carcinogens) contained in tobacco (103). Moreover, the prevalence of frameshift mutations was significantly higher in SCCHN (16%) than in other cancer types (9%) (104). This is also related to exposure to tobacco carcinogens (such as

benzo[a]pyrenes or nitrosamines), which are known to preferentially induce single base pair deletions (105). In addition, increased incidence of p53 frameshift mutations in SCCHN was linked to concomitant alcohol and tobacco exposure (102), suggesting that the synergistic action of these two substances may contribute to such p53 mutational spectra in SCCHN.

The timing of p53 mutation in SCCHN is still controversial. There is evidence that the mutations can occur prior to the conversion from the premalignant to the invasive state (106). However, the incidence of p53 mutation is higher in the malignant lesions (106) and is closely linked to the exposure of most SCCHN patients to carcinogens, such as tobacco and alcohol (30).

p53 has been found to be mutated in about 50% of head and neck cancers (101), so the mutation prevalence in SCCHN is very similar to other epithelial cancers (107). A large-scale p53 mutational analysis revealed that the prevalence and nature of p53 alterations varies significantly between different anatomical sub-sites (28). The highest rate of alterations, including mutations, overexpression and loss of expression was found in tumours of the hypopharynx (28). Laryngeal cancers, on the other hand, exhibited the lowest frequency of p53 alterations but also had a distinct mutation spectrum with most mutations occurring in exon 5 (28). Interestingly, most hot-spot 248 mutations were also found in the larynx (28). Therefore, the p53 mutation spectrum of the larynx resembled the one seen in lung cancer rather than those observed in other sites of the head and neck, such as hypopharynx (28). This observation is consistent with the exposure of the laryngeal surface mucosa to tobacco alone (similar to lungs), while in the case of other tumour sites of the head and neck (oral cavity, oropharynx, hypopharynx) there is frequently concomitant exposure to both tobacco and alcohol.

While the presence of p53 mutations was found to have limited prognostic value in SCCHN (28, 108), p53 mutation was associated with reduced overall survival (HR = 1.48; 95% CI = 1.03-2.11) and disease-free survival (HR = 1.47; 95% CI = 1.12-1.93) in oral cancer (108). Surprisingly, the presence of p53 mutation had a favourable effect on disease-free survival in the oropharynx (HR = 0.45; 95% CI = 0.27-0.73) (108). This discrepancy between two head and neck sub-sites may be due to sampling issues or the underlying biological differences. It is tempting to speculate that high prevalence of HPV-positive oropharyngeal cancers might account for the survival advantage observed here (HPV-positive tumours have a favourable prognosis, as discussed in section 1.2.3.2). However, HPV-positive tumours usually carry wild-type p53 (see section 1.2.5.3) so the situation observed here is far from clear and requires further study.

1.2.5.2. Alterations of the Rb pathway and cyclin D1 expression

In addition to the p53 pathway, another pathway frequently altered in SCCHN is the retinoblastoma (Rb) pathway (109). Rb is an important tumour suppressor protein, which plays a role in the regulation of the cell cycle. The activity of Rb is regulated through its phosphorylation level by cell cycle regulators such as p16 and cyclin D1 (109). Underphosphorylated Rb forms a complex with E2F transcription factor, hence preventing it from activating S-phase genes (necessary for cell proliferation) and resulting in inhibition of the cell cycle at the G1-S checkpoint (110). Cyclin D1, in complexes with CDK4/6 partners, initiates Rb phosphorylation, resulting in release of E2F and cell proliferation (110). The tumour suppressor p16, on the other hand, interferes with the binding of cyclin D1 to CDKs (see Figure 1.6), thus preventing Rb phosphorylation (111).

Cyclin D1 overexpression occurs in 49-79% of SCCHN (112, 113) and is consistently associated with poor prognosis (highly invasive and metastatic tumours, reduced disease-free survival, early recurrence) (113, 114). Moreover, loss of p16 expression (through homozygous deletions and methylations) was reported in 52-82% of head and neck cancers (115, 116), which was also associated with decreased disease-specific survival and early recurrence (69). This further emphasizes the importance of the Rb pathway inactivation in head and neck carcinogenesis.

1.2.5.3. The mechanism of HPV-mediated oncogenesis

Human papillomaviruses are small DNA viruses, which infect the squamous epithelial cells of the skin and mucous membranes (117). While they have been known for a long time as the causal agents of cervical cancer (47), their role in SCCHN became of interest only in the 1980s. Since then it has been determined that HPV, especially HPV-16, is involved in 25% of head and neck cancers (52). Moreover, it has been observed that the majority of HPV-positive tumours express wild-type p53 (99, 118), which can be easily explained by the mechanism of HPV-mediated oncogenesis (see Figure 1.6).

The two main viral oncoproteins are HPV E6 and E7 (50). The E6 oncoprotein is targeted to the nuclear matrix and by binding to p53 of the host cell, it targets it for ubiquitin-mediated degradation (119). Therefore, p53 mutation in HPV-positive tumours would simply be redundant. HPV E6 has also been suggested to mediate telomerase activation (120, 121), an enzyme responsible for elongating the ends of the eukaryotic chromosomes (telomeres), which is crucial for cellular immortalization, and thus helps cells avoid replicative senescence. Active telomerase has been detected in about 90% of SCCHN cases analysed (122).

HPV E7 is also a small nuclear protein, which binds to and destabilises (through ubiquitin-mediated proteolysis) another tumour suppressor protein – retinoblastoma (Rb), which is a negative regulator of cell growth (123). This results in overexpression of $p16^{INK4a}$ (a cyclin-dependent kinase inhibitor), which normally inhibits Rb phosphorylation and blocks cell cycle progression (as described in section 1.2.5.2) (124). While loss of p16 function is a frequent event in SCCHN, high level of p16 could be a surrogate marker for HPV, and was found to be associated with increased overall and disease-free survival (99, 125).

1.2.5.4. Dysregulation of the EGF signalling pathway

An important signalling pathway dysregulated in SCCHN is the epidermal growth factor (EGF) signalling pathway. Epidermal growth factor receptor (EGFR) has been found to be overexpressed in many head and neck cancers (126, 127). EGFR belongs to the ErbB family of receptor tyrosine kinases and can bind multiple ligands. EGF and transforming growth factor α (TGF-α), which have 40% sequence similarity, are believed to be the most important ligands for EGFR. Upon ligand binding EGFR dimerises, which triggers internalisation and autophosphorylation of its cytoplasmic domain due to its intrinsic tyrosine kinase activity. This in turn initiates a signalling cascade through Ras-Raf and PI3K-AKT, resulting in a mitogenic response (128). Interestingly, there is some evidence that EGF-bound EGFR can be translocated into the nucleus, where it can function as a transcription factor (individually or in cooperation with other transcription factors) to induce cyclin D1 expression, promoting cell cycle progression (as described in section 1.2.5.2) (129). High EGFR expression in SCCHN has been correlated with poorer response to therapy and worse overall and disease-free survival (99).

Recently, one of the first targeted therapies has been introduced into the clinic in the UK for treatment of locally advanced, nonresectable or metastatic SCCHN. Cetuximab, a monoclonal antibody against EGFR, has recently been approved for treatment in combination with radiotherapy in patients deemed unsuitable for treatment with cisplatin-based chemoradiation and resulted in a sharp improvement in response rate and survival of these patients compared to standard therapy (130, 131). Anti-angiogenic treatments and tyrosine kinase inhibitors, such as gefitinib and erlotinib, have proved promising in the clinical trials (132).

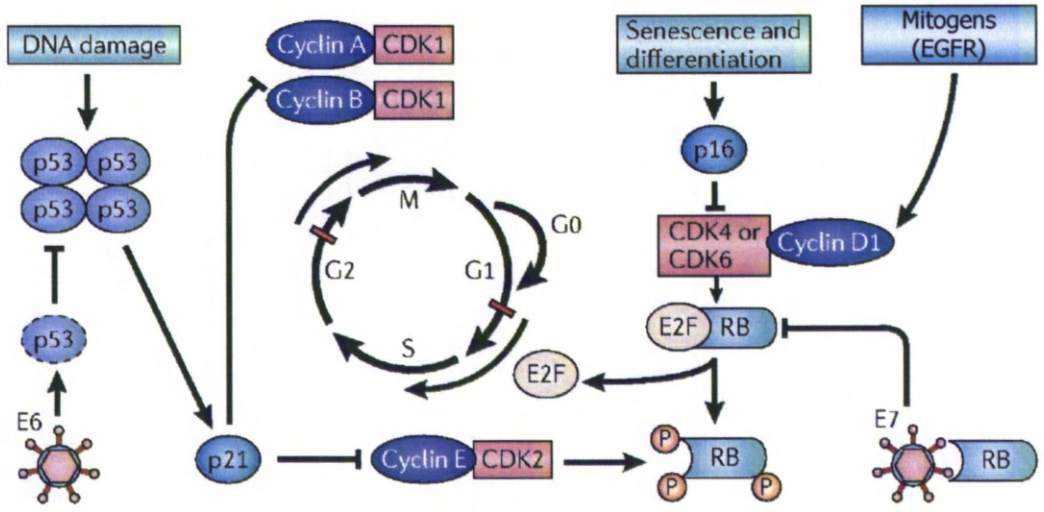

Figure 1.6: A schematic representation of the major molecular pathways altered in SCCHN. Two major tumour suppressor pathways involved in the pathogenesis of SCCHN are the p53 and Rb pathways. Upon DNA damage p53 is induced and stimulates p21 expression (among many others). p21 inhibits cyclin A/B-CDK1 complexes, thus preventing G2-to-M transition. HPV E6 protein binds to p53 and targets it for proteasomal degradation. Another tumour suppressor, Rb, binds to E2F preventing it from activating the S-phase genes. Mitogenic signalling (including EGFR overexpression) stimulates cyclin D1 expression, which complexes with CDK4/6 and phosphorylates Rb, resulting in E2F dissociation and cell cycle entry. HPV E7 protein also inactivates Rb, preventing it from binding to E2F, which results in cell proliferation. Finally, p16, an inhibitor of the CDK-cyclin D1 complexes, is frequently lost in SCCHN. Figure adapted from reference (133).

The number of different molecular alterations (some of which are described here) underlying the pathogenesis of head and neck cancer emphasizes the heterogeneity of this disease and the need for development of personalised treatments for individual patients. Understanding the molecular basis of SCCHN is crucial for finding predictive biomarkers and developing novel treatment strategies tailored to the individual tumour.

1.3. The p53 tumour suppressor protein

One of the key molecular pathways altered in cancer cells is focused upon the p53 tumour suppressor protein (134). When it was first discovered in 1979 (135), p53 was identified as a cellular oncogene due to the ability of the cloned tumour-derived p53 cDNAs to accelerate the cell cycle, immortalize some cell types and cooperate with other oncogenes in cellular transformation (136). It was not until 10 years later when it was discovered that the *TP53* cDNAs initially studied in different laboratories encoded mutant p53 proteins and wild-type p53 was found to have growth-suppressive properties and to inhibit cellular transformation (137). Currently, p53 is one of the most intensely studied proteins in human cancer with nearly 60,000 citations in PubMed.

1.3.1. Structural organisation of the p53 protein

p53 is encoded by the *TP53* tumour suppressor gene located on the short arm of chromosome 17 (17p13.1, a chromosomal locus frequently altered in human cancers) (138). This 20 kbp (kilobase pair) gene consists of 11 exons (2-11 coding) yielding a 393 amino acid protein (139), which functions as a tetramer (140). Structurally, the

p53 protein can be divided into three parts: the N-terminal domain, central core and the C-terminal domain (Figure 1.7).

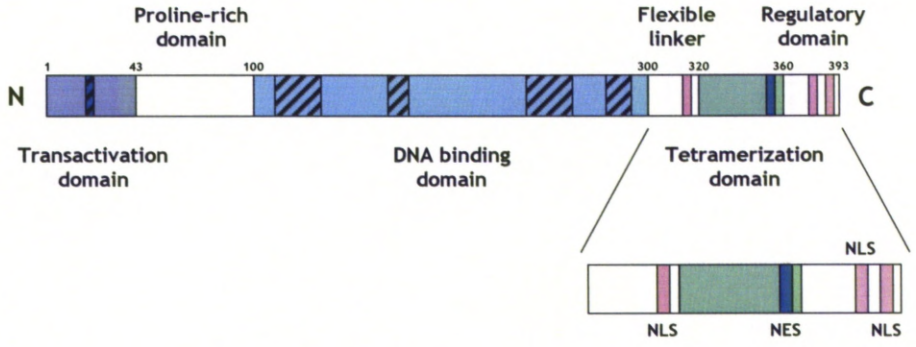

Figure 1.7: Structure of the p53 protein. Hatched boxes represent evolutionarily conserved regions. The protein contains the N-terminal transcriptional activation domain, central sequence-specific DNA binding domain and the C-terminal domain, including the tetramerization and regulatory domains. p53 contains three nuclear localization signals (NLSs) in its C-terminal domain and two nuclear export signals (NESs) – one in the tetramerization domain and another in the N-terminal transactivation domain.

The N-terminal domain contains the acidic transcriptional activation domain and encompasses residues 1-43 (141). The transactivation domain of p53 interacts with several general transcription factors, including the TATA box-binding protein (TBP) (142) and the TBP-associated factors TAFII70 and TAFII31 (143), all being part of the general transcription factor TFIID, and the p62 subunit of the TFIIH transcription factor (144). The residues F19, L22 and W23 have been shown to be essential for transcriptional activation by p53 as they make direct contact with the components of the transcriptional machinery (145).

The central core contains the sequence-specific DNA-binding domain (DBD) of p53 and lies between amino acids 100-300 (146). There are four evolutionarily conserved regions within the core domain (region II: 117-142; III: 171-181; IV: 234-258; V: 270-286), which comprise a DNA-binding element, responsible for

contacting the major and minor grooves of the bound DNA (147). The remaining regions of the central core make up a β-sandwich, which forms a scaffold to support the α-helical DNA binding element (147). The DNA binding central core is a protease-resistant domain, chelating a Zn^{2+} ion, which is necessary for its sequence-specific DNA binding (148). Residues K120, S241, R273, A276 and R283 are also responsible for the sequence-specificity of p53 as they make direct contact with the phosphate backbone in the major grove of DNA, while residues K120, R248, C277 and R280 form hydrogen bonds with DNA bases in the minor grove of DNA (147). The majority of p53 mutations found in human cancers are located in the central core domain, especially within the highly conserved regions (104), leading to the loss (or modification) of sequence-specific DNA binding.

The C-terminal domain (residues 300-393) is multifunctional. It can be further subdivided into three regions: a flexible linker (residues 300-320), a tetramerization domain (residues 320-360) (148) and a regulatory domain, which is rich in basic residues (residues 363-393). The tetramerization domain contains a β-sheet-turn-α-helix motif, which can homodimerize (Figure 1.8) and a pair of such dimers forms the p53 tetramer (149, 150). The pair of dimers is held together by strong hydrophobic interactions between the surfaces of each helix pair (150). The C-terminal regulatory domain contains 9 basic residues and is capable of non-specific DNA binding (148). It has also been reported to bind damaged DNA (151, 152) and to promote reannealing of complementary DNA or RNA strands (153).

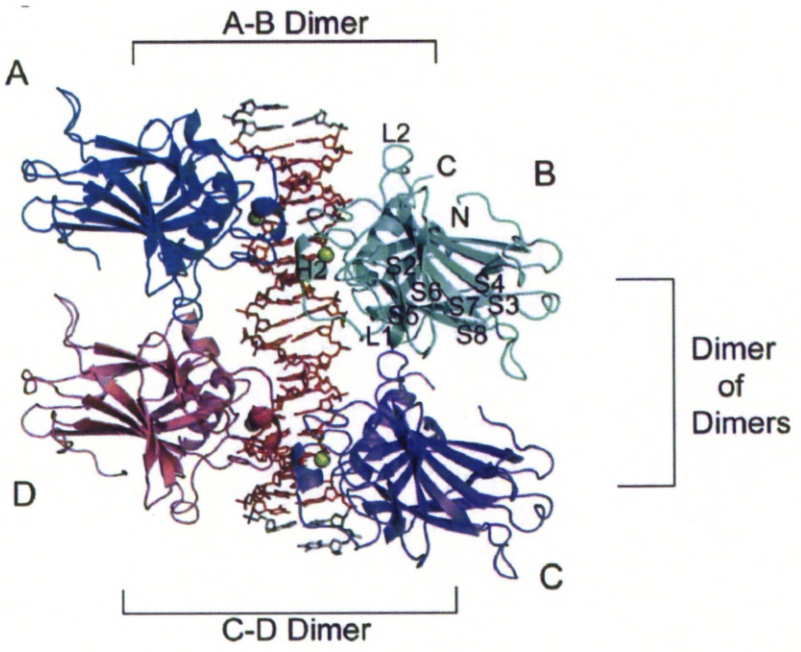

Figure 1.8: Structure of the tetrameric DNA binding domain of p53 binding to DNA. Subunits A (blue) and B (green) form one dimer, subunits C (purple) and D (pink) form the other dimer. Zn^{2+} ions are depicted as bright green spheres. The consensus DNA binding sequence is presented in red and the remaining DNA bases in grey. Figure reproduced from reference (154).

1.3.2. Functions of p53

The p53 protein acts as a multitarget, sequence-specific transcription factor (reviewed in (155)). Most of the promoters bound by p53 contain a consensus binding sequence with an internal symmetry. The consensus binding site consists of two copies of a 10 base pair motif 5'-PuPuPuC(A/T)(T/A)GPyPyPy-3' separated by 0-13 base pairs (156). The symmetry of the four half-sites in the consensus sequence is striking given the fact that p53 binds DNA as a tetramer (140). Importantly, while the majority of the described and validated p53 response elements (REs) are associated with transcriptional activation of gene expression, many of the REs (up to 15%) are also linked to transcriptional repression (157). Although the mechanisms of p53-mediated transcriptional repression are less well understood, the following mechanisms have

been proposed: binding of p53 to transcription factor Sp1, hence inhibiting its ability to bind other promoters (158), direct repression of certain promoters (159) or competing with the TATA-box binding protein (TBP) for binding to some promoters (160). p53-dependent transrepression has also been suggested to be mediated by deacetylation of core histones at the promoter region of repressed genes (161) due to the interaction of p53 with a corepressor mSin3a and histone deacetylases (HDACs) in response to hypoxia (162).

As a transcription factor p53 controls the expression of a large number of genes with various functions, involved in regulation of the cell cycle, apoptosis, senescence, DNA repair after genotoxic stress, oxidative stress, angiogenesis, differentiation (163), cell adhesion, cell migration, extracellular matrix and cytoskeleton organisation (164, 165). Given such a long list of p53-regulated processes, it comes as no surprise that *TP53* mutation is found in about 50% of human cancers (107). Moreover, it is believed that in many other tumours p53 is inactivated indirectly via binding to viral proteins or through alterations of other components of the p53 pathway (interacting with or transmitting signals to or from p53) (134). Germline mutations of p53 have been found to underlie Li-Fraumeni syndrome, a rare autosomal dominant hereditary disorder, which greatly increases susceptibility to cancer (166).

1.3.2.1. Cell cycle regulation by p53

One of the main functions of p53 in the majority of mammalian cells is the inhibition of progression through the cell cycle. There are a number of pathways via which p53 induces cell cycle arrest. First of all, p53 transcriptionally activates the expression of $p21^{WAF1/CIP1}$, which inhibits cyclin-dependent kinases (CDK1 and CDK2) (167). CDKs are the key regulators of the cell cycle checkpoints (168). They become active

only in complexes with cyclins (169) and are essential for successful progression through the cell cycle (G1→S→G2→M phase transitions) (170). By inhibiting the activity of the cyclin/CDK family members (cyclin E-CDK2, cyclin A-CDK1/2 and cyclin B-CDK1), p21 blocks cell cycle progression at G1 and G2 phases (171). p21 is also able to bind proliferating cell nuclear antigen (PCNA), hence blocking the activity of PCNA as a DNA polymerase processivity factor in DNA replication and causing G1 arrest (172). p21 was shown to be essential for p53-mediated G1 arrest (173).

Another p53-induced gene involved in cell cycle regulation is GADD45 (growth arrest and DNA-damage-inducible) (174). GADD45 is implicated in the induction of the G2 arrest as it was reported to inhibit the activity of the CDK1-cyclin B1 complexes (175). This ensures that cell cycle progression can be halted, if necessary, even in the absence of p21.

p53 can also achieve cell cycle arrest via up-regulation of 14-3-3σ in epithelial cells lining internal organs (176). 14-3-3σ promotes a pre-mitotic cell cycle arrest in the G2 phase via sequestering cyclin B1-CDK1 complexes and preventing them from entering the nucleus (177). Cyclin B1 and CDK1 are cytoplasmic during interphase and are translocated into the nucleus at the end of G2 phase to stimulate mitosis (178). This DNA damage checkpoint and sequestration of cyclin B1-CDK1 complexes prevents the cells from entering mitosis, which could be potentially lethal if the cellular DNA is damaged (179).

Similarly to 14-3-3σ, Reprimo, a newly identified candidate tumour-suppressor gene, is a potential mediator of the p53-dependent cell cycle arrest (180). Overexpression of Reprimo inhibits progression through the cell cycle, arresting cells at the G2 phase, likely through inhibition of CDK1 activity (180). While the

mechanism of Reprimo-mediated cell cycle arrest is not fully understood, the accumulation of cyclin B1 in the cytoplasm and the presence of inactive CDK1 in Reprimo-overexpressing cells suggests that it may stimulate G2 arrest via inhibition of CDK1 activity and cytoplasmic sequestration of the CDK1-cyclin B1 complexes (180). Although there is no evidence for the presence of a p53 consensus binding site within the promoter region of Reprimo, its induction upon p53 expression suggests that Reprimo expression is regulated by p53 (180).

The number of p53-responsive genes involved in regulation of the cell cycle suggests that induction of cell cycle arrest is an important mechanism of p53-mediated tumour suppression.

1.3.2.2. The role of p53 in apoptosis

The most important role of p53 is the induction of apoptosis, where it acts to selectively eliminate stressed or abnormal cells, hence protecting the organism from developing cancer. It does so predominantly by transcriptional induction or repression of expression of numerous genes (181) although transcriptionally-independent p53 activities have also been well documented (182). While transcriptional activation of gene expression has been extensively studied, the mechanisms of p53-mediated transcriptional repression are less well understood.

p53 can directly activate each of the three most important apoptotic pathways in the cell (summarized in Figure 1.9): the intrinsic (mitochondrial) apoptotic pathway, the extrinsic (death receptor-mediated) apoptotic pathway and apoptosis mediated by reactive oxygen species (ROS) (183).

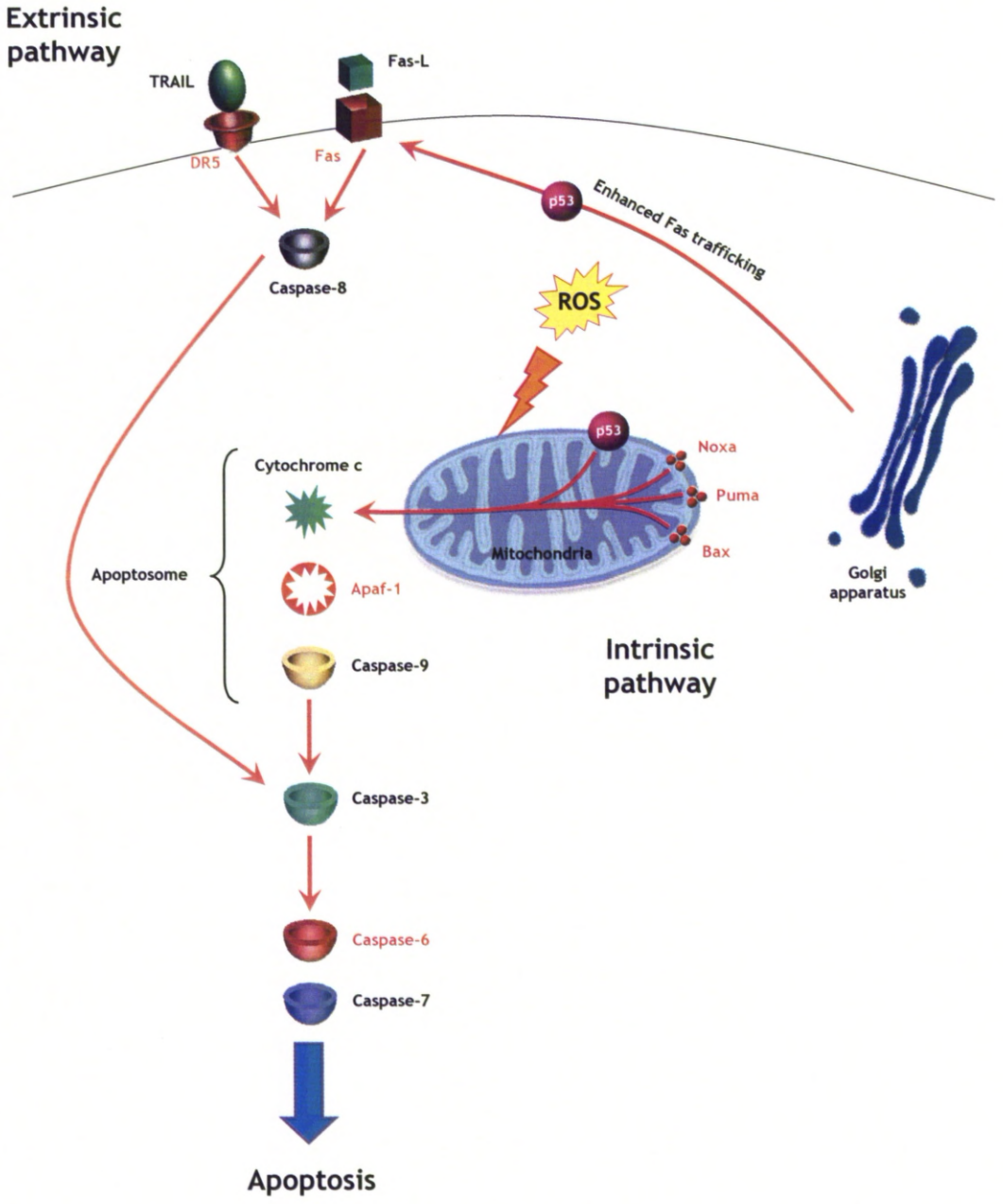

Figure 1.9: A model of p53-mediated apoptosis. The diagram outlines the modes of p53-induced apoptosis: the intrinsic and extrinsic apoptotic pathways and induction of apoptosis through ROS. p53 transcriptional targets are shown in red. Figure adapted from reference (184).

The first two converging pathways, the extrinsic and the intrinsic apoptotic pathway, both lead to the activation of caspases that mediate apoptosis (185). The extrinsic pathway is a type of "instructive" apoptosis, which allows the organism to

actively direct selected cells to commit suicide. It involves a type of cell surface receptors, the so-called death receptors, which upon binding their extracellular ligands transmit apoptotic signals, leading to an activation of caspase-8 and initiation of a caspase cascade (186). The intrinsic or mitochondrial pathway involves the alteration of the mitochondrial membrane potential due to the opening of the mitochondrial transition pores and the release of cytochrome c from the mitochondrial intermembrane space into the cytoplasm (187). Cytochrome c, apoptotic protease-activating factor 1 (Apaf-1) and procaspase-9 form a complex known as the apoptosome, in which procaspase-9 is cleaved and auto-activated, thence initiating a caspase cascade (188). The third apoptotic pathway mediated by p53 involves the production of ROS (189). Increased levels of ROS inflict serious damage to mitochondria, resulting in a leakage of calcium and mitochondrial proteins (including cytochrome c) into the cytoplasm and activation of a caspase cascade (182).

1.3.2.2.1. The extrinsic apoptotic pathway

p53 can initiate the death receptor apoptotic pathway by transcriptional activation of a number of death receptors, including Fas/Apo1 and DR5/KILLER (183). Ligand binding triggers receptor trimerization and clustering of the intracellular death domains (DD), which then recruit intracellular adaptor molecules to form a death-inducing signalling complex (DISC) (186). This leads to the activation of caspase-8, triggering a caspase cascade and induction of apoptosis (190).

Fas (also known as CD95 or Apo1) is a cell-surface receptor belonging to the tumour necrosis factor receptor (TNF-R) family (191). It becomes activated by binding of its ligand, FasL, which is expressed predominantly in activated T cells (191). In response to γ-irradiation, p53 can not only induce Fas expression (192), but

also enhance trafficking of Fas from the Golgi apparatus to the cell surface (193). Moreover, FasL has also been observed to be up-regulated by p53 (194), providing yet another way, in which p53 could activate this apoptotic pathway.

DR5/KILLER is another member of the TNF-R family. Similarly to Fas, it is up-regulated by p53 in response to DNA damage (195) and upon binding of its ligand, TNF-related apoptosis-inducing ligand (TRAIL), activates the apoptotic caspase cascade (196).

A recently discovered gene found to play a role in this pathway is PIDD (p53-induced protein with a death domain), which is a transcriptional target of p53 (197). PIDD is a cytoplasmic protein, which upon binding an adaptor protein RAIDD activates caspase-2, resulting in an activation of a caspase cascade and induction of apoptosis (198).

1.3.2.2.2. The intrinsic apoptotic pathway

In addition to apoptosis triggered by extracellular signals, apoptosis can also be initiated through the mitochondrial pathway. This pathway represents another type of apoptosis mediated by p53. It is dominated by the proteins belonging to the Bcl-2 family, which control the release of cytochrome c from the mitochondria. The Bcl-2 family comprises the anti-apoptotic Bcl-2 and Bcl-X_L, and the pro-apoptotic Bax, Bak, Bid, Noxa and PUMA.

One of the first genes identified to be an apoptotic target of p53 was *Bax*, encoding an apoptosis-inducing mediator – a member of the Bcl-2 family (199). Bax binds to the survival factor Bcl-2 and antagonizes its anti-apoptotic function (200). This suggests that the ratio of Bcl-2 to Bax could be responsible for determining the response (death or survival) to an apoptotic stimulus. However, Bax is not required

for apoptosis under all circumstances and the requirement for Bax was reported to be cell type and context dependent (184). For example, Bax was found to be dispensable for the induction of p53-mediated cell death in T-lymphocytes after ionising radiation (201), in which apoptosis is induced through Fas (see section 1.3.2.2.1) and the death receptor pathway (202). This emphasizes the importance of the numerous p53-mediated apoptotic pathways discussed here.

More recently, two additional pro-apoptotic members of the Bcl-2 family, Noxa (203) and PUMA (204), have been identified as transcriptional targets of p53. These proteins, along with another p53 transcriptional target, non-Bcl-2 family member p53AIP1 (p53-regulated Apoptosis-Inducing Protein 1) (205), localize to the mitochondria and through their binding to Bcl-2 stimulate the opening of the mitochondrial permeability transition pore, resulting in the loss of mitochondrial membrane potential, release of cytochrome c into the cytoplasm and stimulation of a caspase cascade. Moreover, p53 has also been reported to transcriptionally activate the expression of Apaf-1 (206) and caspase-6 (207), further contributing to the stimulation of the intrinsic apoptotic pathway.

As mentioned previously, determining the death or survival of a cell is dependent on the balance of the pro- and anti-apoptotic members of the Bcl-2 family. While p53 can transcriptionally activate the expression of the pro-apoptotic Bcl-2 family proteins, Bcl-2 can specifically suppress p53-mediated apoptosis (208). Therefore, it can be envisaged that p53 should be able to antagonize the action of Bcl-2 for efficient induction of the apoptotic response. Indeed, p53 was reported to down-regulate Bcl-2 gene expression (209). It was further shown that this is achieved through transcriptional repression of the Bcl-2 gene containing a negative p53 response element (in the 5'-untranslated region) (210). Furthermore, p53 was shown

to bind to p2 promoter of Bcl-2 and to suppress Bcl-2 transactivation by another transcription factor, Brn-3a (208), hence tipping the balance towards apoptosis.

Additionally, it was reported that in response to cellular stress p53 can form an inhibitory complex with the anti-apoptotic proteins Bcl-X_L and Bcl-2, leading to mitochondrial membrane permeabilization and apoptosis (211).

Therefore, concomitant transcriptional repression of anti-apoptotic Bcl-2 and induction of pro-apoptotic Bax, Noxa and PUMA as well as physical inhibition of the anti-apoptotic proteins Bcl-X_L and Bcl-2 by wild-type p53 provide a plausible mechanism of p53-mediated apoptosis.

1.3.2.2.3. ROS-mediated apoptosis

Disturbances of mitochondrial integrity may also be influenced by the redox status of the cell and the levels of reactive oxygen species (ROS). The genes implicated in this process are the so called p53-induced genes (PIGs) (189), which encode proteins with activities related to the redox status of cells. So far a number of such genes have been identified including: *PIG1* – a member of the galectin family, stimulating superoxide production (212); *PIG3* – an NADPH-quinone oxidoreductase, a potent generator of ROS (213); *PIG4* – a serum amyloid protein inducible by oxidative stress (214); *PIG6* – a homologue of proline oxidoreductase catalysing the first stage in the conversion of proline to glutamate in the mitochondria (215); *PIG8* – a homologue of murine *Ei24* gene induced by etoposide, which generates ROS (216) and *PIG12* – a member of the glutathione S-transferase family (189). The proteins encoded by the above mentioned genes altogether contribute to the increase of the cellular levels of ROS, which damage mitochondria (189). Release of cytochrome c from the leaking mitochondria

leads to the activation of a caspase cascade, a common event during the apoptotic process.

While hyper-physiological levels of p53 were reported to promote the induction of the pro-oxidant genes, basal p53 levels are known to play an important role in maintaining ROS at a non-toxic level (217). At physiological level p53 induces the expression of a number of antioxidant genes, including *SESN1* (mammalian sestrin homolog), *SESN2* and *GPX1* (glutathione peroxidase 1), hence lowering the levels of ROS in cells (218, 219, 220). This dual action of p53 with respect to ROS ensures that in unstressed cells the levels of ROS are kept low (preventing DNA damage and genetic instability), while in the context of cellular stress ROS up-regulation results in programmed cell death.

Although p53 is predicted to target many other genes than the ones described here, each of these p53-inducible proteins has been shown to be indispensable for the full apoptotic response, at least under certain circumstances, *in vitro*. These results await to be confirmed using *in vivo* models.

1.3.2.3. Choice of response to p53

The fact that p53 induces both cell cycle arrest and apoptosis has led to postulating the question of how the cell decides which response to choose. It appears that the key factor determining the cell's response to p53 might be the cell type (221). Interestingly, p53 has been suggested to selectively induce apoptosis in transformed versions of certain cell types, compared to their normal counterparts, which might preferentially undergo a theoretically reversible cell cycle arrest (222). Some normal cell types, such as gut epithelium, clearly do undergo apoptosis in response to p53 induction, and this is believed to be one of the main causes of the adverse side effects

associated with many anti-cancer treatments (223). However, other cell types, including some epithelial cells and fibroblasts, become more susceptible to apoptosis following oncogenic transformation (224), giving rise to the exciting idea that it might be possible to selectively kill cancer cells while sparing the normal untransformed tissue.

The question of contribution of p53 to the choice of response still remains unanswered. The two suggested models are the 'p53 dumb' and 'p53 smart' model (225).

The 'p53 dumb' model suggests that p53 may have no influence on the cell's response to it, but sends exactly identical signals upon activation in all cases, resulting in stimulation of both pro-apoptotic and cell cycle arrest-inducing target genes. In this scenario, p53 activation would always send an apoptotic signal, which could be either hindered by survival signals or amplified by independent apoptotic signals to reach a threshold necessary to kill the cells (225). This model is supported by the fact that in case of inhibition of p53-dependent apoptosis, p53-mediated cell cycle arrest takes over. However, the fact that apoptotic and cell cycle arrest target genes can be differentially regulated by p53 and that some p53-dependent apoptotic genes are expressed only in cells undergoing p53-mediated apoptosis (226) suggests that the 'p53 dumb' model might not always be correct and needs adjusting. It has therefore been suggested that in the presence of identical signals sent by p53 in every situation, successful transcriptional activation of apoptotic target genes relies on the presence of other transcription factors binding to those promoters (227).

While it is clear that p53-independent factors play a role in determining the cellular response to p53, there is accumulating evidence for the existence of a direct role of p53 in modulating which response pathways are activated. This 'p53 smart' model

suggests that p53 activities differ depending on whether the cell is destined to undergo apoptosis or cell cycle arrest. The type and intensity of cellular stress may influence p53 function by affecting the level and activity of the induced p53. The choice of response can be heavily affected by the abundance of p53, with increasing amounts of the protein turning cell cycle arrested cells into apoptotic cells (228), which could be explained by the lower affinity of the apoptotic target gene promoters for p53. Alternatively, the affinity for certain target genes might be influenced by the conformation of p53 (229). Moreover, post-translational modifications of p53 can also affect promoter binding. An example of the latter is the phosphorylation of p53 on serine 46, which has been correlated with the onset of apoptosis and which enables p53 to induce an apoptotic target p53AIP1 (205). This altered action of phosphorylated p53 could be explained either by subtle changes in conformation affecting its DNA binding specificity or altered capacity to interact with coactivators essential for induction of apoptotic genes. Nevertheless, the retention of the cell cycle arrest response in apoptotic cells indicates that forms of p53 capable of inducing cell death may also have the capacity to drive other responses.

The selection of target genes by p53 has also been suggested to be modulated by p53-binding proteins. p53 forms complexes with a transcriptional coactivator p300/CBP, which opens up the chromatin around the p53-binding sites to make it accessible to both p53 and the transcriptional machinery (230). While this interaction allows p53 to function efficiently as a transcriptional activator in general, the cooperation of JMY with p300 was reported to enhance the ability of p53 to stimulate apoptotic target genes, such as Bax, without having a significant impact on the transcription of cell cycle arrest genes, such as p21 (231). A direct interaction of ASPP family members with p53 has also been found to enhance the ability of p53 to

bind apoptotic target genes (232). Finally, stimulation of apoptosis by p53 has recently been reported to require the presence of at least one other member of the p53 family, p63 or p73 (233). Since wild-type p53 does not directly bind either of these proteins, p63 or p73 may influence the binding of p53 to certain promoters indirectly.

In summary, the available evidence suggests that the consequences of p53 activation are influenced by a number of factors, including the cell type, the nature of stress signals (strength, duration) and the cellular context (presence and abundance of other factors) (221). The possibility to selectively induce apoptosis in cancer cells by modulating the above mentioned factors creates an attractive therapeutic avenue for development of effective anti-cancer treatments targeting p53.

1.3.2.4. The role of p53 in senescence

Apoptosis and cell cycle arrest are not the only anti-proliferative functions of p53. p53 has also been suggested to exert its tumour suppressor properties via regulating the process of cellular senescence (234).

Senescence or proliferative aging is a type of irreversible cell cycle arrest, which differs from quiescence (reversible cell cycle arrest) in the specific morphological changes and gene expression (235). Normal cells undergo a limited number of cell divisions (236). Every cell cycle is accompanied by shortening of telomeres (repetitive DNA sequences at the ends of linear chromosomes) and telomere erosion results in an irreversible growth arrest known as replicative senescence (237). More recently, other stimuli such as DNA damage and oncogene activation have also been reported to cause cells to adopt a senescent phenotype (236). Since aging predisposes cells to accumulate mutations that could eventually lead to malignant transformation, senescence appears to provide a fail-safe mechanism, which prevents organisms from

developing cancer (238). Therefore, it comes as no surprise that a number of tumour suppressors, including p53 and Rb, are involved in controlling cellular senescence (239).

p53 is induced in response to all three senescence-inducing signals (telomere erosion, DNA damage and oncogenic signalling). Oncogene activation and DNA damage lead to the induction of another tumour suppressor, $p14^{ARF}$ (240). $p14^{ARF}$ binds and sequesters MDM2, hence releasing p53 from the negative regulation by MDM2 (as discussed in section 1.3.3.1), leading to the stabilisation and activation of p53 (241). Another protein implicated in the process of senescence is the promyelocytic leukaemia (PML) tumour suppressor. PML is induced by telomere shortening and oncogene activation (242) and interacts with the p300/CBP acetyltransferases, which also acetylate p53 resulting in its activation (see section 1.3.3.2) (243). As a result p53 induces p21 transcription, which may facilitate the onset of senescence (244).

1.3.2.5. The role of p53 in DNA repair and maintaining genomic stability

The ability of p53 to influence the cellular life and death decisions has implications also for maintaining genetic stability. First of all, p53-mediated induction of apoptosis in response to DNA damage directly eliminates abnormal cells harbouring mutations that would otherwise contribute to genomic instability. The induction of cell cycle arrest (a reversible pause in the cell cycle) by p53, on the other hand, allows time for DNA repair, which prevents the propagation of potentially deleterious mutations, again contributing to the maintenance of genomic stability. In addition to DNA damage, p53 was also reported to be activated in response to specific depletion of ribonucleotide pools (245). Ribonucleotide depletion was associated with prolonged

p53 induction, resulting in p21 up-regulation and Rb dephosphorylation, leading to cell cycle arrest at the G1 phase (246), hence preventing DNA replication in conditions that could result in chromosome breakage. Chromosome breakage or dsDNA breaks are the most deleterious type of DNA damage, resulting in a high rate of chromosomal rearrangements, deletions and mutations, resulting in genomic instability (247). Therefore, p53-mediated cell cycle arrest in response to ribonucleotide depletion can stop DNA replication before damage occurs. Moreover, in the context of existing DNA damage, p53 was reported to induce the expression of a ribonucleotide reductase gene *p53R2*, which functions to increase the pool of free dNTPs when DNA repair is required (248).

In addition to the above described indirect role in DNA repair, p53, known as the guardian of the genome (249), is also directly involved in repair of damaged DNA. p53 plays a role at multiple levels of many DNA repair programmes, including MMR and NER.

In NER p53 is involved in DNA damage recognition by activating the transcription of XPC (Xeroderma pigmentosum group C) (250) and XPE/DDB2 (Xeroderma pigmentosum group E/damage-specific DNA binding protein 2) (251). Xeroderma pigmentosum (XP) is an autosomal recessive disorder caused by defects in any of at least 7 genes (XPA to XPG) encoding components of the NER machinery, leading to extreme sensitivity to UV light and high predisposition to skin cancers (8). The transcriptional target of p53, XPC plays an important role in the early steps of global genome NER, especially in damage recognition, and is essential for the recruitment of additional NER factors for the repair complex formation (252, 253), while XPE is required for binding the damaged DNA (251). Following DNA damage recognition and binding, a multi-protein complex is assembled to repair the damage (8).

Following excision of the DNA lesion, DNA polymerase δ and ε are recruited along with their processivity factor PCNA, which is an indispensable component of a number of repair pathways (such as MMR, NER and BER), to fill the gap created by the excised lesion (254). p53 not only induces PCNA expression (255), but also up-regulates two other targets, p21 and GADD45, which interact with PCNA. p21 was reported to have differential effects on PCNA – while it is able to inhibit the function of PCNA in DNA replication, it does not stop the PCNA-dependent NER (256, 257). Similarly, GADD45 was found to stimulate global genomic repair (GGR), which is a subtype of NER, and inhibit entry of cells into S phase (258). Therefore, through transcriptional activation of the above mentioned genes, p53 contributes to NER at multiple levels.

In addition to facilitating NER, p53 has also been implicated in mismatch repair (MMR). p53 induces the expression of human MutS homologue 2 (hMSH2) (259), whose main function is recognition of DNA mismatch, binding to it and stimulating a cascade of reactions leading to DNA repair (260). hMSH2 was also found to interact with PCNA to form an active mismatch repair complex, which facilitates hMSH2 transfer to DNA mismatches (261). By inducing PCNA expression (as described above) p53 also contributes to MMR at another level.

Apart from its functions in promoting DNA repair, p53 has been implicated in the regulation of centrosome replication during mitosis (262). Centrosomes are major microtubule organising centres, which play a role in establishing the two poles of mitotic spindle, formation of the cleavage furrow plane and balanced segregation of chromosomes (263). It was reported that p53-null cells generate multiple copies of functional centrosomes during a single cell cycle (262), which has deleterious effects for mitotic fidelity and leads to unequal segregation of chromosomes between the

daughter cells. However, p53-null mice develop normally but are highly susceptible to spontaneous tumours (264). While wild-type mice did not develop any tumours by the age of 9 months, mice with a homozygous p53 deletion developed obvious cancers by the age of 6 months in 74% of cases. This suggests that p53 is crucial for tumour suppression, as its lack might contribute to chromosomal abnormalities and tumour formation. Therefore, regulating centrosome duplication is yet another mechanism, through which p53 may contribute to maintaining genomic stability.

1.3.2.6. The role of p53 in angiogenesis

As a part of its repertoire of tumour suppressive functions, p53 has also been implicated in suppressing angiogenesis. This is supported by the fact that tumours bearing p53 mutations are more highly vascularized (as measured by the microvessel density) than p53 wild-type tumours (265) and are associated with poor survival (266). This suggests that p53 plays a critical role in controlling tumour vascularization.

p53 inhibits angiogenesis via three main mechanisms: inhibition of systems responsible for sensing hypoxic conditions, down-regulation of pro-angiogenic factors and up-regulation of anti-angiogenic factors (267). By combining these mechanisms p53 is able to efficiently shut down the angiogenic potential of cancer cells.

Angiogenesis is stimulated in response to oxygen deprivation associated with an up-regulation of hypoxia inducible factor (HIF) (268). HIF functions as a heterodimer comprising two subunits, HIF-1α and HIF-1β, and transcriptionally activates expression of the vascular endothelial growth factor (VEGF) in hypoxic conditions resulting in enhanced angiogenesis (269). p53 can directly bind to HIF-1α and

promote its MDM2-mediated ubiquitylation and degradation, resulting in inhibition of angiogenesis (270).

In addition to interfering with the hypoxia-sensing systems, p53 is also able to repress the expression of pro-angiogenic factors, including VEGF (158), basic fibroblast growth factor (bFGF) (159), bFGF-binding protein (bFGF-BP) (271) and cyclooxygenase-2 (COX-2) (160). The mechanisms of transcriptional repression by p53 include: binding of p53 to transcription factor Sp1, hence inhibiting its ability to bind other promoters (VEGF); direct repression of certain promoters (bFGF and bFGF-BP) or competing with the TATA-box binding protein (TBP) for binding to some promoters (COX-2).

Finally, p53 is also involved in transcriptional activation of anti-angiogenic factors, including maspin (272), α(II) collagen prolyl-4-hydroxylase [α(II)PH] (273), thrombospondin-1 (TSP-1) (274) and brain-specific angiogenesis inhibitor 1 (BAI1) (275). Maspin is a member of the serpin family, which inhibits new blood vessel formation, tumour invasion and metastasis (272). α(II)PH catalyses the formation and extracellular release of anti-angiogenic peptides derived from collagen type 4 and 18 (273). TSP-1 inhibits angiogenesis in a number of ways, for example through negative regulation of growth and migration of endothelial cells (276). Finally, BAI1 is cleaved into an anti-angiogenic fragment called vasculostatin, which is secreted into the extracellular matrix (277). Collectively, the expression of the discussed proteins results in the inhibition of angiogenesis through many different pathways. The fact that p53 is involved in angiogenesis suppression at multiple levels suggests that inhibiting this process may be critical for effective tumour suppression.

Angiogenesis is crucial in tumours, especially in those at a late stage of development as they need a constant supply of oxygen and nutrients (278). This stage

is also the time when most p53 mutations in human cancers occur (279, 280). This suggests that loss of p53 and the unrestrained recruitment of new blood vessels provide a critical growth advantage to tumours at a late stage of development.

1.3.2.7. The role of p53 in tumour invasion and metastasis

In addition to the roles of p53 in inhibiting tumour formation (through the induction of cell cycle arrest, apoptosis, senescence and DNA repair, and inhibition of angiogenesis – see sections 1.3.2.1-6), it is becoming clear that p53 also regulates invasiveness of tumours and the process of metastasis (see Figure 1.10).

The main cause of cancer mortality is usually not the primary tumour but distant metastases. In order to obtain metastatic potential cancers cells must be able to detach from the primary tumour, invade the stroma and basement membrane of the blood and lymphatic vessels and finally extravasate to seed a new tumour.

Frequently, one of the first steps of cancer cells on the road to metastasis is undergoing epithelial-mesenchymal transition (EMT). EMT is a process implicated in wound healing, in which epithelial cells at the edge of the wound, normally displaying cell-cell adhesions, undergo a major change in phenotype by losing cell-cell junctions and restructuring of the cytoskeleton to assume a motile mesenchymal-like appearance (110). EMT is transcriptionally regulated by Slug/Snail and Twist proteins, which were reported to down-regulate E-cadherin, involved in stabilising cell-cell junctions, and up-regulate proteins stimulating cell migration (281, 282).

EMT is implicated in the formation of invasive and metastatic tumour cells in the course of tumour progression (283). Since p53 loss has been linked to activation of the EMT programme and high tumour grade, wild-type p53 has been suggested to play a role in EMT suppression through maintaining a transcriptional programme,

which prevents EMT (284, 285). As part of this programme, p53 has been proposed to stimulate MDM2-mediated degradation of Slug, which was associated with up-regulation of E-cadherin and decreased invasiveness of cancer cells (286). However, these finding have been questions by other studies, which reported that MDM2 actually promotes cell motility and invasiveness (287, 288). While MDM2 was suggested to promote ubiquitylation and degradation of E-cadherin (288), a more recent study demonstrated that the MDM2-mediated increase in motility and invasiveness of cells is independent of its E3 ubiquitin ligase activity, since a RING-finger MDM2 mutant (lacking the E3 ubiquitin ligase activity) was also able to promote motility and invasion (287). Altogether these data suggest that p53-dependent down-regulation of Slug likely occurs through a different mechanism than MDM2-mediated degradation of Slug.

An alternative pathway could involve p53-mediated up-regulation of miRNA-192 and miRNA-200 family members, which suppresses EMT (284, 289). These miRNAs have been found to inhibit transcriptional repressors of E-cadherin (ZEB1/2), which is considered to be an epithelial cell marker (as discussed above) (284, 289). p53 knock-down in MCF12A cells resulted in a conversion of the epithelial phenotype to an EMT phenotype, which correlated with down-regulation of E-cadherin and up-regulation of mesenchymal cell markers, such as Vimentin or ZEB1 (284). These observations provide an insight into how p53 could be involved in inhibiting the invasive potential of tumours.

Upon acquiring the ability to detach from the primary tumour, the cancer cells must gain the ability to invade and migrate through the stroma. They achieve this by remodelling of the actin cytoskeleton and changing their morphology. In order to be able to migrate, a cell needs to become polarized before forming actin-containing

protrusions for recognition and binding to the ECM. Invasive cancer cells may generate cell protrusions called invadopodia, which trigger degradation of the surrounding ECM (290). Functionally similar structures formed by macrophages and oncogene-transformed fibroblasts are known as podosomes (291). p53 has recently been reported to suppress invadopodia formation through transcriptional activation of Caldesmon expression (292). Caldesmon is an actin-binding protein shown to inhibit the formation of podosome/invadopodium structures (293). Moreover, p53 has been shown to regulate a number of microRNAs (miRNAs), including miRNA-143 and miRNA-145 (co-expressed from a single promoter), which inhibit podosome formation (294). Another piece of evidence linking p53 to the invasiveness of cancer cells is the fact that p53-null cells display altered morphology and increased migratory potential (295). A number of p53-regulated genes are implicated in cell shape and motility, including fibronectin (296), keratin, collagens and macrophage-stimulating protein (Msp) (164) as well as smooth muscle α-actin (297).

Interestingly, in addition to transcriptional regulation of cytoskeletal and ECM components, p53 has also been suggested to influence signalling pathways regulating cell migration. The most important signalling pathway controlling actin polymerization (reorganization) and adhesion involves the Rho family of small GTPases, which includes Cdc42, Rac and Rho (298).

Cdc42 controls cell polarity and triggers formation of filopodia (microspikes) involved in sensing the extracellular environment and providing spatial information to the cell to direct movement (298). In contrast to active invasion by cancer cells through promotion of ECM degradation, it has been shown using intravital imaging that invasive squamous cell carcinoma cells may also collectively follow tracks in the ECM created by other motile cells (such as fibroblasts), which is known as collective

invasion (299). Such SCC cells retain epithelial markers (such as E-cadherin), are unable to remodel ECM and rely on mesenchymal cells (such as stromal fibroblasts) to promote tumour progression (299). This also emphasizes the great influence that the tumour microenvironment might have on tumour invasion and metastasis. Importantly, the process of collective invasion in the fibroblast-following squamous carcinoma cells was found to depend on Cdc42 and its effector kinases MRCK and knock-down of either of the molecules inhibited the invasion of cancer cells in this system (299).

Another member of the Rho GTPase family, Rac, promotes formation of lamellipodia, large membrane protrusions at the leading edge of migrating cells, associated with elongated cell motility (300). Finally, RhoA and RhoC, acting through their effector Rho kinases (ROCKs), are responsible for regulating the formation of focal adhesions and actin stress fibres (301), generating a mode of motility resembling amoeboid movement (302). Rho GTPases are active in their GTP-bound state and are inactivated by GTP hydrolysis (303). Their activity is regulated by GEFs (guanine nucleotide exchange factors), which activate them, and GAPs (GTPase activating proteins), which turn them off (304). p53 has been suggested to modulate the activity of Rac by transactivation of the PTEN gene (305). The tumour suppressor PTEN is a lipid phosphatase, that dephosphorylates and down-regulates the levels of phosphatidylinositol 3,4,5-trisphosphate (PIP_3) (306), which is an important messenger of cell growth signalling, activating the Akt survival pathway (307). PIP3 is also necessary for GEF-mediated Rac and Cdc42 activation (308). Therefore, by inducing PTEN, p53 inhibits Rac activation and contributes to suppression of Rac-mediated invasiveness and metastatic potential of cancer cells (309). In addition to its role in the regulation of Rac activity, p53 has also been suggested to influence

the processes mediated by the other members of the Rho GTPase family. p53 was found to prevent actin cytoskeleton reorganization and the initiating step of filopodia formation, cell spreading and polarization (310), induced by active Cdc42 and necessary for efficient migration.

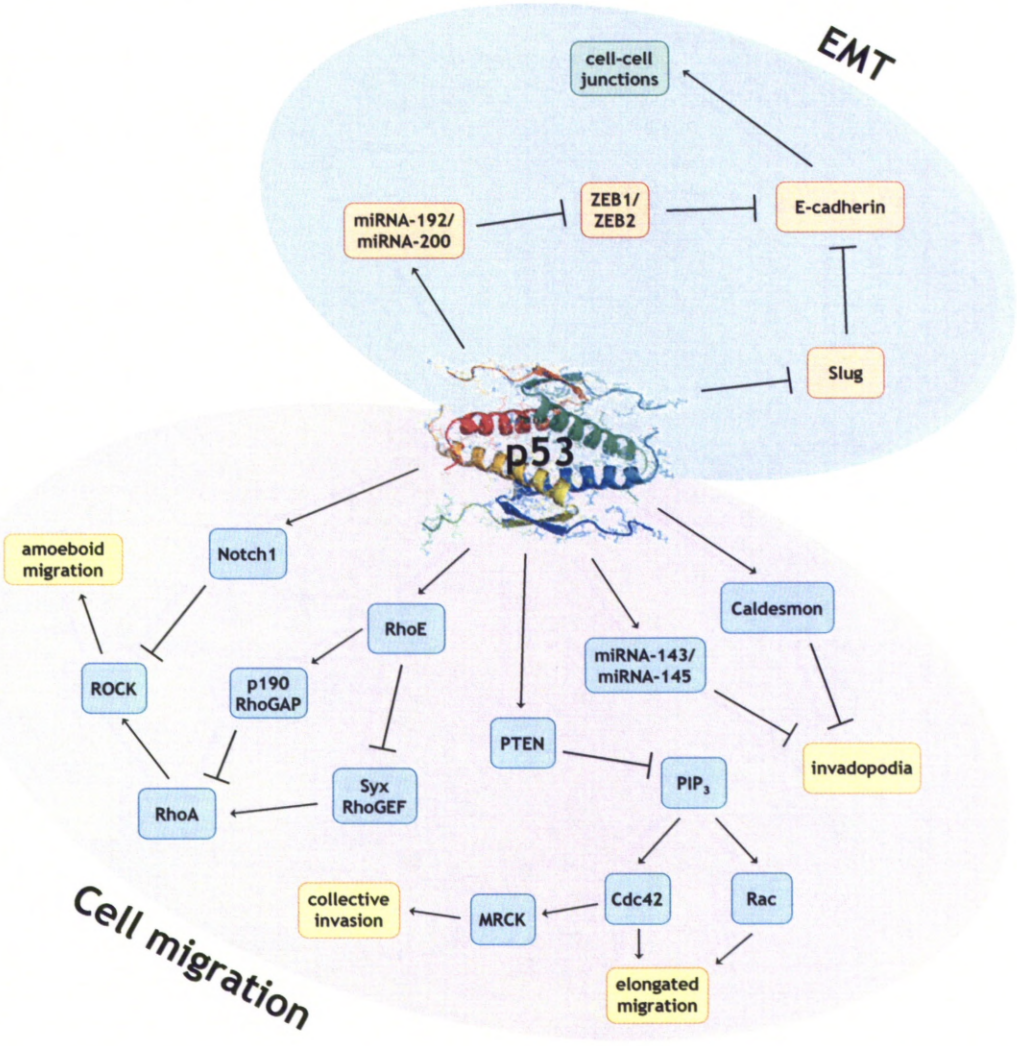

Figure 1.10: Functional connections between p53 and regulation of EMT and cell migration. p53 may oppose EMT by inhibiting Slug and transcriptional activation of miRNA-192/200, resulting in up-regulation of E-cadherin (an epithelial marker). p53 is also implicated in the inhibition of invasive migration. p53 may oppose: invadopodia formation through Caldesmon or miRNA-143/145 up-regulation; elongated migration through transactivation of PTEN; collective invasion through inhibition of Cdc42 and amoeboid migration through Notch1 and RhoE induction. Figure adapted from reference (311).

Finally, p53 loss was reported to be associated with increased RhoA (and consequently ROCK) activity and contributed to increased invasiveness (312). RhoA stimulates contractility, which favours rounded amoeboid movement (302). While this mode of motility is difficult to reconcile with the process of EMT in tumour progression, it has been shown that many cancer cells migrate in this way *in vivo* (313), especially during collective migration through fibroblast-created channels (299). p53 may suppress ROCK activation via transcriptional activation of Notch1, which down-modulates Rho effectors (314). Moreover, RhoE, which interferes with RhoA activation, is a transcriptional target of p53 (315). RhoE is believed to achieve its inhibition of RhoA through suppression of a GEF for RhoA (Syx) activating RhoA (316) and activation of p190 RhoGAP, which inactivates RhoA (317).

All these observations provide evidence for the functional connections between p53 and cytoskeletal and ECM components as well as signalling pathways involved in controlling cell morphology and migration, and suggest mechanisms through which p53 loss could promote invasiveness and metastatic potential of cancer cells.

1.3.3. Regulation of the p53 pathway

Since p53 regulates such a large number of cellular processes and is a potent inhibitor of cell growth, its activity has to be tightly regulated during development and normal growth (225). This is accomplished through a number of mechanisms including regulation of protein stability, subcellular localization and transcriptional activity of p53 (318). Under normal conditions p53, which has as short half-life (approximately 20 min.), is kept at low, often undetectable levels (mostly due to the function of its negative regulator MDM2) (319, 320). In response to many types of cellular stress,

p53 is stabilised and activated through post-translational modifications (summarised in Figure 1.12).

1.3.3.1. Regulation of p53 protein stability

Two critical proteins involved in regulation of p53 are MDM2 (murine double minute 2) and MDMX (321). The importance of the MDM2-p53 and MDMX-p53 interaction is best demonstrated by *in vivo* studies, in which lack of MDM2 or MDMX is lethal to mice at early embryonic stages even before implantation (322, 323). These phenotypes are rescued completely by accompanying deletion of p53, indicating that unrestrained p53 activity is lethal to mouse embryos (324) and that MDM2 and MDMX play non-redundant roles in regulating p53 activity (321).

MDM2 can inhibit the transcriptional activity of p53 and promote its degradation. MDM2 is a RING-finger E3 ubiquitin ligase targeting p53 for ubiquitylation and proteasomal degradation (325, 326). MDM2 binds to p53 and monoubiquitylates it at multiple lysine residues (327) and other proteins, such as p300/CBP, cooperate with MDM2 in the polyubiquitylation and degradation of p53 (328, 329).

The function of MDMX in regulating p53 stability is less clear. MDMX, a homologue of MDM2, lacks the robust E3 ubiquitin ligase activity but has been suggested to regulate p53 stability indirectly (discussed in more detail below) (330).

p53 and MDM2 form an auto-regulatory feedback loop (Figure 1.11) (331). p53 stimulates the expression of MDM2 by binding the *MDM2* P2 promoter (332). Since MDM2 inhibits p53 function, a negative feedback loop is created, which tightly regulates p53 activity (Figure 1.11). Low p53 activity, in turn, results in decreased steady state levels of MDM2. To ensure that MDM2 is not present in excessive

amounts, it can also ubiquitylate and target itself for degradation (333), which titrates the levels of both p53 and MDM2.

However, the E3 ubiquitin ligase activity of MDM2 towards itself and p53 also has to be regulated to facilitate efficient degradation of p53 without concomitant depletion of MDM2 in unstressed cells. This may be achieved through regulation by MDMX, which might facilitate ubiquitylation of p53 through stabilisation of MDM2 and inhibition of MDM2 autoubiquitylation by modifying substrate preference of the MDM2 ubiquitin ligase activity (330). Another protein implicated in the regulation of the MDM2 E3 ligase activity is MTBP (MDM2-binding protein), which promotes ubiquitylation and degradation of p53 while reducing autoubiquitylation and hence stabilising MDM2 (334).

In normal cells the p53 levels are kept low and p53 becomes up-regulated and activated in stressed or damaged cells (134). This is an inbuilt defence mechanism against cancer since such cells are more likely to carry mutations or have abnormal cell cycle control and hence be dangerous to the organism.

In order to perform its tumour suppressor functions, p53 has to be stabilised and this involves inhibition of p53 degradation by MDM2. The p53 network can be activated by a number of independent mechanisms (Figure 1.11). One of the pathways to be considered here is triggered by DNA damage. The activation of the p53 network in response to double-strand DNA breaks (induced by ionising radiation or some chemotherapeutic drugs) depends on two protein kinases – ATM (ataxia telangiectasia mutated) and checkpoint kinase Chk2. Double-strand DNA breakes activate ATM kinase, which in turn activates Chk2 (335). They further stabilise p53 by phosphorylating it on serines 15 and 20, respectively (336, 337, 338, 339). These modifications interfere with MDM2 binding, thus preventing p53 ubiquitylation and

degradation (340). UV-induced DNA damage (such as pyrimidine dimers) or hypoxia, on the other hand, result in the activation of ATR (ataxia telangiectasia related) kinase, which phosphorylates p53 at serines 15, 37 and 392 (341, 342) and Chk1, which can also phosphorylate p53 at serine 20 (343). These modifications alleviate the effects of p53 inhibition by MDM2 (344).

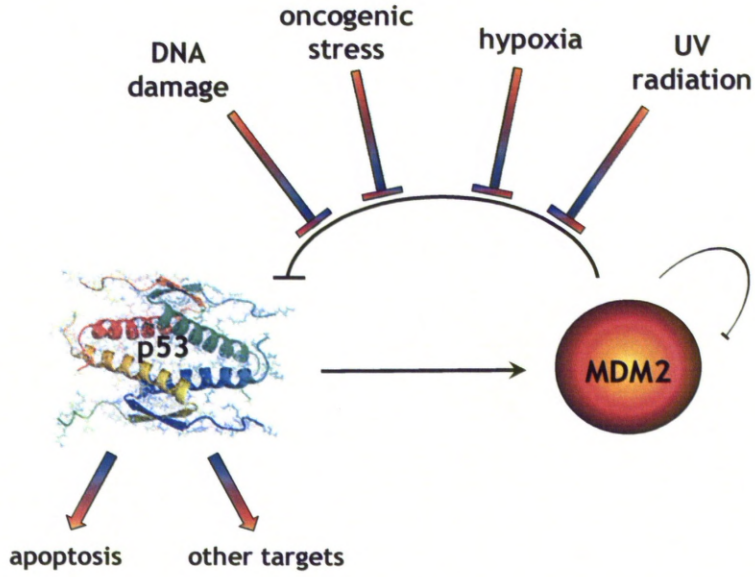

Figure 1.11: p53-MDM2 auto-regulatory feedback loop. MDM2 is a transcriptional target of p53. A rise in the level of p53 results in increased MDM2 production and enhanced degradation of both proteins. Therefore, in normal cells the levels of both p53 and MDM2 are kept low. A number of cellular stresses, such as DNA damage or oncogenic signalling, involve inhibition of p53 degradation by MDM2, leading to the stabilisation and activation of p53, which can then function as a transcriptional regulator to control the expression of its target genes.

Another pathway is induced by aberrant growth signals, which can be the result of the expression of oncogenes, such as Ras or Myc (134). This leads to $p14^{ARF}$ expression, which binds to MDM2 and prevents MDM2-mediated inhibition of p53, (345). The exact mechanism, through which $p14^{ARF}$ inhibits MDM2 is not entirely clear and may be tissue-specific. $p14^{ARF}$, which is mostly a nucleolar protein, was

suggested to relocalise MDM2 to the nucleolus (241, 346, 347). In addition, $p14^{ARF}$ was also reported to block the ubiquitin ligase activity of MDM2 (345) and interfere with the nucleoplasm-cytoplasm shuttling ability of MDM2 (347). Consequently, $p14^{ARF}$-dependent inhibition of MDM2 results in p53 stabilisation and activation.

A summary of the processes and molecules involved in the regulation of p53 stability and activity is presented in Figure 1.12.

1.3.3.2. Regulation of p53 activity

In addition to modulation of p53 protein stability, transcriptional activity of p53 can also be regulated. MDM2 for instance, apart from promoting p53 degradation, binds to the N-terminal transcriptional activation domain of p53 and prevents binding of the components of the transcription machinery, hence suppressing the activity of p53 as a transcriptional regulator (348). Moreover, MDM2 has also been suggested to inhibit p53 acetylation (see below), thus preventing its activation (349). Similarly, MDMX was also reported to inhibit p53 activity (350) in a manner independent of MDM2, since MDM2 cannot compensate for MDMX loss *in vivo* (351). While the mechanistic details of the MDMX-mediated regulation of p53 activity still remain unclear, it has been suggested that MDMX (similarly to MDM2) may inhibit the acetylation of p53 by p300/CBP (see below), thus preventing its activation (352).

On the other hand, a number of post-translational modifications of p53, such as the addition or removal of acetyl, phosphoryl or ribosyl chemical groups as well as ubiquitin or 'SUMO' modification, which result in a conformational change of the protein, have been suggested to enhance the sequence-specific DNA binding and transcriptional activities of p53 in response to stress (353). In the unmodified protein the C-terminus usually folds back inhibiting the DNA binding domain situated in the central core of p53. It has been suggested that acetylation or phosphorylation of p53

near the C-terminus can interfere with this folding, hence enhancing the DNA binding capacity of p53 (354). Therefore, the C-terminus has been shown to allosterically regulate the conversion of p53 between the latent and active forms (355).

For example, casein kinase II, responsible for phosphorylating p53 at serine 389 (356), activates sequence-specific DNA binding (357) and transcriptional activity of p53 (358). Histone acetyltransferases, including p300/CBP and PCAF, by acetylating lysines in the C-terminal domain of p53 (359) also stimulate the classical conformational change of p53 (seen also after other post-translational modifications of the C-terminus), thus enhancing its DNA binding capacity. Interestingly, p300/CBP are also involved in destabilisation of p53 by cooperating with MDM2 in its polyubiquitylation (see section 1.3.3.1). These seemingly contradictory functions were reported to be achieved through compartmentalisation of p300/CBP (328), with cytoplasmic ubiquitylation and nuclear acetylation of p53. However, the fact that MDM2-mediated degradation can occur both in the nucleus and in the cytoplasm (360) suggests that other factors (such as other interacting partners) may also be important in regulating the p300/CBP activity towards p53.

The efficiency of p53 acetylation by p300/CBP can also be modulated by other proteins. PML for instance, mentioned previously in the context of senescence (see section 1.3.2.4), has been reported to recruit p53 to a subset of PML nuclear bodies and to facilitate p300/CBP-mediated acetylation (243) and Chk-2-mediated phosphorylation of p53 (361) hence leading to its activation. In addition, $p14^{ARF}$, described previously to sequester MDM2 hence protecting p53 from degradation (see section 1.3.3.1), can also contribute to p53 activation by regulating its acetylation (as MDM2 can no longer inhibit p53 acetylation) (349).

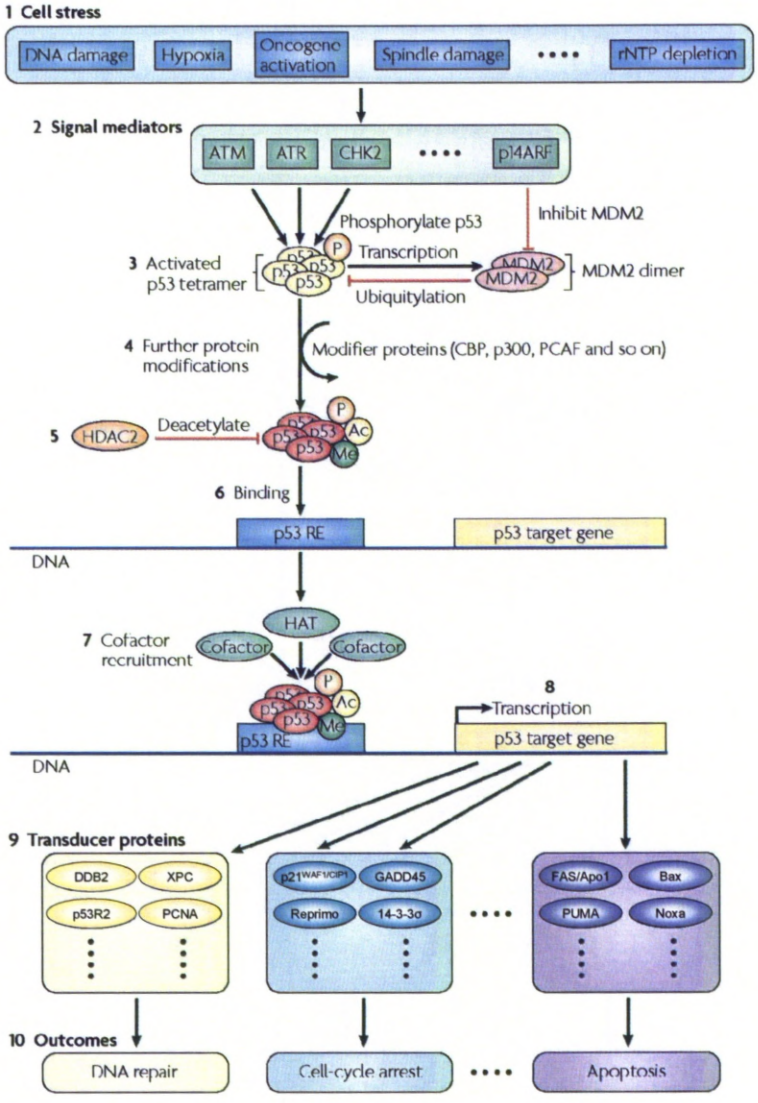

Figure 1.12: A summary of p53 stabilisation, activation and regulation of downstream target genes (adapted from reference (157)). 1) Cells are subjected to one of a number of cellular stresses. 2) Signal mediator proteins are up-regulated/activated and stabilise p53 by inhibiting its interaction with MDM2 – either through direct suppression of MDM2 or through p53 phosphorylation. 3) Ubiquitylation and degradation of p53 is inhibited and p53 levels rise. 4) Additional proteins can also modify p53 (by acetylation or methylation), leading to further stabilization and enhanced sequence-specific DNA binding of p53. 5) DNA binding can also be hindered by proteins removing those modifications (like HDAC). 6) An active p53 tetramer binds to a p53 response element (RE) and 7) recruits cofactors (including TAFs) to regulate transcription of the nearby gene. 8) p53 activates transcription (as shown here) or represses expression of its target gene. 9) p53 up-regulates a number of transducer proteins, 10) which are involved in numerous pathways important in tumour suppression, including DNA repair, cell-cycle arrest, apoptosis, senescence and many others.

p53 deacetylation, on the other hand, either through inhibition of histone acetyltransferases by MDM2 (362) or direct interaction of p53 with the histone deacetylase 1 (HDAC1)-containing complex (363), inhibits p53 transcriptional activity.

p53 acts as a transcription factor and this role is crucial for its tumour suppressor functions. In cancer the DNA binding and transcriptional activity of p53 is frequently compromised due to missense mutations, which distort the folding of the core domain. It has been observed that conformational changes caused by posttranslational modifications can also be induced with the help of short peptides, antibodies or drugs interacting with the C-terminus of p53 (364), which might be a way of reactivating mutant p53 and restoring its normal function.

1.3.3.3. Regulation of subcellular localization of p53

The transcriptional activity of p53 relies on its nuclear localization (365). Since p53 is a potent inhibitor of cell growth, the activity and hence nuclear import and export of p53 have to be tightly regulated.

The nuclear import of p53 is enabled by the three nuclear localization signals (NLSs) within the C-terminal domain of p53 (Figure 1.7), which target it for transport into the nuclear compartment and allow efficient nuclear import (366). In order to be transported into the nucleus by the import machinery, p53 has to be present in the vicinity of the nucleus. It has been reported that p53 is actively transported through the cytoplasm towards the nucleus along the microtubule network by dynein, a minus-end-directed microtubule-associated motor protein (367).

p53 also possesses a nuclear export signal (NES), located in the tetramerization domain (Figure 1.7) (368). Following nuclear import, p53 undergoes tetramerization

and can perform its functions as a transcription factor (155). It has been proposed that p53 tetramerization conceals its NES, hence contributing to the nuclear retention of the fully functional protein (368). Ubiquitylation of p53 by MDM2, on the other hand, could expose the NES by affecting p53 tetramerization (369), resulting in export of p53 into the cytoplasm for ubiquitin-mediated proteolysis by the proteasome (Figure 1.13). While the NES of p53 was shown to be both necessary and sufficient for nuclear export (368), more recent studies have suggested that the ubiquitylation of p53 within its C-terminal domain by MDM2 is critical for nuclear export of p53 (370, 371).

In a number of tumour types harbouring wild-type p53, including some neuroblastomas and breast cancers, loss of p53 function is suggested to be due to cytoplasmic sequestration of the protein (372, 373). The mechanisms involved in the cytoplasmic accumulation of p53 are far from clear. It has been suggested that wild-type p53 might be shuttled into the cytoplasm due to hyperactive nuclear export (374). It has also been reported that wild-type p53 might accumulate in the cytoplasm due to the cytoplasmic anchorage mediated by interaction of p53 with parkin-like ubiquitin ligase (PARC) or with the glucocorticoid receptor (GR) (375). Treatment of neuroblastoma cells with GR inhibitors resulted in the dissociation of the p53-GR complex, redistribution of both proteins into the nucleus and restoration of p53 functions (375). Therefore, the use of drugs disrupting the GR-p53 interaction might have a significant therapeutic potential in certain types of cancer displaying cytoplasmic p53 sequestration.

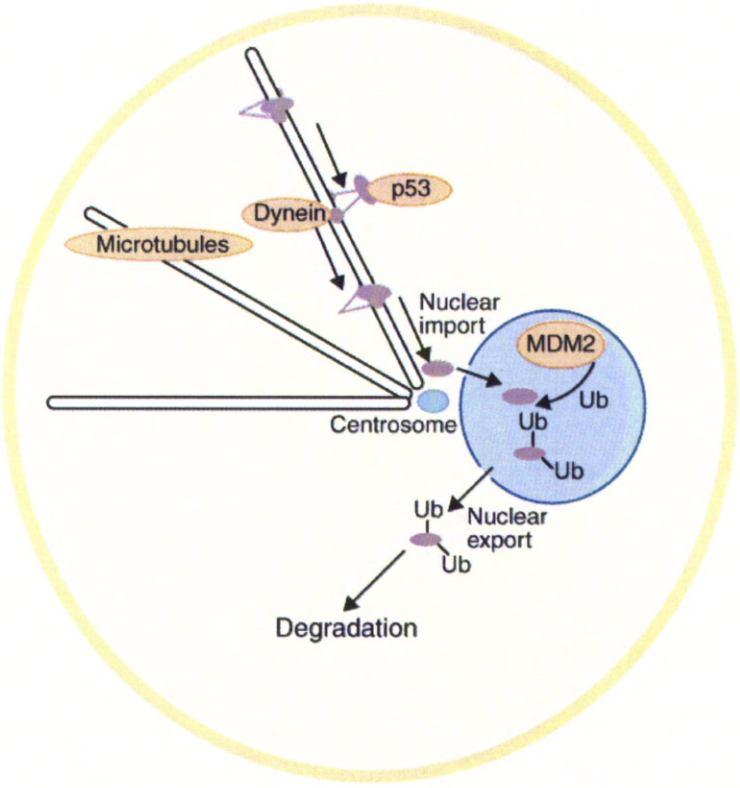

Figure 1.13: Intracellular transport of p53. p53 associates with microtubules and is actively transported towards the nucleus with the help of a motor protein, dynein. Import receptors located in the nuclear envelope recognise the NLS of p53. Export of p53 into the cytoplasm occurs most likely upon p53 ubiquitylation by MDM2, which reveals the NES of p53. Figure reproduced from reference (365).

1.3.4. Loss of p53 function in cancer

The most common alteration found in human cancers is inactivation of the p53 tumour suppressor pathway, which can happen via a number of mechanisms, including altered subcellular localization of the p53 protein, defects preventing p53 activation, mutations or deletions of the *TP53* gene itself or lesions in the signalling pathways downstream of p53 (376).

Loss of p53 function increases cancer risk. Li-Fraumeni syndrome patients, carrying germline p53 mutations, have increased susceptibility to various types of cancer (166) and p53-null mice are highly tumour-prone (264). Somatic *TP53*

mutations are found in ~50% of human cancers (107). The vast majority of p53 alterations are missense mutations resulting in the production of a full-length protein with single amino acid substitutions, which accumulates in the nucleus of cancer cell (377). Theoretically, based on the frequency of STOP codons in the codon table (3 out of 64), missense mutations are more likely to occur than nonsense mutations. This hypothesis is confirmed by a large-scale mutational analysis of genomes of colorectal and breast cancers (sequencing of 13,000 genes in a total of 22 tumours, without a preference for oncogenes or tumour suppressors) (378). The overall frequency of missense mutations was 81%, while nonsense, splice mutations and deletions/insertions (frame-shift mutations) comprised 7%, 4% and 8% of all mutations, respectively (378). This spectrum is strikingly similar to the mutational spectrum of p53 in human cancer with missense mutations representing 74%, nonsense mutations 8% and frame-shift mutations 9% of all p53 mutations (139). This also suggests that the mutational spectrum of p53 reflects a general mutagenesis mechanism.

In contrast, the mutational spectra of other tumour suppressors like Rb or APC are significantly different and comprise primarily deletions, nonsense or frameshift mutations (Figure 1.14), resulting in the production of a truncated protein or no protein expression at all (107). This suggests that loss of protein expression is the most efficient mechanism to inactivate the functions of these tumour suppressors in a developing tumour. However, most of the tumour suppressor genes are believed to be recessive and inactivation of one allele is not sufficient for tumour development. According to Knudson's two-hit hypothesis both functional copies of a tumour suppressor gene need to be lost to initiate a cancer (379). This loss of the second allele, known as the loss of heterozygosity (LOH), may occur through deletion of part

or the entire chromosome carrying the tumour suppressor gene, gene conversion, mitotic recombination or a second inactivating mutation (110).

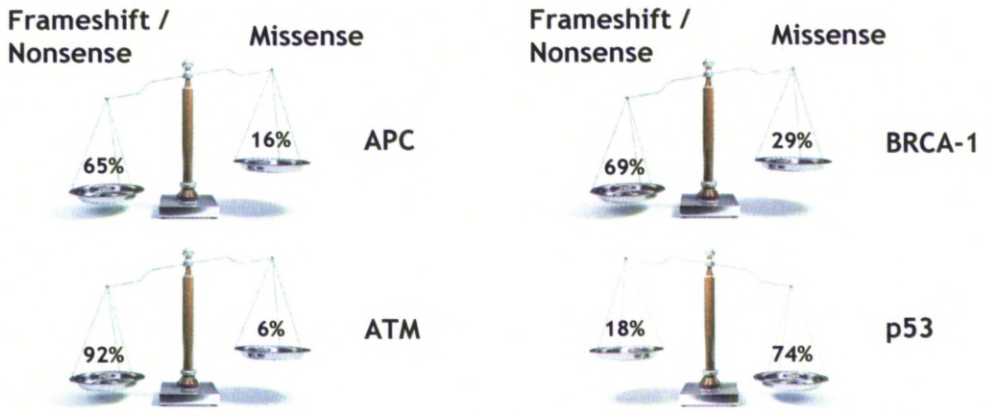

Figure 1.14: Mutation types in tumour suppressor genes (data adapted from reference (380)). While the predominant mutation types in many other tumour suppressor genes are nonsense or frameshift, the majority of p53 mutations are missense. This suggests that there is a selective advantage of the mutant p53 protein over the truncation.

The fact that mutation in only one copy of p53 results in tumour development (as demonstrated by mice heterozygous for mutant p53 (6)) suggests that the p53 tumour suppressor gene does not strictly follow the Knudson's model (see section 1.3.4.1). The majority of tumour-derived p53 mutations (more than 95%) cluster in the central DNA binding domain of the protein (see section 1.3.4.2) and most of them result in the loss of wild-type p53 transcriptional activity (381), suggesting that it is the loss of p53 function that leads to cancer development. Moreover, the fact that missense mutations are significantly more common than nonsense mutations suggests that there is a selective advantage of the mutant protein over the truncation. This apparent selection bias might be explained by the fact that p53 functions as a tetramer. The presence of nonsense mutation in one of *TP53* alleles would potentially result in no protein expression or expression of a truncated protein, most likely lacking the

C-terminal tetramerization domain. However, wild-type p53 expressed from the second allele could retain its transcriptional activity and suppress tumour formation. On the other hand, DNA binding domain missense p53 mutants, lacking wild-type p53 transcriptional activity, might oligomerize with the remaining wild-type p53 and abrogate its function (as discussed below in section 1.3.4.1).

1.3.4.1. Dominant negativity of p53 mutants

Due to the fact that p53 functions as a tetramer, hetero-oligomerisation between mutant and wild-type forms of p53 may have a dominant-negative effect, which neutralises the wild-type protein (382). Specifically, p53 mutants were reported to inhibit the sequence-specific DNA binding of wild-type p53 and transactivation of its target genes (383), explaining why such mutations could be preferentially selected in a developing tumour. Indeed, mice heterozygous for a dominant-negative p53 mutant develop tumours (382) indicating that the inhibition of the wild-type p53 by the mutant might give some selective advantage in tumour progression.

Since this hetero-oligomerisation underlies the mutant p53 transdominant suppression, it is not surprising that the DBD mutants have the tetramerization domain fully functional (384). It has also been suggested that in these complexes mutant p53 is capable of shifting the wild-type p53 into a mutant conformation (385).

However, frequent loss of heterozygosity (LOH) in cancers harbouring *TP53* mutations (eliminating the wild-type allele) (386) suggests that the dominant-negative effects of the mutants might not lead to complete loss of p53 function. In this respect p53 also partly complies with the Knudson's two-hit model of tumorigenesis (see section 1.3.4).

1.3.4.2. Types of p53 mutations

Some *TP53* codons have a high frequency of mutation, with more than 40% of all mutations found at only six p53 residues – 175, 245, 248, 249, 273 and 282 (139), the so-called mutational hot-spots (Figure 1.15). These residues are located in the conserved regions within the DNA-binding domain of p53 and are critical for the structural integrity and sequence-specific DNA binding of the protein (147).

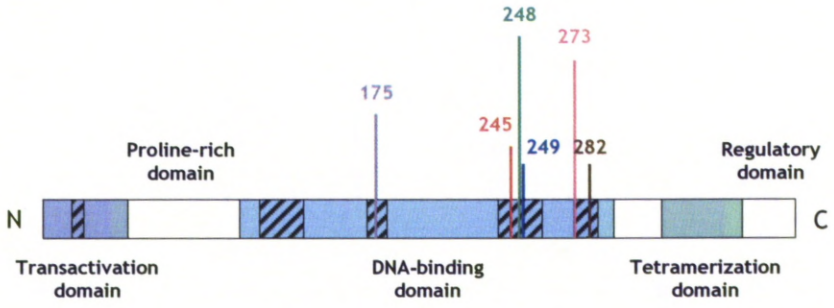

Figure 1.15: Mutational hot-spots in the p53 tumour suppressor gene (data adapted from reference (139)). The majority of p53 mutations are found in the DNA binding domain of the protein with six mutational hot-spots at residues 175, 245, 248, 249, 273 and 282.

It is now commonly recognised that different DBD mutants of p53 display varying oncogenic potency (387). Determination of the crystal structure of the core domain of p53 revealed that p53 mutations can be divided into two main classes: contact and structural (147).

The contact mutations affect residues that make direct contact with DNA. Hence, they occur on the L3 loop or the nearby loop-sheet-helix (L1 loop-S2-S2' sheet-H2 helix) motif of p53 (Figure 1.16) (147). The two most common contact mutations are found at residues R248 and R273, with frequencies of 8% and 7.5%, respectively (139).

The structural mutations, on the other hand, disrupt the folding of the p53 protein. They occur at residues R175 (5.5%), G245 (3.5%), R249 (3%) and R282 (3%) (139).

The R175 residue is located on the L2 loop near the Zn^{2+} binding site (Figure 1.16), which is buried away from the surface of the protein (147). The R249 residue is located on the L3 loop and makes multiple contacts via van der Waals forces, hydrogen bonds and salt bridges with the surrounding residues on the L2 and L3 loops (147). The residue R282 located on the H2 helix is crucial for maintaining the structure of the loop-sheet-helix motif as it is involved in the packing of the H2 helix against the S2-S2' hairpin and the L1 loop (147). It is important to note that all these three mutations occur at arginine residues. These residues are structurally important because arginines fully utilize the potential of their guanidinium groups to form hydrogen bonds with the carbonyl groups of the polypeptide backbone and hence are critical for stabilizing the structure of the DNA binding core domain. Finally, the G245 residue located on the L3 loop is the only non-arginine residue being a mutational hot-spot (147). This residue appears to be critical because of its small size, which allows the L3 loop to adopt a conformation not favoured by residues with a side chain (147). Moreover, due to the tight packing, any residue with a side chain would lead to the disruption of the L2 loop, which is located in close proximity to G245 (147). Therefore, mutations at any of the above mentioned residues disrupt the stable folding of the core domain of p53 and such mutants are generally unfolded. This is supported by several lines of evidence. First of all, the structural mutants associate with the heat shock protein HSC70 (388), suggesting that they are denatured or misfolded. Secondly, they are recognised by the PAb240 monoclonal antibody, which is specific for unfolded p53, but not the PAb1620 antibody specific for the native p53 conformation (389). Finally, the structural mutants, unlike wild-type p53, are highly sensitive to proteases, suggesting that their core domains are unfolded and exposed (146).

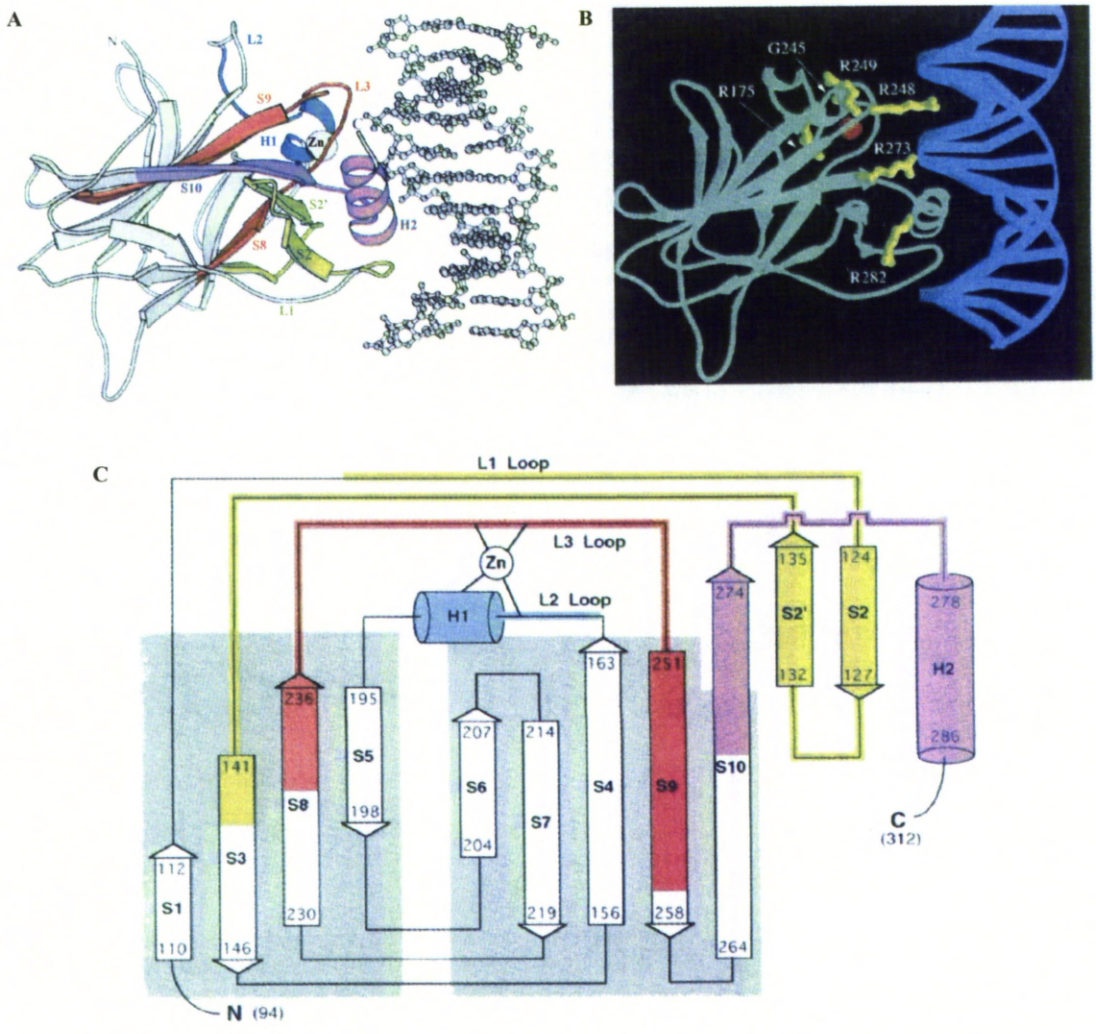

Figure 1.16: Structure of the core domain of p53 (reproduced from reference (147)).

A. Schematic representation of the core domain-DNA complex. The β-strands (S), α-helices (H), loops (L) and the zinc atom (Zn) are shown. The conserved regions are shown in yellow, blue, red and fuchsia. The loop L3 and the loop-sheet-helix (consisting of loop L1, β-sheet comprising the S2-S2' hairpin and the terminus of β-strand S10, and α-helix H2) are responsible for contacting DNA in the minor and major groove, respectively.

B. Ribbon representation of the core domain-DNA complex showing the six most frequently mutated residues of p53 (yellow). The core domain is coloured green, the DNA – blue and the zinc atom is depicted as a red sphere.

C. Topological diagram of the secondary structures of the core domain. The residue numbers at the beginning and end of each structure are shown. The conserved regions are coloured as in A. The shaded areas correspond to the two β-sheets that make up the β-sandwich.

In contrast, contact mutants of p53 display none of the above properties. They do not bind HSC70 (388), they yield a stable core domain (similarly to wild-type p53) upon proteolytic cleavage (146) and are usually recognised by the native conformation specific antibody PAb1620 (389).

In spite of these differences, both the structural and contact mutations of p53 result in the loss of sequence-specific DNA binding of this protein (390, 391). However, they have been suggested to have different oncogenic potency with the structural mutations being more tumorigenic (387). It can be speculated that this is due to the fact that structural mutants can shift the remaining wild-type p53 into a mutant conformation upon hetero-oligomerisation (392), resulting in complete loss of p53 function while the contact mutants might retain native conformation and therefore when incorporated into tetramers with wild-type p53, they may retain some residual wild-type activity (393). It might therefore be expected that in a developing tumour the structural mutations would be preferentially selected compared to the contact mutations. Clearly, this is not the case as residues R273 and R248 are the two most common mutational hot-spots of p53 (139). This seemingly unexpected observation can probably be explained by the fact that in carcinogenesis, which is a multistep process, the lower oncogenicity of the contact mutants will result in a number of subsequent tumorigenic steps. For example, it was reported that in SCCHN expression of the contact p53 mutants (in 13 patients) was associated with 100% LOH, while expression of the structural mutants (in 24 patients) was associated with LOH in only 50% of cases ($p = 0.0034$) (394). This finding is in line with the structural mutants exerting a stronger dominant-negative effect on wild-type p53 (392), hence decreasing the selective pressure for losing the wild-type allele. Nevertheless, SCCHN carrying the contact mutations were associated with higher

tumour stages, increase in lymph node metastasis and shorter recurrence-free and overall survival, than tumours expressing the structural mutations (394). This suggests that dominant-negative inhibition of the wild-type allele by the mutant is not complete and LOH remains an important event during tumorigenesis. This conclusion is consistent with studies of mouse models of Li-Fraumeni syndrome, where mice hemizygous for the mutant p53 allele ($p53^{R270H/-}$ or $p53^{R172H/-}$) had a much shorter overall survival (8 vs. 24 months) than mutant p53-heterozygous mice ($p53^{R270H/+}$ or $p53^{R172H/+}$) (6). Note that the structural R172H mutation in mice corresponds to the R175H mutation in human p53, while the contact R270H mutation in mice is equivalent to the R273H mutation in humans.

1.3.4.3. Oncogenic gain of function of mutant p53

Apart from the dominant-negative effects on the wild-type protein, some p53 mutants have been suggested to acquire oncogenic properties contributing to accelerated cell growth and tumorigenic potential (395). The fact that the majority of p53 mutations are missense indicates that there is a selective advantage of a mutated protein over the truncation in cancer cells. The first idea that mutant p53 might not be just an inactivated tumour suppressor came from a study showing that point mutations in wild-type *TP53* activate it for cellular transformation in cooperation with the *RAS* oncogene (320). The term 'oncogenic gain of function' (GOF) of p53 mutants was first suggested in 1990 when different mutant forms of p53 were reported to gain transforming potential (396). Moreover, p53 mutants were also suggested to enhance metastatic potential and tissue invasiveness (397), hinder differentiation (398) and induce gene amplification (399). However, convincing evidence for the gain of function of mutant p53 was only provided by more recent studies of two mouse

models of Li-Fraumeni syndrome (5, 6). These studies focused on two p53 mutants containing missense mutations, which result in single amino acid (arginine to histidine) substitutions at positions 172 and 270. These mutations in the murine *Tp53* correspond to R175H and R273H mutations in the human gene, respectively. These mutants represent two mutational classes: the R175H mutation is a structural mutation causing a significant conformational shift of p53, while the R273H mutation belongs to the class of contact mutations affecting the p53 residues that make direct contact with DNA (discussed in detail in section 1.3.4.2) and leading to a loss of p53-specific DNA binding (147). Although the two p53 mutations did not affect overall survival (Figure 1.17A), mice heterozygous for the mutant p53 ($p53^{M/+}$) developed different tumour spectra than mice hemizygous for wild-type p53 ($p53^{+/-}$). Moreover, mice hemizygous for the mutant p53 allele ($p53^{M/-}$) developed novel tumours compared to p53-null ($p53^{-/-}$) mice suggesting that these two p53 mutants play a role in stimulating tumorigenesis (Figure 1.17B).

In human cancer, mutations in the conserved regions of p53 have been associated with high tumour grade, worse prognosis (400) and tumour resistance to treatment (401, 402). Various p53 mutants have been suggested to confer resistance to apoptosis in response to a number of agents used in cancer therapy including etoposide and cisplatin (393), 5-fluorouracil (403), UV and ionising radiation (404). Moreover, the strength of these effects has been found to vary between different p53 mutants (393).

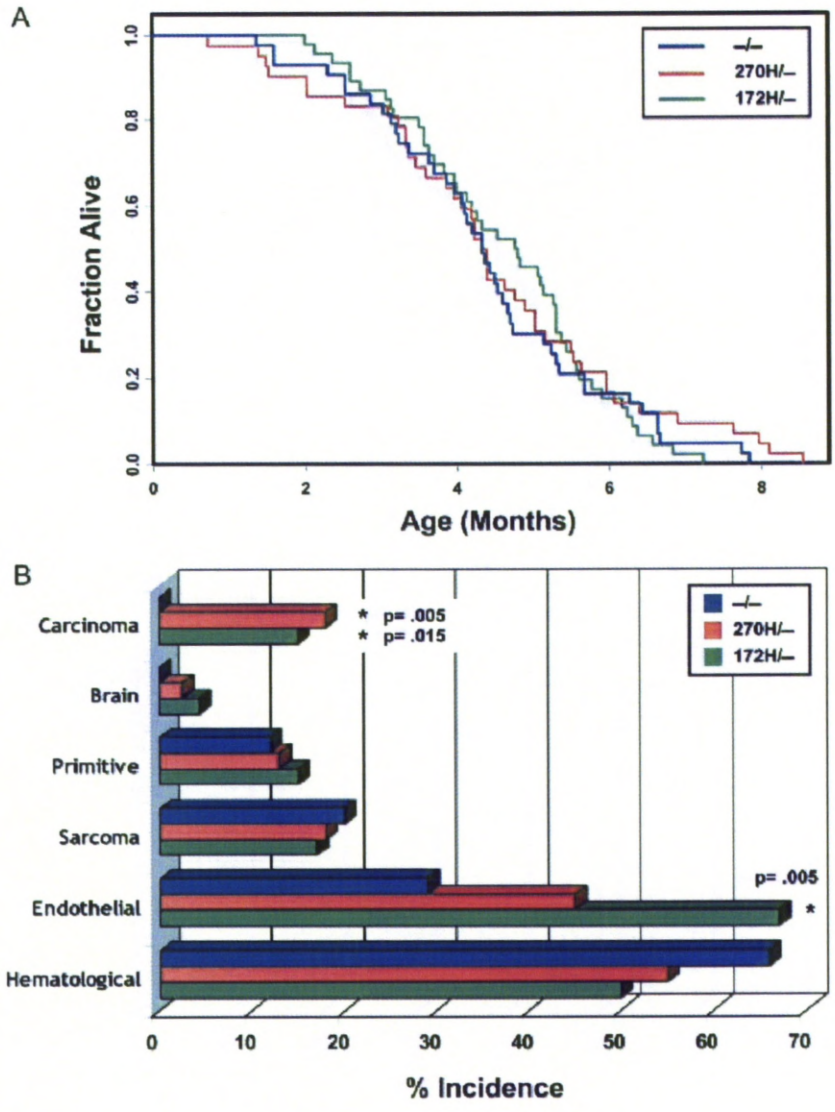

Figure 1.17: Overall survival and tumour spectra of mice carrying one mutant p53 allele (reproduced from reference (6)).

A. Kaplan-Meyer plot demonstrating similar overall survival of $p53^{-/-}$, $p53^{R270H/-}$ and $p53^{R172H/-}$ mice.

B. Histograms representing the spectrum of tumours developed by $p53^{-/-}$ (blue), $p53^{R270H/-}$ (red) and $p53^{R172H/-}$ (green) mice.

Note: The R270H and R172H mutations in murine *Tp53* correspond to R273H and R175H mutations in the human gene, respectively.

1.3.4.3.1. Mechanisms of mutant p53 gain of function

The mechanism of action of the GOF mutants is not well understood but it has been suggested that the mutant proteins may exert their oncogenic effects via inhibition of other members of the p53 family, transactivation of a distinct set of target genes (involved in cellular proliferation, cell survival or angiogenesis) or participation in novel protein-protein interactions (405).

1.3.4.3.1.1. Dominant-negative effects on other p53 family members

Unlike wild-type p53, many GOF mutants have been reported to bind to and inhibit function of other members of the p53 family – p73 and/or p63 (406), which share some functions with p53. For p73 and mutant p53, interaction occurs between the DNA binding domains of the two proteins (407), and not through the tetramerization domains (408) as in the case of wild-type and mutant p53, hence preventing transactivation and p53-independent apoptosis induced by p73 in response to DNA damage (409). Recently, increased chemoresistance of tumours overexpressing some of the GOF mutants has been mechanistically linked to hetero-oligomerisation between mutant p53 and p73 (410).

The binding affinity of different p53 mutants for p73 varies and is also influenced by the status of the p53 polymorphism at amino acid 72 (411). An arginine at position 72 has been correlated with a stronger interaction between mutant p53 and p73 as well as stronger inhibition of p73-mediated apoptosis (412). It has been further shown that p53-72R mutants are capable of inhibiting chemotherapy-induced apoptosis more efficiently than p53-72P mutants and in a group of SCCHN patients those with tumour-specific expression of the 72R allele had both a decreased response to cisplatin chemotherapy and an overall worse survival than those with p53-72P

expression (413). Consequently, it can be concluded that tumour chemosensitivity is influenced by the type of p53 mutation and its efficiency of binding p73 as well as the status of the p53 polymorphism at position 72.

1.3.4.3.1.2. Transactivation-dependent mechanism

p53 mutants may function as oncogenic transcription factors. The genomic sequences bound by mutant p53 are notoriously heterogeneous and so far there has been no success in establishing a linear consensus sequence for mutant p53 binding sites. The mutant proteins associate with DNA either due to their intrinsic DNA binding ability (direct binding) or by interacting with other DNA binding proteins (passive binding) to activate transcription of genes that do not contain the canonical p53 DNA binding sites (414).

The remarkable heterogeneity of the mutant p53 response elements may be partly due to passive binding of p53 mutants to DNA. In such cases the specificity of mutant p53 association with certain DNA sequences may be dependent on the DNA binding specificity of mutant p53 interacting partners. In support of this notion, mutant p53 was found to associate with a number of sequence-specific transcription factors, including Sp1 (415), Ets-1 (416) and NF-Y (417). Interestingly, such tethering to non-mutant p53 specific binding sites is not unique to p53 mutants. Interactions between wild-type p53 and other sequence-specific DNA binding proteins play an important role in p53-mediated transcriptional repression. By interacting with other transcription factors wild-type p53 can inhibit their DNA binding and transcriptional activity. Importantly, the association of wild-type and mutant p53 with non-canonical binding sites can have functionally opposite outcomes (418). For example, association of wild-type p53 with Ets-1 results in transcriptional repression of Ets-1-regulated

genes (419) while p53 mutants were found to cooperate with Ets-1 to enhance the transcription of cancer-related genes (416). One of the genes regulated in this manner is *MDR1* (multi-drug resistance-1 gene) (418), encoding an ATP-dependent efflux pump responsible for pumping various hydrophobic cytotoxic drugs out of the cell. MDR1 plays an important role in the response of tumours to chemotherapeutic agents, such as taxanes. Analogously to Ets-1, transcriptional activation by NF-Y is repressed by wild-type p53 but augmented by p53 mutants (417). The presence of mutant p53/NF-Y complexes results in increased DNA synthesis and up-regulation of cyclin A, cyclin B1, cyclin B2, CDK1 and CDC25 expression (all of which are involved in cell cycle control) in response to DNA damage (417).

The inverse effects of wild-type and mutant p53 interactions with other transcription factors with respect to transcriptional regulation of target genes may stem from the different chromatin modifying activities recruited by wild-type and mutant p53 proteins to the regulated gene promoters. Mutant p53 was found to recruit p300 to NF-Y target promoters (417), resulting in histone acetylation and hence increased accessibility of chromatin to transcription machinery. Interestingly, differences between gene regulation by mutant and wild-type p53 become apparent only under stress conditions, suggesting that association of p53 proteins with DNA is a prerequisite rather than an initiating event for control of NF-Y-mediated transcription.

Remarkably, the interaction between mutant p53 and DNA binding proteins, including Sp1, Ets-1 and NF-Y, is dependent on the presence of an intact C-terminal domain of p53, where the binding sites for these proteins are located (420).

Other genes transactivated by p53 mutants include: *BAG-1* (421), *PCNA* (proliferating cell nuclear antigen) (422), *c-MYC* (423), *IL-6* (424), *HSP70* (heat

shock protein 70) (425), *EGFR* (426), *IGF-II* (insulin-like growth factor receptor II) (427), *EGR1* (428) and *dUTPase* (403).

It is believed that mutant p53 requires an intact N-terminal acidic transactivation domain to exert its gain of function (429). While the tumour-derived GOF p53-281G mutant acts as a transcriptional activator of *MDR1* and *c-MYC* and enhances the tumorigenic potential of cells, additional mutations at residues 22 and 23, which prevent interaction with TAF and C-terminal modifications, completely abolish these functions (429).

Independently of binding to other factors, p53 mutants exhibit DNA structure-selective binding, associating with divergent sequences of DNA, containing numerous repetitive DNA elements and capable of adopting a non-B-DNA conformation (430). Among such sequences mutant but not wild-type p53 was found to bind with high affinity to the MAR/SAR (nuclear matrix/scaffold attachment region) DNA elements (431), which are important in a number of nuclear processes, such as maintaining genomic organisation and controlling transcription and DNA replication. It is suggested that association of p53 mutants with MAR/SAR elements may interfere with these processes, resulting in multiple oncogenic effects (431). Moreover, p53 mutants were found to interact with the trinucleotide CTG•CAG repeats, which act as nucleosome positioning elements (432) and promote the maintenance of an inactive state of chromatin (heterochromatin) (433). Therefore, mutant p53 binding to such CTG•CAG tracts was suggested to play a role in formation and maintenance of a repressive state of chromatin (414).

All of this evidence suggests that mutant p53 may be a key molecule in the oncogenic signalling pathways. Its ability to interact with DNA and coordinate chromatin remodelling and gene transcription is remarkable and indicates that altering

the transcriptome of cancer cells may be one way through which mutant p53 proteins exert their gain-of-function properties.

1.3.4.3.1.3. Novel protein-protein interactions

Last but not least, the GOF p53 mutants have been suggested to have transcription-independent functions and act through novel protein-protein interactions. Specific binding to mutant but not wild-type p53 might be due to the differences in structure and conformation between the two proteins. For example, p42 and p38 MAPKs have been found to interact with mutant p53 rather than the wild-type in a cell cycle specific manner, with increased interactions during S phase, suggesting a cell growth promoting role of these proteins (434). More recently, MBP1 (Mutant p53-Binding Protein 1) has been identified as a mutant p53-175H interacting protein (435). Since overexpression of MBP1 accelerates malignant transformation and has tumour cell growth enhancing properties, it has been suggested to be an oncogene (435). Therefore, interaction of mutant p53 with MBP1 could serve as an example of cooperation of two oncogenes.

The GOF properties of mutant p53 can also be mediated by its prolonged half-life (405). Both the wild-type and mutant proteins interact with MDM2. However, mutant p53 seems to accumulate in cancer cells and remain stable (436). Since p53 mutants have been shown to associate with MDM2 and to be inherently unstable (437, 438), there must be additional mechanisms that stabilize the mutant protein. The most plausible mechanism for the absence of the MDM2-p53 negative-feedback loop is one, in which p53 mutants fail to transactivate the *MDM2* promoter. This leads to insufficient MDM2 levels for efficient targeting of p53 for degradation (437). Interestingly though, mutant p53 also stabilises MDM2, which normally has a very

short half-life (5-15 min) (439). Therefore, an alternative theory suggests that mutant p53 could be protected from MDM2-mediated degradation by associating with heat shock proteins (440), including HSP90 (441). Mutant p53 enables HSP90 to bind to MDM2, hence blocking the ARF binding site (442). Since MDM2 can stimulate hyperproliferation and aneuploidy in p53-null mice (443), MDM2 stabilisation provides yet another mechanism how mutant p53 can contribute to tumorigenesis.

1.3.4.3.2. Biological manifestations of mutant p53 gain of function

GOF mutations in p53 are frequently associated with poor prognosis (444) and tumour resistance to treatment (401, 402). These could result from the acquired capabilities of mutant p53 such as enhancement of cell proliferation, promotion of genetic instability, migration and invasion, and interference with apoptosis. In order to tailor specific therapies for individual cancer patients it is important to understand the biological mechanisms employed by mutant p53 to achieve its oncogenic potential.

1.3.4.3.2.1. GOF p53 mutants promote genomic instability

Genomic instability is one of the key characteristics driving tumour progression. Mutant p53 can enhance genetic instability by affecting overall chromosome number and structure, and by influencing DNA repair and thus affecting mutation rates.

Abnormal centrosome numbers were observed with high frequency in tumour cells from mice expressing the p53-175H GOF mutant as opposed to p53-null mice (445) although another study showed that p53-null cells *in vitro* also exhibit centrosomal abnormalities (262), suggesting that this effect could be a result of mere loss of function by mutant p53. Because centrosomes are duplicated once per cell cycle, an

increased number of centrosomes would result in unequal segregation of chromosomes between the daughter cells.

Moreover, GOF p53 mutants have been reported to disrupt spindle checkpoint control, resulting in S-phase re-entry (instead of arrest) of cells with a 4n DNA content in the presence of spindle depolymerising agents and generation of polyploid cells (446). This activity was also found to be independent of the N-terminal domain of p53, as expression of mutant p53 with additional mutations at residues 22 and 23 resulted in similar degrees of polyploidy (446). This suggests that GOF p53 mutants promote aneuploidy via a transcription-independent mechanism. As discussed previously, GOF p53 mutants inhibit the activity of the other p53 family members, p63 and p73 (406). In the absence of p53, p73 can suppress aneuploidy and polyploidy (447). Therefore, inhibition of p73 by p53 mutants could provide a potential mechanism, through which mutant p53 might promote genomic instability.

1.3.4.3.2.2. GOF of p53 mutants through inhibition of apoptosis

In addition to genomic instability, many GOF p53 mutants have been shown to confer resistance to various pro-apoptotic signals in cancer cells, hence contributing to tumour promotion and tumour resistance to treatment.

First of all, it was observed that p53 mutants are able to suppress apoptosis induced by oncogenic signalling, such as deregulated c-Myc expression (448), which is a frequent event in many cancer cells. c-Myc expression results in the induction of p53-mediated apoptosis through $p14^{ARF}$ up-regulation and inhibition of MDM2-mediated degradation of p53 (345) and the resistance to c-Myc-induced apoptosis may be a result of neutralising wild-type p53 activity by the GOF p53 mutants. In this way, cancer cells can fully benefit from the pro-proliferative potency

of c-Myc, without the danger of undergoing c-Myc-mediated apoptosis. Mutant p53 has also been suggested to protect cells from undergoing apoptosis in response to growth factor deprivation (449). Growth factor deprivation down-regulates c-Myc expression but may also up-regulate $p14^{ARF}$, triggering the same p53-dependent apoptotic pathway (450). Moreover, p53 mutants have also been implicated in suppression of p53-independent apoptosis, which might be a result of inhibition of p73 functions by GOF p53 mutants (as described in section 1.3.4.3.1.1).

Importantly, many GOF p53 mutants are associated with increased resistance of tumours to various anti-cancer treatments, including γ-irradiation, doxorubicin, cisplatin (451), etoposide (393), 5-FU (403), UV and methotrexate (404). Moreover, knock-down of endogenous mutant p53 expression was observed to sensitise cancer cells to apoptosis induced by such agents and other pro-apoptotic signals (452), providing further links between apoptosis resistance and mutant p53.

Mechanistically, there are a number of ways to explain the increased resistance of tumours to anti-cancer treatment. As mentioned previously, p53 mutants are known to inhibit p73 function (see section 1.3.4.3.1.1), which is responsible for induction of p53-independent apoptosis in response to DNA damage (409). Hence, it is conceivable that p73 inhibition by mutant p53 could render cells expressing GOF p53 mutants resistant to many types of anti-cancer treatments (410).

Another possible mechanism of increased resistance to apoptosis could be the transcriptional activation of expression of EGR1 by mutant p53 (428). EGR1 (early growth response 1) is a transcription factor implicated in regulating proliferation, apoptosis and angiogenesis (453). Its induction by mutant p53 enhances transforming properties and has an anti-apoptotic effect on cancer cells (428). It was further shown that this apoptosis resistance may be also due to down-regulation of procaspase-3,

a key component of the apoptotic caspase cascade (see Figure 1.9), by some p53 mutants (452).

All this evidence suggests that mutant p53 might promote resistance to apoptosis via a number of mechanisms, which may vary depending on the cellular context. By doing so it may not only promote tumour progression but also enhance tumour resistance to anti-cancer therapy.

1.3.4.3.2.3. The role of GOF p53 mutants in cell migration, invasion and metastasis

Although p53 mutations are known to occur at many different stages of tumorigenesis, in some cancers they are significantly more frequent at later stages and are associated with advanced, metastatic tumours (9). As discussed previously tumour progression is associated with acquisition of invasiveness and metastatic potential by cancer cells. In addition to losing the wild-type p53-mediated suppression of these characteristics, p53 mutants have been implicated in active promotion of cell migration, invasiveness and metastasis (454).

Firstly, wild-type p53 was suggested to suppress migration and invasiveness through MDM2-mediated degradation of an invasion promoter Slug, resulting in up-regulation of E-cadherin (286). On the other hand, the presence of mutant p53 was associated with low MDM2 expression, stabilisation of Slug, down-regulation of E-cadherin and short metastasis-free survival of non-small cell lung cancer patients (286). Importantly, these effects seemed to go beyond the simple loss of wild-type p53 function. It was suggested that mutant p53 might promote Slug up-regulation by repressing MDM2 expression since knockdown of mutant p53 resulted in increased MDM2 levels (286), providing the first potential mechanism for mutant p53-mediated invasiveness of cancer cells. However, more recent studies demonstrated that MDM2

actually promotes invasiveness of cells in a RING-finger-independent manner (287) and since MDM2 is usually maintained at a low level in the presence of mutant p53 (which is unable to transactivate MDM2), mutant p53 is likely to promote motility and invasiveness via an alternative mechanism.

Interestingly, induction of cell migration by mutant p53 is strongly dependent on the cellular context. It was suggested that cooperation between mutant p53 and oncogenic Ras may be critical for some of the malignant phenotypes displayed by mutant p53 expressing tumours (455) explaining why some studies reported dominant-negative rather than GOF effects of mutant p53 in promoting cell migration (456). Moreover, oncogenic Ras and mutant p53 were found to be essential for TGF-β-induced invasiveness and metastatic spread (457).

Transforming growth factor β (TGF-β) plays a dual role in cancer progression. At early stages of tumour development it functions as a tumour suppressor putting a break on proliferation of epithelial cells, while in advanced cancers it is paradoxically diverted into a potent enhancer of invasion and metastasis (458). Smad2 and Smad3 are the key mediators of TGF-β signalling, which are phosphorylated upon TGF-β receptor activation and accumulate in the nucleus, eliciting gene responses to TGF-β (459). The molecular basis of the switch of TGF-β from tumour suppressor to oncogene is not fully understood. Recently, mutant p53 has been reported to be crucial for TGF-β-mediated invasiveness (457). Mutant p53 inhibits the activities of p63, which was shown to suppress TGF-β-induced malignant responses (457). p63 inhibits invasiveness and metastatic potential of cancer cells by induction of its transcriptional targets, Sharp-1 and cyclin G2, suggested to function as metastasis suppressors (457). Indeed, knockdown of either of these targets mimics the ability of mutant p53 to drive migration and invasiveness (457).

However, most stratified epithelia express predominantly ΔNp63, an isoform of p63 unable to bind to mutant p53 (406). In this context, Smads were found to be essential for complex formation between mutant p53 and p63 (457). Moreover, oncogenic Ras was required for phosphorylation of mutant p53 at the N-terminus, which was a prerequisite of the TGF-β-induced mutant p53/Smad/p63 ternary complex formation (457). Hence, TGF-β signalling induces phosphorylation of Smads, which serve as a platform for a ternary complex formation by Ras-activated mutant p53 and p63, resulting in the acquisition of invasiveness and metastatic proclivity. These findings demonstrate yet another role for the GOF p53 mutants in promoting cancer invasion and metastasis.

However, TGF-β signalling is not always indispensable for mutant p53 to exhibit its function in promoting migration and invasiveness (460). In addition to suppression of Sharp-1 and cyclin G2 expression, p63 inhibition by mutant p53 was reported to result in increased α5β1 integrin and EGFR recycling, driving cancer cell migration and invasion (454). Integrin recycling is driven by Rab-coupling protein (RCP), which by associating with α5β1 integrin directs it from the recycling endosomes back to the plasma membrane, where it can bind its substrate, fibronectin, and promote cell migration (461). Moreover, RCP was suggested to function as a scaffold for coordinated trafficking of α5β1 integrin and EGFR, resulting in enhanced EGFR autophosphorylation and signalling via Akt (461). Importantly, Akt in addition to its pro-survival activities has recently been reported to promote cell migration and invasiveness (462). Transcriptionally active TAp63 was found to inhibit activation of RCP hence inhibiting integrin and EGFR recycling and consequently blocking cell migration (454). However, direct transcriptional targets of p63 regulating the association of RCP with α5β1 integrin are currently unknown. The anti-migratory

effect of p63 was relieved by mutant p53 expression, promoting tumour cell migration and invasion (454). Altogether, these observations suggest that through increased integrin and EGFR recycling, mutant p53 drives migration and invasion via the Akt signalling pathway.

While mutant p53 is likely to be involved in numerous other pathways, which are dysregulated in human cancer, the findings discussed above shed light onto how the oncogenic gain of function of mutant p53 could contribute to tumour invasiveness, metastatic potential and resistance to treatment. However, many of the mechanisms through which mutant p53 promotes tumour progression are still not well understood and there are areas, which require further investigation. Poor prognosis associated with expression of mutant p53 underlies the need for screening, developing novel therapies and better prediction of treatment response. Elucidating the mechanism of action of individual GOF p53 mutants will be crucial for developing targeted therapies tailored to individual patients and perhaps improving survival of cancer patients with mutant p53 expressing tumours.

1.4. Aim of this project

p53 is an important tumour suppressor protein, whose function is lost through *TP53* mutations in about 50% of human tumours (107), making it arguably the most frequently altered gene in human cancer. The majority of p53 mutations are missense, resulting in the expression of full-length protein with single amino acid substitutions, which tends to accumulate in tumour cells (436). These missense p53 mutants not only lack wild-type p53 tumour-suppressor activity but in addition evidence suggests that some of these also gain new functions that can promote tumorigenesis (see

section 1.3.4.3). This oncogenic 'gain of function' of p53 mutants is proposed to be achieved via modulating the transcriptome of a cancer cell or through novel protein-protein interactions (as discussed in section 1.3.4.3.1) but the molecular details of the mechanisms involved are still not entirely understood.

Therefore, the aim of this project was to investigate the mechanisms and functional consequences of mutant p53 GOF in LSCC cells, which are important preclinical models in the search for new therapies for treatment of laryngeal cancer (463). The mutants chosen for these studies represent two different mutational classes:

- R175H – a structural mutation causing a significant conformational shift of p53,
- R273H – a contact mutation affecting a p53 residue that makes direct contact with DNA and hence leading to a loss of wild-type p53-specific DNA binding; note that mutants of this class may retain altered ability to transactivate p53-responsive genes.

Both of these mutants have been shown to display GOF properties using *in vivo* models (5, 6) and have been documented to occur in laryngeal cancer (139). The mechanism of action of the GOF p53 mutants mentioned above was investigated by identifying mutant p53 interacting proteins and studying the gene expression changes in cells expressing those p53 mutants. Since mutant p53 expression is frequently linked to poor prognosis (101), the functional consequences of GOF p53 mutations in laryngeal cancer were studied with respect to cellular motility and invasiveness, which may be used as surrogate indicators of metastatic potential. In addition, GOF p53 mutants are frequently associated with resistance to treatment (401, 402) and hence the response of mutant p53 expressing LSCC cells to ionising radiation (a common treatment modality for laryngeal cancer) was also studied.

Since many biological functions involve interactions of proteins with other proteins and with DNA, identifying the interacting partners of mutant p53 and studying the gene expression changes in mutant p53 expressing cells may elucidate, which molecular networks and pathways mutant p53 proteins are involved in, and the components of these networks (including the identified mutant p53 interacting proteins) may represent important new therapeutic targets. Moreover, better understanding of the impact of mutant p53 expression on response to treatment may make the choice of treatment suitable for particular patients easier as well as facilitate development of novel therapies tailored to the individual tumours.

Chapter 2

Materials and Methods

2. Materials and Methods

2.1. List of reagents

2.1.1. General reagents

Reagent or product	Manufacturer
Acetic acid (glacial) 100% anhydrous	Merck
Acetone	Prolabo
Acetonitrile	Fisher
Acrylogel 2.6 (40%) solution	BDH
Adenosine 5'-triphosphate, disodium salt hydrate	Sigma
Agar	ForMedium
Amaxa® Nucleofector® Kit V	Lonza
Ammonium bicarbonate	Sigma
Ammonium persulfate (APS)	Sigma
Ampicillin sodium salt	Sigma
Aprotinin	Roche
Albumin from bovine serum (BSA), minimum 96% electrophoresis	Sigma
Blotting Grade Blocker Non Fat Dry Milk	Bio-Rad
Bromophenol Blue	Sigma
Crystal Violet	Sigma
d-Biotin	SUPELCO Analytical
Dimethyl sulfoxide (DMSO)	Sigma
Dimethylformamide (DMF)	BDH
DL-Dithiothreitol, for molecular biology, minimum 99% titration	Sigma
DPX Mountant for histology	Sigma

Reagent or product	**Manufacturer**
Dual-Luciferase® Reporter 1000 Assay System	Promega
EndoFree Plasmid Mega Kit (5)	Qiagen
Ethanol, absolute, 200 proof, for molecular biology	Sigma
Ethanol (Abs), reagent grade	Department of Chemistry University of Liverpool
Ethidium Bromide solution	Sigma
Ethylenediaminetetra-acetic acid (EDTA) disodium salt	BDH
Ethylene glycol-bis(β-aminoethyl ether)-N,N,N',N'-tetracetic acid (EGTA)	Sigma
Gelatin from porcine skin	Sigma
Geneclean Turbo Kit	Qbiogene
GenSieve LE agarose	Flowgen Bioscience
25% Gluteraldehyde solution	BDH
Glycerol, ≥ 99.5%, A.C.S. reagent	Sigma
Glycine	Fisher Scientific
HEPES, Free Acid, Molecular Biology Grade	Calbiochem
Hybond™ ECL™ Nitrocellulose Membrane	GE Healthcare
Iodoacetamide (IAA)	Sigma
InterPlay™ Mammalian TAP System	Stratagene
Kanamycin sulphate, from *Streptomyces kanamyceticus*	Sigma
Leupeptin	Roche
Luria Broth	Sigma
Magnesium acetate tetra-hydrate, Minimum 99%	Sigma
Magnesium chloride	Sigma
β-mercaptoethanol	Sigma
Methanol, analytical reagent grade	Fisher Scientific

Reagent or product	**Manufacturer**
Pepstatin	Roche
Phenol red	BDH
Phenylmethanesulfonyl fluoride (PMSF)	Fluka
Ponceau S, practical grade	Sigma
Potassium hexacyanoerrate(II) 3-hydrate (potassium ferrocyanide)	BDH
Potassium hexacyanoerrate(III) (potassium ferricyanide)	BDH
Prestained Protein Marker, Broad Range (7-175 kDa)	NEB
Protein Assay Dye Reagent Concentrate	Bio-Rad
Protein G Sepharose®	Sigma
QIAprep Spin Miniprep Kit (50)	Qiagen
Qiashredder™ (50)	Qiagen
REASTAIN Quick-Diff Kit	Reagena
Rely+On™ Virkon® Tablets	DuPont
RNase-Free DNase Set (50)	Qiagen
RNeasy® Mini Kit (50)	Qiagen
SeaKem® GTG® Agarose	Lonza
Sequencing Grade Modified Trypsin	Promega
Silver Stain Plus Kit	Bio-Rad
Sodium chloride (NaCl)	VWR
Sodium dodecyl sulphate (SDS)	BDH Prolabo
Sodium dihydrogen phosphate dihydrate $(NaH_2PO_4 \cdot 2H_2O)$	Fluka BioChemika
Sodium fluoride	Fluka BioChemika
Sodium phosophate dibasic dihydrate $(Na_2HPO_4 \cdot 2H_2O)$	Sigma
Soybean Trypsin Inhibitor (STI)	Roche

Reagent or product	**Manufacturer**
TA Cloning kit	Invitrogen
N,N,N',N'-tetramethylenediamine (TEMED)	BDH
Trichloroacetic acid (TCA)	BDH Prolabo
Trifluoroacetic acid	Applied Biosystems
Tris Base, ULTROL® Grade	Calbiochem
Triton X-100	Amersham Biosciences
Tween 20	Sigma
Western Lightning *Plus*-ECL chemiluminescence reagent	PerkinElmer
Whatman 3 mm Chromatography Paper	VWR
X-Gal (5-Bromo-4-chloro-3-indolyl-B-D-galactopyranoside)	BDH
Xylene cyanole FF	Sigma

All H_2O used was ultra-pure H_2O $(> 18\,M\Omega \cdot cm)$ produced by PURELAB Ultra-pure Water Purification System (ELGA Process Water).

2.1.2. Tissue culture reagents

Reagent	**Manufacturer**
Dulbecco's Modified Eagle's Medium, HEPES Modification	Sigma
Dulbecco's Phosphate Buffered Saline	Sigma
Fetal Bovine Serum	Sigma
FuGENE® HD Transfection Reagent	Promega
G418 Sulfate, Cell Culture Tested	Calbiochem
GeneJuice® Transfection Reagent	Novagen
L-Glutamine 200 mM	Sigma
Lipofectamine™ 2000 Transfection Reagent	Invitrogen
MEM Non-essential amino acid solution 100×	Sigma
Opti-MEM® I Reduced Serum Medium	Invitrogen
Penicillin-Streptomycin, BioReagent	Sigma
Phosphate Buffered Saline (Dulbecco A), non-sterile	Oxoid
Puromycin	InvivoGen
RPMI-1640 Medium	Sigma
Trypsin-EDTA solution (1×)	Sigma

2.1.3. Enzymes and cloning reagents

Reagent	**Manufacturer**
Adenosine 5′-Triphosphate (ATP)	NEB
Anatarctic Phosphatase	NEB
10× Antarctic Phosphatase Reaction Buffer	NEB
BamHI	NEB
DNA Polymerase I, Large (Klenow) Fragment	NEB
dNTP Mix	NEB
EcoRI	NEB
EcoRV	NEB
Hexamminecobalt(III) chloride (HCC)	Sigma
NdeI	NEB
NotI	NEB
pCR2.1 vector (25 ng/μl)	Invitrogen
Phusion® High-Fidelity DNA polymerase	Finnzymes
5× Phusion® HF Buffer	Finnzymes
Quick-Load 1 kb DNA Ladder	NEB
SmaI	NEB
10× Standard Taq Reaction Buffer	NEB
StuI	NEB
T4 DNA ligase	Ambion
10× T4 DNA Ligase Reaction Buffer	Ambion
Taq DNA polymerase	NEB

2.2. Cloning

10× DNA/RNA native loading buffer

Concentration	Reagent
0.1% (w/v)	bromophenol blue
0.1% (w/v)	xylene cyanol
1 mM	EDTA
50% (v/v)	glycerol

1.2% (w/v) agarose gel

Reagent	Amount
agarose	0.6 g
ethidium bromide (10 µg/µl)	2.5 µl
TAE buffer	50 ml

TAE (Tris-acetate-EDTA) buffer (50×)

Concentration	Reagent
2 M	Tris
5.71% (v/v)	glacial acetic acid
50 mM	EDTA

For restriction digests, 3 µg of the plasmid containing the insert of interest and 1 µg of the vector "backbone" DNA were digested routinely with 10-fold excess of enzyme (restriction endonuclease of interest), e.g. 10 U of enzyme were used to digest 1 µg of DNA. The digests were carried out under conditions indicated for the respective enzymes by the manufacturer. The backbone DNA was further dephosphorylated (to minimise the rate of religation) by adding 0.5 µl Antarctic phosphatase and

10× Antarctic Phosphatase Reaction Buffer (to a final concentration of 1×) and incubating at 37°C for 15 min.

The digested DNA was then resolved by gel electrophoresis on a 1.2% (w/v) agarose gel (prepared using SeaKem GTG Agarose, which contains low levels of polyanionic contaminants that could inhibit DNA modifying enzymes) containing 0.5 μg/ml ethidium bromide, in a horizontal electrophoresis unit (Scie-Plas) connected to a PowerPac power supply (Bio-Rad). The insert and backbone of interest were then cut out of the gel using a sterile scalpel and purified using a Geneclean Turbo Kit according to the manufacturer's instructions. The ligation was set up as follows.

Component	**Volume**
insert DNA	6.5 μl
backbone DNA	1 μl
T4 DNA ligase	1 μl
10× T4 DNA ligase reaction buffer	1 μl
ATP	0.5 μl
Total volume:	10 μl

"No insert" and "no ligase" controls were also set up. The ligations were incubated at 14°C overnight. For blunt-end ligations 0.2 μl of 100 μM HCC was also added.

2.3. Bacterial strains, transformation and plasmid purification

One Shot TOP-10 Chemically Competent *E. coli* (Invitrogen) were used as a cloning strain and chemically competent *E. coli* strain XL-1 Blue (Stratagene) were used for large-scale plasmid preparation.

Luria-Bertani (LB) liquid medium

Reagent	**Amount**
powdered LB	12.5 g
H_2O	500 ml

Sterilised by autoclaving (121°C for 15 min.).

Luria-Bertani (LB) medium with agar

Reagent	**Amount**
powdered LB	12.5 g
agar	7.5 g
H_2O	500 ml

Sterilised by autoclaving (121°C for 15 min.). After the medium partially cooled down, antibiotics were added as required, the medium was then poured into 10 cm Petri dishes and allowed to set.

For transformation, competent cells were thawed on ice. 5 µl of the ligation mix was added to the TOP-10 competent cells and incubated on ice for 30 min. to allow even distribution of the plasmid. Next, the cells were incubated at 42°C for 30 sec. and then placed back on ice immediately for 2 min. 200 µl of SOC medium was then added to the cells and they were incubated in a shaker at 37°C, 220 rpm for 1 hour. Following incubation, the transformations were plated on LB/Agar plates containing the appropriate antibiotic (10% and 90% of the entire volume per plate). The plates were incubated at 37°C overnight.

Usually, between 5 and 10 colonies were inoculated into 4 ml liquid LB containing the appropriate antibiotic. The cultures were incubated at 37°C with shaking at 220 rpm, overnight. The cultures were then centrifuged at 16,000×g for 5 min. and DNA was extracted using the QIAprep Spin Miniprep Kit according to the

instructions. This procedure is based on the original alkaline extraction method by Birnboim and Doly (464). The method relies on the fact that under carefully selected alkaline pH (12-12.5) linear genomic DNA is denatured while plasmid DNA remains in its native state. Lysis was achieved with lysozyme (to weaken the cell wall), SDS and NaOH. The lysate was then neutralised by acidic NaAc solution, resulting in renaturation and aggregation of the chromosomal DNA and high molecular weight RNA and precipitation along with protein while plasmid DNA remained in solution. Genomic DNA, some RNA and protein was then removed in a single centrifugation step.

The QIAprep Miniprep is a modification of this method. Briefly, the bacterial pellets were resuspended in 250 µl of Buffer P1 (containing LyseBlue reagent). The cells were lysed by alkaline lysis by adding 250 µl of Buffer P2 and inverting the tube a few times. The presence of LyseBlue in the resuspension buffer helped to ensure thorough mixing of the solutions until a homogenously coloured blue suspension was obtained. 350 µl of neutralization Buffer N3 was then added and the tubes were inverted a few times until all trace of blue disappeared. The tubes were centrifuged at 16,000×g for 10 min. and the supernatants were applied to the QIAprep spin columns (containing a silica membrane). Due to the specifically optimised high-salt conditions during the lysis procedure only DNA binds to the silica membrane, while RNA and proteins are found in the flow-through. The columns were centrifuged at 16000×g for 1 min. The flow-through was discarded. The columns were washed by adding 500 µl of Buffer PB (to remove endonucleases) and centrifuged at 16000×g for 1 min. The flow-through was discarded. A second wash to remove salts was performed by adding 750 µl of Buffer PE and centrifugation at 16000×g for 1 min. The flow-through was discarded. The columns were centrifuged at 16000×g for an additional 1 min. to

remove residual ethanol from wash buffer. The columns were then placed in fresh 1.5 ml microcentrifuge tubes and DNA was eluted with a low-salt solution – usually 30-50 µl of H_2O was added to the centre of each column, which were then incubated for 1 min. at room temperature and centrifuged at 16,000×g for 1 min.

The colonies were screened by restriction digestion and agarose gel electrophoresis (using GenSieve LE agarose) for the presence and orientation of the insert.

XL-1 Blue competent cells were then transformed with the plasmid DNA from a positive clone as described previously. A single colony was inoculated into 4 ml liquid LB containing the appropriate antibiotic and the culture was incubated at 37°C with shaking at 220 rpm, overnight. 50 µl of this culture was then used to set up a 500 ml culture. The culture was then incubated at 37°C with shaking at 220 rpm, overnight. The bacterial cells were pelleted by centrifugation at 6,000×g for 15 min. at 4°C and DNA was extracted using the EndoFree Plasmid Mega Kit according to the manufacturer's instructions. Similarly to the miniprep procedure, the Megaprep plasmid purification is also based on a modified alkaline lysis procedure. The plasmid DNA is then bound to a QIAGEN Anion-Exchange Resin under optimized low-salt and pH conditions. RNA, protein and other impurities are removed by a medium-salt wash and plasmid DNA is eluted using a high-salt buffer. It is then concentrated and desalted by isopropanol precipitation. The EndoFree kit used includes also an endotoxin removal step. Bacteria shed small amounts of endotoxins into their surroundings during active growth and large amounts when they are dying. Bacterial endotoxins are lipopolysaccharides (LPSs), which are toxic to eukaryotic cells. Due to their chemical properties and tendency to form micellar structures they tend to co-purify with plasmid DNA. For example, they can interact with the anion-exchange resins due to the negatively charges phosphate groups present on the endotoxins. The

endotoxin removal buffer prevents the LPS molecules from binding to the anion-exchange resin, yielding a high quality plasmid DNA preparation, which is suitable for transfections.

Briefly, the bacterial pellet was resuspended in 50 ml of Buffer P1 (containing LyseBlue). The cells were lysed by adding 50 ml of Buffer P2 and inverting the tube a few times until a homogenously coloured blue suspension was obtained. The lysate was incubated for 5 min. at room temperature. 50 ml of pre-chilled Buffer P3 was then added and the tube was inverted a few times until all trace of blue disappeared. The lysate was then poured into the QIAfilter Mega-Giga Cartridge (attached to a vacuum source) and incubated for 10 min. at room temperature. The vacuum source was then switched on and the liquid pulled through. The vacuum source was switched off. 50 ml of Buffer FWB2 was added to the QIAfilter Cartridge and the precipitate was stirred gently using a clean pipette tip. The vacuum source was switched on until all the liquid was pulled through. The QIAfilter Cartridge was then detached and disposed. 12.5 ml of Buffer ER was added to the filtered lysate, mixed by inverting the bottle a few times and incubated on ice for 30 min. During this time, a QIAGEN-tip 2500 was equilibrated with 35 ml of Buffer QBT and the column was emptied by gravity flow. Following the incubation the lysate was applied onto the column. The flow-through was discarded. The column was washed with 200 ml of Buffer QC. The DNA was eluted with 35 ml of Buffer QN and collected into a 50 ml Falcon tube. The DNA was then precipitated by adding 24.5 ml of room-temperature isopropanol, mixed and centrifuged immediately at 5,000×g for 1 hour at 4°C. The supernatant was carefully decanted and the pellet was transferred into a fresh microcentrifuge tube in 1 ml of endotoxin-free room-temperature 70% ethanol. The tube was centrifuged at 16,000×g for 10 min. at 4°C. The supernatant was carefully

decanted and the wash with ethanol to remove salts was repeated twice. The DNA pellet was then air-dried until the pellet became translucent. It was then redissolved in a suitable volume (based on the size of the pellet) of 0.1× Buffer TE. DNA was quantified with a BioPhotometer (Eppendorf) using the dsDNA program.

2.4. DNA constructs and plasmids

Vector maps were generated using Vector NTI Advance™ 11 (Invitrogen). Wherever indicated, 2 μg of DNA was vacuum dried and sent for sequencing to Eurofins MWG Operon. The obtained sequence was compared to the reference sequence from the NCBI (National Center for Biotechnology Information) database using NCBI BLAST (Basic Local Alignment Search Tool) (465), which allows for alignment of two sequences.

In order to investigate protein interactions of mutant and wild-type p53 proteins using TAP-tag purification, the p53 cDNAs (wt and two mutants) were cloned into pNTAP vector, which resulted in N-terminally TAP-tagged forms of p53. The cDNAs were also subcloned into pCMV-Script vector for validation studies without the TAP-tag.

2.4.1. pCMV-Script.p53

pCMV-Script.p53, containing human p53 cDNA, was a kind gift from Dr Carlos Rubbi (University of Liverpool). The p53 cDNA was sequenced.

2.4.2. pNTAP-B.p53

p53 cDNA was excised from pCMV-Script.p53 and inserted into pNTAP-B vector (Stratagene) using BamHI and EcoRI restriction sites. The B version of the pNTAP

vector (containing one extra nucleotide in front of the multiple cloning site) was used to ensure that p53 is in frame with the TAP-tag (consisting of the CBP- and SBP-tags). The generated pNTAP-B.p53 was sequenced.

2.4.3. pCB6+.p53-175H

pCB6+.p53-175H vector, containing cDNA of human p53 with a mutation at position 175 (arginine to histidine) was a kind gift from Dr Karen Vousden (Beatson Institute of Cancer Research). Since no vector map or sequence was available, the regions upstream and downstream of p53, as well as the entire p53 cDNA itself, were sequenced.

2.4.4. pCR2.1.p53-175H

Due to the lack of appropriate restriction sites to excise p53-175H cDNA from pCB6+.p53-175H that would allow insertion into the pNTAP vector, the cDNA of the mutant p53 was amplified by PCR from the pCB6+.p53-175H vector using primers introducing a BamHI site at the 5'-end (forward: 5'-GAG AGG ATC CAT GGA GGA GCC GCA GTC AGA TC-3') and an EcoRI site at the 3'-end (reverse: 5'-GAG AGA ATT CTC AGT CTG AGT CAG GCC CTT C-3'). Phusion High-Fidelity DNA Polymerase was used for amplification. The following reaction was set up.

Component	**Volume**
template DNA (100 ng)	3.84 µl
primer-F (0.1µg/µl)	1 µl
primer-R (0.1µg/µl)	1 µl
Phusion DNA polymerase (2 U/µl)	0.2 µl
5× Phusion HF Buffer	4 µl
dNTPs (10 mM)	0.4 µl
H_2O	9.56 µl
Total:	20 µl

The following thermal cycling reaction conditions were used.

denaturation:	98°C, 30 sec.	
denaturation:	98°C, 10 sec.	15 cycles
annealing:	60°C, 30 sec.	
extension:	72°C, 1 min.	
final extension:	72°C, 5 min.	
inactivation:	94°C, 20 min.	

2 µl of Taq DNA Polymerase (5 U/µl) and 2 µl of 10mM dATP were then added to the reaction to add 3'-A-overhangs to the PCR product and incubated at 72°C for 20 min. The reaction was resolved on a 1% (w/v) agarose gel. The PCR product was excised from the gel, purified using Geneclean and ligated into pCR2.1 vector from the TA Cloning kit. pCR2.1 is a linearized vector containing single 3'-deoxythymidine (dT) overhangs, allowing for efficient ligation of PCR products.

TOP-10 competent cells were transformed with the overnight ligations. The transformants were plated on LB/Agar plates containing 50 µg/ml Amp and 50 µg/ml X-Gal and screened using the blue-white selection. White colonies were inoculated into 4 ml of LB with 50 µg/ml Amp. The culture was incubated at 37°C

with shaking at 220 rpm, overnight. Following a miniprep DNA extraction, the p53 cDNA was sequenced to confirm that no additional mutations had been introduced during PCR.

2.4.5. pNTAP-B.p53-175H

p53-175H cDNA was then subcloned from pCR2.1.p53-175H into pNTAP-B using BamHI and EcoRI sites so that p53 is in frame with the TAP-tag.

2.4.6. pCMV-Script.p53-175H

p53-175H cDNA was also subcloned from pCR2.1.p53-175H into pCMV-Script (Stratagene) using BamHI and EcoRI sites.

2.4.7. pET24a(+).p53-273H

pET24a(+).p53-273H vector, containing cDNA of human p53 with a mutation at position 273 (arginine to histidine), was a kind gift from Prof. Sir Alan Fersht (University of Cambridge). The p53 cDNA was sequenced.

2.4.8. pNTAP-B.p53-273H

p53-273H cDNA was excised from pET24a(+).p53-273H using NdeI and EcoRI sites and inserted into BamHI and EcoRI sites of pNTAP-B so that p53 is in frame with the TAP-tag. This involved blunting of the ends cut with NdeI and BamHI using 2 µl of DNA Polymerase I, Large (Klenow) Fragment (5 U/µl) and 10× NEBuffer 2 (added to a final concentration of 1×) at 25°C for 15 min. and a subsequent digestion with EcoRI.

2.4.9. pCMV-Script.p53-273H

p53-273H cDNA was also subcloned from pET24a(+).p53-273H into pCMV-Script using SmaI and EcoRV sites (both produce blunt ends). Digestion with StuI was performed on 5 of the clones to confirm that p53 cDNA was inserted into pCMV-Script in the correct orientation.

2.4.10. Other constructs

pβ-gal is an expression vector encoding β-galactosidase (β-gal) under the regulation of an SV40 promoter.

pp53-TA-luc is a p53 luciferase reporter construct. It drives firefly luciferase expression from a minimal herpes simplex virus (HSV) thymidine kinase promoter, located downstream of a p53 response element comprising a fragment of the putative replication origin of the human ribosomal gene cluster (RGC) p53 binding element and a p53 consensus binding sequence (466). The construct was obtained from BD Clontech.

pRL-TK is a luciferase reporter construct. It drives constitutive *Renilla* luciferase expression from an HSV thymidine kinase promoter. The construct was a kind gift from Prof. Mike White (University of Liverpool).

pSUPER.GFP is an expression vector encoding GFP under the regulation of the PGK promoter. The vector was obtained from Oligoengine.

pSUPER.puro.shp53 is an expression vector encoding a short hairpin specific for p53 and a fluorescent protein mCherry. The vector was generated by Dr Radosław Polański (University of Liverpool).

pSUPER.puro.shScr is an expression vector encoding a control (scrambled) short hairpin and a fluorescent protein mCherry. The vector was generated by Dr Radosław Polański (University of Liverpool).

2.5. Cell culture

H1299 cells (non-small cell lung carcinoma) were obtained from the American Type Culture Collection (Manassas, VA). They were maintained in RPMI-1640 medium supplemented with 10% FBS. H1299 cells are p53-null. They were used in this study because they are well known, grow quickly and are relatively easy to transfect.

UM-SCC-12 cells (laryngeal squamous cell carcinoma) were a kind gift from Prof. Thomas Carey (University of Michigan). They were maintained in Dulbecco's Modified Eagle's Medium (HEPES Modification) supplemented with 10% FBS, 1% penicillin/streptomycin, 1% L-glutamine and 1% Non-Essential Amino Acids. These cells are functionally p53-null, as they carry a homozygous p53 truncation (Q104X).

All cells were grown at 37°C in a humidified atmosphere of 5% CO_2.

In order to prepare cryostocks, cells were harvested by trypsinization and pelleted by centrifugation at 300×g for 5 min. The media was aspirated and the pellets were resuspended in 1 ml of freezing medium (10% DMSO in FBS). The cell suspensions were transferred into cryovials (Nunc). To ensure slow freezing, the vials were placed in a cryogenic freezing container (Nalgene) filled with 100% isopropanol and stored at -80°C overnight. The following day the vials were transferred to liquid nitrogen.

When recovering cells from liquid nitrogen, the stocks were thawed as quickly as possible in a 37°C water bath. Since DMSO is toxic to cells at concentrations above 0.5%, the cells were resuspended in at least 20 ml of complete growth media and

transferred to an appropriate tissue culture flask. As soon as the cells adhered to the surface (usually the following day), the media was changed.

2.6. Transfections

H1299 cells were routinely transfected with GeneJuice (Novagen) at 3 µl per µg of DNA (ratio 3:1) with empty vectors added to ensure equal DNA content of transfections.

For transfection efficiency testing H1299 and UM-SCC-12 cells were seeded into 6-well plates and transfected with 1 µg of pβ-gal per well using GeneJuice at ratios 2:1, 3:1 and 4:1; Lipofectamine 2000 (Invitrogen) at ratios 2:1, 2.5:1 and 3:1; and FuGENE HD (Roche) at ratios 2:1, 2.5:1 and 3:1. UM-SCC-12 cells were also transfected by electroporation using the Amaxa® Nucleofector® Kit, in an attempt to achieve higher transfection efficiency.

Small interfering RNAs were delivered to cells using Lipofectamine 2000.

2.6.1. GeneJuice transfection

The day before transfection cells were plated at such a density (20% confluent for H1299) so that they were approximately 50-80% confluent before transfection.

Before transfection, serum-free (SF) medium, GeneJuice and DNA were equilibrated to room temperature. For one well of a 6-well plate 100 µl of SF medium was placed in a sterile tube. 3 µl of GeneJuice was added directly to the serum-free medium (making sure that GeneJuice does not come in contact with the walls of the tube) and mixed thoroughly by vortexing. The GeneJuice/SF medium mixture was incubated at room temperature for 5 min. 1 µg of DNA was then added and the mixture was mixed by flicking the tube with a finger. The reaction mix was incubated

at room temperature for 15 min. The GeneJuice/DNA mixture was then added drop-wise to cells in complete growth media, distributing the drops over the entire dish surface. The dish was then rocked gently to ensure even distribution of the transfection mixture and the cells were incubated at 37°C, 5% CO_2. The cells were analysed 24 hours post transfection.

The GeneJuice:DNA ratio used in the above example was 3:1. The volumes used were adjusted based on the amount of DNA and GeneJuice:DNA ratio used.

2.6.2. Lipofectamine transfection

The day before transfection cells were plated at such a density (35-40% confluent for H1299) so that they were approximately 90% confluent before transfection.

Before transfection, SF Opti-MEM medium, Lipofectamine and DNA were equilibrated to room temperature. For one well of a 6-well plate 1 μg of DNA was diluted in 250 μl of SF Opti-MEM medium and 2.5 μl of Lipofectamine was diluted in 250 μl of SF Opti-MEM medium. The mixtures were incubated for 5 min. at room temperature. Following incubation the diluted DNA was added to the diluted Lipofectamine. The transfection mixture was mixed by flicking the tube with a finger and incubated for 20 min. at room temperature. The entire transfection mixture was then added drop-wise to cells in complete growth media, distributing the drops over the entire dish surface. The dish was then rocked gently to ensure even distribution of the liposome complexes and the cells were incubated at 37°C, 5% CO_2. The cells were analysed 24 hours post transfection.

The Lipofectamine:DNA ratio used in the above example was 2.5:1. The volumes used were adjusted based on the amount of DNA and Lipofectamine:DNA ratio used.

2.6.3. FuGENE transfection

The day before transfection cells were plated at such a density (30-35% confluent for H1299) so that they were approximately 85% confluent before transfection.

Before transfection, SF medium, FuGENE and DNA were equilibrated to room temperature. For one well of a 6-well plate 1 μg of DNA was diluted in 100 μl of SF medium. 3 μl of FuGENE was then added to the diluted DNA (making sure that FuGENE does not come in contact with the walls of the tube). The transfection mixture was mixed by flicking the tube with a finger and incubated for 15 min. at room temperature. The entire transfection mixture was then added drop-wise to cells in complete growth media, distributing the drops over the entire dish surface. The dish was then rocked gently to ensure even distribution of the liposome complexes and the cells were incubated at 37°C, 5% CO_2. The cells were analysed 24 hours post transfection.

The FuGENE:DNA ratio used in the above example was 3:1. The volumes used were adjusted based on the amount of DNA and FuGENE:DNA ratio used.

2.6.4. Nucleofection

The day before nucleofection UM-SCC-12 cells were sub-cultured so that they were approximately 70-85% confluent before nucleofection. A protocol for nucleofection of UM-SCC-14A cells (a cell type similar to UM-SCC-12) was found in Lonza's cell line database and tested on UM-SCC-12.

On the day of nucleofection a 6-well plate with 1.5 ml of complete growth media per well was placed in the incubator to prewarm the media. The Nucleofector Solution, supplement and DNA were equilibrated to room temperature.

The cells were harvested by trypsinization and counted using the Z2 Coulter Particle Count and Size Analyzer (Beckman Coulter). 1×10^6 cells were then aliquoted in separate 15 ml polypropylene centrifuge tubes (Corning) and pelleted by centrifugation at 90×g for 10 min. at room temperature. The media was then aspirated and one pellet was resuspended in complete growth media and transferred directly into one well of the prewarmed 6-well plate (untreated control). The remaining pellets were resuspended in 100 µl of Nucleofector mix (prepared freshly by combining 82 µl Nucleofector Solution V with 18 µl of supplement) each. 3 µg of DNA was then added to the cell suspensions and the mixtures were transferred to individual nucleofection cuvettes, making sure that the sample covered the bottom of the cuvette and no air bubbles were present. One sample was kept without DNA (untransfected control). The cuvettes were then inserted into the Cuvette Holder of the Nucleofector™ II Device (Lonza) and the U-031 program was applied by pressing the X-button. Extra care was taken to ensure that the cells did not stay in the Nucleofector mix for more than 15 min., as this can reduce cell viability and transfection efficiency. Approximately 500 µl of the prewarmed culture medium was added to each of the cuvettes using a supplied sterile Pasteur pipette and the samples were gently transferred into the prepared 6-well plate avoiding repeated aspiration of the samples. The cells were then incubated at 37°C, 5% CO_2 and analysed 18 hours post nucleofection.

2.6.5. siRNA delivery

The day before transfection with siRNA, cells were plated into 10 cm dishes at such a density (30% confluent for UM-SCC-12) so that they were approximately 40% confluent before transfection.

On the day of transfection, the media on the 10 cm dishes was aspirated and replaced with 6.4 ml of complete growth media (to obtain a final volume of 8 ml after adding the transfection mixture). Before transfection, SF Opti-MEM medium and Lipofectamine were equilibrated to room temperature, siRNA was thawed just before transfection. Cells were transfected with siRNA at a final concentration of 40 nM. For one 10 cm dish 320 pmoles of siRNA was diluted in 800 µl of SF Opti-MEM medium and 16 µl of Lipofectamine was diluted in 800 µl of SF Opti-MEM medium. The mixtures were incubated for 5 min. at room temperature. Following the incubation the diluted siRNA and Lipofectamine were combined. The transfection mixture was mixed by flicking the tube with a finger and incubated for 20 min. at room temperature. The entire transfection mixture (1.6 ml) was then added drop-wise to cells in 6.4 ml of complete growth media, distributing the drops over the entire dish surface, resulting in a final volume of 8 ml and a 40 nM final concentration of siRNA. The dish was then rocked gently to ensure even distribution of the liposome complexes and the cells were incubated at 37°C, 5% CO_2. The media was changed and replaced with 10 ml of complete growth media 6 hours post transfection. The cells were analysed 48 hours post transfection.

The following siRNAs were used:

p53 (5'-GGA CAU ACC AGC UUA GAU U-3') – as described in reference (467),

MDM2 (5'-GCC ACA AAU CUG AUA GUA U-3') – synthesized by Dharmacon,

scrambled (5'-GGA CGC AUC CUU CUU AAU U-3') – synthesized by Dharmacon.

2.7. Bradford assay

Cells were harvested by trypsinization and pelleted by centrifugation at 300×g for 5 min. The pellets were washed with 1 ml of PBS and the cells were pelleted by

centrifugation as previously. The pellets were frozen at -80°C prior to further processing.

SLIP (Stuart Linn Immunoprecipitation) buffer

Concentration	**Reagent**
50 mM	HEPES, pH 7.5
150 mM	NaCl
10% (v/v)	glycerol
0.1% (v/v)	Triton X-100

Protein sample loading buffer (4×)

Concentration	**Reagent**
250 mM	Tris, pH 6.8
8% (w/v)	SDS
40% (v/v)	glycerol
4 mg/ml	bromophenol blue
1% (v/v)	β-mercaptoethanol

2.7.1. Preparation of protein standards

SLIP buffer was supplemented with protease inhibitors: aprotinin (2 µg/ml), leupeptin (0.5 µg/ml), pepstatin A (1 µg/ml), soybean trypsin inhibitor (100 µg/ml) and phenylmethylsulfonyl fluoride (1 mM). 20 mg of BSA was dissolved in 1 ml of SLIP buffer. A serial dilution was then made to obtain the following BSA concentrations: 10 mg/ml, 5 mg/ml, 2.5 mg/ml, 1.25 mg/ml, 0.6 mg/ml and 0.3 mg/ml. 2 µl of the standards were then added to 1 ml of protein assay dye reagent (diluted 1:5 with H_2O). 2 µl of the SLIP buffer was also added to 1 ml of protein assay dye reagent and used as a blank. A standard curve was prepared on the BioPhotometer (Eppendorf)

using the Bradford program, which measures absorbance at 595 nm. The calibration was considered acceptable if the obtained CV was below 5.

2.7.2. Protein extraction and quantification

Cell pellets were lysed on ice in SLIP buffer supplemented with protease inhibitors (as above). After incubation on ice for 10 minutes, the lysates were centrifuged at 16,000×g for 10 min. at 4°C and the supernatants were transferred to fresh tubes. 2 µl of the lysates were then added to 1 ml of protein assay dye reagent and the protein concentrations were determined based on the prepared standard curve.

Typically, 50 µg of total protein was then made up in sample loading buffer (final concentration of the buffer 1×) to a total volume of 20 µl.

2.8. SDS-PAGE (polyacrylamide gel electrophoresis)

Tris-Glycine electrophoresis buffer (running buffer)

Concentration	**Reagent**
25 mM	Tris
250 mM	glycine
0.1% (w/v)	SDS

Table 2.1: Composition of SDS-PAGE gels (volumes needed for 2 gels).

Reagent	**Resolving gel**		**Stacking gel**
	10%	**12%**	
40% acrylamide mix	2 ml	2.4 ml	510 µl
1.5 M Tris, pH 8.8	2 ml	2 ml	—
1 M Tris, pH 6.8	—	—	500 µl
10% SDS	80 µl	80 µl	40 µl
H_2O	3.83 ml	3.43 ml	2.9 ml
TEMED	6.4 µl	6.4 µl	4 µl
10% APS	80 µl	80 µl	40 µl

The percentage of acrylamide in the resolving gel was chosen based on the size of proteins to be analysed. The glass slides for making 0.75 mm thick gels were assembled and the resolving gel was poured into the sandwich, overlaid with water and allowed to polymerize. After the gel had set, the water was poured off and the stacking gel was poured, a comb inserted and the gel allowed to polymerize. Following polymerization, the comb was removed and the glass sandwich was placed in an electrophoresis tank filled with running buffer.

The protein samples were denatured by boiling for 5 min, vortexed, spun down and placed on ice. Typically 50 µg of total protein in 1× sample loading buffer was loaded on the gel alongside a pre-stained protein marker. SDS-PAGE was performed using a two-gel Mini-PROTEAN® Tetra cell (Bio-Rad) at 200 V for 1 hour.

2.9. Silver Staining

After resolving proteins on SDS-PAGE, it is possible to visualize them by staining with silver. Silver staining is very sensitive and can detect as little as nanogram quantities of protein (468). Silver Stain Plus Kit (Bio-Rad) was used for this purpose.

Fixative Enhancer Solution

Reagent	**Volume** (1 gel)
Reagent Grade Methanol	10 ml
Reagent Grade Acetic Acid	2 ml
Fixative Enhancer Concentrate	2 ml
H_2O	6 ml

Staining Solution

Reagent	**Volume** (1 gel)
H_2O	3.5 ml
Silver Complex Solution	0.5 ml
Reduction Moderator Solution	0.5 ml
Image Development Reagent	0.5 ml
Development Accelerator Solution	5 ml

The components were added in the indicated order.

All the reagents were prepared freshly immediately before use. Development Accelerator Solution was prepared by dissolving 0.5 g of Development Accelerator Reagent in 10 ml of H_2O.

Following SDS-PAGE the gel was transferred to a clean tray and incubated in the Fixative Enhancer Solution with gentle agitation for 20 min. The solution was then decanted and the gel was rinsed in 20 ml of H_2O for 10 min. with gentle agitation. The water was decanted and the rinse step was repeated. The gel was then placed in the Staining Solution and incubated with gentle agitation until the desired staining intensity was reached. The staining was stopped by placing the gel in 5% (v/v) acetic acid solution and incubating for 15 min. with gentle agitation. Afterwards, the gel was rinsed in H_2O for 5 min., scanned and dried using a Model 543 Gel Dryer (Bio-Rad) attached to a LABOPORT® Vacuum Pump (KNF Neuberger).

2.10. Western blotting

Western blotting is a technique, which allows for detection of specific proteins in the studied sample. Proteins are first separated by size using SDS-PAGE and then

transferred to a membrane, which is probed with antibodies specific to the proteins of interest.

Transfer Buffer

Concentration	**Reagent**
25 mM	Tris
192 mM	glycine
20% (v/v)	methanol

PBS/Tween

Concentration	**Reagent**
65 mM	$Na_2HPO_4 \cdot 2H_2O$
15 mM	$NaH_2PO_4 \cdot 2H_2O$
75 mM	NaCl
0.1 % (v/v)	Tween 20

Ponceau S solution

Concentration	**Reagent**
0.2% (w/v)	Ponceau S
5% (v/v)	acetic acid

Following SDS-PAGE proteins were transferred onto a Hybond ECL nitrocellulose membrane using the Mini Trans-Blot® Electrophoretic Transfer Cell (Bio-Rad). The gel was removed from between the glass slides onto pre-wetted Whatman paper. The nitrocellulose membrane was placed gently over the gel making sure that no air bubbles were trapped in between. It was then covered with another piece of Whatman paper, placed between a pair of sponges and inserted into the blotting cassette. The cassette was placed in the tank along with an ice pack (to prevent overheating during

the transfer) and the tank was filled with transfer buffer. The transfer was performed at 100 V for 1 hour. Following the transfer, the membrane was stained briefly with Ponceau S and rinsed with H_2O to check whether the transfer of proteins was successful. The membrane was destained briefly in PBS/Tween and blocked in 5% (w/v) non-fat dry milk in PBS/Tween solution at 4°C overnight (to prevent non-specific binding of antibodies to the membrane).

The membrane was sliced into strips based on the size of studied proteins as required and incubated with primary antibodies (in 5% milk-PBS/Tween solution) for 1 hour at room temperature. The membranes were then washed thrice for 15 min. in PBS/Tween. The horseradish peroxidase (HRP)-conjugated secondary antibodies (in 5% milk-PBS/Tween solution) were then applied and the membranes were incubated for 1 hour at room temperature. The membranes were washed 3 times as previously. All the incubation and washing steps were performed on a shaker with gentle agitation. Following the final wash, the membranes were transferred to dry trays and the Western Lightning *Plus*-ECL chemiluminescence reagent was applied for 1 min. The signal was detected by chemiluminescence and recorded using a Kodak IM4000 image station.

The primary antibodies used included:

- anti-actin antibody C-2 (sc-8432, Santa Cruz Biotechnology) – 3 μg/ml; a mouse monoclonal antibody, which recognizes an epitope within amino acids 350-375 of human actin,
- anti-Bcl-2 antibody 124 (M0887, DakoCytomation) – 1:100 dilution, a mouse monoclonal antibody raised against a synthetic peptide comprising amino acids 41-54 of human Bcl-2,

- anti-GFP antibody (Roche) – 0.4 μg/ml; a mixture of two mouse monoclonal antibodies (from clone 7.1 and 13.1) raised against partially purified GFP from *Aequorea victoria*,
- anti-MDM2 antibody IF2/Ab-1 (OP46T, Calbiochem) – 3 μg/ml; a mouse monoclonal antibody, which recognizes an epitope within amino acids 26-169 of human MDM2,
- anti-MDMX goat polyclonal antibody D-19 (sc-14738, Santa Cruz) – 3 μg/ml; a goat polyclonal antibody, which recognizes an epitope within an internal region of human MDMX,
- anti-MTBP antibody T-14 (ProMab Biotechnologies) – 3 μg/ml; a mouse monoclonal antibody raised against recombinant MTBP by ProMab Biotechnologies using their standard protocol for monoclonal antibody production (469),
- anti-p21 antibody F-5 (sc-6246, Santa Cruz Biotechnology) – 3 μg/ml; a mouse monoclonal antibody raised against amino acids 1-159 representing full-length p21 of mouse origin, cross-reacts with human p21,
- anti-p53 antibody DO-1/Ab-6 (OP43, Calbiochem) – 3 μg/ml; a pantropic mouse monoclonal antibody, which recognizes an epitope within amino acids 21-25 of human p53,
- anti-p53 antibody (ab2433, Abcam) – 3 μg/ml; a rabbit polyclonal antibody raised against a synthetic peptide comprising amino acids 277-296 of human p53,
- anti-Tmod3 antibody (R5168) – 3 μg/ml; a rabbit polyclonal antibody raised against recombinant human Tmod3; the antibody was a kind gift from Prof. Velia Fowler (The Scripps Research Institute).

The secondary antibodies used were HRP-conjugated and included:

- sheep anti-mouse antibody (RPN4201, GE Healthcare) – used at a 1:2500 dilution,
- donkey anti-rabbit antibody (NA934, GE Healthcare) – used at 1:5000 dilution,
- rabbit anti-goat antibody (305-036-003, Jackson ImmunoResearch Laboratories) – used at a 1:20,000 dilution.

2.10.1. Densitometry

Wherever indicated signal intensity was estimated by performing densitometry. Kodak Molecular Imaging Software v. 4.0.3K1 was used for this purpose. When collecting data, the software records intensity value for each pixel. The areas for analysis were defined by creating manual regions of interest (ROIs) on the image using the ROI Rectangle tool. Volume measurement was then performed by the software using the recorded pixel information. One of the ROIs was selected on a blank part of blot (without any samples) and used as background. The signal intensity for each sample was calculated by subtracting the sum intensity of the blank ROI from the sum intensity (the sum of all the pixel intensities within the ROI, including the background) of each of the sample ROIs.

2.11. Dual-luciferase reporter assays

Luciferase reporter assays are a commonly used technique to study eukaryotic gene expression. In dual-reporter assays the simultaneous expression of two individual reporter enzymes is measured within a single system. Typically, one reporter enzyme reflects the specific experimental conditions and the other serves as a baseline control

and can indicate whether the transfection efficiency between different conditions was equal.

The Dual-Luciferase® Reporter 1000 Assay System (Promega) was used for performing dual-reporter assays (as descriebd previously (470)). In this assay, the activities of firefly luciferase (from *Photinus pyralis*) and *Renilla* luciferase (from *Renilla reniformis* also known as sea pansy) are measured sequentially from a single sample. It is possible to distinguish between the respective bioluminescent reactions of firefly and *Renilla* luciferases due to different structures and substrate requirements of these two enzymes. None of these enzymes requires post-translational modifications for its enzymatic activity and hence they can function as genetic reporters immediately following translation. Firefly luciferase catalyzes a luminescent reaction, in which photon emission is achieved through oxidation of beetle luciferin to oxyluciferin. *Renilla* luciferase catalyzes a luminescent reaction, in which light is generated as a result of oxidation of coelenterazine (coelenterate-luciferin) to coelenteramide. In this assay, the firefly and *Renilla* luciferase reactions produce stabilized luminescence signals, which decay slowly over time. Both reporters yield linear assays, which are extremely sensitive (ranging from sub-attomole amounts of enzyme per reaction over seven orders of magnitude).

For reporter assays, cells were seeded into 6-well plates and co-transfected with 1.2 µg of pp53-TA-luc (firefly luciferase), 0.12 µg of pRL-TK (*Renilla* luciferase) and 0.3 µg of pSUPER.GFP per well (constructs described in detail in section 2.4.10). 24 hours post transfection the cells were lysed on plates by adding 500 µl of Passive Lysis Buffer (diluted 1:5 in H_2O) per well and incubating the plates for 10 min. at room temperature with gentle agitation. Passive Lysis Buffer promotes rapid lysis of cultured mammalian cells, provides optimum stability of the firefly and *Renilla*

luciferases as well as minimum background luminescence. The lysates were transferred into microcentrifuge tubes and centrifuged for 1 min. at 16,000×g at 4°C. The supernatants were then transferred into fresh microcentrifuge tubes. The firefly luciferase signal was measured first. 100 µl of LAR II (Luciferase Assay Reagent II) was placed in a fresh tube. 20 µl of the sample was added, the tube was vortexed for 1 sec. and luminescence was measured at 560 nm in a Glomax 20/20 luminometer (Turner BioSystems). The reaction was then quenched and the *Renilla* luciferase reaction was initiated by adding 100 µl of Stop & Glo® Buffer (supplemented with 50× Stop & Glo® Substrate). The tube was vortexed for 5 sec. and the *Renilla* luciferase activity was measured with an integration period of 10 sec. The results were normalised to protein concentrations in the samples, which were measured using a microBradford assay. A microBradford assay was performed analogically to Bradford assay (described in section 2.7) with the following BSA concentrations prepared by serial dilution and used for calibration: 5 mg/ml, 2.5 mg/ml, 1.25 mg/ml, 0.625 mg/ml, 0.313 mg/ml, 0.156 mg/ml and 0.078 mg/ml.

2.12. In situ β-galactosidase assay

In situ β-galactosidase staining was used for determination of transfection efficiency. Cells were transfected with pβ-gal containing the lacZ gene, which encodes β-galactosidase. β-galactosidase cleaves X-Gal into galactose and 5-bromo-4-chloro-3-hydroxyindole, which upon oxidation forms an insoluble blue product. Therefore, the cells, which were transfected with pβ-gal and express β-galactosidase will turn blue.

Substrate Buffer

Concentration	**Reagent**
3 mM	potassium ferrocyanide
3 mM	potassium ferricyanide
1 mM	magnesium chloride
2% (w/v)	X-Gal

24 hours post transfection the cells were washed in PBS and fixed using Fixing Buffer (0.5% (v/v) glutaraldehyde in PBS) for 15 minutes at room temperature. Following the incubation the Fixing Buffer was removed, the cells were washed twice with PBS and incubated in Substrate Buffer overnight at 37°C, 5% CO_2. The following day the Substrate Buffer was removed, the cells were washed twice in H_2O and the plates were dried.

2.13. Establishing stable cell lines

2.13.1. Stable cell lines expressing TAP-tagged forms of p53

In order to study protein interactions of the two mutant forms of p53 in laryngeal cancer, large numbers of UM-SCC-12 cells expressing TAP-tagged p53-175H and p53-273H were required. Given the low transfection efficiency of UM-SCC-12, establishing lines with a stable expression of the p53 mutants was attempted.

To determine the optimal concentration of G418 antibiotic to be used for selection, UM-SCC-12 cells were grown in the presence of G418 at the following concentrations: 100μg/ml, 200μg/ml, 400μg/ml, 800μg/ml, 1000μg/ml. The concentration of the selective marker that killed all the cells in approximately 12 days was chosen.

For establishing stable cell lines, UM-SCC-12 cells were transfected with pNTAP-B.p53, pNTAP-B.p53-175H or pNTAP-B.p53-273H using FuGENE at a ratio 3:1. Stable clones were selected by growing the transfected cells in full growth medium containing 400 μg/ml G418. After individual colonies were formed, they were picked using a sterile pipette tip containing 5 μl of trypsin, transferred to 24-well plates and expanded. Following selection, the G418 concentration was reduced to 200 μg/ml for maintenance of the stable clones. The clones were screened by western blotting for the expression of the TAP-tagged p53 proteins.

2.13.2. Stable p53-knock-down cell lines

Following the generation of UM-SCC-12 clones expressing the TAP-tagged p53-175H or TAP-tagged p53-273H, a stable knock-down of p53 expression in these clones was attempted to determine whether the results observed in the generated mutant p53-expressing clones are due to mutant p53 and to exclude the possibility of clonal variation.

To determine the optimal concentration of selective marker to be used for selection, UM-SCC-12 cells were grown in the presence of Puromycin at the following concentrations: 0.2μg/ml, 0.4μg/ml, 0.6μg/ml, 0.8μg/ml, 1μg/ml. The concentration of the selective marker that killed all the cells in approximately 5 days was chosen.

For establishing stable cell lines, UM-SCC-12 clones were transfected with pSUPER.puro.shp53 or pSUPER.puro.shScr using FuGENE at a ratio 3:1. Stable clones were selected by growing the transfected cells in full growth medium containing 0.5 μg/ml Puromycin. Following the selection, the Puromycin concentration was reduced to 0.25 μg/ml for maintenance of the stable clones. The

clones were screened by western blotting for the expression of the TAP-tagged p53 proteins.

2.14. Live imaging of cell migration

Live cell imaging is a technique that allows for long-term observation of living cells and analysis of cell migration. Over the course of an experiment the cell culture vessel is kept in a microscope chamber, which is heated to 37°C and the cells are supplied with a humidified CO_2-containing atmosphere (see Figure 2.1 for an illustration of the microscope chamber setup).

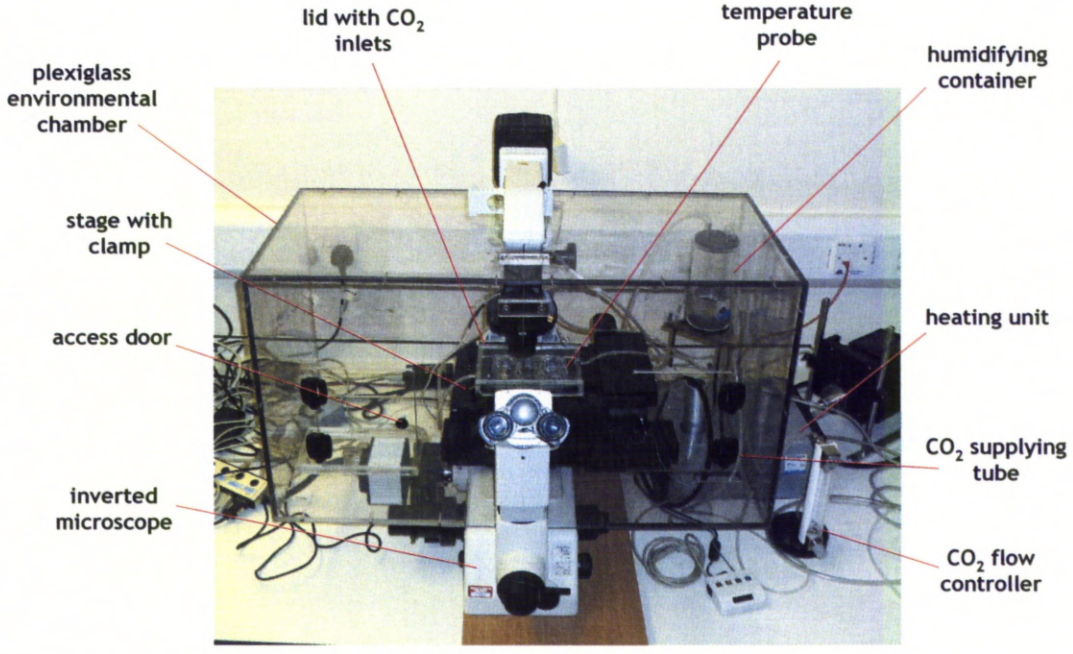

Figure 2.1. Microscope configuration for live-cell imaging. The culture plate (typically a 6-well plate) with cells was inserted into the plexiglass environmental chamber through the access door and fitted on the stage with a clamp. The temperature probe was inserted into the water-filled space of the plate in-between the wells. CO_2 was passed through a jar with water placed over the heating unit to facilitate evaporation and this humidified CO_2 was delivered to the plate through two inlets in the lid.

Typically, between 150,000 and 200,000 cells were seeded per well of a 6-well plate one day before the start of the experiment. On the day of the experiment the microscope chamber was pre-heated to 37°C. The media was replaced with 6 ml of fresh full growth media per well and 2 ml of H_2O was placed in the spaces between the wells to minimise evaporation. The cell culture plate was placed inside the microscope chamber and the temperature probe was placed in the water-containing space between the wells. The CO_2 supply was switched on and imaging was started.

A few positions (2-3) were selected per well and these were imaged with a time-lapse of 3 min. for 12 to 24 hours using Simple PCI software (Hamatsu Corporation). The recorded images were then combined to create movies.

The motility of cells was analysed using ImageJ software (National Institutes of Health). Plugins enabling tracking of individual cells were written by Dr Carlos Rubbi (University of Liverpool). Between 20 and 50 cells per condition were selected and tracked. The following parameters were determined and compared:

- total distance travelled – the length of the entire track of each cell,
- net distance travelled – distance in straight line between the first and last position of each cell,
- speed – total distance travelled divided by the duration of experiment in minutes,
- directionality – net distance travelled divided by total distance travelled.

2.14.1. Live imaging of migration in cells manipulated by RNAi

Transfection with siRNA was performed as described in section 2.6.5. 6 hours post transfection the media was changed and replaced with full growth media. 8 hours post transfection the cells were trypsinized and counted. Two 6-well plates were prepared for live imaging to ensure that the cells did not become overconfluent during the

imaging, which could affect motility. One plate was seeded with 200,000 cells per well (one well per condition) to be imaged 24-36 hours post transfection and 175,000 cells per well (one well per condition) were seeded into another plate to be imaged 36-48 hours post transfection. Imaging was performed as described in section 2.14.

The remaining cells from each condition were seeded into 6-well plates (one plate per condition) distributing the cells evenly between all wells. 3 wells per condition were harvested for a western blot in the middle of each of the imaging intervals (at 30 hours and 42 hours post transfection, respectively) to determine the knock-down efficiency.

2.15. Boyden chamber migration assays

The Boyden chamber migration assay measures the migratory potential of cells as determined by their ability to migrate from one medium-filled compartment to another through a microporous membrane.

BD Falcon™ Cell Culture Inserts for 24-well plates with a membrane containing 8.0 μm pores at a density of $6 \pm 2 \cdot 10^4$ per cm^2 (BD Biosciences) were used for migration assays. The cell culture inserts were placed in a 24-well Companion Plate (BD Biosciences) containing 600 μl of full growth media. Typically, 15,000 cells in 300 μl of full growth media were seeded into the insert and the plate was incubated at 37°C, 5% CO_2 for 18 hours. Following incubation the inner side of the insert was scraped rigorously with a cotton bud to remove all the cells that did not migrate through the porous membrane. The inside of the insert was further washed with a cotton bud soaked in PBS. The cells that migrated through the membrane were fixed and stained using the REASTAIN Quick-Diff Kit. The cells were first fixed by

placing the cell culture insert in a well with 500 µl of REASTAIN Quick-Diff Fix solution for 10 min. The insert was then stained with 500 µl of REASTAIN Quick-Diff Red solution for 2 min., followed by a 2 min. staining with 500 µl of REASTAIN Quick-Diff Blue solution. The inserts were then rinsed in a large volume of H_2O and left upside down on a piece of towel to dry.

Once the cell culture inserts were completely dry, the membranes were excised from the inserts using a sharp scalpel blade and mounted on a microscope glass slide under a cover slip using DPX Mountant. The slides were allowed to dry and the cells that migrated through the membrane were counted using a phase contrast microscope.

2.16. Boyden chamber invasion assays

The Boyden chamber invasion assay enables to study invasiveness of cells *in vitro* as determined by their ability to penetrate through a reconstituted basement membrane and migrate from one medium-filled compartment to another (containing chemoattractant) through a microporous membrane.

BD BioCoat™ Matrigel™ Invasion Chambers for 24-well plates with a membrane containing 8.0 µm pores (BD Biosciences) were used for invasion assays. The membrane of the invasion inserts is coated with a thin layer of Matrigel Matrix, serving as a reconstituted basement membrane, which completely occludes the pores of the membrane. Therefore, only the cells, which are capable of invading through the Matrigel Matrix can migrate through the membrane pores.

The invasion inserts were removed from -20°C storage and allowed to warm to room temperature. They were then placed in a 24-well Companion Plate and 500 µl of pre-warmed SF bicarbonate-based media was added to the interior of the inserts and the wells. The chambers were allowed to rehydrate for 2 hours in a humidified tissue culture incubator (37°C, 5% CO_2).

Towards the end of the incubation period the cells were harvested by trypsinization and pelleted by centrifugation at 90×g for 10 min. at room temperature. The media was aspirated and the cells were resuspended in DMEM supplemented with 0.1% FBS, 1% L-glutamine and 1% Non-Essential Amino Acids.

The Companion Plate was removed from the incubator. The media from the inside of the inserts was aspirated gently without disturbing the layer of Matrigel. The inserts were then transferred to fresh wells containing 750 µl of full growth media (with 10% FBS serving as a chemoattractant). 50,000 cells in 500 µl of media containing 0.1% FBS (thus generating a serum gradient) were then seeded into the inserts and the plate was incubated at 37°C, 5% CO_2 for 30 hours. Following the incubation the inner side of the inserts was scraped rigorously with a cotton bud to remove all the cells that did not migrate through the porous membrane. The inside of the inserts was further washed with a cotton bud soaked in PBS. The inserts were then placed in a well with 500 µl of REASTAIN Quick-Diff Fix solution (methanol) for 10 minutes to fix the cells that migrated through the membrane. The inserts were then stained with 500 µl of 0.5% Crystal Violet solution for 30 min. The inserts were rinsed in a large volume of H_2O and left upside down on a piece of towel to dry.

Once the cell culture inserts were completely dry, the membranes were excised from the inserts using a sharp scalpel blade and mounted on a microscope glass slide under a cover slip using DPX Mountant. The slides were allowed to dry and the cells that migrated through the membrane were counted using a phase contrast microscope.

2.17. RNA isolation and quality testing

In order to study gene expression in UM-SCC-12 cells (p53-null) and UM-SCC-12 derivatives expressing high levels of the GOF p53 mutants (p53-175H or p53-273H)

total cellular RNA was extracted using the RNeasy Mini Kit. Briefly, cells are lysed in a buffer containing guanidine thiocyanate, which inactivates RNases and prevents RNA degradation. The total RNA is then bound to the silica membrane of the RNeasy column under high-salt conditions. The on-column DNase treatment allows for removal of the contaminating DNA, which is washed away along with other contaminants during the washes. High-quality RNA is then eluted in RNase-free H_2O. This procedure provides an enrichment for mRNA since RNA molecules smaller than 200 nucleotides (15-20% of total RNA) are selectively excluded. RNA purified using this method is suitable for downstream applications such as microarrays or qRT-PCR.

Typically, 3×10^6 cells were seeded into a tissue culture flask and incubated overnight. The following day the cells were harvested by trypsinization and pelleted by centrifugation at 300×g for 5 min. at room temperature. The media was aspirated and the cells were washed in 1 ml of PBS. The cells were centrifuged again at 300×g for 5 min. at room temperature and the supernatant was removed completely. The cells were lysed in 350 µl of Buffer RLT (for processing up to 5×10^6 cells) by pipetting up and down. The lysate was then pipetted directly into a QIAshredder spin column (to ensure complete homogenization) and the column was centrifuged for 2 min. at 16,000×g. 350 µl of 70% ethanol were then added to the homogenized lysate and mixed by pipetting. The sample was then transferred into an RNeasy spin column and centrifuged for 15 sec. at 8,000×g. The flow-through was discarded. The column was washed with 350 µl of Buffer RW1 and centrifuged for 15 sec. at 8,000×g. The flow-through was discarded. 80 µl of DNase I incubation mix, prepared directly before use by adding 10 µl of DNase I to 70 µl of Buffer RDD, was then pipetted into the centre of the column membrane and incubated for 15 min. at room temperature. Following the incubation 350 µl of Buffer RW1 was added to the column, which was

then centrifuged for 15 sec. at 8,000×g. The flow-through was discarded. The column was then washed with 500 µl of Buffer RPE and centrifuged for 15 sec. at 8,000×g. The flow-through was discarded. The column was washed again with 500 µl of Buffer RPE and centrifuged for 2 min. at 8,000×g. The column was then placed in a fresh collection tube and centrifuged for 1 min. at 16,000×g. The column was then transferred to a 1.5 ml RNase-free microcentrifuge tube, 30-50 µl of RNase-free H_2O was pipetted directly onto the column membrane and the RNA was eluted by centrifugation for 1 min. at 8,000×g.

RNA was quantified by spectrometry at 260 nm with a BioPhotometer using the RNA program. The integrity was tested by running 500 ng of total RNA on a 1% (w/v) agarose gel (prepared using GenSieve LE agarose).

2.18. Expression microarrays

Microarray technology enables monitoring of genome-wide expression levels of genes in a given organism. Thousands of DNA molecules (of known identity, called probes) are immobilised on a glass slide in a highly organised manner at specific positions known as features. A microarray may contain thousands of features, each containing a few million copies of identical probes that are unique to specific genes. Determining the gene expression levels is based on complementary binding between the unknown sequences and the probes.

First, RNA is extracted from cells or tissue. It is then reverse-transcribed and subjected to linear amplification to create sense strand cDNA. The sense strand cDNA is fragmented (to aid exon array hybridisation), providing a template for the synthesis of either reverse strand cDNA or cRNA, which is fluorescently labelled either directly, by incorporation of fluorescently labelled nucleotides, or in the case of single

colour microarrays, indirectly by the incorporation of biotinylated nucleotide residues. cRNA may be used because RNA-DNA hybridization is more stable (stronger) than DNA-DNA hybridization. The sample (cDNA or cRNA) is hybridized onto a microarray glass slide (chip). Immediately following hybridization, the array is washed and, if using biotinylated cDNA, the array is stained with streptavidin phycoerythrin conjugate. Phycoerythrin is derived from cyanobacteria and eukaryotic algae and exhibits extremely bright fluorescence. The labelled cDNA is then excited by a laser and the chip with the fluorescing features is scanned to quantify the emitted fluorescence, which corresponds to the amount of nucleic acid bound to the probes (and the initial mRNA present).

Expression profiles of mutant p53-expressing (p53-273H) laryngeal cancer cells (12-273H-39) were compared with parental UM-SCC-12 cells (p53-null). The RNA samples for each cell line were prepared in triplicate on three separate occasions. The microarray hybridization of biotinylated cDNA was performed using an Affymetrix GeneChip® Human Exon 1.0 ST Array (as described previously (471)) within the Cancer Research UK Affymetrix GeneChip Microarray Service hosted by the Molecular Biology Core Facility (Paterson Institute for Cancer Research). The array consisted of 5,362,207 features, used to investigate 1,084,639 exon clusters (collections of overlapping exons) with over 1.4 million probe sets (472). A probe set contains typically between 11 and 20 probe pairs, which interrogate the same sequence (e.g. a transcript). The probes were 25 bp long. Most of the exon-based probe sets contained 4 probes for each exon and there were approximately 40 probes per gene.

Following hybridisation, the microarray chip was scanned using a GeneChip® Scanner 3000 (Affymetrix). Affymetrix GeneChip Command Console software

(AGCC) was used to extract pixel intensities from the generated image and to calculate single intensity values for each gene. Data analysis was performed by Dr Bryony Lloyd (University of Liverpool). Quality control analysis was performed on the raw array data using Expression Console software (Affymetrix). Normalisation was performed to minimise systematic errors and ensure that the majority of observed differences are due to biological variation. The data was then analysed to identify differentially expressed genes and clustered to identify groups of co-regulated genes and the pathways involved.

The generated microarray data was MIAME compliant (Minimum Information About a Microarray Experiment) and was logged in a secure database known as MIAME VICE (measuring Variations In Cellular Expression) (473), which was written by the Bioinformatics Department at the Paterson Institute for Cancer Research.

2.19. Quantitative real-time PCR

The results obtained from the expression array analysis were validated using two-step quantitative real-time PCR (qRT-PCR). qRT-PCR was performed by members of the Applied Biology team (led by Prof. D. Ross Sibson and Dr Bryony Lloyd, University of Liverpool). Data analysis was performed by Dr Bryony Lloyd.

2.19.1. Reverse transcription

1.5 μg of total RNA was reverse transcribed using a SuperScript™ First-Strand Synthesis System for RT-PCR (Invitrogen) according to manufacturer's instructions. The following mixture was prepared.

Component	**Volume**
total RNA (1.5 µg)	*n* µl (depending on the RNA concentration)
50 µM oligo(dT)$_{20}$	1 µl
10 mM dNTP mix	1 µl
DEPC-treated water	up to a total volume of 10 µl

The mixture was incubated at 65°C for 5 min. and then placed on ice for at least 1 min. The cDNA Synthesis Mix was prepared by combining the following components in the indicated order.

Component	**Volume** (1 reaction)
10× RT buffer	2 µl
25 mM $MgCl_2$	4 µl
0.1 M DTT	2 µl
RNaseOUT (40 U/µl)	1 µl
SuperScript™ III RT (200 U/µl)	1 µl

10 µl of the cDNA Synthesis Mix was added to each RNA/primer mixture and incubated at 50°C for 50 min. The reaction was terminated by heating to 85°C for 5 min. and then chilled on ice. 1 µl of RNase H was added to each reaction and incubated at 37°C for 20 min.

Each RNA sample was reverse transcribed in duplicate and the no RT control was performed once per sample. A 1:20 dilution of the resulting cDNA and no RT control was prepared and stored at -20°C. 5 µl of the respective cDNA/no RT control was used for each qRT-PCR reaction.

2.19.2. Standard preparation

Genes of interest selected from the expression microarray data analysis were amplified by PCR from the cDNA using the primers and thermal cycling reaction

conditions listed in Appendix 1. The PCR products were cloned into pCR2.1 vector from the Topo TA cloning kit (Invitrogen). The identity of the PCR products was confirmed by direct sequencing using DYEnamicET Dye Terminator Cycle Sequencing Kit for MegaBACE (Amersham Biosciences) and analysed on a MegaBACE1000 (Amersham Biosciences). Once confirmed, plasmid purification was performed using the QIAPrep Spin Miniprep Kit (Qiagen). The DNA was quantified using NanoDrop ND-1000 (Thermo Scientific) and the following 7 standard amounts of each plasmid were prepared: 2×10^{3}, 2×10^{2}, 2×10^{1}, 2, 2×10^{-1}, 2×10^{-2} and 2×10^{-3} attomoles per reaction.

2.19.3. qRT-PCR

iQ™ SYBR® Green Supermix (Bio-Rad) was used for qRT- PCR (performed as described previously (474)). iQ SYBR Green Supermix is a 2× mix for real-time PCR application containing a 2× proprietary reaction buffer with dNTPs, iTaq DNA polymerase, 6 mM $MgCl_2$, SYBR Green I, fluorescein and stabilizers. The reactions were set up in 96-well PCR microplates by combining the following components.

Component	**Volume** (1 reaction)
2× iQ SYBR Green Supermix	10 µl
primer 1 (10 µM)	1 µl
primer 2 (10 µM)	1 µl
sterile water	3 µl
cDNA	5 µl
Final reaction volume:	20 µl

The final concentration of the primers was 500 nM. The qRT-PCR was carried out in triplicate for each reverse transcription (see Figure 2.2) and in duplicate for each no

RT control. The 7 concentrations of the standards (plasmid DNA containing the PCR product of interest) were also present in triplicate on each plate. The thermal cycling reaction conditions and primers used for each gene are included in Appendix 1. The qRT-PCR was performed using an iQ5 Multicolour Real-Time PCR Detection System (Bio-Rad).

2.19.4. Data analysis

The cycle number (C_T) at which the fluorescence passes a certain threshold was determined. C_T determined for the 7 standards was plotted against the log of the standard amounts to create a standard curve, from which the amount of product in the unknown samples could be determined. This was performed using the CFX Manager™ Software (Bio-Rad).

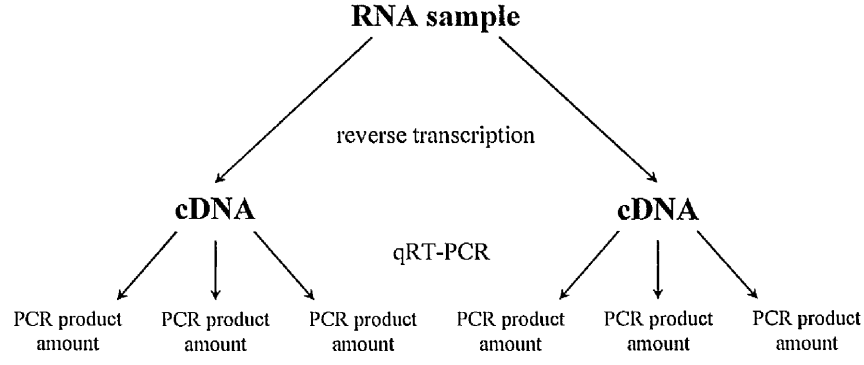

Figure 2.2: A schematic representation of the qRT-PCR experimental setup. Additionally, each RNA sample was present in triplicate.

Average values for each gene (for each transcription reaction separately) were determined. The results were normalised by dividing the average gene expression value by the average expression value of the reference gene (histone H3) for the corresponding reverse transcription reaction. This normalised relative value was then

averaged between the two reverse transcription reactions. Since the RNA samples were also present in triplicates, the normalised relative values for each gene were averaged between the triplicates and the standard deviation was calculated. The relative gene expression was obtained by dividing the gene expression level in the test sample (e.g. expressing mutant p53) by the gene expression level in the control sample (e.g. p53-null).

2.20. TAP-tag purification

Tandem affinity purification (TAP) is a technique, which enables purification of a protein complex of interest using two different affinity purification tags: streptavidin-binding peptide (SBP) and calmodulin-binding peptide (CBP). SBP is a synthetic sequence isolated from a random peptide library, which has a high affinity for streptavidin $\left(\sim 2\times10^{-9}\ \mathrm{M}\right)$ and can be specifically eluted with biotin (475). CBP is a peptide derived from a C-terminal fragment of skeletal muscle myosin light-chain kinase, which has a high affinity for calmodulin $\left(\sim 1\times10^{-9}\ \mathrm{M}\right)$ in the presence of calcium (476) and can be specifically eluted by removing calcium with a chelating agent (477). The lysate containing the tagged protein of interest is passed through two consecutive columns with streptavidin and calmodulin resins, respectively (Figure 2.3). The gentle washing and elution conditions allow for isolation of whole protein complexes without disrupting them. TAP-tag purification is a method of isolating highly purified protein complexes thanks to two rounds of specific binding and specific elution.

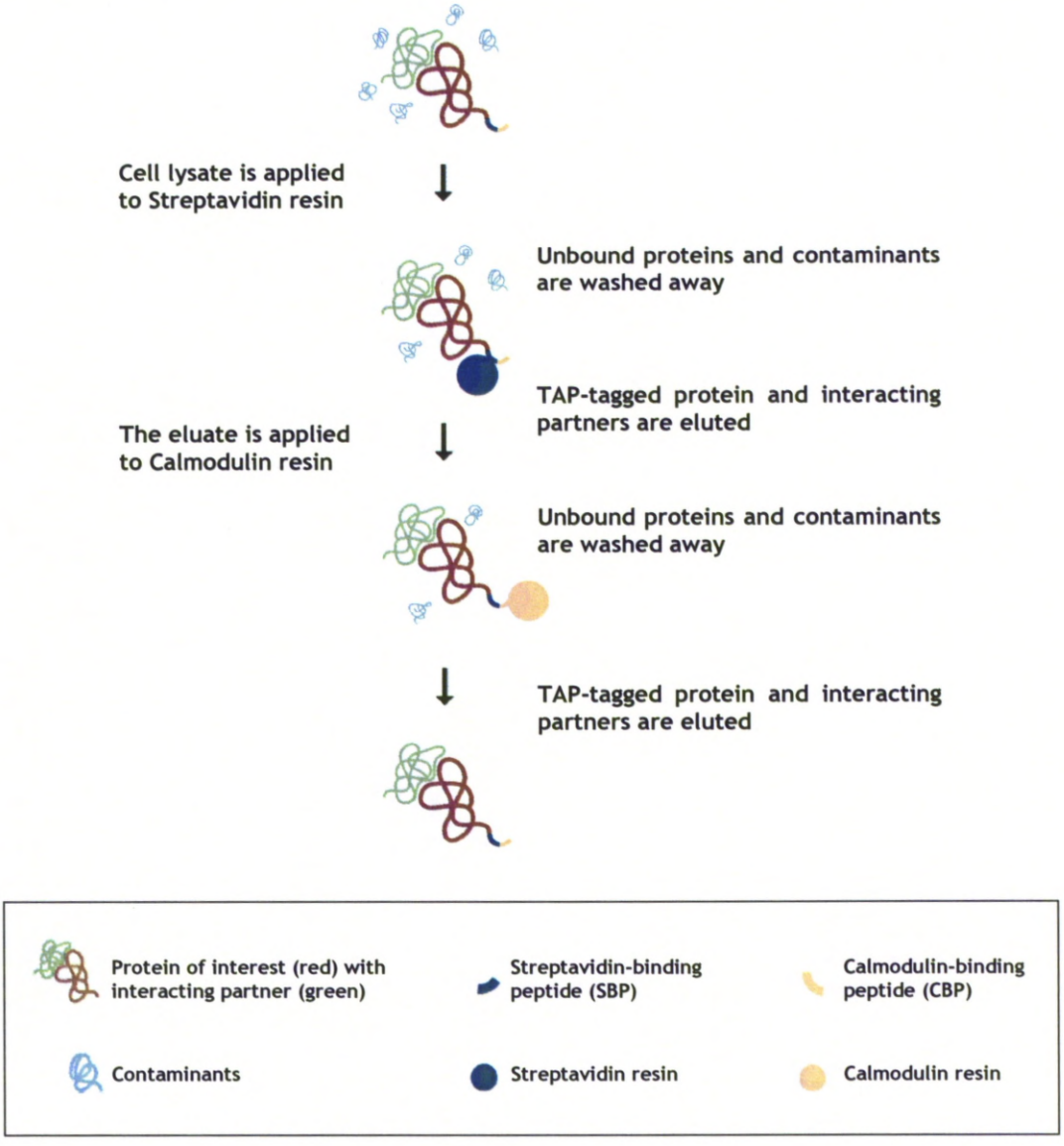

Figure 2.3: A schematic representation of the tandem affinity purification procedure.

The InterPlay Mammalian TAP System was used to isolate TAP-tagged p53-175H and p53-273H binding proteins according to the manufacturer's instructions. The reagents necessary for the purification were prepared directly before use and kept on ice. Lysis buffer was supplemented with protease inhibitors: aprotinin (2 µg/ml), leupeptin (0.5 µg/ml), pepstatin A (1 µg/ml), soybean trypsine inhibitor (100 µg/ml) and phenylmethylsulfonyl fluoride (1 mM). Streptavidin binding buffer (SBB),

streptavidin elution buffer (SEB) and calmodulin binding buffer (CBB) were supplemented with protease inhibitors (as described above) and β-mercaptoethanol (10 mM). Calmodulin elution buffer was supplemented only with β-mercaptoethanol (10 mM). All centrifugation steps were performed at 4°C and the samples were kept on ice at all times. Samples from each step of the purification were kept for analysis.

10×10^6 cells were lysed in 1 ml of the supplemented lysis buffer by three rounds of freeze-thawing. The lysate was centrifuged at 16,000×g for 10 min. at 4°C. The pre-cleared lysate was transferred to a fresh tube and supplemented with 4 µl of 0.5 M EDTA and 0.7 µl of 14.4 M β-mercaptoethanol.

50 µl of 50% streptavidin resin slurry was centrifuged for 5 min. at 1,500×g. The supernatant was discarded and the resin was washed twice with 1 ml of SBB followed by centrifugation for 5 min. at 1,500×g to collect the resin. The supernatant was discarded and the resin was resuspended in 25 µl of SBB.

The pre-cleared lysate was then incubated with the streptavidin resin for 2 h at 4°C on a Clay Adams Brand Nutator (Becton Dickinson). Following the incubation the resin was collected by centrifugation for 5 min. at 1,500×g and the supernatant was removed. The resin was washed twice with 1 ml of SBB and collected by centrifugation for 5 min. at 1,500×g. The bound proteins were eluted in 100 µl of SEB by rotating the tube for 30 min. at 4°C on a nutator. Following the incubation the resin was collected by centrifugation for 5 min. at 1,500×g. The eluate was transferred to a fresh tube and supplemented with 2 µl of streptavidin supernatant supplement and 400 µl of CBB.

25 µl of 50% calmodulin resin slurry was centrifuged for 5 min. at 1,500×g. The supernatant was discarded and the resin was washed twice with 1 ml of CBB followed

by centrifugation for 5 min. at 1,500×g to collect the resin. The supernatant was discarded and the resin was resuspended in 12.5 µl of CBB.

The supplemented streptavidin eluate was then incubated with calmodulin resin for 2 h at 4°C on a nutator. Following the incubation the resin was collected by centrifugation for 5 min. at 1,500×g and the supernatant was removed. The resin was washed twice with 1 ml of CBB and collected by centrifugation for 5 min. at 1,500×g. The bound proteins were eluted in 50 µl of CEB by rotating the tube for 30 min. at 4°C on a nutator. Following the incubation the resin was collected by centrifugation for 5 min. at 1,500×g. The eluate was transferred to a fresh tube.

The streptavidin and calmodulin resins used for purification were resuspended in a volume of 1× sample loading buffer (see section 2.7) equal to the volume of packed resin used (25 µl and 12.5 µl, respectively).

The eluted proteins were resolved by SDS-PAGE and analysed using Silver Staining and western blotting. The purified proteins were identified using nanospray mass spectrometry.

2.20.1. Optimisation of the TAP-tag purification procedure

Due to the very low efficiency of the original TAP-tag purification procedure (see section 3.6), optimisation was necessary. Since the composition of the buffers provided with the kit was proprietary, a different protocol (including buffer composition) was obtained from reference (478) and used as a starting point for optimisation. All the buffers prepared in the course of optimisation will be referred to as custom buffers.

Lysis buffer

Concentration	**Reagent**
10% (v/v)	glycerol
50 mM	HEPES
150 mM	NaCl
2 mM	EDTA
0.1% (v/v)	Triton X-100
2 mM	DTT
10 mM	NaF

Supplemented with protease inhibitors (as described previously).

Streptavidin elution buffer (SEB)

Concentration	**Reagent**
10 mM	β-mercaptoethanol
50 mM	HEPES
150 mM	NaCl
1 mM	MgAc
1 mM	imidazole
0.1% (v/v)	Triton X-100
2 mM $CaCl_2$	2 mM $CaCl_2$
10 mM	D-biotin

Calmodulin binding buffer (CBB)

Concentration	**Reagent**
10 mM	β-mercaptoethanol
50 mM	HEPES
150 mM	NaCl
1 mM	MgAc
1 mM	imidazole
0.1% (v/v)	Triton X-100
2 mM	$CaCl_2$

Calmodulin rinsing buffer (CRB)

Concentration	**Reagent**
50 mM	ammonium bicarbonate
75 mM	NaCl
1 mM	MgAc
1 mM	imidazole
2 mM	$CaCl_2$

Calmodulin elution buffer (CEB)

Concentration	**Reagent**
50 mM	Ammonium bicarbonate
25 mM	EGTA

The reagents necessary for the purification were prepared directly before use and kept on ice. The streptavidin and calmodulin resins provided with the InterPlay Mammalian TAP System were used also for the optimisation experiments. All centrifugation steps were performed at 4°C and the samples were kept on ice at all times. Samples from each step of the purification were kept for analysis.

10×10^6 cells were lysed in 1 ml of custom lysis buffer by rotating the tube for 15 min. at 4°C on a nutator and performing two rounds of freeze-thawing. The lysate was centrifuged at 16,000×g for 15 min. at 4°C. The pre-cleared lysate was transferred to a fresh tube.

20 µl of 50% streptavidin resin slurry was centrifuged for 1 min. at 800×g. The supernatant was discarded and the resin was washed twice with 800 µl of custom lysis buffer followed by centrifugation for 1 min. at 800×g to collect the resin. The supernatant was discarded leaving between 20 µl and 50 µl of buffer on the beads to prevent them from drying.

The pre-cleared lysate was then incubated with the streptavidin resin at 4°C overnight on a nutator. After the incubation the resin was collected by centrifugation for 1 min. at 800×g and the supernatant was removed. The resin was washed twice with 800 µl of custom lysis buffer, followed by three washes with 800 µl of custom CBB. The resin was then collected by centrifugation for 1 min. at 800×g, the supernatant was removed leaving some liquid on the beads. The bound proteins were eluted in 20 µl of custom SEB by rotating the tube for 30 min. at 4°C on a nutator. The resin was collected by centrifugation for 1 min. at 800×g, the eluate was transferred to a fresh tube and the elution was repeated with another volume of custom SEB. The eluates were pooled together and supplemented with 40 µl of custom CBB and 5 µl of 0.1 M $CaCl_2$.

20 µl of 50% calmodulin resin slurry was centrifuged for 1 min. at 800×g. The supernatant was discarded and the resin was washed twice with 800 µl of custom CBB followed by centrifugation for 1 min. at 800×g to collect the resin. The supernatant was discarded leaving some liquid on the beads to prevent them from drying.

The supplemented streptavidin eluate was then incubated with calmodulin resin for 2 h at 4°C on a nutator. The resin was washed twice with 800 µl of custom CBB, followed by three washes with 800 µl of custom CRB. The resin was then collected by centrifugation for 1 min. at 800×g, the supernatant was removed leaving some liquid on the beads. The bound proteins were eluted in 10 µl of custom CEB by rotating the tube for 30 min. at 4°C on a nutator. The resin was collected by centrifugation for 1 min. at 800×g, the eluate was transferred to a fresh tube and the elution was repeated with another volume of custom CEB. The eluates were pooled together.

The streptavidin and calmodulin resins used for purification were resuspended in a volume of 1× sample loading buffer (see section 2.7) equal to the volume of packed resin used (10 µl each).

The eluted proteins were analysed as described previously. The details of optimisation of the above procedures are described in section 3.6.

2.21. Mass spectrometry

Mass spectrometry (MS) is an analytical technique, which enables determination of the composition of a sample by measuring the mass-to-charge ratio (m/z) of charged particles. In this procedure a sample is loaded onto the MS instrument and undergoes vaporization. The sample then passes through an ionisation source, where it is bombarded with a beam of electrons (electrospray ionisation, ESI), which displace electrons from organic molecules to form radical cations (also called molecular ions). The collection of ions is accelerated into the magnetic field and deflected according to their mass-to-charge ratio within the mass analyzer. The separated ions are then detected along with their relative abundance by the detector and recorded. The ion signal is processed into mass spectra.

MS is also frequently combined with liquid chromatography (LC), which may be used to physically separate the compounds before they are introduced into the ionisation source. LC-MS is a highly sensitive technique oriented at specific detection and identification of components in a complex mixture.

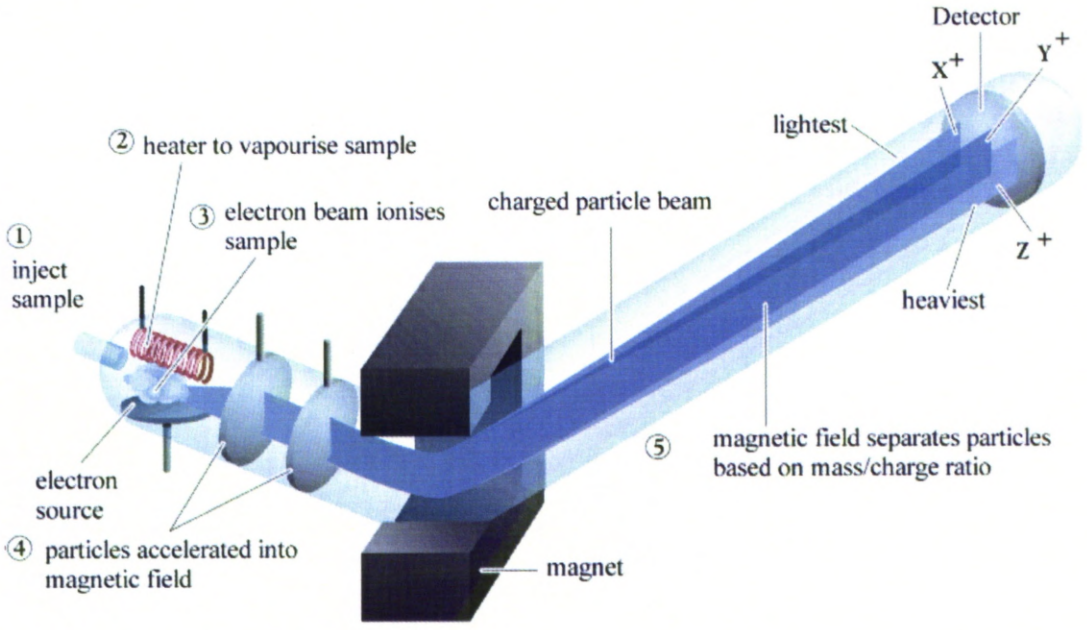

Figure 2.4: A diagrammatic representation of the operating principle of mass spectroscopy (adapted from reference (479)).

LC-ESI-MS/MS (as described previously (480)) was used to identify the binding partners of p53-175H and p53-273H in the protein complexes isolated using TAP-tag purification. The eluted proteins were precipitated by mixing one volume of 100% (w/v) TCA with four volumes of the sample (final TCA concentration 20%) and incubating on ice for 1 hour. The samples were centrifuged at 16,000×g for 10 min. at 4°C. The supernatant was discarded and the pellet was washed twice with ice-cold acetone. Following a centrifugation at 16,000×g for 5 min. at 4°C, the supernatant was discarded and the pellet was air-dried briefly. The pellets were resuspended in 20 µl of 50 mM ammonium bicarbonate and treated with 0.1 mM DTT for 15 min. at room temperature. They were then treated with 55 mM iodoacetamide for 15 min. at room temperature. Finally, the samples were treated with 250 ng of trypsin overnight at 37°C, to digest the purified proteins into peptides.

Following the trypsin digest, the samples were cleaned up using Zip-Tips (Millipore). A Zip-Tip is a 10 µl pipette tip with a small bed of chromatography

media fixed at its end, which is used for purifying protein, peptide and oligonucleotide samples to remove salts, buffers or detergents that could interfere with mass spectrometry. Briefly, 10 µl of a sample was transferred to a fresh tube and acidified by adding 1 µl of 1% (v/v) TFA. The Zip-Tip was wetted by pipetting 10 µl of 100% (v/v) ACN through it twice. It was then washed 3 times with 0.1% (v/v) TFA. The sample was bound to the Zip-Tip by pipetting it up and down approximately 10 times. The Zip-Tip was washed 3-5 times with 0.1% (v/v) TFA and the sample was eluted with 10 µl of 75% (v/v) ACN by pipetting it up and down 5-6 times.

Following clean-up using Zip-Tips the samples were delivered into an API QSTAR Pulsar *i* system (Applied Biosystems) by automated in-line chromatography, using an integrated LC Packings System and a PepMap™ 100 C18 column of 75 µm internal diameter × 15 cm long (Dionex), via a nanoelectrospray source head and a 10 µm internal diameter PicoTip (New Objective). The LC conditions were the following: 5% (v/v) ACN, 0.05% (v/v) TFA for 15 min; 5-45% (v/v) ACN, 0.05% (v/v) TFA for 60 min; 99% (v/v) ACN, 0.05 % (v/v) TFA for 10 min; 5% (v/v) ACN, 0.05% (v/v) TFA for 10 min; with a flow rate of 0.35 µl/min throughout. MS and MS/MS spectra were acquired using the Analyst QS software (Applied Biosystems). The proteins present in the purified complexes were identified with Protein Pilot software (Applied Biosystems) using the Paragon™ algorithm (481) and the most recent version of SwissProt database. The identified proteins were accepted if they fell within the 1% local false discover rate (FDR) and if at least two peptides were identified with a confidence >95%. The mass accuracy of each peptide ion was determined at 5-30 ppm (parts per million).

Mass spectroscopy and data analysis was performed by Dr Rosalind Jenkins (University of Liverpool).

2.22. Immunoprecipitation

Immunoprecipitation is a technique used to isolate protein complexes containing a protein of interest using an antibody specific for that protein. Immunoprecipitation coupled with SDS-PAGE and western blotting is frequently used to study protein-protein interactions.

Immunoprecipitation was performed to determine whether the mutant p53 interacting proteins identified by mass spectrometry in the complexes isolated by TAP-tag purification were present in protein complexes in cells.

H1299 cells were seeded into 15 cm dishes and transfected with 15 μg of p53, p53-175H, p53-273H or empty vector per dish. The cells were co-transfected with 15 μg of β-gal per well to estimate transfection efficiency. One day post transfection the cells were trypsinized and split into two 15 cm dishes per transfection with a small aliquot placed in a 6-well plate for *in situ* β-galactosidase assay.

SLIP buffer (with BSA)

Concentration	**Reagent**
50 mM	HEPES, pH 7.5
150 mM	NaCl
10% (v/v)	glycerol
0.1% (v/v)	Triton X-100
0.5 mg/ml	BSA

Supplemented with protease inhibitors (as described in section 2.7.1).

The following day the cells were harvested, lysed in SLIP buffer for 10 min. on ice and the lysates were clarified by centrifugation at 16,000×g for 10 min. at 4°C. The supernatants were transferred to fresh tubes and protein concentration in the samples was determined using Bradford assay. 4 mg of total protein was used for immunoprecipitation. The volume of the lysate was made up to 500 µl with SLIP buffer. All centrifugation steps were performed at 4°C and the samples were kept on ice at all times.

Protein G Sepharose beads (100 µl of 50% slurry per sample) were washed 3 times with 1 ml of SLIP buffer and collected by centrifugation at 16,000×g for 30 sec. After the last wash the beads were resuspended in SLIP buffer to obtain 50% slurry.

50 µl of the 50% slurry of Protein G Sepharose beads was then added to each protein sample. The tubes were incubated for 1 hour at 4°C on a nutator to remove the proteins that bind non-specifically to the beads. Following the incubation the beads were collected by centrifugation at 16,000×g for 30 sec. and the supernatants were transferred to fresh tubes.

2 µg of anti-p53 antibody Ab-1 (PAb421, Calbiochem) was added to each of the samples and incubated for 1 hour at 4°C on a nutator to allow the antibody to bind to p53. Following the incubation 50 µl of the 50% slurry of Protein G Sepharose beads was added to each of the samples and incubated for 2 hours at 4°C on a nutator to capture the immune complexes on the beads. The beads were then collected by centrifugation at 16,000×g for 30 sec. The supernatant was discarded and the beads were washed 3 times with 500 µl of SLIP. After the last wash the supernatant was removed completely, draining the beads of any residual SLIP buffer. The beads were then resuspended in 60 µl of 1× sample loading buffer (see section 2.7) and boiled for

5 min. at 99°C. 20 µl of the immunoprecipitated complexes were analysed by SDS-PAGE and western blotting.

2.23. Clonogenic assay

Clonogenic assay (colony formation assay) is an *in vitro* cell survival assay, which measures the ability of single cells to proliferate and form colonies. Since radiation therapy is one of the treatment modalities for laryngeal cancer, clonogenic assays (as described previously (482)) were used to investigate the response to γ-radiation of the mutant p53 expressing laryngeal cancer cell lines.

Immediately before the experiment the required number of 6-well plates was coated with gelatin. 0.1% (w/v) gelatin solution was prepared in H_2O. A few drops of phenol red were added until a bright yellow colour was achieved. The solution was sterilised by autoclaving (121°C for 15 min.). 2 ml of the gelatin solution were added per well of a 6-well plate and incubated for 2 hours. Following the incubation, the gelatin solution was aspirated and the plates were ready to use.

The day before irradiation, 1.1×10^6 cells were seeded into 25 cm^2 flasks (2 flasks per condition) such that they were subconfluent on the day of the treatment. The following day the cells (in flasks) were treated with 0 Gy (untreated), 2 Gy, 4 Gy or 6 Gy at room temperature using a ^{137}Cs source delivering ~ 6.25 Gy/min of γ-radiation. Subsequently, the cells were trypsinized and counted using the Coulter Counter. The cells were seeded in triplicates into gelatin-coated 6-well plates at the following concentrations (number of cells per well): 800, 1,600, 3,200, 6,400, 12,800, 25,600, 51,200, 102,400. Pre-gassed (kept in tissue culture flasks inside a humidified tissue culture incubator for 48 hours prior to the experiment) full growth media was used for plating. The plates were then placed in the incubator (37°C, 5% CO_2) and

incubated for 14 days until sufficiently large colonies have been formed. A colony was defined as a group of ≥ 50 cells corresponding to more than 5 cell divisions (482).

Fixing/staining solution

Concentration	**Reagent**
6% (v/v)	glutaraldehyde
0.5% (w/v)	crystal violet
	in PBS

Following incubation, the media was aspirated and the cells were washed with PBS. The cells were then incubated with the fixing/staining solution for 30 min. at room temperature. The plates were washed by immersing them gently in a sink filled with tap water. The plates were then left upside down on a piece of towel to dry.

The colonies were counted under the light microscope for at least 2 different seeding concentrations (in triplicate) for each treatment. The plating efficiency (PE) was calculated for the untreated cells by dividing the number of colonies formed by the number of cells seeded.

$$PE = \frac{\text{no. of colonies formed}}{\text{no. of cells seeded}}$$

The number of colonies formed after treatment was then used to calculate the surviving fraction (SF) taking the plating efficiency into account:

$$SF = \frac{\text{no. of colonies formed}}{\text{no. of cells seeded} \times PE}$$

The results were plotted on a logarithmic scale and fitted to the linear-quadratic equation $y = \exp\left(-\left(a \cdot x + b \cdot x^2\right)\right)$, where y is the surviving fraction and x is the treatment dose (483).

Chapter 3

Results

3. Results

p53 is an important tumour suppressor protein, whose function is lost through *TP53* mutations in about 50% of human tumours, making it arguably the most frequently altered gene in human cancer. The majority of p53 mutations are missense, resulting in the expression of full-length protein with single amino acid substitutions, which tends to accumulate in tumour cells. These missense p53 mutants not only lack wild-type p53 tumour-suppressor activity but in addition evidence suggests that some of these also gain new functions that can promote tumorigenesis. This oncogenic 'gain of function' of p53 mutants is proposed to be achieved via modulating the transcriptome of a cancer cell or through novel protein-protein interactions (as discussed in section 1.3.4.3.1).

To investigate the mechanism of action of a GOF p53 mutant, two defined GOF mutants, which represent distinct mutational classes, were chosen for these studies:

- R175H – single amino acid substitution (arginine to histidine) at position 175 is an example of a structural mutation, causing a significant conformational shift of p53,
- R273H – single amino acid substitution (arginine to histidine) at position 273 is a contact mutation, affecting a residue that makes direct contact with DNA and hence leading to a loss of wild-type p53-specific DNA binding; note that mutants of this class may retain altered ability to transactivate p53-responsive genes.

In order to study the mechanisms of gain of function of p53 mutants, protein interactions of the two defined GOF mutants (R175H and R273H) were identified as well as gene expression of the R273H mutant of p53 was studied.

To enable purification of p53-containing complexes, cDNAs encoding wt and two mutant forms of p53 were cloned into TAP-tag vectors (section 3.1). The vectors were tested for expression and p53 transcriptional activity in a p53-null cell line (H1299) using western blotting and luciferase p53 transcriptional activity assays (section 3.2).

In order to study protein interactions of the GOF p53 mutants in laryngeal cancer, a p53-null laryngeal cancer cell line was required. A functionally p53-null LSCC cell line (UM-SCC-12) has been identified in the panel of available cell lines and tested for p53 expression (section 3.3). To engineer these cells to express the GOF p53 mutants of interest, the cells had to be transfected with the generated TAP-tag vectors. Therefore, the transfection efficiency of UM-SCC-12 cells was tested and optimised (section 3.4). Since the transfection efficiency of UM-SCC-12 cells remained extremely low in spite of optimisation, in order to obtain a sufficient amount of protein for TAP-tag purification, stable laryngeal cancer cell lines expressing either of the two GOF p53 mutants have been established (section 3.5).

TAP-tag purification of mutant p53-containing complexes has been performed and the purified proteins have been identified using mass spectroscopy (section 3.7). Validation of some of the identified binding partners was performed using immunoprecipitation and western blotting (section 3.8).

The migratory potential (a surrogate indicator of metastatic potential) of the established LSCC cell lines expressing the GOF p53 mutants was investigated using live cell imaging and Boyden chamber motility assays (section 3.9). Down-regulation of mutant p53 by RNAi in the generated cell lines was performed to investigate whether the observed increase in motility was due to mutant p53 expression (section 3.10). The invasiveness of the highly motile mutant p53 expressing cells was also studied using Boyden chamber invasion assays (section 3.11).

To study gene expression changes in the highly motile cells expressing one of the GOF p53 mutants, exon array analysis was performed and the obtained results were validated by qRT-PCR (section 3.12).

Finally, the response to ionising radiation (one of the main treatment modalities for head and neck cancer) of the mutant p53 expressing cells was investigated using clonogenic assays (section 3.13).

3.1. DNA construct maps and sequencing

Table 3.1: List of all the constructs generated or used in the current study and their application.

Construct	Purpose/Use
pCMV-Script.p53	validation studies using untagged forms of p53; source of p53 cDNA for subloning into other vectors
pNTAP-B.p53	purification of p53 containing complexes using the TAP-tag purification system
pCB6+.p53-175H	source of p53-175H cDNA for subcloning into other vectors
pCR2.1.p53-175H	temporary vector, into which p53-175H cDNA amplified by PCR was ligated; used for subcloning p53-175H cDNA into other vectors
pNTAP-B.p53-175H	purification of p53-175H containing complexes using the TAP-tag purification system
pCMV-Script.p53-175H	validation studies using untagged forms of p53
pET24a(+).p53-273H	source of p53-273H cDNA for subcloning into other vectors
pNTAP-B.p53-273H	purification of p53-273H containing complexes using the TAP-tag purification system
pCMV-Script.p53-273H	validation studies using untagged forms of p53

3.1.1. pCMV-Script.p53

pCMV-Script.p53 vector was used for subcloning of the human p53 cDNA into a TAP-tag vector (pNTAP) and was utilised for validation studies using untagged forms of p53. The p53 cDNA was sequenced to confirm its identity. The obtained sequence was compared with the reference sequence of p53 (accession number: NM_000546) and no mutations were found. Based on the sequencing results (Appendix 2) and the pCMV-Script sequence found in the Addgene Vector Database (484) a vector map was generated (Figure 3.1).

3.1.2. pNTAP-B.p53

p53 cDNA was subcloned from pCMV-Script.p53 into pNTAP-B (as described in section 2.4.2) to enable protein purification using the TAP-tag purification system. Based on the sequencing results (Appendix 3) and the vector sequence provided by Stratagene a vector map was generated (Figure 3.2).

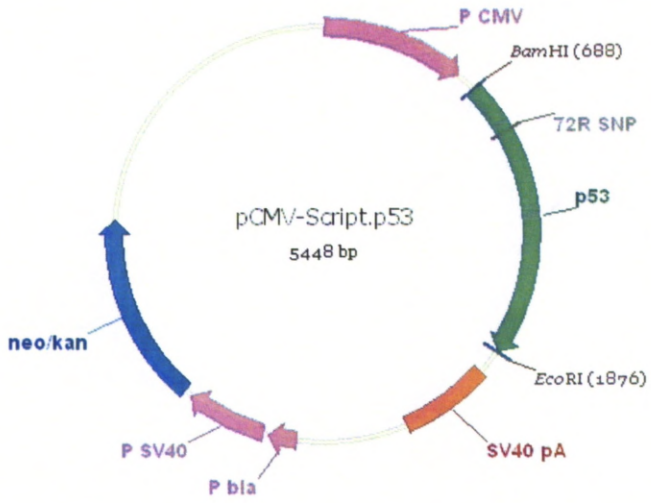

Figure 3.1: Map of the pCMV-Script.p53 vector. The size of the vector is 5448 bp. Features: P CMV – CMV promoter; BamHI, EcoRI – restriction sites for the indicated endonucleases; 72R SNP – single nucleotide polymorphism at amino acid 72 (arginine); p53 – human p53 cDNA; SV40 pA – SV40 polyadenylation signal; P bla – *bla* promoter; P SV40 – SV40 promoter; neo/kan – neomycin/kanamycin resistance cassette.

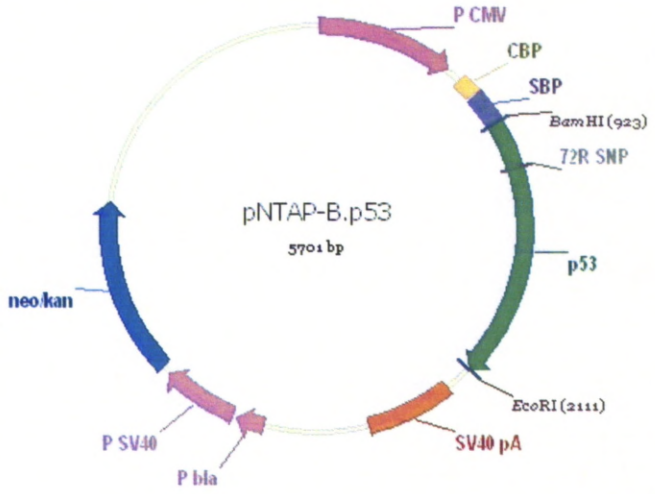

Figure 3.2: Map of the pNTAP-B.p53 vector. The size of the vector is 5701 bp. Features: P CMV – CMV promoter; CBP – calmodulin binding peptide; SBP – streptavidin binding peptide; BamHI, EcoRI – restriction sites for the indicated endonucleases; 72R SNP – single nucleotide polymorphism at amino acid 72 (arginine); p53 – human p53 cDNA; SV40 pA – SV40 polyadenylation signal; P bla – *bla* promoter; P SV40 – SV40 promoter; neo/kan – neomycin/kanamycin resistance cassette.

3.1.3. pCB6+.p53-175H

pCB6+.p53-175H vector was used for subcloning of the cDNA encoding human p53 with in a single amino acid substitution at position 175 (arginine to histidine) into a TAP-tag vector (pNTAP). The entire sequence of the pCB6+ vector was not available. To determine the strategy for cloning p53-175H into pNTAP vector, the regions upstream and downstream as well as the entire coding sequence of p53 were sequenced (Appendix 4). Based on these sequencing results, an approximate map of pCB6+.p53-175H was generated (Figure 3.3). The features known to be present in the pCB6+ vector (such as the pCMV promoter or the antibiotic resistance cassettes) are also outlined.

3.1.4. pCR2.1.p53-175H

The p53 cDNA was amplified by PCR from pCB6+.p53-175H and subcloned into pCR2.1 vector (as described in section 2.4.4) for further subcloning into a TAP-tag vector (pNTAP). Sequencing results (Appendix 5) confirmed that p53 cDNA contained only the desired mutation at codon 175 (R to H). Based on the sequencing results and pCR2.1 sequence found in the Addgene Vector Database (484) a vector map was generated (Figure 3.4).

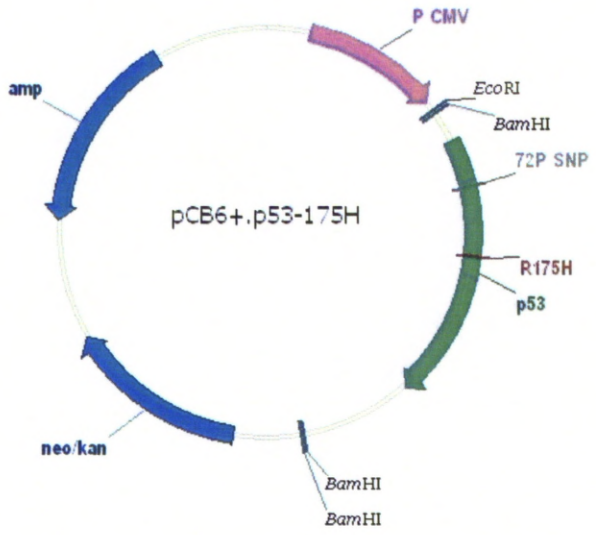

Figure 3.3: An approximate map of the pCB6+.p53-175H vector. Features: P CMV – CMV promoter; BamHI, EcoRI – restriction sites for the indicated endonucleases; 72P SNP – single nucleotide polymorphism at amino acid 72 (proline); R175H – single amino acid substitution at position 175 (arginine to histidine); p53 – human p53 cDNA; neo/kan – neomycin/kanamycin resistance cassette; amp – ampicillin resistance cassette. Note that the features are not drawn to scale.

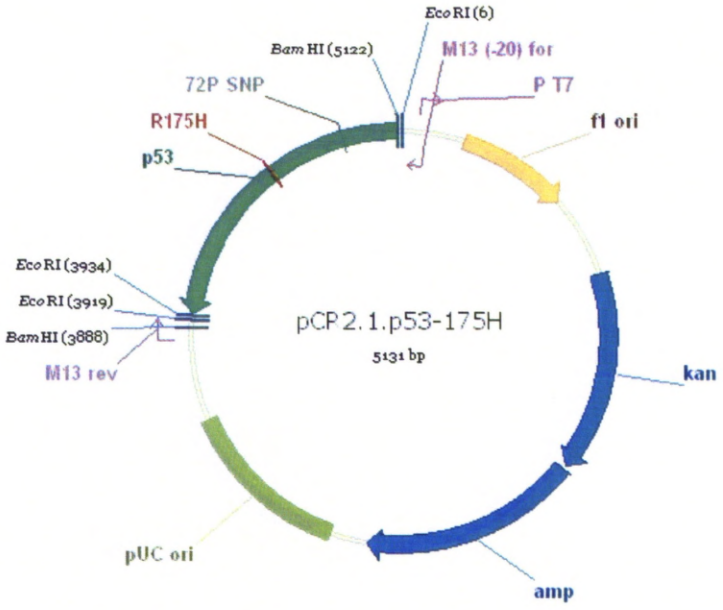

Figure 3.4: Map of the pCR2.1.p53-175H vector. The size of the vector is 5131 bp. Features: M13 (-20) for – M13 (-20) forward priming site; P T7 – T7 promoter; f1 ori – f1 origin; kan – kanamycin resistance cassette; amp – ampicillin resistance cassette; pUC ori – pUC origin; M13 rev – M13 reverse priming site; BamHI, EcoRI – restriction sites for the indicated endonucleases; p53 – human p53 cDNA; R175H – single amino acid substitution at position 175 (arginine to histidine); 72P SNP – single nucleotide polymorphism at amino acid 72 (proline).

3.1.5. pNTAP-B.p53-175H

The p53-175H cDNA was then subcloned from pCR2.1.p53-175H into pNTAP-B vector (as described in section 2.4.5) to enable protein purification using the TAP-tag purification system. The p53/pNTAP-B junctions were sequenced to confirm that the cDNA was cloned correctly and that it is in frame with the TAP-tag (Appendix 6). A vector map was generated based on the sequencing results and the vector sequence provided by Stratagene (Figure 3.5).

3.1.6. pCMV-Script.p53-175H

The p53-175H cDNA was also subcloned from pCR2.1.p53-175H into pCMV-Script vector (as described in section 2.4.6). The vector was utilised for validation studies using untagged forms of p53. Based on the pCMV-Script sequence found in the Addgene Vector Database (484) a vector map was generated (Figure 3.6).

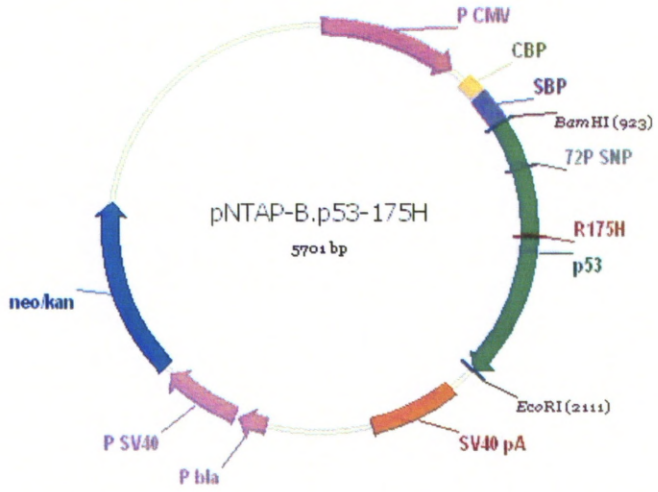

Figure 3.5: Map of the pNTAP-B.p53-175H vector. The size of the vector is 5701 bp. Features: P CMV – CMV promoter; CBP – calmodulin binding peptide; SBP – streptavidin binding peptide; BamHI, EcoRI – restriction sites for the indicated endonucleases; 72P SNP – single nucleotide polymorphism at amino acid 72 (proline); R175H – single amino acid substitution at position 175 (arginine to histidine); p53 – human p53 cDNA; SV40 pA – SV40 polyadenylation signal; P bla – *bla* promoter; P SV40 – SV40 promoter; neo/kan – neomycin/kanamycin resistance cassette.

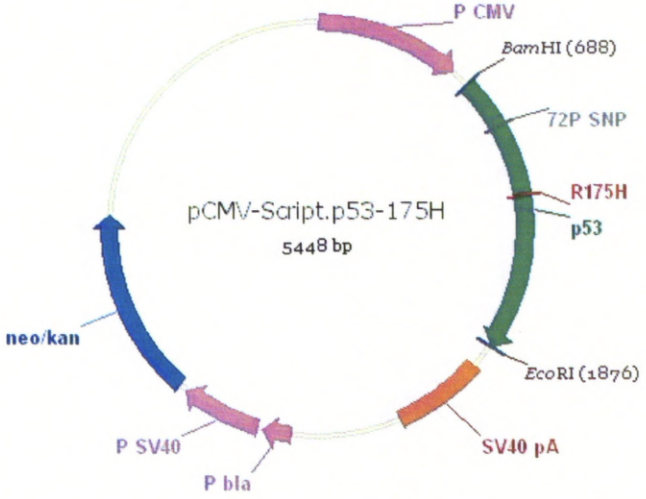

Figure 3.6: Map of the pCMV-Script.p53-175H vector. The size of the vector is 5448 bp. Features: P CMV – CMV promoter; BamHI, EcoRI – restriction sites for the indicated endonucleases; 72P SNP – single nucleotide polymorphism at amino acid 72 (proline); R175H – single amino acid substitution at position 175 (arginine to histidine); p53 – human p53 cDNA; SV40 pA – SV40 polyadenylation signal; P bla – *bla* promoter; P SV40 – SV40 promoter; neo/kan – neomycin/kanamycin resistance cassette.

3.1.7. pET24a(+).p53-273H

The pET24a(+).p53-273H vector was used for subcloning of the cDNA encoding human p53 with a single amino acid substitution at position 273 (arginine to histidine) into a TAP-tag vector (pNTAP). The p53 cDNA was sequenced to confirm its identity. Based on the sequencing results (Appendix 7) and the pET24a(+) sequence found in the Addgene Vector Database (484) a vector map was generated (Figure 3.7).

3.1.8. pNTAP-B.p53-273H

The p53-273H cDNA was subcloned from pET24a(+).p53-273H into pNTAP-B vector (as described in section 2.4.8) to enable protein purification using the TAP-tag purification system. The p53/pNTAP-B junctions were sequenced to confirm that the cDNA was cloned correctly and that it is in frame with the TAP-tag (Appendix 8). A vector map was generated based on the sequencing results and the vector sequence provided by Stratagene (Figure 3.8).

3.1.9. pCMV-Script.p53-273H

The p53-273H cDNA was also subcloned from pET24a(+).p53-273H into pCMV-Script vector (as described in section 2.4.9). The vector was utilised for validation studies using untagged forms of p53. Based on the pCMV-Script sequence found in the Addgene Vector Database (484) a vector map was generated (Figure 3.9).

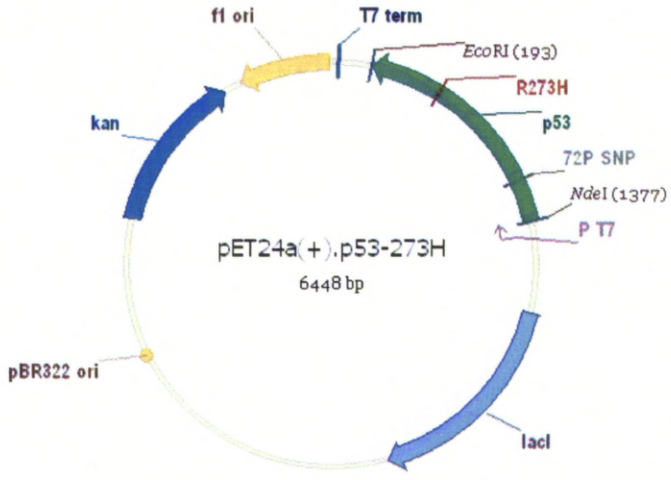

Figure 3.7: Map of the pET24a(+).p53-273H vector. The size of the vector is 6448 bp. Features: T7 term – T7 terminator; EcoRI, NdeI – restriction sites for the indicated endonucleases; R273H – single amino acid substitution at position 273 (arginine to histidine); p53 – human p53 cDNA; 72P SNP – single nucleotide polymorphism at amino acid 72 (proline); P T7 – T7 promoter; lacI – lactose repressor coding sequence; pBR322 ori – pBR322 origin; kan – kanamycin resistance cassette; f1 ori – f1 origin.

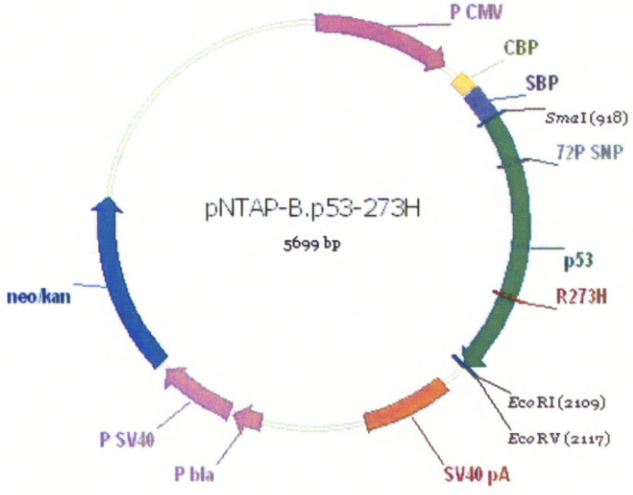

Figure 3.8: Map of the pNTAP-B.p53-273H vector. The size of the vector is 5699 bp. Features: P CMV – CMV promoter; CBP – calmodulin binding peptide; SBP – streptavidin binding peptide; SmaI, EcoRI, EcoRV – restriction sites for the indicated endonucleases; 72P SNP – single nucleotide polymorphism at amino acid 72 (proline); p53 – human p53 cDNA; R273H – single amino acid substitution at position 273 (arginine to histidine); SV40 pA – SV40 polyadenylation signal; P bla – *bla* promoter; P SV40 – SV40 promoter; neo/kan – neomycin/kanamycin resistance cassette.

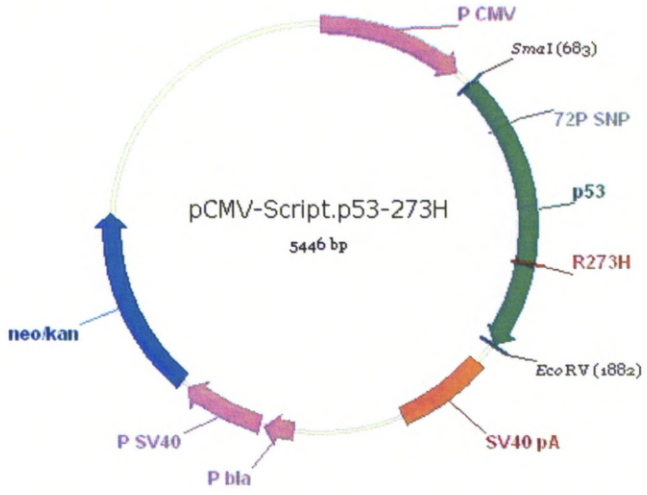

Figure 3.9: Map of the pCMV-Script.p53-273H vector. The size of the vector is 5446 bp. Features: P CMV – CMV promoter; SmaI, EcoRV – restriction sites for the indicated endonucleases; 72P SNP – single nucleotide polymorphism at amino acid 72 (proline); p53 – human p53 cDNA; R273H – single amino acid substitution at position 273 (arginine to histidine); SV40 pA – SV40 polyadenylation signal; P bla – *bla* promoter; P SV40 – SV40 promoter; neo/kan – neomycin/kanamycin resistance cassette.

3.2. R175H and R273H p53 mutants display dominant-negative effects on wild-type p53

Wt and two mutant forms of p53 (R175H and R273H) cloned into TAP-tag vectors were tested for expression and transcriptional activity in a p53-null NSCLC cell line (H1299). H1299 cells were chosen for these studies because they grow quickly and are relatively easy to transfect with transfection efficiencies of approximately 30-50% being obtained routinely.

H1299 cells were transfected with a constant amount (20 ng) of untagged wt p53 and co-transfected with increasing amounts of the TAP-tagged p53 mutants (Figure 3.10 and 3.11). With increasing amount of the mutant p53 there is a fall in p53 activity, which demonstrates that both p53 mutants display a dominant-negative effect on wt p53, which is dose-dependent (Figures 3.10A and 3.11A). 100 ng of TAP-tagged p53-175H reduces the activity of 20 ng of untagged wt p53 12.4-fold, while 100 ng of TAP-tagged p53-273H reduces the activity of 20 ng of untagged wt p53 9-fold. This suggests that the structural p53 mutant (R175H) is more effective in inhibiting wt p53 activity than the contact mutant (R273H). A possible explanation could be the fact that upon hetero-oligomerization the structural mutant may shift wt p53 into mutant conformation (as discussed in section 1.3.4.2) while the contact mutants might retain native conformation and in tetramers with wt p53 they may have some residual wild-type transcriptional activity. Note, however, that the TAP-tagged p53 mutants discussed above display no wild-type transcriptional activity.

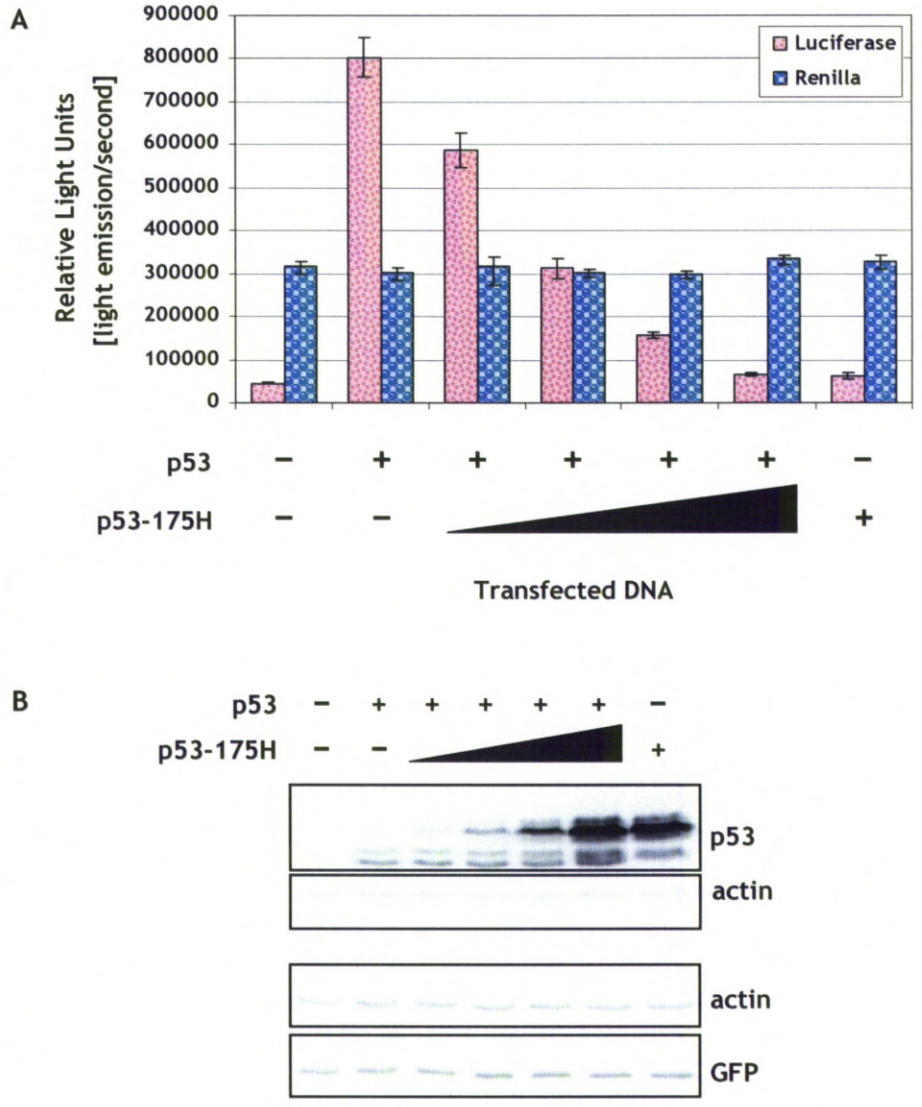

Figure 3.10: Expression and dominant-negative activity of TAP-tagged p53-175H mutant. H1299 cells were transfected with 20 ng of pCMV-Script.p53 encoding untagged wt p53 (as indicated with "+") and increasing amounts of pNTAP-B.p53-175H encoding TAP-tagged p53-175H (3 ng, 10 ng, 30 ng, 100 ng). The experiment was performed once.

A. Luciferase reporter p53 transcriptional activity assay. The histograms represent the mean of three replicates, the error bars represent standard error of mean.

B. Western blot analysis with the indicated antibodies (DO-1 for p53) showing the expression of TAP-tagged p53-175H. Actin is a loading control and GFP is a transfection efficiency control.

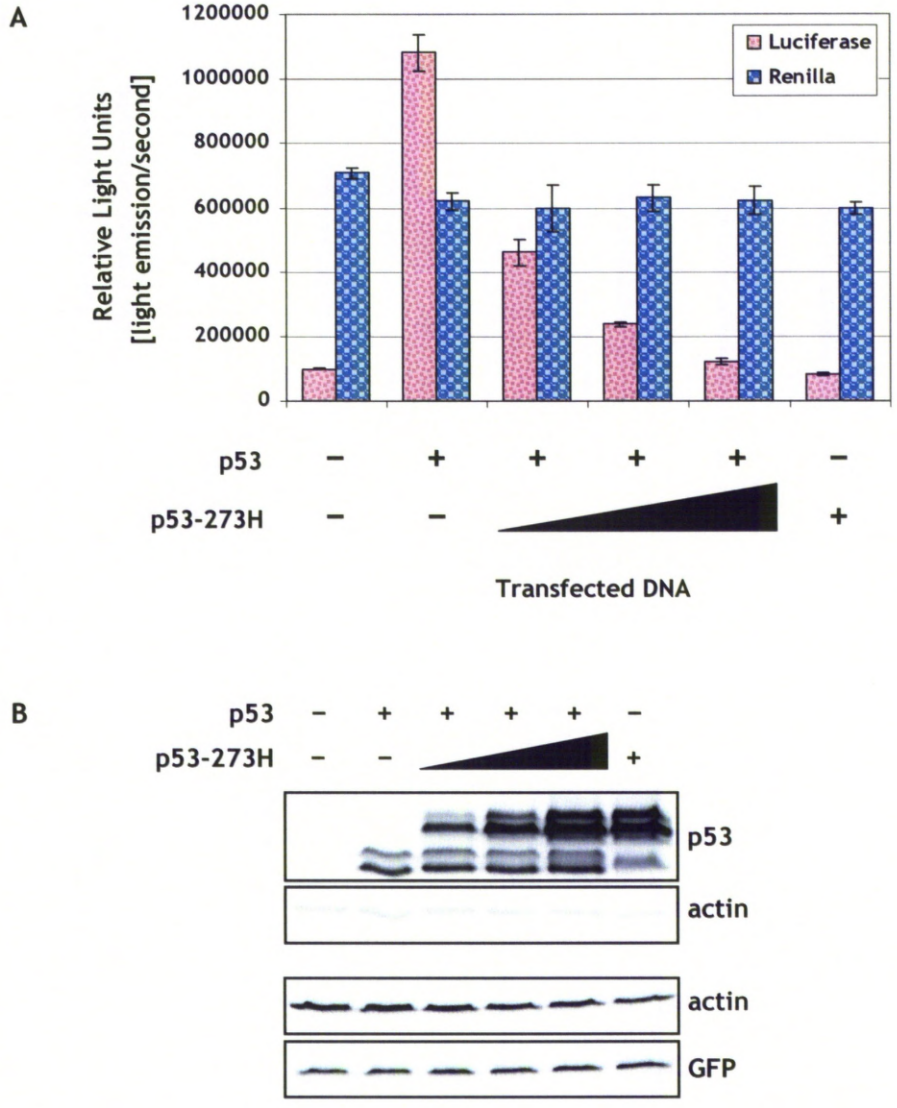

Figure 3.11: Expression and dominant-negative activity of TAP-tagged p53-273H mutant. H1299 cells were transfected with 20 ng of pCMV-Script.p53 encoding untagged wt p53 (as indicated with "+") and increasing amounts of pNTAP-B.p53-273H encoding TAP-tagged p53-273H (10 ng, 30 ng, 100 ng). The experiment was performed once.

A. Luciferase reporter p53 transcriptional activity assay. The histograms represent the mean of three replicates, the error bars represent standard error of mean.

B. Western blot analysis with the indicated antibodies (DO-1 for p53) showing the expression of TAP-tagged p53-273H. Actin is a loading control and GFP is a transfection efficiency control.

As shown in Figures 3.10B, 3.11B, 3.12 B and 3.13B expression of wt p53 from pCMV-Script vector resulted in a double band on western blots at approximately 52 kDa. The expected mobility of wt p53 corresponds to the lower band. Careful analysis of the sequence upstream of p53 cDNA in pCMV-Script revealed the presence of an alternative translation initiation codon CTG (485, 486), which was in frame with p53 cDNA and was not followed by an in-frame STOP codon. If translation was initiated from this codon, the resulting p53 would be 15 amino acids longer and hence its predicted molecular weight would be approximately 1.7 kDa greater than that of wt p53 translated from its original ATG. This could explain the presence of two bands recognised by a p53 specific antibody on a western blot.

Expression of TAP-tagged p53 forms from pNTAP-B vector resulted in multiple bands at approximately 58 kDa and 52 kDa, recognised by a p53-specific antibody on a western blot. The presence of these multiple bands can also be explained by alternative initiation of translation. It is important to note that CBP, SBP and p53 cDNA each have their own ATG so translation could be initiated from any of these START codons. Moreover, since the pNTAP-B vector differs from the pCMV-Script vector only by the presence of the TAP-tag coding sequence, alternative initiation of translation from codon CTG could also occur, explaining the number of different bands observed in Fiugres 3.10B, 3.11B, 3.12 B and 3.13B.

TAP-tagged wt p53 displays wt p53 transcriptional activity, which is lower than the activity of the untagged protein and this becomes more apparent with increasing p53 dose (Figure 3.12A). Moreover, the efficiency of transfecting TAP-tagged wt p53 was higher than that of untagged wt p53 as judged by the levels of co-transfected GFP (Figure 3.12B), resulting in a higher level of expression of TAP-tagged wt p53 compared to untagged wt p53. This means that a higher level of TAP-tagged wt p53

results in a comparable transcriptional activity when 10 ng of each vector are transfected and the transcriptional activity of the TAP-tagged wt p53 does not increase proportionately with the increasing amounts of the vector transfected (although the level of expressed protein increases proportionately). This suggests that the TAP-tagged wt p53 might have some auto-inhibitory effect when higher levels of the protein are present.

It was also observed that TAP-tagged wt p53 reduces the activity of the untagged protein when co-transfected (Figures 3.13A). 100 ng of TAP-tagged wt p53 reduced the activity of 100 ng of untagged wt p53 1.5-fold. One interpretation of this observation is that TAP-tagged p53 is acting as a partial dominant-negative in this system. However, the inhibitory effect of the TAP-tagged wt p53 on untagged wt p53 is much weaker than that of the dominant-negative p53 mutants, p53-175H or p53-273H (1.5-fold reduction compared to 12.4-fold and 9-fold, respectively). Moreover, increasing amounts of TAP-tagged wt p53 co-transfected with a constant amount (100 ng) of untagged wt p53 did not result in a dose-dependent inhibition but actually in gradual increase of wt p53 transcriptional activity. This also suggests that TAP-tagged wt p53 has intrinsic wt p53 transcriptional activity.

Ultimately, derivatives of a p53-null LSCC cell line were to be engineered to express these TAP-tagged constructs to permit purification of protein complexes containing the wt and mutant forms of p53. Since TAP-tagged wt p53 has wt p53 transcriptional activity and since it was not intended to be transfected in combination with untagged wt p53, this partial dominant-negative effect described above would not take place. Moreover, since wt p53 has strong growth-inhibitory properties, if cells expressing TAP-tagged wt p53 were established, they would most likely express it at a low level, at which TAP-tagged wt p53 was shown to behave similarly to its

untagged counterpart. Finally, any results obtained using the TAP-tagged wt p53 can be further validated in studies using cDNAs that lack the TAP-tag.

The activity of the *Renilla* luciferase, which is expressed constitutively in this system, serves as an internal control of the transfection efficiency. Similar activity indicates comparable transfection efficiencies between the conditions (Figure 3.10A and 3.11A). These results, however, have to be analysed with caution as wild-type p53 was reported to modulate the activity of some promoters (487), including HSV-TK used here for *Renilla* expression. In experiments shown in Figures 3.12A and 3.13A it appears that as the amount of wt p53 expressing plasmid increases, the *Renilla* activity also seems to increase and this is particularly clear for the combination of TAP-tagged and untagged wt p53 (Figure 3.13A). Therefore, the firefly luciferase activity was not normalized to the *Renilla* activity as recommended by the kit manufacturer, but the two luciferase activities were presented side by side. Such approach helps to avoid artefacts, which could occur due to normalization to another reporter construct, which may be influenced by many variables (in addition to wild-type p53 expression) including oncogene activity or DNA damage (488).

Since *Renilla* activity is not an ideal internal control for transfection efficiency for the reasons described above, GFP levels were also monitored by western blotting as an additional indicator of the efficiency of transfection between the conditions.

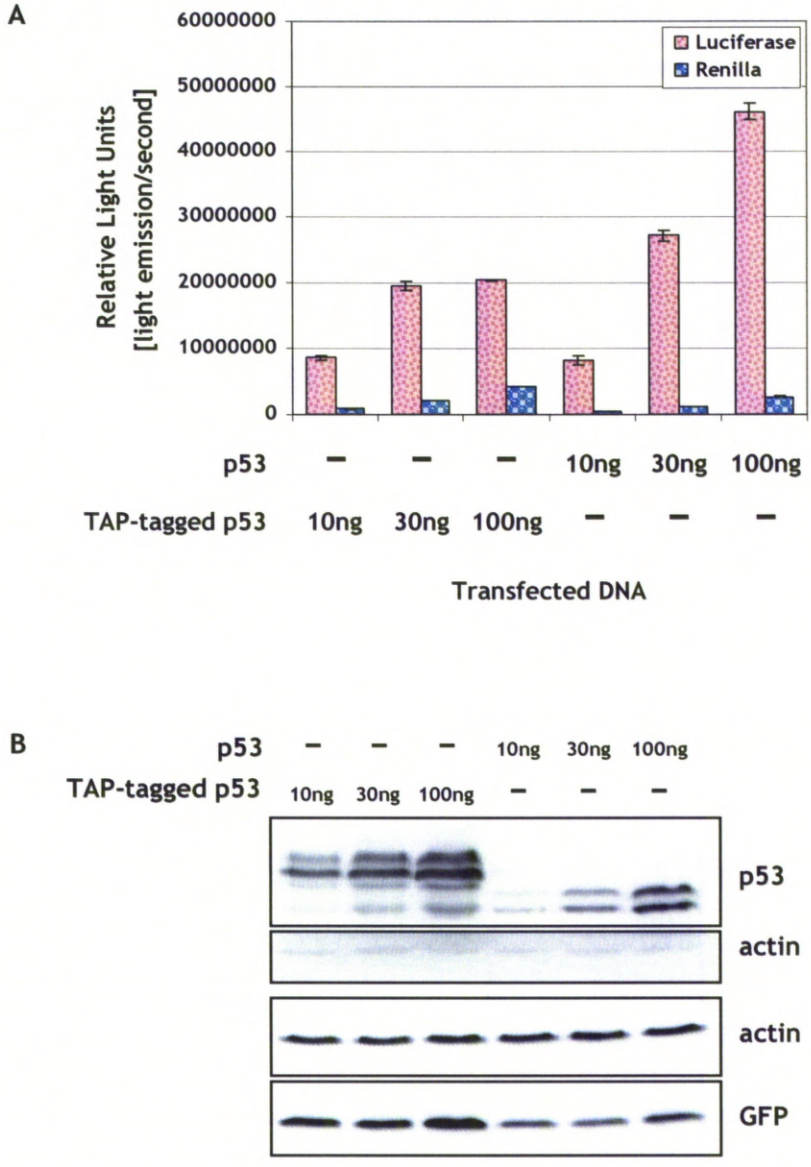

Figure 3.12: Expression and transcriptional activity of TAP-tagged p53 compared to untagged p53. H1299 cells were transfected with the indicated amounts of pCMV-Script.p53 encoding untagged wt p53 or pNTAP-B.p53 encoding TAP-tagged wt p53. The experiment was performed thrice.

A. Luciferase reporter p53 transcriptional activity assay. The histograms represent the mean of three replicates, the error bars represent standard error of mean.

B. Western blot analysis with the indicated antibodies (DO-1 for p53) showing the expression of TAP-tagged and untagged p53 forms. Actin is a loading control and GFP is a transfection efficiency control.

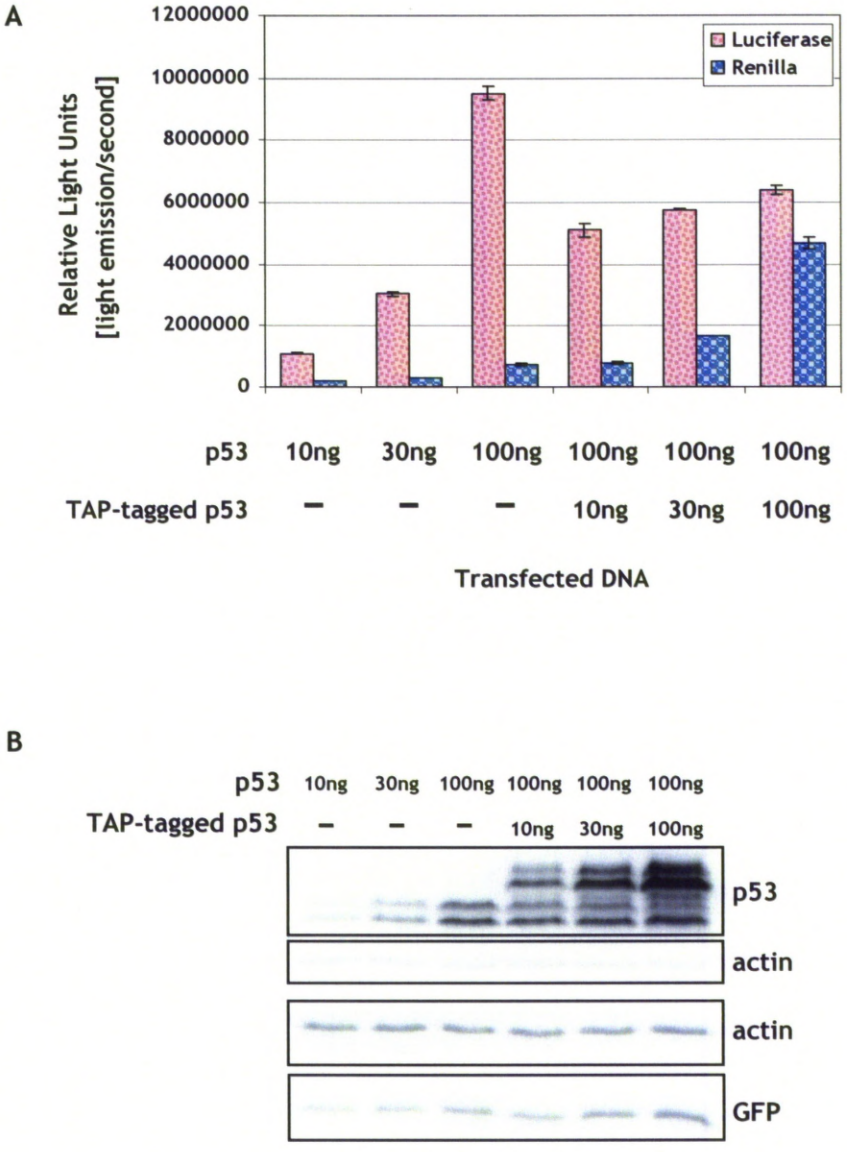

Figure 3.13: Expression and transcriptional activity of TAP-tagged p53. H1299 cells were transfected with the indicated amounts of pCMV-Script.p53 encoding untagged wt p53 or pNTAP-B.p53 encoding TAP-tagged wt p53. The experiment was performed once.

A. Luciferase reporter p53 transcriptional activity assay. The histograms represent the mean of three replicates, the error bars represent standard error of mean.

B. Western blot analysis with the indicated antibodies (DO-1 for p53) showing the expression of TAP-tagged and untagged p53 forms. Actin is a loading control and GFP is a transfection efficiency control.

3.3. UM-SCC-12 is functionally p53-null

As presented above, mutant p53 exerts dominant-negative effects on wild-type p53. Therefore, in order to investigate the true gain of function of p53 mutants, studies have to be performed in cells that are p53-null, which is now a common practice in the field. Clearly, a functionally p53-null cell line is desirable for both studying the gene expression changes mediated by mutant p53 and to avoid potential interference from endogenous p53 in the purification of mutant p53 protein complexes.

A laryngeal cancer cell line with a nonsense mutation of the glutamine residue at amino acid 104 (Q104X), leading to a homozygous p53 truncation (UM-SCC-12) has been identified in the panel of available cell lines and tested for p53 expression. If the truncated protein was expressed it would be expected to be approximately 11 kDa. As shown in Figure 3.14A UM-SCC-12 cells have no detectable p53 expression. The faint band observed at approximately 23 kDa is most likely non-specific as it is not affected by transfection with siRNA for p53 (Figure 3.14A). A control experiment using siRNA for MDM2 confirmed knock-down efficacy in this cell line (Figure 3.14B).

While no p53 was detected in UM-SCC-12, there is always a possibility of alternative p53 isoforms being expressed in these cells. Such isoforms could theoretically be a result of alternative initiation of translation or alternative splicing. The p53 sequence contains two alternative in-frame start codons – at residues 40 and 44, respectively. These alternative translational start sites both fall in exon 4 of p53, which is the largest exon of p53 and encompasses base pairs 97-375 of the coding sequence. These alternative start codons are located upstream of and within the same exon as the nonsense mutation in UM-SCC-12 cells, resulting in a stop codon at residue 104. Therefore, alternative initiation of p53 translation seems rather unlikely

as the ribosome would have to read through the stop codon at residue 104. Alternative splicing, however, still remains possible. The alternative splice isoforms could be composed of any combination of exons 2-11 with the exception of exon 4, as this would result in polypeptide chain termination.

The expression of alternative splice variants is usually lower than the expression of the main transcript (in this case truncated). It could be expected that some of the produced splice variants should contain exon 2 and hence be detected using the anti-p53 antibody DO-1 (recognising epitope within residues 20-25). Since no truncated p53 or other p53 isoforms containing exon 2 were detected, it is likely that the expression of the other splice variants is also very low or absent. Therefore, it can be concluded that there is little or no p53 protein being expressed in the UM-SCC-12 cell line.

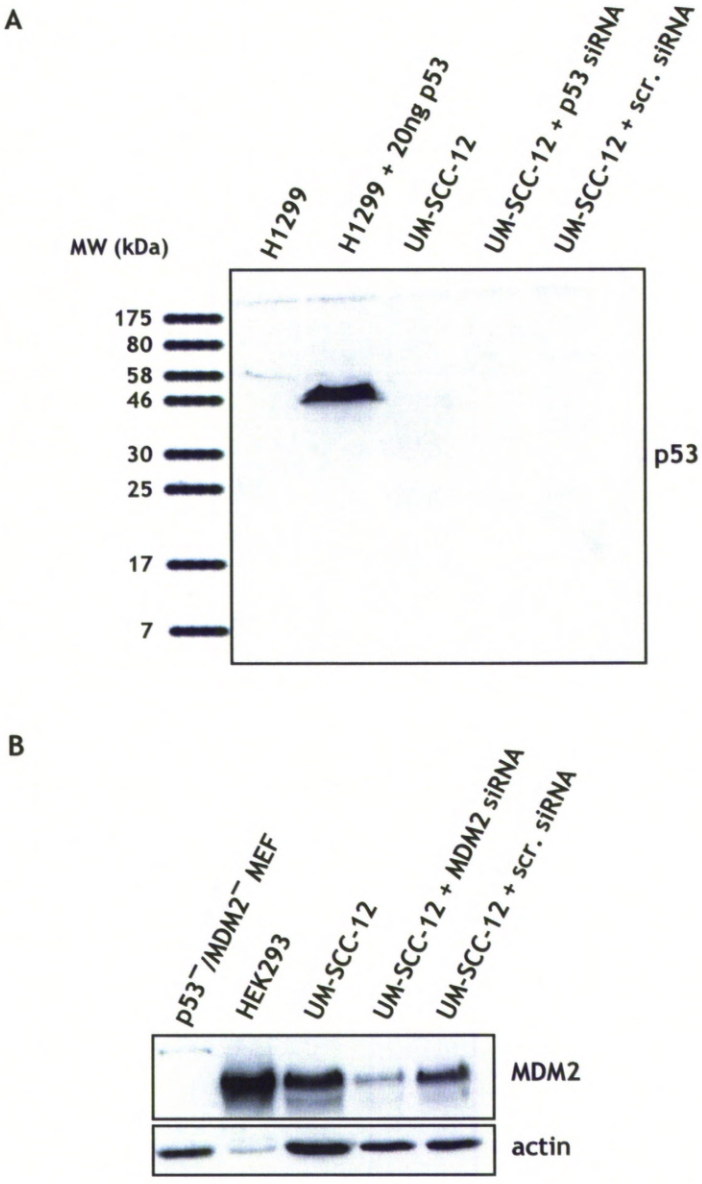

Figure 3.14: UM-SCC-12 is a p53-null laryngeal cell line with no detectable p53. UM-SCC-12 cells were transfected with control (scrambled) siRNA, siRNA for p53 or MDM2. The cells were analysed 48 hours post transfection. The experiment was performed once.

A. Western blot for p53 with DO-1. UM-SCC-12 cells were tested for p53 expression following transfection with siRNA for p53. A lysate from untransfected H1299 cells and H1299 cells transfected with 20 ng of p53 were used as a negative and positive antibody control, respectively.

B. Western blot analysis with the indicated antibodies. The level of MDM2 in UM-SCC-12 was tested following transfection with siRNA for MDM2. A lysate from $p53^{-}/MDM2^{-}$ MEF (p53-null/MDM2-null) cells and HEK293 cells were used as a negative and positive antibody control, respectively.

3.4. Transfection optimisation of UM-SCC-12

In order to study the mechanisms of mutant p53 GOF in laryngeal cancer, the p53-null UM-SCC-12 cells had to be engineered to express wt and the two mutant forms of p53. This could be achieved through either transient or stable transfection of UM-SCC-12 cells with the generated TAP-tag constructs (described in section 3.1). Since very little information was available on UM-SCC-12 prior to this study, the transfection efficiency had to be tested and if required, the conditions optimised.

UM-SCC-12 and H1299 cells (as a positive control) were transfected with 1 μg of pβ-gal per well of a 6-well plate using different transfection reagents at different ratios to find the conditions yielding the highest transfection efficiency of UM-SCC-12 cells. Following transfection, the transfection efficiency was estimated based on *in situ* β-gal staining.

The highest transfection efficiency (~40%) of H1299 cells was obtained using Lipofectamine at a 2:1 ratio (Figure 3.15G) while UM-SCC-12 cells were transfected most efficiently (1-2%) using FuGENE at a 3:1 ratio (Figure 3.15R). In further optimisation experiments it was determined that the highest transfection efficiency of UM-SCC-12 cells was obtained when they were seeded at a 50% confluence (data not shown).

In spite of extensive optimisation studies, the best transfection efficiency achieved on UM-SCC-12 was still low (1-2%). Therefore, in order to obtain a population of cells with a moderate to high level expression of the TAP-tagged proteins, stable cell lines had to be generated. High level of expression would clearly reduce the number of cells needed to perform TAP-tag purification of p53 containing complexes. On the other hand, high level of expression could disturb the cellular balance and force protein interactions that would not normally occur due to the abundance of the

transfected p53. Therefore, generating cell lines with a moderate (physiological) level of expression of the TAP-tagged p53 forms would be most desirable in an attempt to reproduce physiologically relevant conditions and interactions.

Towards the end of the studies described in this thesis, a new transfection system became available to our laboratory – transfection by electroporation (nucleofection). This system was tested on UM-SCC-12 cells using condition recommended by the manufacturer for a similar SCC cell line (UM-SCC-14A). The transfection efficiency achieved using this system without optimisation was significantly better than any other transfection method used so far and reached 50% (Figure 3.16A).

This technique is, however, much more toxic to the cells than lipofection (~60% viable cells after the nucleofection). Because it was expected that more cells (than the recommended 1×10^6 per reaction) would be needed for further experiments, the technique was tested for use with a larger number of cells $\left(3\times10^6\right)$. While the cell viability was higher for 1×10^6 cells used, the transfection efficiency was very similar between the two conditions. The apparent difference in confluence between the two conditions (Figure 3.16) was due to difference in seeding density (different sizes of dishes used). Based on this test it was decided that 3×10^6 cells would be used for future nucleofection experiments.

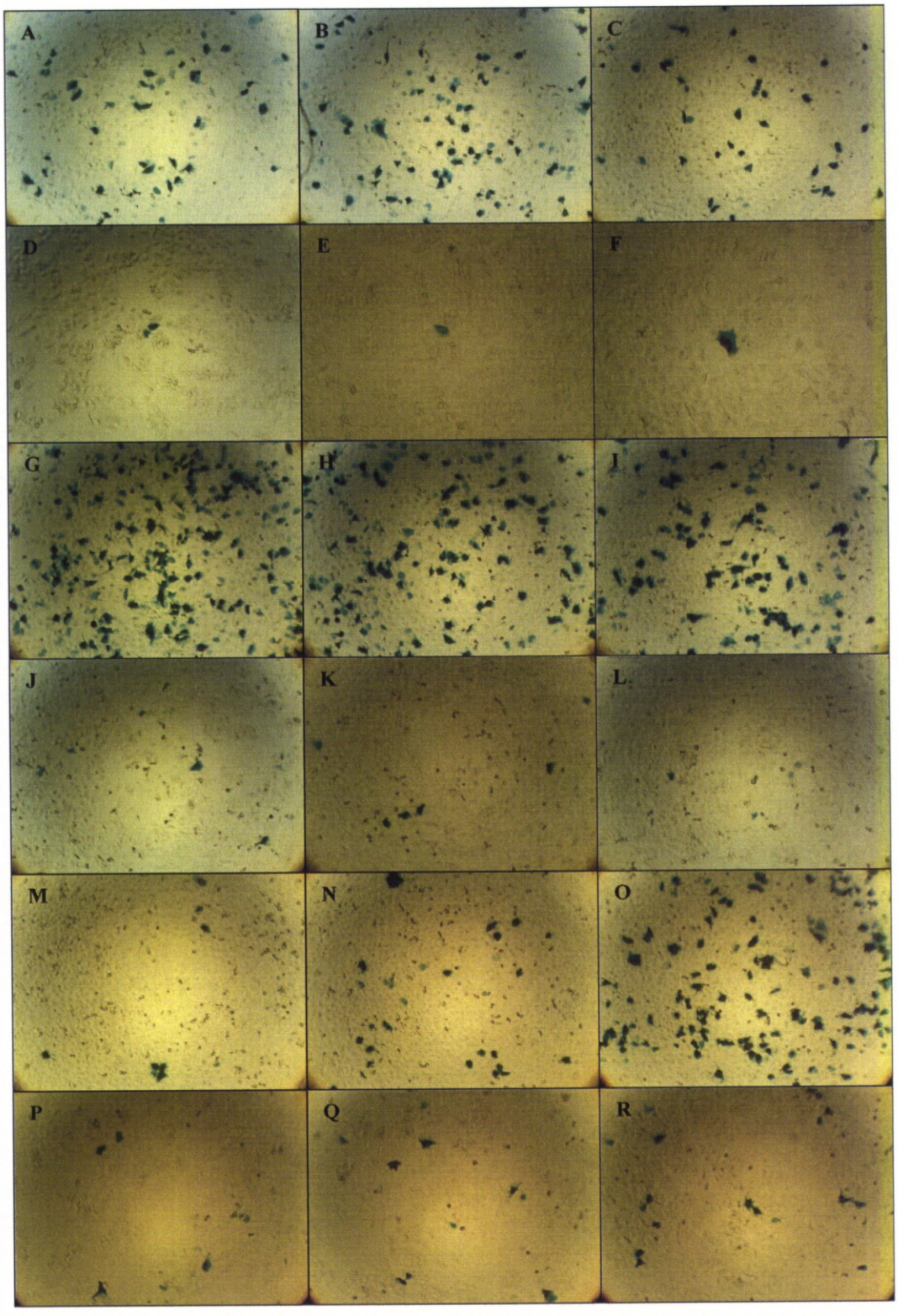

Figure 3.15: β-galactosidase transfection efficiency testing of H1299 and UM-SCC-12 cells. UM-SCC-12 cells were transfected with 1 μg of pβ-gal per well of a 6-well plate and analysed by *in situ* β-galactosidase staining 24 hours post transfection (as described in section

2.12). Transfection efficiency was estimated by judging the number of blue cells compared to the total number of cells in the dish. The experiment was performed at least thrice.

A, B, C. H1299 cells transfected using GeneJuice at 2:1, 3:1 and 4:1 ratios, respectively.

D, E, F. UM-SCC-12 cells transfected using GeneJuice at 2:1, 3:1 and 4:1 ratios, respectively.

G, H, I. H1299 cells transfected using Lipofectamine at 2:1, 2.5:1 and 3:1 ratios, respectively.

J, K, L. UM-SCC-12 cells transfected using Lipofectamine at 2:1, 2.5:1 and 3:1 ratios, respectively.

M, N, O. H1299 cells transfected using FuGENE at 2:1, 2.5:1 and 3:1 ratios, respectively.

P, Q, R. UM-SCC-12 cells transfected using FuGENE at 2:1, 2.5:1 and 3:1 ratios, respectively.

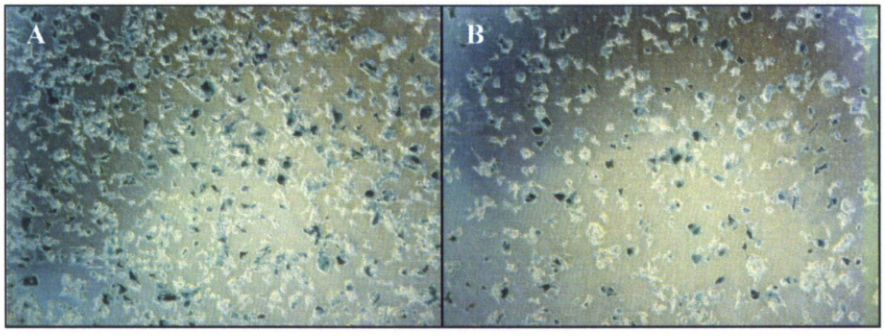

Figure 3.16: β-galactosidase testing of nucleofection efficiency of UM-SCC-12 cells. UM-SCC-12 cells were transfected by nucleofection as described in section 2.6.4. The experiment was performed once.

A. 1×10^6 cells were transfected with 3 μg of pβ-gal and seeded into a well of a 6-well plate.

B. 3×10^6 cells were transfected with 3 μg of pβ-gal and seeded into a 10 cm dish.

3.5. Establishing stable UM-SCC-12 cell lines expressing mutant p53

Due to extremely low transfection efficiency of UM-SCC-12 cells using lipofection, establishing stable cells lines expressing the TAP-tagged forms of wt and mutant p53 was attempted. Stable UM-SCC-12 derived cell lines expressing TAP-tagged p53-175H (12-175H-20) and TAP-tagged p53-273H (12-273H-39 and 12-273H-41) have been established. The level of the mutant p53 expression in the generated clones has been compared to tumour-derived UM-SCC cell lines expressing wt (UM-SCC-17AS) or mutant p53 (UM-SCC-81B) (Figure 3.17). While two of the generated clones (12-175H-20 and 12-273H-39) show moderate overexpression of the TAP-tagged p53, 12-273H-41 seems to express the mutant p53 closer to physiological level.

Attempts to produce similar clones expressing TAP-tagged wt p53 were unsuccessful in spite of performing the process of cloning and selection twice. More than 100 colonies, both fast and slowly growing ones, were selected for further expansion but many of them were lost during the expansion process because they failed to grow exhibiting signs of senescence – the cells were flat, enlarged (often more than two times larger than normal dividing cells) and had irregular, heterogeneous shapes. The clones that survived and proliferated were screened by western blotting but showed no detectable p53 expression. Given the potent growth inhibitory effects of wt p53 it could be expected that the cells would not tolerate p53 expression and therefore the failure of these attempts is not surprising.

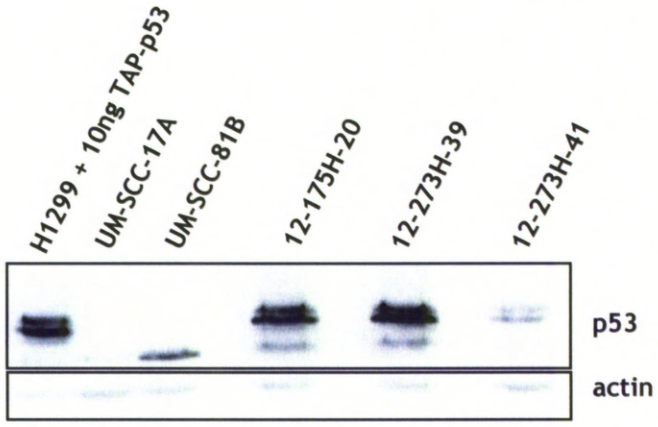

Figure 3.17: Expression levels of the TAP-tagged p53 mutants in the established clones of UM-SCC-12. Western blot analysis with the indicated antibodies (DO-1 for p53) of cell lysates of H1299 transfected with 10 ng of pNTAP-B.p53, UM-SCC-17AS (wt p53), UM-SCC-81B (mutant p53) compared to the stable clones of UM-SCC-12 expressing TAP-tagged p53-175H or p53-273H. The stable clones were tested for p53 expression multiple times.

3.6. Optimisation of the TAP-tag purification of mutant p53 complexes

In order to identify the binding partners of mutant p53, TAP-tag purification of protein complexes was performed using 12-175H-20 cells according to the manufacturer's protocol. 16×10^6 cells were used for this purification and the amounts of the resins and buffers used were scaled-up proportionately to the volumes described in section 2.20. This purification was performed once.

As shown in Figure 3.18A p53 is purified using this method. MDM2, the main negative regulator known to bind p53, was also identified in the purified protein complexes by western blotting (inset of Figure 3.18B), validating the technique as a means to purify p53-interacting proteins. Note however that other known wt p53-interacting partners, such as Bcl-2 and MDMX (discussed in sections 1.3.2.2.2 and 1.3.3.1-2, respectively), were not detected. This suggests that these proteins might specifically interact with wt p53 but not mutant p53 or that the interaction with p53 mutants is much weaker and not detectable using this system (TAP-tag purification and western blotting). Indeed, Bcl-2 was reported to be bound specifically by wt but not the tumour-derived mutants of p53 (211).

The discrete bands on the silver-stained gel suggest that there are numerous proteins in the purified complexes (indicated with arrows in Figure 3.18B) and that the sample is not degraded.

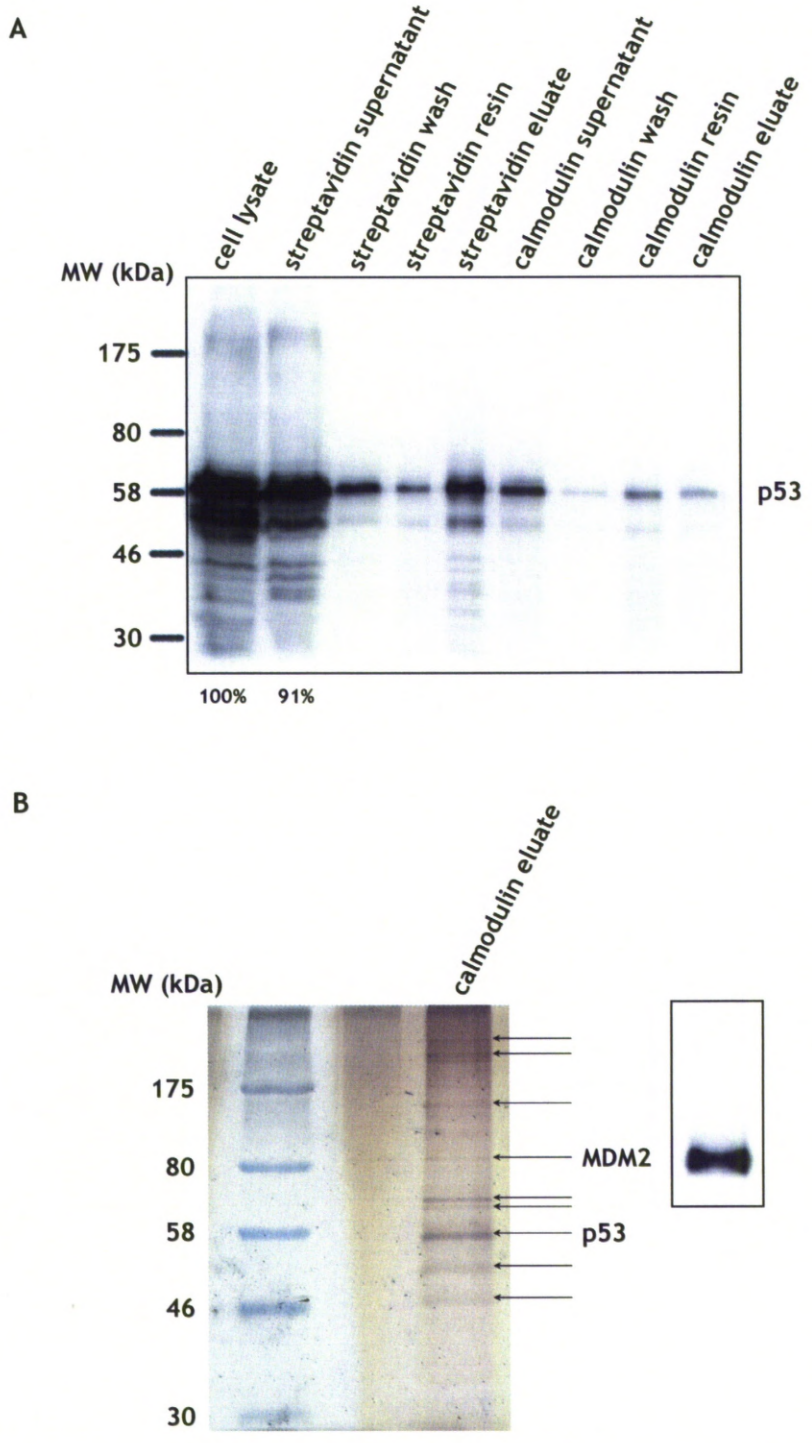

Figure 3.18: TAP-tag purification of protein complexes containing p53-175H.

A. Western blot for p53 (using DO-1) of equivalent amounts (1%) of the fractions of a TAP-tag purification from 12-175H-20 cells, resolved on a 10% polyacrylamide gel.

B. Silver staining of the proteins in 12.5% of the calmodulin eluate fraction resolved on a 10% polyacrylamide gel (representative of two replicate gels). Inset shows western blot for MDM2 in 10% of the calmodulin eluate fraction resolved on a 10% polyacrylamide gel. There is no evidence for the presence of Bcl-2 or MDMX in this fraction.

While the TAP-tag purification clearly works in principle since p53 is demonstrably purified, it is also very inefficient. The major problem seems to be the first step of the purification – binding the TAP-tagged p53 to the streptavidin resin. Densitometry was performed on western blots from samples representing the equivalent amounts (1%) of the purification fractions (Figure 3.18A) and it appeared that ~90% of p53 present in the lysate did not bind to the streptavidin resin and remained in the supernatant. The elution from streptavidin resin was fairly efficient. However, a significant proportion of the eluted p53 did not bind to calmodulin resin and remained in the calmodulin supernatant. Finally, the elution of the purified complexes from calmodulin resin was also very difficult with more protein staying on the beads than was present in the final eluate.

3.6.1. Optimisation 1 – scaling-up the amount of starting material

The first attempt to obtain a sufficient amount of protein for mass spectrometry identification involved scaling up the amount of starting material. 47×10^6 12-175H-20 cells were used for this purification but the volumes of resins and buffers used were kept the same as previously. This was based on the assumption that the streptavidin resin was not saturated (not all of the binding sites were occupied by the TAP-tagged p53) and perhaps only part of the total p53 pool was in the conformation allowing it to bind to the resin. In such a situation increasing the amount of starting material should increase the amount of protein binding to the resin. This optimisation attempt was performed once.

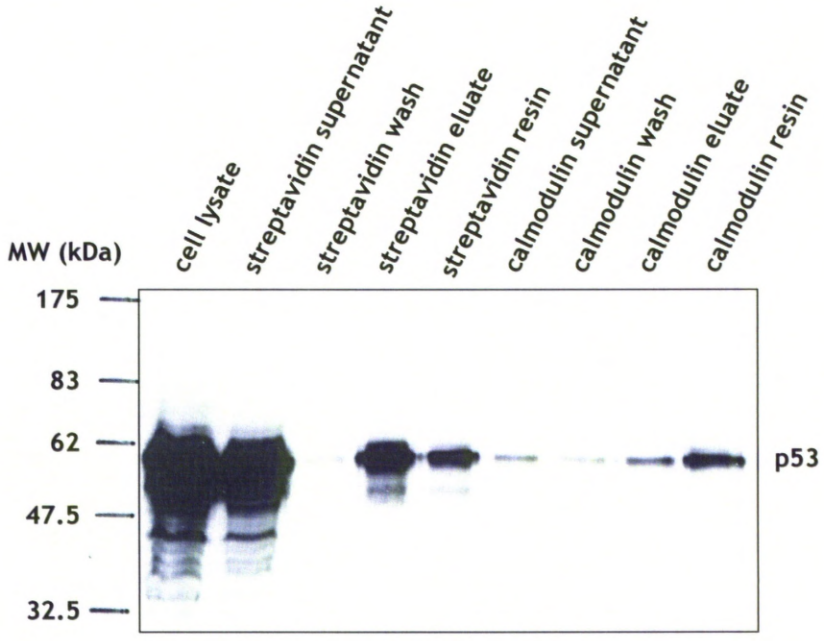

Figure 3.19: TAP-tag purification of protein complexes containing p53-175H.

Western blot for p53 (using DO-1) of equivalent amounts (0.3%) of the fractions of a TAP-tag purification from the 12-175H-20 cells, resolved on a 10% polyacrylamide gel.

Based on the strength of the signal of the streptavidin eluate fraction (Figure 3.19) and bearing in mind that three times less of each fraction was resolved on the gel this time (due to a larger volume of the lysate and to keep the amount of each fraction on the gel equal) compared to the previous experiment (Figure 3.18A), it can be concluded that the amount of TAP-tagged p53, which bound and was eluted from streptavidin resin increased to some extent although not as much as expected. Moreover, it appears that the vast majority of the TAP-tagged p53 never bound to streptavidin resin remaining in the streptavidin supernatant, suggesting that increasing the amount of starting material does not improve binding significantly. The majority of the eluted protein bound to calmodulin resin. However, most of it was not eluted and remained on calmodulin beads. Although it is a common practice in the field to boil the proteins off the calmodulin resin, this approach would increase contamination with proteins bound non-specifically to the beads and therefore on this occasion this approach was not used.

90% of the calmodulin eluate was subjected to nanospray mass spectrometry. Only two proteins were identified in the purified sample: calmodulin (99.3% coverage) and p53 (11.5% coverage). Any p53-interacting proteins that might have been purified were most likely below the threshold of detection of the mass spectrometer.

3.6.2. Optimisation 2 – extending binding and elution times

57×10^6 12-175H-20 cells were used for this purification keeping the volumes of resins and buffers used the same as previously. Since the composition of the buffers provided with the InterPlay TAP-tag kit is proprietary, manipulation of concentrations of individual components was not possible. Therefore, a composition of a custom calmodulin elution buffer was obtained from reference (489).

Calmodulin elution buffer (CEB)

Concentration	**Reagent**
10 mM	Tris, pH 7.9
10 mM	β-mercaptoethanol
0.1% (v/v)	Triton X-100
200 mM	KAc
20 mM	EGTA

The time of binding to streptavidin resin was extended and the lysate was incubated on the beads overnight. The elution time was extended to 90 min. The calmodulin binding conditions remained the same. Following binding the calmodulin resin was divided into two equal aliquots and the proteins were eluted with either the proprietary CEB or the freshly prepared CEB by rotating the tubes on a nutator at 4°C overnight. The supernatants were then transferred to fresh tubes and another elution step was performed by placing the tubes on a vortexer for 1 h at room temperature. This optimisation attempt was performed once.

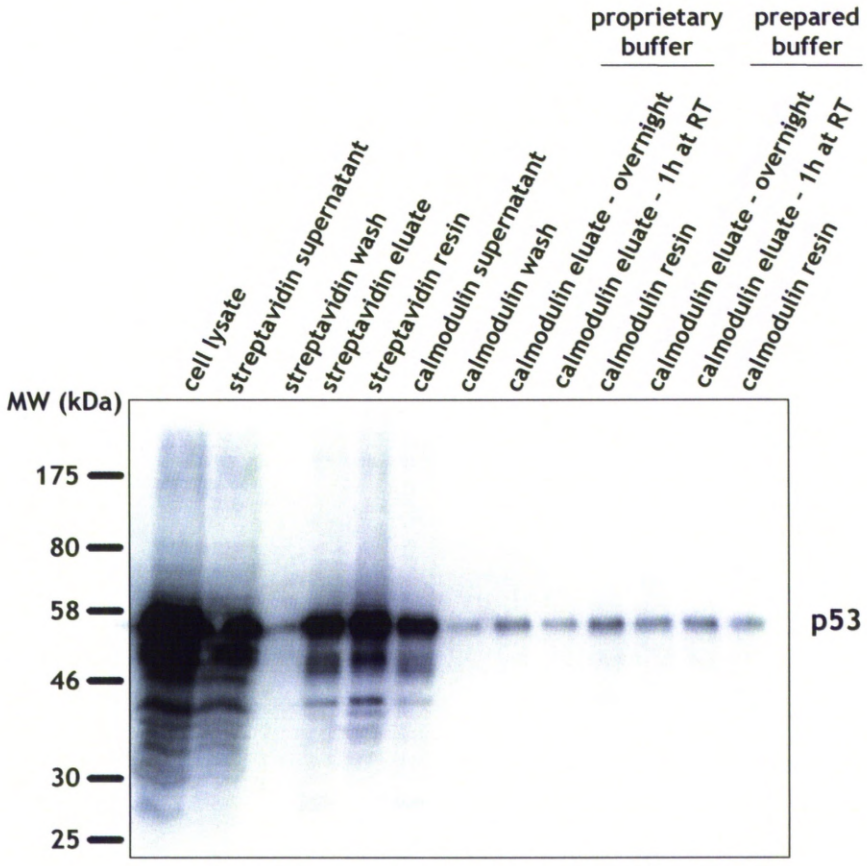

Figure 3.20: TAP-tag purification of protein complexes containing p53-175H.

Western blot for p53 (using DO-1) of equivalent amounts (0.3%) of the fractions of a TAP-tag purification from the 12-175H-20 cells, resolved on a 10% polyacrylamide gel.

The extended binding time seems to have increased the amount of p53 bound to streptavidin resin (Figure 3.20). The extended elution time did not have much influence on the amount of protein recovered and in this purification more protein stayed on streptavidin beads than was eluted in streptavidin eluate. It is possible that the extended binding time allowed for more non-specific interactions of p53 with the resin and only the specifically-bound p53 could then be eluted from the streptavidin resin. This could mean that the resin was actually saturated and the hence increasing the amount of protein was not the correct approach. The assumption that the resin is unlikely to be saturated was initially made because TAP-tag purification (performed according to manufacturer's instructions) was previously successfully used in our laboratory to purify MDM2-interacting proteins. Moreover, the amount of proteins purified this way was sufficient for mass spectroscopy identification. However, in this case it appears that all the binding sites on the streptavidin resin might actually be occupied.

The vast majority of the eluted protein did not bind to calmodulin resin, which could suggest that the resin might be saturated. Elution from calmodulin resin was improved slightly by an additional incubation of the beads for 1 h at room temperature in the elution buffer. By comparing the amount of the protein that remained on the calmodulin beads after the elution, it can be concluded that the freshly prepared CEB was slightly better than the proprietary CEB in eluting the proteins.

3.6.3. Optimisation 3 – extending binding and elution times further

Since increasing the amount of starting material did not have much influence on the amount of protein recovered from the purification, the approach of overloading the resins was abandoned and 10×10^6 12-175H-20 cells were used for this purification.

In addition to EDTA and β-mercaptoethanol the lysate was supplemented with EGTA to a final concentration of 10 mM. EDTA and EGTA are added to the lysate to chelate any Ca^{2+} and hence prevent binding of the cellular calmodulin to the calmodulin-binding peptide (CBP) of the TAP-tagged protein, which could potentially conceal the streptavidin-binding peptide and interfere with binding to streptavidin resin. Moreover, binding of intracellular calmodulin to the CBP could also hinder later binding of the tagged protein to calmodulin (discussed in reference (490)).

Binding and elution from streptavidin resin and binding to calmodulin resin were performed overnight at 4°C. The prepared CEB (section 3.6.2) was used and two consecutive elutions from calmodulin resin were performed for 1 h at room temperature on a vortexer. The amounts of resins and buffers used were as indicated in section 2.20 for processing 10×10^6 cells. This optimisation attempt was performe once.

While binding to streptavidin resin was significantly better compared to the first purification (Figure 3.18A), the overnight elution from streptavidin resin does not seem to have improved the elution efficiency suggesting that the proteins remaining on streptavidin resin might be bound to it non-specifically. Most of the eluted protein bound to calmodulin resin supporting the hypothesis that the calmodulin resin may have been overloaded in the previous optimisation attempt (section 3.6.2). Although the two consecutive elution steps with prepared CEB (see section 3.6.2) at room temperature resulted in nearly complete elution of the bound proteins from calmodulin resin, the amount of TAP-tagged p53 in the calmodulin eluate (as judged by the western blot signal in Figure 3.21) was still insufficient for mass spectrometry identification.

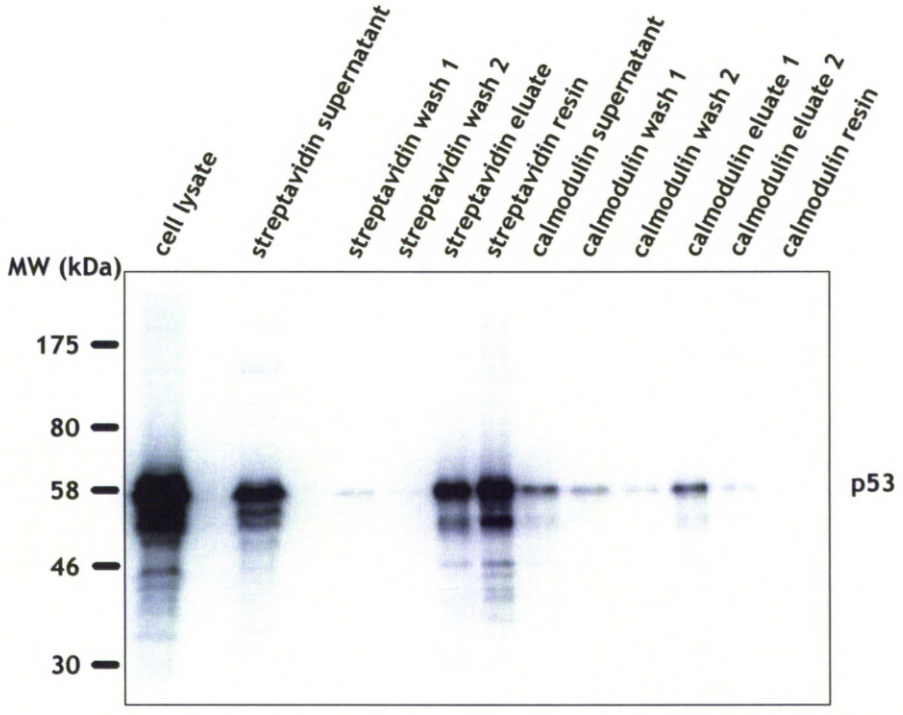

Figure 3.21: TAP-tag purification of protein complexes containing p53-175H.

Western blot for p53 (using DO-1) of equivalent amounts (0.75%) of the fractions of a TAP-tag purification from the 12-175H-20 cells, resolved on a 10% polyacrylamide gel.

3.6.4. Optimisation 4 – custom buffers and increasing the amount of streptavidin resin

No significant improvement in the efficiency of purification was achieved in the previous optimisation attempts. Since the composition of the buffers provided with the kit was proprietary, the buffers were replaced with custom buffers and the purification was performed as described in section 2.20.1. Two purifications were performed in this optimisation attempt – both using 10×10^6 12-175H-20 cells. For one purification the amounts of resins used were as described in section 2.20.1 (Figure 3.22A) and for the other – 10 times greater amount of streptavidin resin and the respective elution buffer were used while the amount of calmodulin resin used was kept the same (Figure 3.22B). Densitometry was performed on the western blots to obtain an estimation of signal intensity of the purification fractions. This optimisation attempt was performed once.

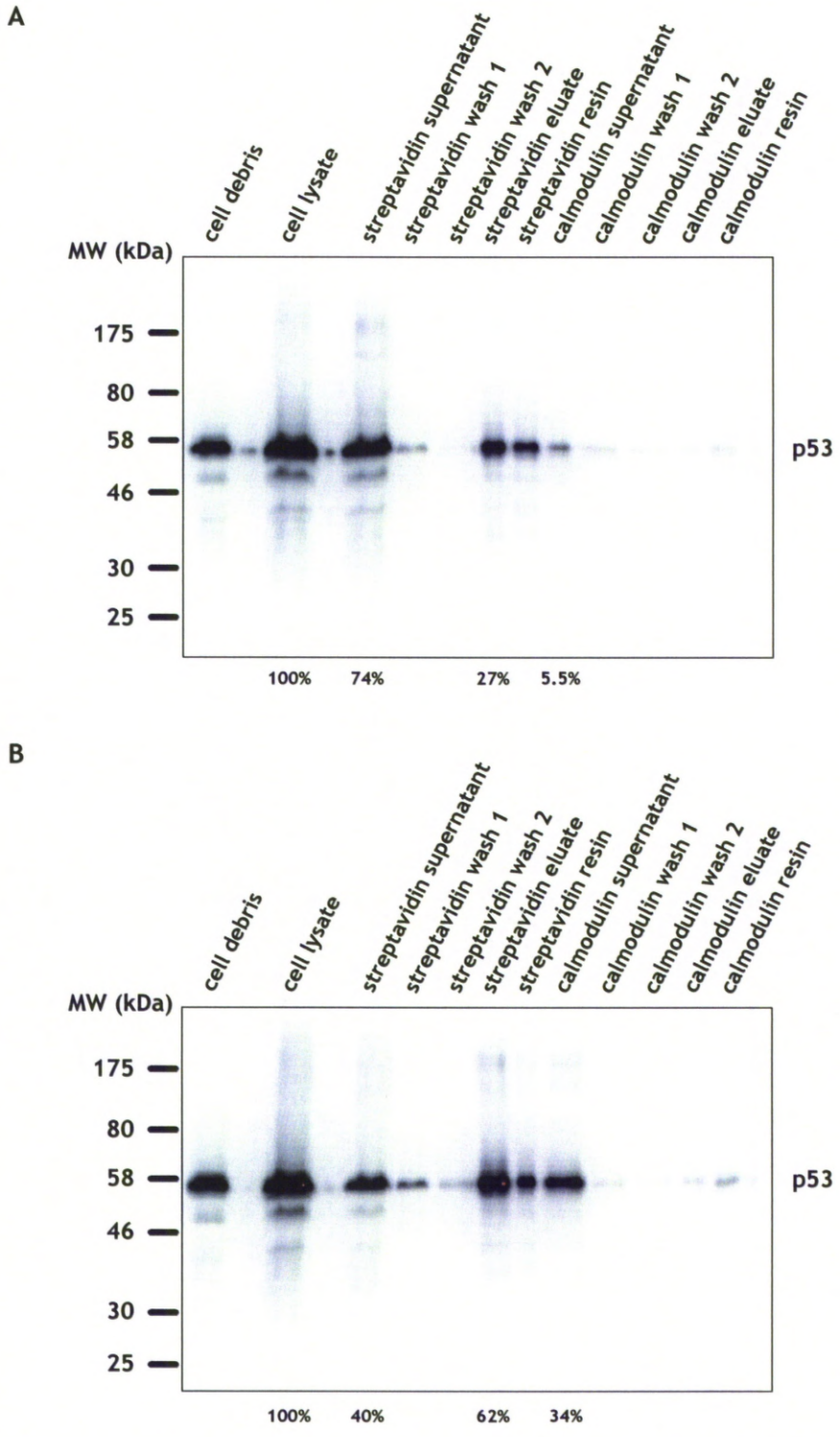

Figure 3.22: TAP-tag purification of protein complexes containing p53-175H.

Western blot for p53 (using DO-1) of equivalent amounts (0.75%) of the fractions of a TAP-tag purification from the 12-175H-20 cells, resolved on a 10% polyacrylamide gel. The purification was performed using the recommended amount of streptavidin resin (A) or 10 times the recommended amount of streptavidin resin (B).

In this purification custom buffers were used. In order to check whether the lysis of the cells is complete using the custom lysis buffer, the pellet of the cell debris was resuspended in 1× sample loading buffer, boiled at 99°C and loaded onto the polyacrylamide gel alongside all the other purification fractions. As shown in Figure 3.22, although some TAP-tagged p53 remains in the cell debris, the majority of the protein is in the lysate. Using 10-fold more than the recommended amount of streptavidin resin significantly increases binding efficiency with only 40% remaining in the unbound fraction (streptavidin supernatant, Figure 3.22B) compared to 74% when the recommended amount of resin was used (Figure 3.22A). Elution from the streptavidin resin was successful in both cases with more protein being eluted than staying on streptavidin resin.

When binding to calmodulin resin is considered approximately 22% of total TAP-tagged p53 available bound to calmodulin in the first purification (Figure 3.22A) compared to 28% when 10 times more streptavidin resin was used (Figure 3.22B). Clearly, although over twice as much (62% vs. 27%) of the TAP-tagged p53 was applied to calmodulin resin, the amount of protein bound increased marginally (by only 6%). This suggests that the calmodulin resin was saturated and hence no more protein could bind to it. Elution from calmodulin resin was highly inefficient in both cases as more protein remained on the beads than was eluted in the final eluate.

3.6.5. Optimisation 5 – increasing the amount of calmodulin resin

The results from the previous optimisation attempt suggested that the calmodulin resin might be saturated so the next step was to increase the amount of calmodulin resin used. 10×10^6 12-175H-20 cells were used for this purification and in addition to using 10-fold more streptavidin resin, the amount of calmodulin resin and the

respective elution buffer were increased 10-fold. Moreover, since the elution from calmodulin was quite inefficient in the previous optimisation attempt (section 3.6.4), two consecutive elutions were performed for 30 min. at room temperature on a vortexer. The calmodulin elution buffer was prepared based on the recipe used before (section 3.6.2) increasing the concentrations of KAc and EGTA. All the other buffers used were the same as in the previous optimisation attempt (section 3.6.4). This optimisation attempt was performed once.

Calmodulin elution buffer (CEB)

Concentration	**Reagent**
10 mM	Tris, pH 7.9
10 mM	β-mercaptoethanol
0.1% (v/v)	Triton X-100
1 M	KAc
25 mM	EGTA

Similarly to the previous purification (section 3.6.4), approximately 40% of the total TAP-tagged protein did not bind to streptavidin resin and approximately 60% was eluted from the resin, suggesting that the purification efficiency is very consistent. Increasing the amount of calmodulin resin used, however, did not improve the binding significantly as only 32% seemed to bind to calmodulin resin (Figure 3.23) compared to 28% in the previous optimisation attempt (Figure 3.22B).

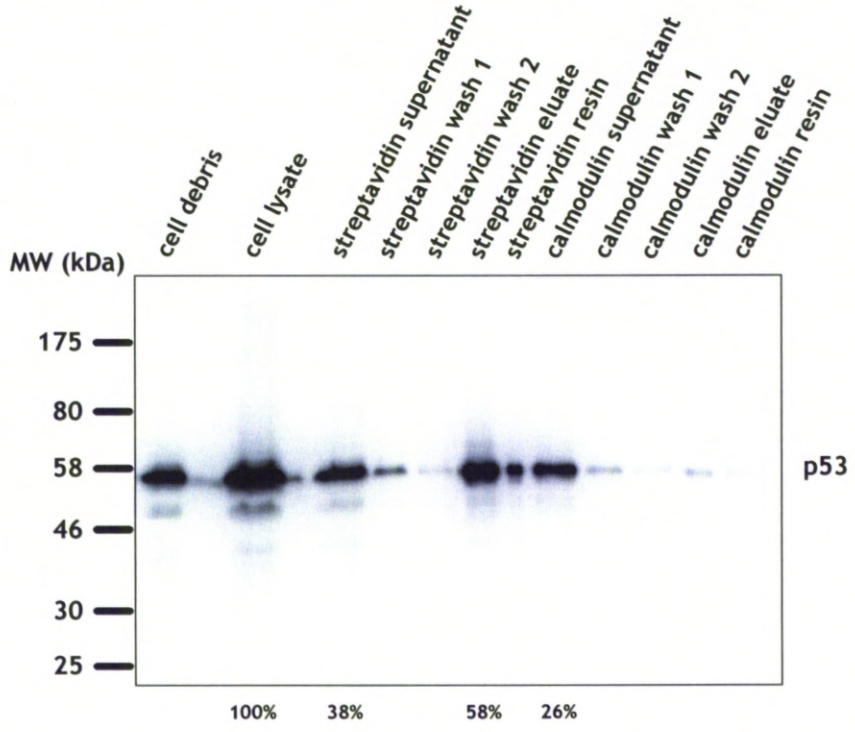

Figure 3.23: TAP-tag purification of protein complexes containing p53-175H.

Western blot for p53 (using DO-1) of equivalent amounts (0.75%) of the fractions of a TAP-tag purification from the 12-175H-20 cells, resolved on a 10% polyacrylamide gel.

3.6.6. Optimisation 6 – adding EGTA to the lysate

Binding to streptavidin was improved significantly by increasing the amount of streptavidin resin used but binding to calmodulin remained highly inefficient. In an attempt to improve binding to calmodulin, the lysate was supplemented with EGTA to a final concentration of 10 mM, as described in section 3.6.3. All the remaining buffers used were the same as in the previous optimisation attempt (section 3.6.5). 10×10^6 12-175H-20 cells were used for this purification. This optimisation attempt was performed once.

While addition of EGTA did not influence binding to streptavidin resin, the elution seemed to be less efficient with 49% of protein recovered from streptavidin resin (Figure 3.24) compared to 58% in the previous optimisation attempt (Figure 3.23). Importantly, binding to calmodulin resin was also not improved with only about 25% binding to the resin.

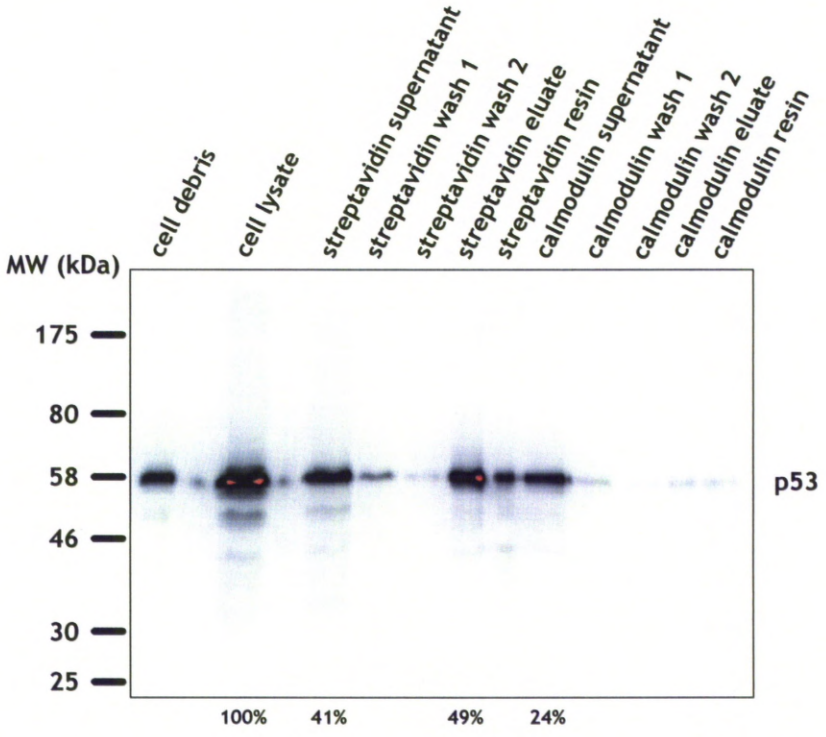

Figure 3.24: TAP-tag purification of protein complexes containing p53-175H.

Western blot for p53 (using DO-1) of equivalent amounts (0.75%) of the fractions of a TAP-tag purification from the 12-175H-20 cells, resolved on a 10% polyacrylamide gel.

3.6.7. Optimisation 7 – lysis in the absence of EDTA

Since addition of EGTA to the lysate seemed to reduce the recovery of TAP-tagged p53 from the streptavidin resin, in this optimisation attempt neither EDTA nor EGTA were added to the lysis buffer or lysate, respectively. All the remaining buffers used were the same as in the previous optimisation attempt (section 3.6.6). 10×10^6 12-175H-20 cells were used for this purification. Additionally, the purification through streptavidin resin only was also performed using 10×10^6 UM-SCC-12 cells (as a negative control for the purification specificity) in order to check whether the p53-175H complexes purified only using streptavidin resin contained a lot of proteins that were bound to the resin non-specifically. This experiment was performed once.

Removing EDTA from the lysis buffer significantly improved binding to streptavidin, with approximately 90% binding and 69% of the protein recovered from streptavidin resin (Figure 3.25A). Binding to calmodulin remained unaffected with 28% binding to the resin. Since no improvement in the second purification stage (calmodulin purification) was achieved in spite of multiple optimisation attempts, it was investigated whether purification of the mutant p53-containing complexes could be performed using streptavidin resin alone. For this purpose, a lysate from UM-SCC-12 cells, which do not express TAP-tagged p53, was used for the first purification stage (streptavidin purification) and equivalent fractions of streptavidin eluates from purifications performed using both cell lines (UM-SCC-12 and 12-175H-20) were compared on a silver-stained polyacrylamide gel (Figure 3.25B). The purification through streptavidin resin alone appeared to be quite specific with only a few proteins (indicated with arrows in Figure 3.25B) being present in both samples. Therefore, it was decided that the mutant p53-containing complexes would be purified using streptavidin resin only.

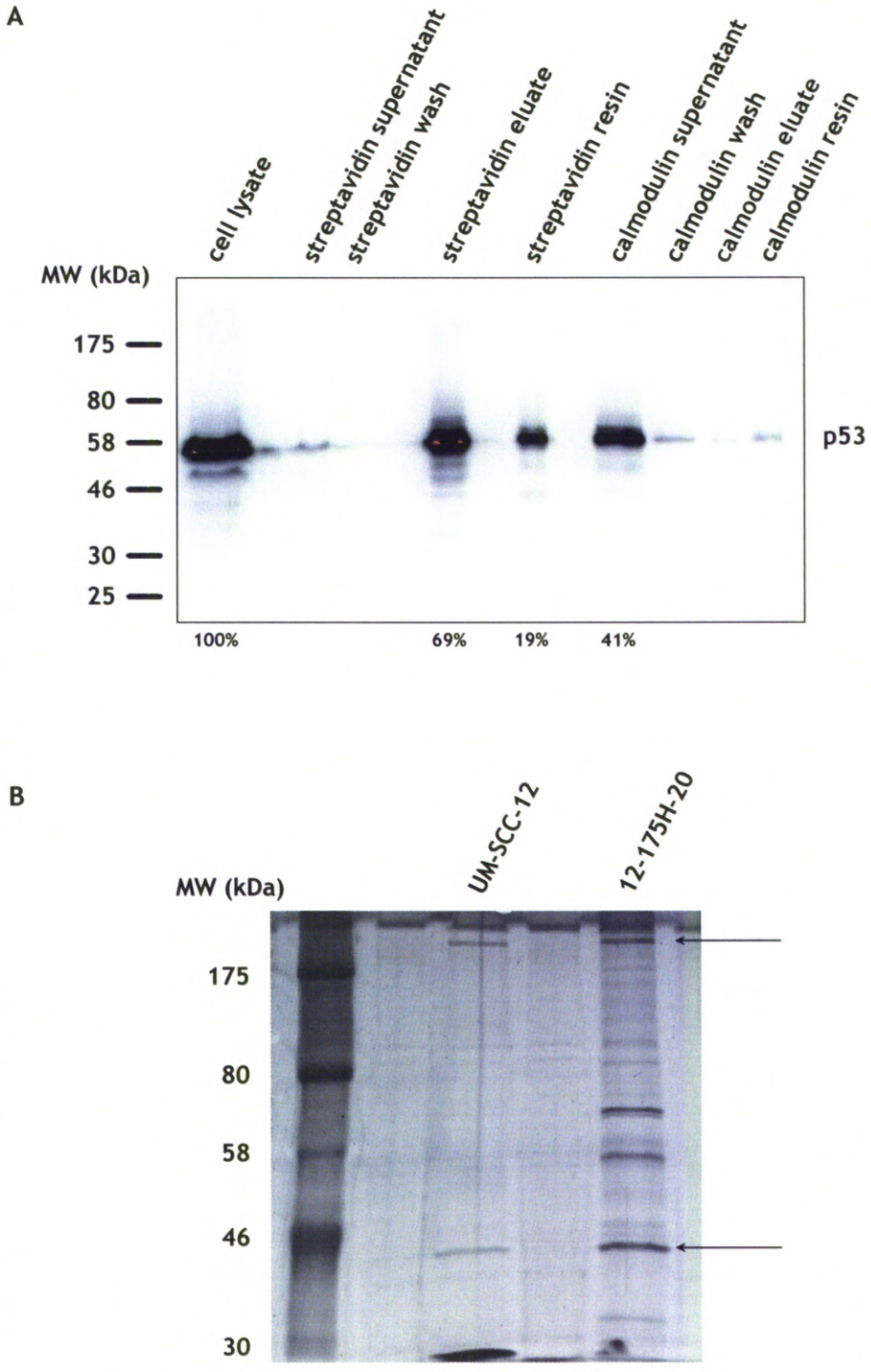

Figure 3.25: TAP-tag purification of protein complexes containing p53-175H.

A. Western blot for p53 (using DO-1) of equivalent amounts (0.75%) of the fractions of a TAP-tag purification from the 12-175H-20 cells, resolved on a 10% polyacrylamide gel.

B. Silver staining of the proteins in 1.75% of the streptavidin eluate fraction from a TAP-tag purification performed using lysates from UM-SCC-12 and 12-175H-20 cells, resolved on a 10% polyacrylamide gel.

3.7. Purification and identification of mutant p53 interacting partners

3.7.1. Purification of mutant p53-containing complexes

Due to the poor efficiency of binding and elution of TAP-tagged p53 from the calmodulin resin, the TAP-tag purification was reduced to purification through streptavidin resin only. 10×10^6 UM-SCC-12 cells, 12-175H-20 cells and 12-273H-39 cells were used for this purification. The buffers used were the same as in the previous optimisation attempt (section 3.6.7) and for clarity the compositions are listed below. To maximise the purification efficiency, three consecutive elutions from streptavidin resin were performed.

Lysis buffer

Concentration	**Reagent**
10% (v/v)	glycerol
50 mM	HEPES
150 mM	NaCl
0.1% (v/v)	Triton X-100
2 mM	DTT
10 mM	NaF

Supplemented with protease inhibitors (as described previously).

Calmodulin binding buffer (CBB) – used for washes before the elution

Concentration	**Reagent**
10 mM	β-mercaptoethanol
50 mM	HEPES
150 mM	NaCl
1 mM	MgAc
1 mM	imidazole
0.1% (v/v)	Triton X-100
2 mM	$CaCl_2$

Streptavidin elution buffer (SEB)

Concentration	**Reagent**
10 mM	β-mercaptoethanol
50 mM	HEPES
150 mM	NaCl
1 mM	MgAc
1 mM	imidazole
0.1% (v/v)	Triton X-100
2 mM $CaCl_2$	2 mM $CaCl_2$
10 mM	D-biotin

Purification using 12-175H-20 cells was perfomed twice, while the other two purifications (using UM-SCC-12 cells and 12-273H-39 cells) were performed once.

An additional, third consecutive elution step significantly increased the recovery of proteins from streptavidin resin with 91% of total TAP-tagged p53-175H being present in the final streptavidin eluate (Figure 3.26A). The streptavidin eluate from the p53-273H purification seems to contain more protein than was present in the lysate (Figure 3.26B), an impression which may be due to pipetting error (unequal loading).

Silver staining of the streptavidin eluates (Figure 3.27) revealed a different pattern of bands in the samples containing the two p53 mutants (p53-175H and p53-273H) suggesting that they have different interacting partners. Performing the purification using the parental UM-SCC-12 cells (p53-null) allowed for exclusion of any proteins binding to the streptavidin resin non-specifically from analysis.

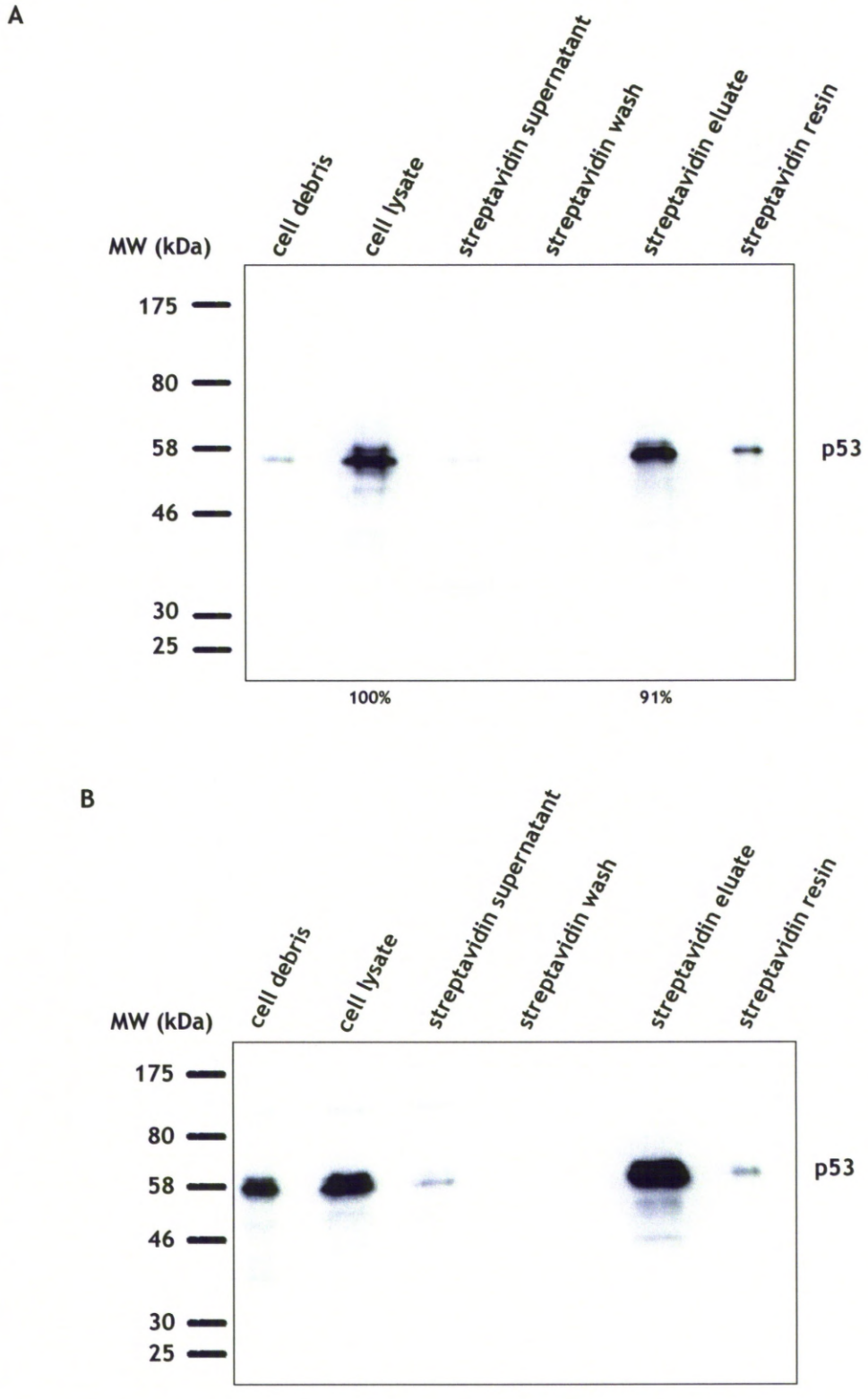

Figure 3.26: Purification of the mutant p53-containing complexes.

Western blot for p53 (using DO-1) of equivalent amounts (0.75%) of the fractions of a TAP-tag purification from the 12-175H-20 cells (A) or 12-273H-39 cells (B), resolved on a 10% polyacrylamide gel.

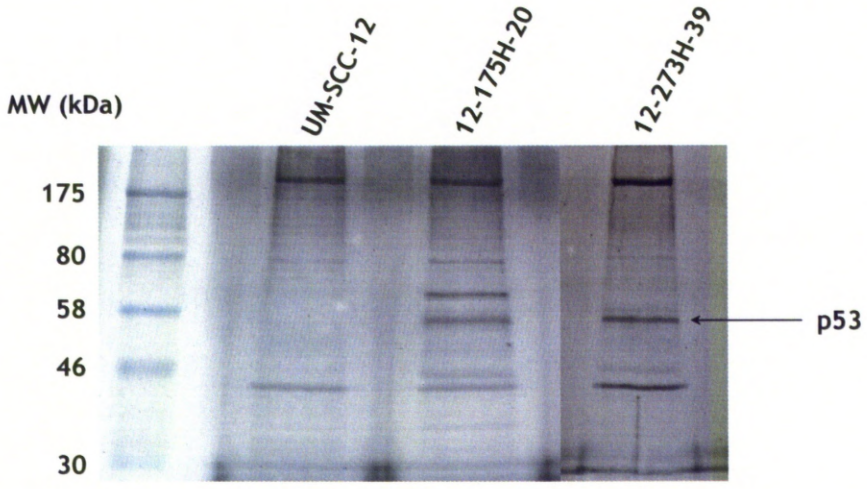

Figure 3.27: Purification of the mutant p53-containing complexes.

Silver staining of the proteins in 2% of the streptavidin eluate fractions from TAP-tag purifications performed using lysates from UM-SCC-12, 12-175H-20 and 12-273H-39 cells, resolved on a 10% polyacrylamide gel.

3.7.2. Identification of mutant p53-interacting proteins

95% of the final streptavidin eluates from section 3.7.1 were subjected to mass spectrometry. A full list of identified proteins is presented in Appendix 9. The proteins present only in the test samples (containing the mutant TAP-tagged p53) and not in the control sample (purified from UM-SCC-12) are shown in Table 3.2.

p53 was detected in both of the test samples (Table 3.2). Another protein identified in both mutant p53-containing complexes was myosin light chain kinase 2 (skeletal/cardiac muscle). Given that the calmodulin-binding peptide was derived from skeletal muscle myosin light-chain kinase, the identified peptides were most likely those comprising the CBP.

HSP70 was identified only in the p53-175H-containing complexes. HSP70 is an inducible chaperone stabilising existing proteins against aggregation and mediating the folding of newly translated proteins (491). p53-175H is a structural mutant and it may be bound by HSP70 because it is most likely misfolded.

Although 3 peptides of heat shock cognate 71 kDa protein (HSP7C, also known as HSC70) were identified in the control sample (from UM-SCC-12), 43 peptides of this protein were found in the test sample from p53-175H purification. The significant enrichment of this heat shock cognate in the p53-175H-containing sample suggests that the interaction of these two proteins is specific, likely because p53-175H is recognised by HSC70 as a misfolded protein. Most likely both HSP70 and HSC70 contribute to the thick band observed on the silver-stained gel slightly above the 58 kDa marker band in p53-175H-containg sample but not in the other two samples (Figure 3.27).

Table 3.2: The list of proteins identified in the mutant p53-containing complexes, purified from 12-175H-20 and 12-273H-39 cells, respectively. The number next to each protein indicates the number of peptides identified. Due to high sequence similarity of some proteins, some of the identified peptides could not be unequivocally assigned to one protein. These ambiguous cases are shaded with the same colour.

12-175H-20 cells		12-273H-39 cells	
Cellular tumour antigen p53	21	Cellular tumour antigen p53	37
Heat shock 70 kDa protein 1 (HSP70)	38	Serum albumin	3
Heat shock cognate 71 kDa protein (HSP7C)	43	CD59 glycoprotein	2
BAG family molecular chaperone regulator 2 (BAG2)	7	Histone H1.2	1
Tropomodulin-3 (Tmod3)	2	Tropomodulin-3 (Tmod3)	2
Myosin light chain kinase 2, skeletal/cardiac muscle	1	Myosin light chain kinase 2, skeletal/cardiac muscle	2
Myosin-VI	1	Myosin-VI	2
		Keratin, type II cytoskeletal 1	4
		Keratin, type I cytoskeletal 10	2
		Keratin, type II cytoskeletal 2 epidermal	3
		Keratin, type II cytoskeletal 6A	2
		Keratin, type II cytoskeletal 75	1
		Keratin, type II cytoskeletal 5	2
		Keratin, type II cytoskeletal 6C	2
		Keratin, type II cytoskeletal 6B	2
		Keratin, type II cytoskeletal 79	1

BAG2 (BCL2-associated athanogene 2) was also identified only in the p53-175H-containing sample. BAG2 binds with high affinity to the ATPase domain of HSC70/HSP70 and promotes substrate release (492), resulting in reduced degradation of misfolded proteins (493). It is possible that BAG2 co-purified with p53-175H due to its interaction with HSP70.

Tropomodulin-3 was identified in both of the mutant p53-containing samples. Tropomodulin-3 regulates actin polymerization by capping pointed ends of actin filaments and sequestering actin monomers, and hence acts as a negative regulator of cell migration. The fact that only 2 peptides of tropomodulin-3 were identified in each of the samples may suggest that the interaction with mutant p53 is relatively weak.

Myosin-VI was identified in both of the mutant p53-containing samples. Myosin-VI is an actin-based motor protein, involved in intracellular vesicle transport and cell migration. However, the small number of peptides actually identified suggests that the interaction with the two p53 mutants is relatively weak.

The proteins identified only in the p53-273H complexes included: serum albumin, CD59 glycoprotein, histone H1.2 and a number of cytoskeletal keratins (Table 3.2). Skeletal keratins have a high sequence similarity and based on the few peptides identified it was impossible to distinguish, which type was actually present (Table 3.2). Generally, only between 1 and 3 peptides were identified in the p53-273H-containing sample for the above proteins suggesting that these interactions are relatively weak.

Interestingly, MDM2 was not identified in the mutant p53 containing complexes by mass spectroscopy although it was detected previously by western blotting in the calmodulin eluate from the first purification of p53-175H-containing complexes (Figure 3.18B). It is important to note that a large proportion (10%) of the final

calmodulin eluate was probed with an anti-MDM2 antibody, which is very sensitive. This likely suggests that the interaction of mutant p53 with MDM2 is relatively weak and the amount of MDM2 present in the purified complexes was below the threshold of detection by the mass spectrometer.

3.8. HSP70 interacts specifically with the R175H mutant of p53

Following purification of the mutant p53 containing complexes using a simplified TAP-tag purification method coupled with identification of the isolated proteins by mass spectroscopy (section 3.7), immunoprecipitation was performed to further determine whether the identified mutant p53 interacting proteins were present in protein complexes in cells. Since this entailed using a different approach, such data would provide additional evidence supporting the validity of the identified protein interactions and of the TAP-tag/mass spectrometry method for identifying mutant p53 binding proteins.

H1299 cells were transfected with wt p53, p53-175H, p53-273H or the corresponding empty vector. The p53-containing complexes were immunoprecipitated using a p53-specific antibody (as described in section 2.22) and analysed by SDS-PAGE and western blotting (Figure 3.28). This experiment was performed once.

Transfection of wt and two mutant forms of p53 into H1299 cells (p53-null) resulted in uneven expression of the p53 forms, with the highest level of expression of wt p53, slightly lower of p53-273H and even lower of p53-175H. Nevertheless, the efficiency of immunoprecipitation of these p53 forms was comparable with perhaps a slightly stronger signal for wt p53 (Figure 3.28). The observed difference in the mobility of the three p53 forms (with wt p53 migrating faster than the p53 mutants) is most likely due to differences in the SNP at amino acid 72. The p53 mutants used in

this project carry a proline at residue 72, while the used wt p53 has an arginine at this position. Difference in mobility of p53 forms differing in the status of the SNP at amino acid 72 was reported previously, with p53-72R exhibiting faster mobility than p53-72P (494).

As expected, wt p53 caused induction of MDM2 (as observed in the lysate of H1299 transfected with wt p53). MDM2 also immunoprecipitated preferentially with wt p53, suggesting that not only is MDM2 induced by wt p53 but also the interaction of MDM2 with wt p53 is probably stronger than with either of the mutant p53s.

HSP70 was found to immunoprecipitate specifically with p53-175H, providing further support that it is a p53-175H-interacting protein. Moreover, the absence of HSP70 in the other immunoprecipitated samples suggests that the interaction of HSP70 with p53-175H is preferential, likely due to misfolded or altered structure of this p53 mutant (as discussed previously).

Tmod3, on the other hand, although identified in the mutant p53-containing complexes, does not seem to immunoprecipitate with p53 in this assay (Figure 3.28). As discussed previously, the interaction of Tmod3 with mutant p53 may be either non-specific or too weak to be identified by western blotting.

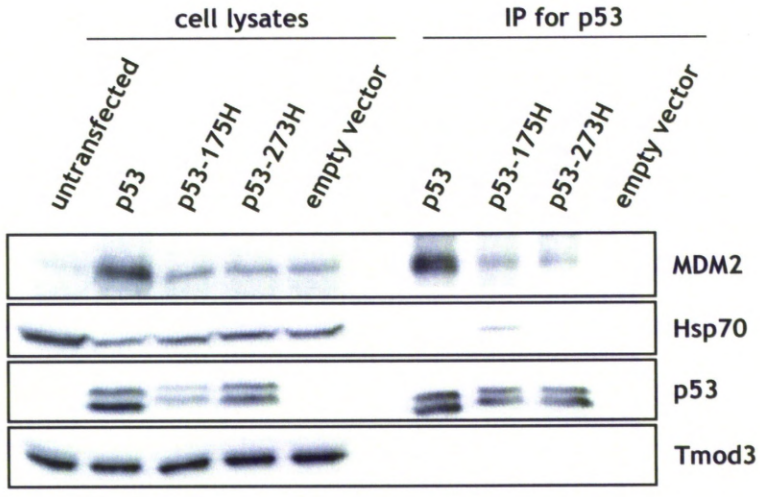

Figure 3.28: Immunoprecipitation of wt and mutant p53-containing complexes. Western blot analysis with the indicated antibodies (ab2433 for p53) of lysates and immunoprecipitated fractions from H1299 cells transfected with 15 μg of p53, p53-175H, p53-273H in pCMV-Script or the corresponding empty vector. Cells were harvested 48 hours post transfection. Immunoprecipitation with a p53-specific antibody (Ab-1) was performed using 4 mg of total protein per condition. This experiment was performed once.

3.9. Cells expressing mutant p53 exhibit increased motility

GOF p53 mutants are associated with highly aggressive and metastatic tumours, which are the main cause of cancer mortality. Therefore, cell migration and invasiveness (surrogate indicators of metastatic potential) of mutant p53-expressing cells were studied in this project.

The motility of the previously generated cell clones expressing TAP-tagged p53-175H and p53-273H (see section 3.5) was studied using Boyden chamber motility assays and live cell imaging. These two assays measure different properties. The Boyden chamber motility assay measures the ability of cells to migrate through pores in a membrane, whilst live cell imaging measures the motility of cells in two dimensions on plastic.

3.9.1. Boyden chamber motility assays

Boyden chamber motility assays were performed as described in section 2.15. The motility of the following cell lines was studied in this experiment:

- UM-SCC-12 – p53-null,
- 12-175H-20 – expressing high level of TAP-tagged p53-175H,
- 12-273H-39 – expressing high level of TAP-tagged p53-273H,
- 12-273H-41 – expressing low level of TAP-tagged p53-273H,
- 12-273H-null – a cell line established as a result of the cloning process but with no detectable p53-273H expression.

This entire experiment was performed once, however the motility of UM-SCC-12 cells in this assay was tested twice.

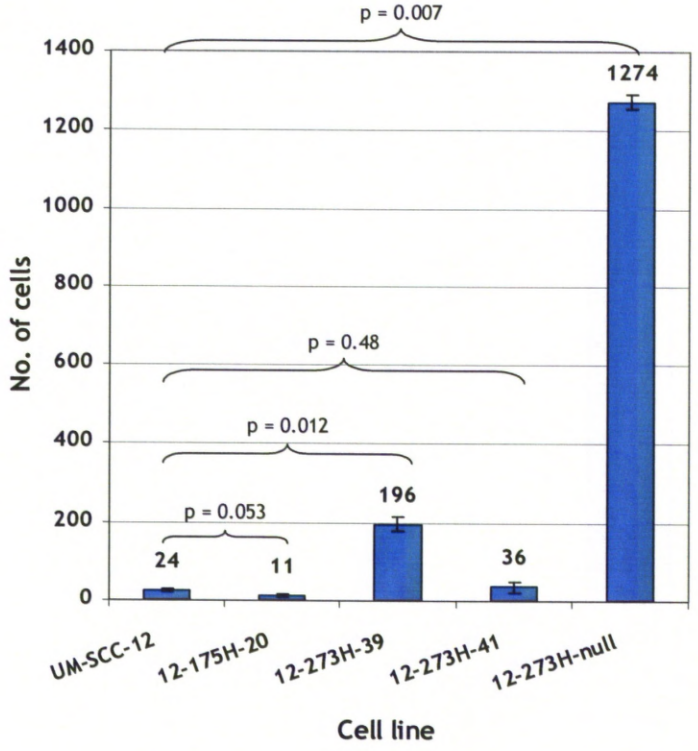

Figure 3.29: Motility of mutant p53-expressing cell lines determined using Boyden chamber motility assays. 15,000 cells were seeded into Boyden chambers and incubated for 18 hours. The number of cells that migrated through the membrane was counted. The values shown above the histograms represent the mean of three replicates, the error bars represent standard error of mean. Statistical analysis was performed using Student's t-Test. The differences were considered significant if $p < 0.05$.

As shown in Figure 3.29, 12-175H-20 cells have a slightly reduced motility in this assay as compared to the parental UM-SCC-12 cells but this difference is not statistically significant ($p = 0.053$). The motility of 12-273H-41 cells was similar to UM-SCC-12 cells ($p = 0.48$). 12-273H-39 cells were over 8-fold more motile than UM-SCC-12 cells and this difference was statistically significant ($p < 0.05$). Interestingly, 12-273H-null cells turned out to be over 50-fold more motile than the parental UM-SCC-12 cells ($p < 0.05$). It was observed that these cells display an elongated, spindle-like morphology and form numerous filopodia. The morphology of these cells is compatible with an EMT. Whilst this has not been investigated specifically, such an EMT could provide an explanation for how the cells are able to migrate more efficiently through the Boyden chamber membrane.

Generally, it can be observed that the laryngeal cancer cell lines studied are not very motile in this system since out of 15,000 cells seeded into the Boyden chambers, only between 11 and 1274 cells (less than 8.5%) migrated through the membrane. These data suggest that this might not be the most appropriate system to study the migratory potential of these cells. This might be partially due to the fact that the cells studied in this project require a considerable time to adhere to the surface of the dish and their plating efficiency is very low. It was observed as part of a different experiment (clonogenic assays, section 3.13) that the plating efficiency (see section 2.23) of UM-SCC-12 cells is very low (~9.5%) and even lower for p53-175H and p53-273H-expressing cells (~5.9% and ~3.8%, respectively). Hence, the number of cells that actually adhered to the surface of the membrane might have influenced the number of migrating cells. Moreover, with an increased time required for the cells to adhere to the membranes, the time during which the cells could have migrated through the pores was considerably shorter. Extending the duration of the experiment,

however, proved to be impractical since most of the cells were able to divide during the experiment making the data impossible to interpret.

3.9.2. Live imaging of cell migration

Live cell imaging was performed as described in section 2.14 using the same cell lines that were used for Boyden chamber motility assays (section 3.9.1). The motility of UM-SCC-12 cells and 12-273H-39 cells was tested in this system of two different occasions. In this experiment the cells were imaged for 14.4 hours with a time-lapse of 3 min. (288 passes). Two fields were selected per cell line and 10 cells from each field were tracked, resulting in a total of 20 cells tracked per cell line. Representative movies are available on the attached CD (see Appendix 10). The tracks of 10 cells on a 2D plane are presented below (Figure 3.30).

Based on the recorded cell tracks (Figure 3.30), UM-SCC-12 cells seem to have travelled the smallest net distance out of all the cell lines. The total distance travelled, net distance travelled, speed and directionality (as defined in section 2.14) were then determined using a plugin for ImageJ based on the coordinates of each of the cells recorded for each frame.

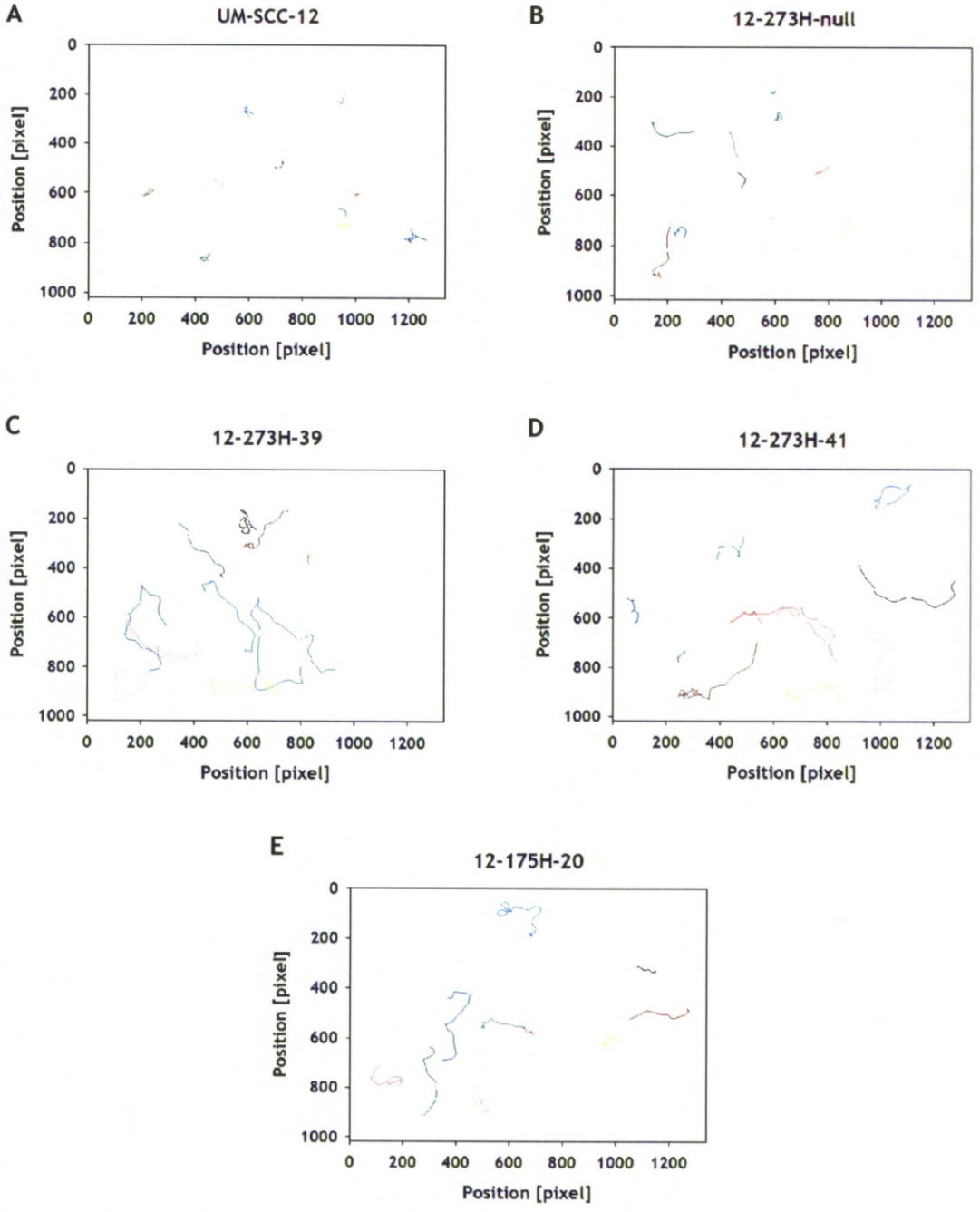

Figure 3.30: Tracks of cells selected for tracking represented on a 2D plane.

The cells were imaged for 14.4 hours with a time-lapse of 3 min. 10 cells per field were tracked. The plane, on which the tracks are shown, represents the actual area, on which the cells were moving. The axes represent the coordinates assigned to the image by ImageJ.

12-273H-39 cells and 12-273H-41 cells display increased motility (approximately 2-fold higher) compared to the parental UM-SCC-12 cells, as judged by the total distance travelled and speed, which are directly proportional (Figure 3.31A and D). The net distance travelled by the cells expressing the 273H mutant of p53 is also significantly larger than that of the parental UM-SCC-12 ($p < 0.05$). The directionality of 12-273H-39 cells and 12-273H-41 cells seems slightly higher than that of UM-SCC-12 cells but this difference is not statistically significant (Figure 3.31B and C). Directionality provides information about whether the movement of cells is random. Directionality is always ≤ 1, as it is defined by the ratio of net distance travelled and total distance travelled (the first cannot exceed the latter). The larger the directionality (closer to 1), the less random the movement is. In this case, the directionality of all three cell lines is below 0.3, suggesting that 12-273H-39 cells and 12-273H-41 cells display an increase in random movement.

12-175H-20 cells also display increased motility compared to the parental UM-SCC-12 cells but the difference in total distance travelled and speed, although significant ($p = 0.02$), was much smaller than in the case of p53-273H-expressing cells (Figure 3.31A and D). 12-175H-20 cells displayed also a significant increase ($p < 0.05$) in net distance travelled and directionality compared to the parental UM-SCC-12 cells (Figure 3.31B and C) suggesting that these p53-175H-expressing cells display an increase in organised, directional movement.

In this assay 12-273H-null cells behaved almost identically to UM-SCC-12 cells, with no significant difference between the two cell lines ($p > 0.05$) in any of the four parameters studied (Figure 3.31).

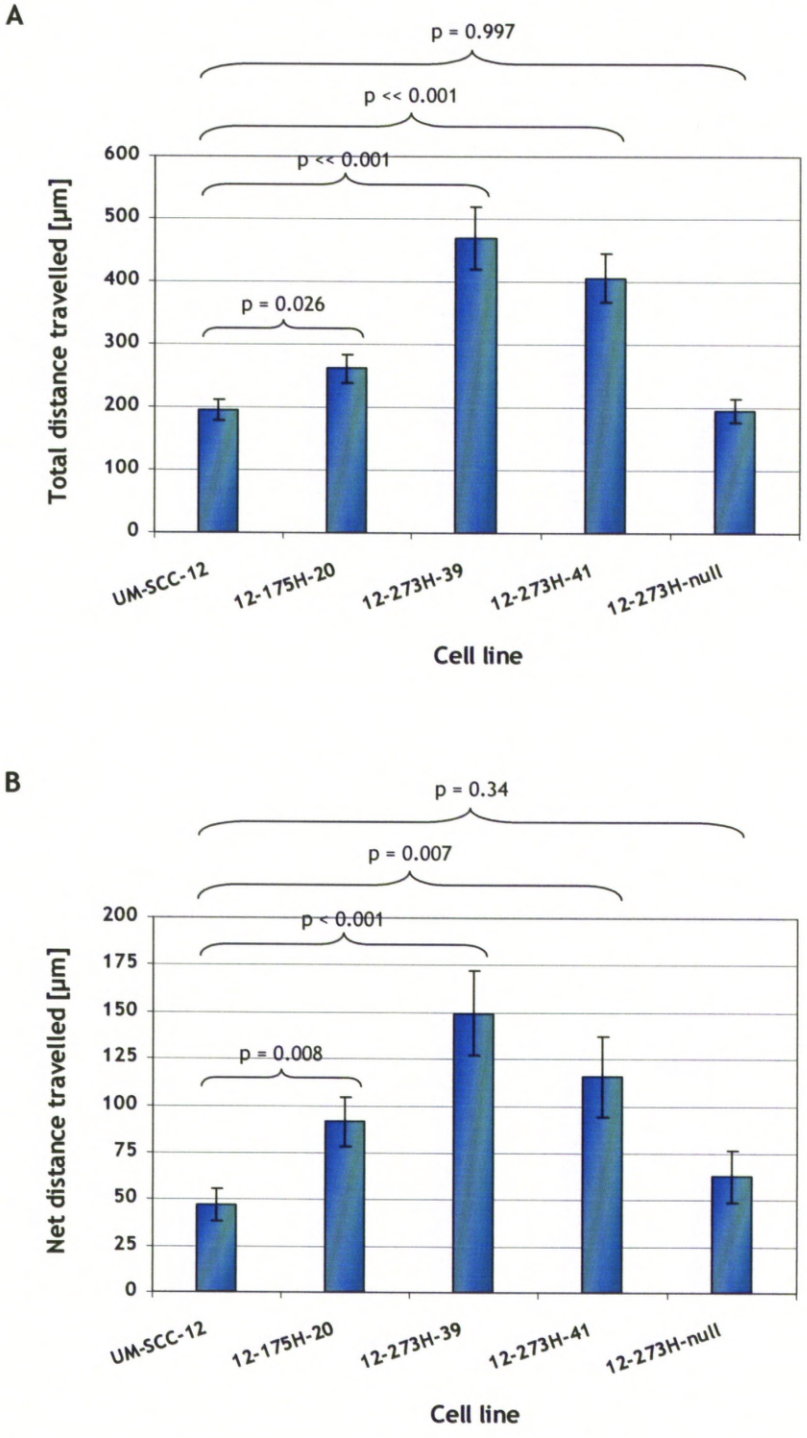

Figure 3.31: Live cell imaging of the mutant p53-expressing cell lines.

A. Total distance travelled by the cells over the course of experiment.

B. Net distance travelled by the cells over the course of experiment.

The histograms represent the mean of 20 cells tracked, the error bars represent standard error of mean. Statistical analysis was performed using Student's t-Test.

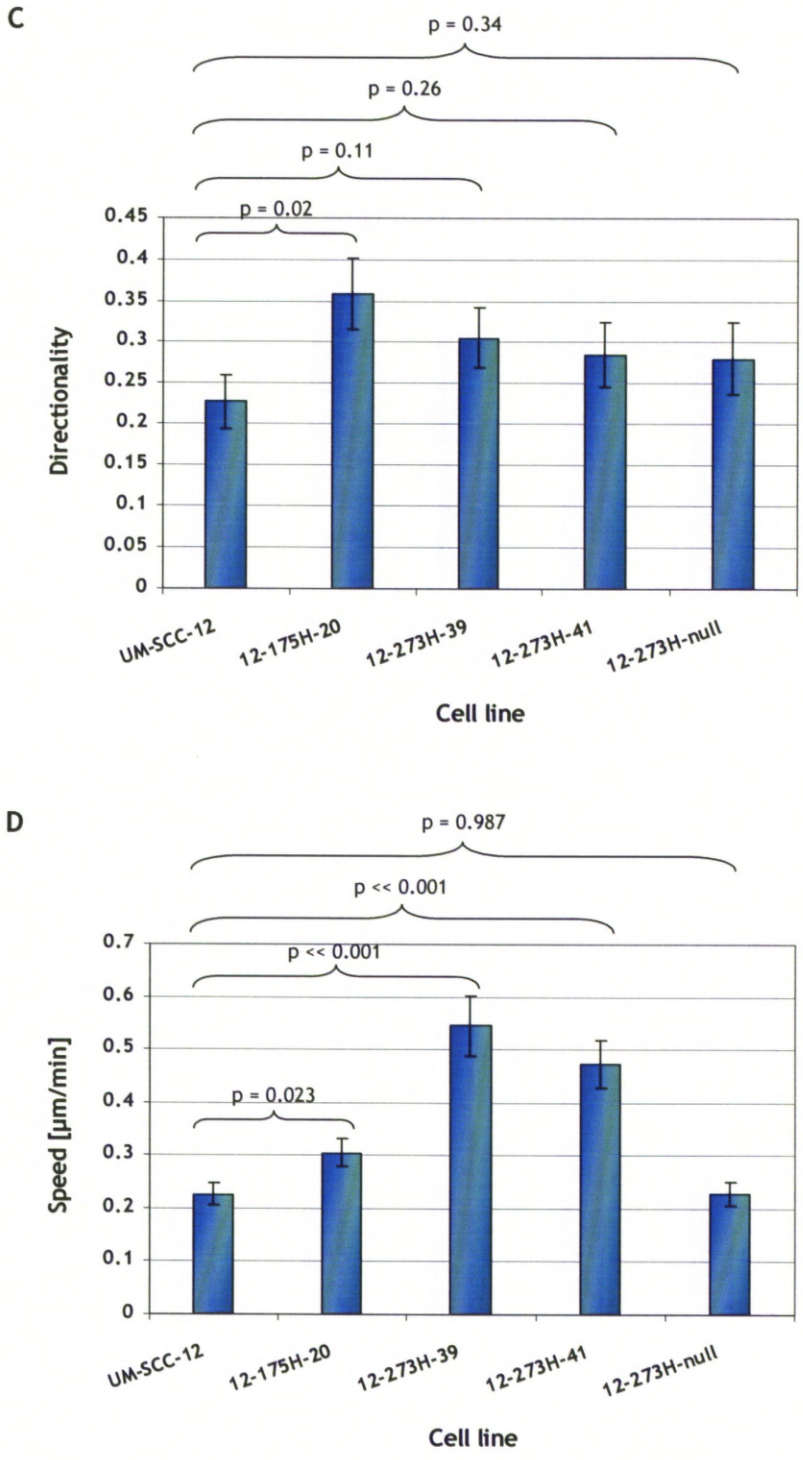

Figure 3.31 (cont.): Live cell imaging of the mutant p53-expressing cell lines.

C. Directionality of the cells over the course of experiment.

D. Average speed of the cells over the course of experiment.

The histograms represent the mean of 20 cells tracked, the error bars represent standard error of mean. Statistical analysis was performed using Student's t-Test.

The live imaging system seems to be suitable for monitoring the migratory potential of the laryngeal cancer cell lines under study, as there are clear differences in motility between the mutant p53-expressing cells and the parental p53-null cells. Moreover, 12-273H-null cells, which serve as a negative control for the process of establishing stable clones, behave as expected in this system with all four parameters studied (total distance travelled, net distance travelled, directionality and speed) comparable to those of UM-SCC-12 cells.

It is important to remember that the cells studied in this project are squamous cell carcinoma cells, which are derived from epithelial cells lining the skin and internal cavities (110). Due to the fact that squamous cells often exhibit flattened morphology and their main function is to line surfaces, it is possible that these cells are more potent in migrating on 2D surfaces (such as laboratory dish surfaces) rather than in 3D space (the Boyden chamber motility assay measures the ability of cells to migrate through pores in a membrane, which might represent three-dimensional migration). These observations suggest a possible explanation why live cell imaging could be a more appropriate assay than Boyden chambers for monitoring the migratory potential of the LSCC under study.

However, it is also important to note that the mutant p53-expressing cells studied are clones of UM-SCC-12 cells and, therefore, the results presented above have to be interpreted with a note of caution. During the process of establishing stable clones, the cells are treated with an antibiotic to select the colonies expressing the resistance marker (present in the same vector as the gene of interest – mutant p53 in this case). This process may result in the selection of rare clonal variants harbouring mutations in genes that affect the phenotype under study. Therefore, when studying stable clones the possibility of clonal variation cannot be underestimated.

3.10. Increased motility of mutant p53-expressing cells is likely due to mutant p53 expression

In order to test whether the observed differences in motility of the established mutant p53-expressing clones are due to mutant p53 expression or whether they can be attributed to clonal variation, down-regulation of mutant p53 expression by RNAi was attempted in the highly motile 12-273H-39 cells.

3.10.1. The impact of transient down-regulation of mutant p53 by RNAi on motility of 12-273H-39 cells

12-273H-39 cells were transfected with siRNAs as described in section 2.6.5. Since the cells were to be used for live imaging and transfection reagents frequently have high toxicity, four different conditions were studied in this experiment:

- untreated cells,
- cells treated with Lipofectamine alone (to estimate the influence of Lipofectamine treatment on cell motility)
- cells transfected with scrambled siRNA (as a control for siRNA specificity),
- cells transfected with siRNA for p53.

Live imaging of cell migration following RNAi manipulation was performed as described in section 2.14.1. Total distance travelled by the cells was studied, as this was one of the most prominently changed parameters when compared to the parental UM-SCC-12 cells (Figure 3.31). This experiment was performed once. Representative movies are available on the attached CD (see Appendix 11).

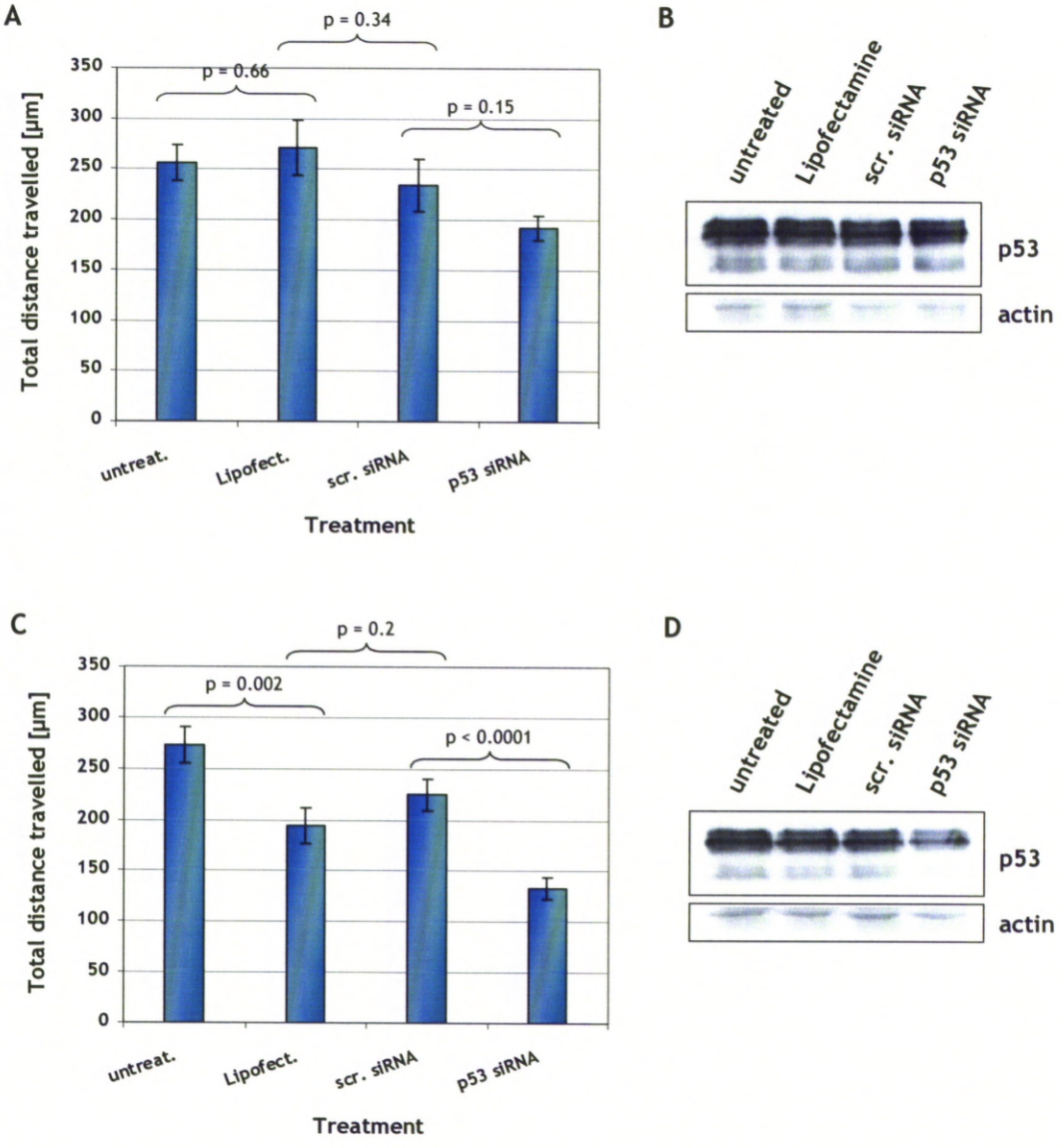

Figure 3.32: Transient knock-down of mutant p53 and motility. 12-273H-39 cells were transfected with control (scrambled) siRNA, siRNA for p53 or an equal volume of Lipofectamine alone. The cells were imaged 24-48 hours post treatment with a time-lapse of 3 min. This experiment was performed once.

A and C. Total distance travelled by the cells 24-36 hours (A) or 36-48 hours (C) post transfection. The histograms represent the mean of 20 cells tracked, the error bars represent standard error of mean. Statistical analysis was performed using Student's t-Test.

B and D. Western blot analysis with the indicated antibodies (DO-1 for p53) showing the expression of p53 at 30 hours (B) or 42 hours (D) post transfection (in the middle of the imaging periods shown in panels A and C, respectively).

As shown in Figure 3.32A in the period 24-36 hours post transfection, treatment with Lipofectamine alone did not have a significant impact on motility of 12-273H-39 cells ($p = 0.66$). Treatment of cells with scrambled siRNA as compared to treatment with Lipofectamine alone resulted in a slight reduction in motility but this difference was not statistically significant ($p = 0.34$). Finally, transfection with siRNA for p53 resulted in a reduction in motility, which was significant when compared to treatment with Lipofectamine alone ($p = 0.014$), but not statistically significant when compared to transfection with scrambled siRNA ($p = 0.15$). However, the small differences observed could be due to poor knock-down efficiency. As shown in Figure 3.32B, there is no visible reduction in the level of p53 in the cells transfected with siRNA for p53 at 30 hours post treatment, which is likely due to poor transfection efficiency of 12-273H-39 cells.

In the following 12 hours of the experiment (36-48 hours post transfection) the toxicity of Lipofectamine became more apparent as treatment of 12-273H-39 cells with Lipofectamine alone resulted in a significant reduction in the total distance travelled by the cells ($p = 0.002$) when compared to untreated cells (Figure 3.32C). Treatment of cells with scrambled siRNA compared to treatment with Lipofectamine alone did not have a significant impact on motility ($p = 0.2$). Transfection with siRNA for p53, on the other hand, resulted in a significant reduction in motility when compared to transfection with scrambled siRNA ($p < 0.0001$). Western blotting confirmed that there was a slight reduction in the p53 level at 42 hours after transfection of cells with siRNA for p53 (Figure 3.32D). Although it seems like the p53 siRNA lane might have been slightly underloaded (as judged by the level of actin), it is unlikely that the difference in p53 level observed would be solely due to a loading difference. In Figure 3.32B the scr. siRNA and p53 siRNA lanes also appear

slightly underloaded (as judged by the level of actin), yet the p53 level is relatively even in all lanes. This is likely because the level of p53-273H in 12-273H-39 cells is high and small loading differences are difficult to spot in terms of p53 level in these cells. This suggests that the reduction in p53 level observed in Figure 3.32D is due to p53 siRNA transfection rather than a small loading difference.

If knock-down of mutant p53 really results in the reduction of motility, then it can be concluded that the increased motility of mutant p53-expressing clones is a result of mutant p53 expression.

3.10.2. Stable knock-down of mutant p53 in the generated clones

Due to persistently low transfection efficiency and knock-down efficiency of the mutant p53-expressing laryngeal cancer cell lines, establishing cell lines with a stable knock-down of mutant p53 has been attempted (as described in section 2.13.2). A number of clones with a significant reduction of mutant p53 expression have been established. Stable clones expressing scrambled short hairpins have also been generated as a negative control for the cloning process.

A number of clones with a reduced level of p53 have been established from 12-273H-39 cells (Figure 3.33A) and 12-273H-41 cells (Figure 3.33C). Cell lines with a comparable level of p53 following transfection with scrambled siRNA have also been generated from these cells (Figure 3.33B and D, respectively). Knock-down of mutant p53-175H in 12-175H-20 cells appeared more difficult and the two clones with the lowest level of p53 out of all the ones screened showed only a partial reduction of the p53 level (Figure 3.33E). A number of control (scrambled siRNA) clones with a comparable p53 level to the parental 12-175H-20 cells have also been generated (Figure 3.33F).

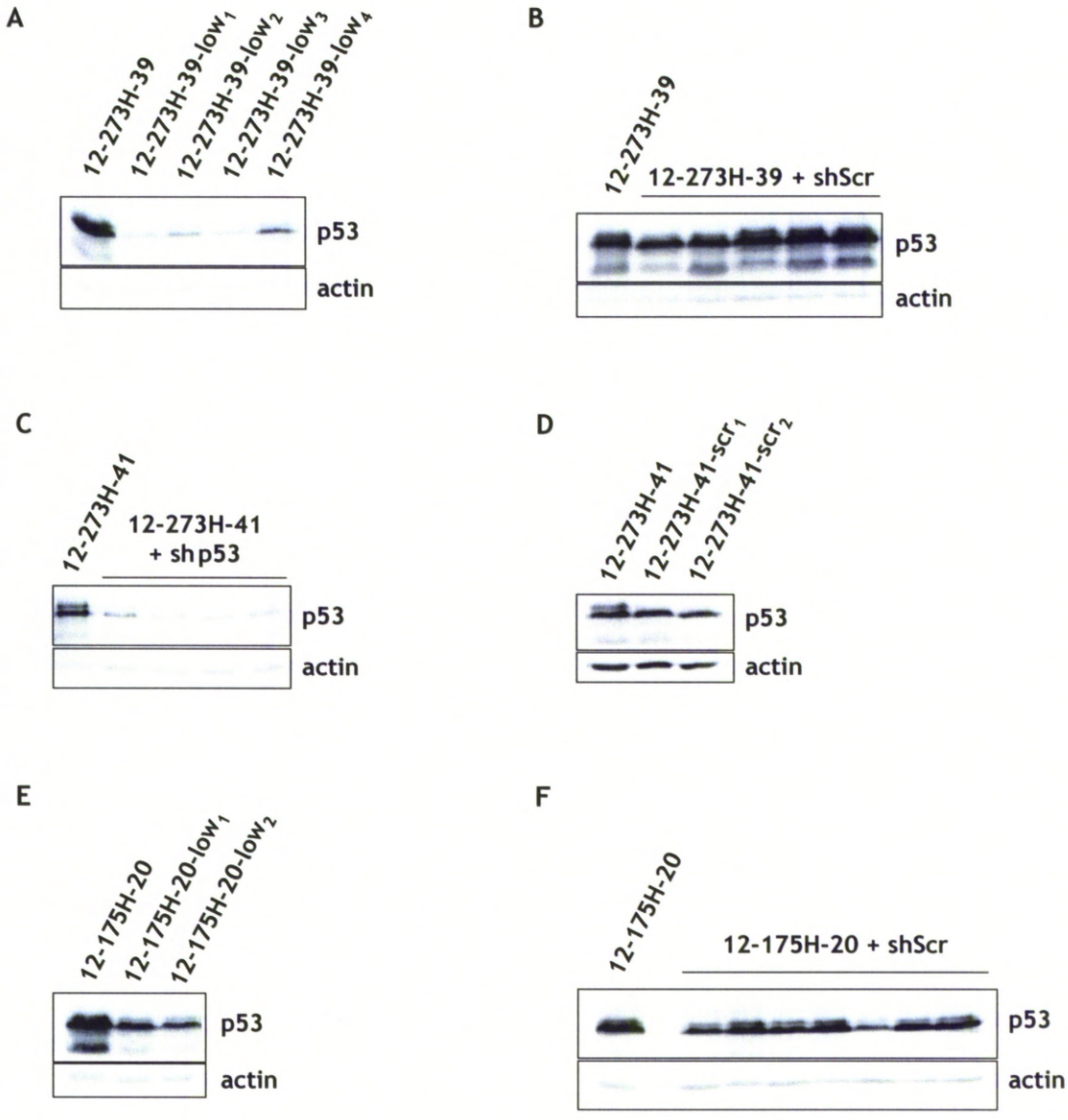

Figure 3.33: Expression levels of the TAP-tagged p53 mutants in the established knock-down clones. The previously established mutant p53-expressing cell lines were transfected with pSUPER.puro.shp53 or pSUPER.puro.shScr and stable clones were established. All the clones presented here were tested for p53 expression at least twice.

A-F. Western blot analysis with the indicated antibodies (DO-1 for p53) of cell lysates of the generated clones as compared to the parental cell line: 12-273H-39 (A and B), 12-273H-41 (C and D) or 12-175H-20 (E and F).

The motility of some of the generated clones was studied using the live cell imaging system. Representative movies are available on the attached CD (see Appendix 12).

12-273H-39 cells were more motile in this experiment than the parental UM-SCC-12 cells ($p < 0.0001$), showing that the data collected using the live cell imaging system are reproducible. The two generated clones of 12-273H-39 cells tested in this experiment, 12-273H-39-low$_1$ and 12-273H-39-low$_3$ (expressing a reduced level of p53-273H), displayed reduced motility compared to the parental cell line (Figure 3.34) and these differences were statistically significant ($p < 0.05$). Moreover, the reduction in motility of 12-273H-39-low$_1$ cells was so large that they became comparably motile to UM-SCC-12 cells, with there being no significant difference in motility between the two ($p = 0.17$). While 12-273H-39-low$_3$ cells were clearly less motile than their parental cells (12-273H-39), there was still a significant difference in motility ($p = 0.012$) between these cells and UM-SCC-12 cells, which could be explained by incomplete p53-knockdown in 12-273H-39-low$_3$. This also suggests that a very low level of mutant p53 is sufficient for the cells to display increased motility.

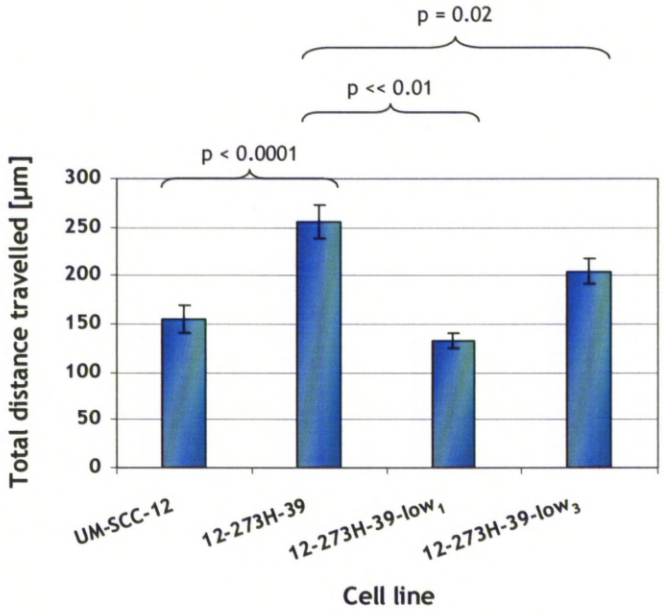

Figure 3.34: Stable knock-down of mutant p53 and motility. 150,000 cells were seeded per well of a 6-well plate. The cells were imaged for 12 hours with a time-lapse of 3 min. The histograms represent the mean of the total distance travelled by 50 tracked cells, the error bars represent standard error of mean. Statistical analysis was performed using Student's t-Test. This experiment was performed once.

In summary, mutant p53 expressing clones display increased motility (section 3.9.2). Transient knock-down of mutant p53 in 12-273H-39 cells results in a statistically significant reduction in motility 36-48 hours post transfection (Figure 3.32C), however, due to poor knock-down efficiency in 12-273H-39 cells (Figure 3.32D), analysis of this result was problematic. Generation of cell clones of 12-273H-39 cells with a stable reduction of p53-273H expression (Figure 3.33A) allowed to address the question of mutant p53 contribution to the observed increased motility of 12-273H-39 cells once again. Both of the tested clones exhibited significantly reduced motility (Figure 3.34). All of these data collectively suggest that the increased motility of the mutant p53-expressing cells is indeed due to mutant p53 expression.

3.11. Mutant p53-expressing LSCC cells do not display increased invasiveness

Since mutant p53 was shown to increase motility of laryngeal cancer cells (section 3.10), it was investigated whether the mutant p53-expressing cells display increased invasiveness *in vitro*, which is another indicator of metastatic potential. Boyden chamber invasion assays were performed on UM-SCC-12 cells, 12-273H-39 cells (highly motile) and 12-273H-39-low$_1$ cells (displaying reduced motility compared to the parental cells) as described in section 2.16.

As previously discussed, Boyden chambers are not an ideal system for studying the LSCC cells used in this project. However, it was expected that the thin layer of Matrigel that the invasion chambers are coated with would facilitate cell adhesion. Indeed the cells appeared to adhere to the Matrigel within an hour from the time of seeding. To encourage cell migration a serum gradient was also used. Moreover, this was the only invasion assay performed routinely and readily available in our

laboratory and therefore, despite the problems observed previously, invasion was investigated using this assay. The experiment was performed twice.

As shown in Figure 3.35, 12-273H-39 cells do not display increased invasiveness compared to the parental UM-SCC-12 cells, as measured by their ability to degrade matrigel and migrate through the pores of a Boyden chamber membrane. In fact, 12-273H-39 cells appear to be slightly less invasive than UM-SCC-12 cells but this difference is not statistically significant ($p = 0.08$). Similarly, the invasiveness of 12-273H-39-low$_1$ cells (reduced expression of p53-273H) does not differ significantly from their parental cells (12-273H-39).

It is important to note that these three cell lines are generally not invasive in this system as out of 50,000 cells seeded only 15 cells (in case of UM-SCC-12) managed to degrade the matrigel and migrate through the membrane, which is less than 0.05% of the entire population. As shown previously, the laryngeal cancer cell lines studied here are generally not very efficient in migrating through the Boyden chamber membranes (see section 3.9.1) and this could partially be a reason why such a small number of cells migrated through the membranes in this assay. Perhaps, as in the case of motility, live imaging of invasion would be a more suitable way to study the invasive potential of these cells (as discussed in section 3.9.2).

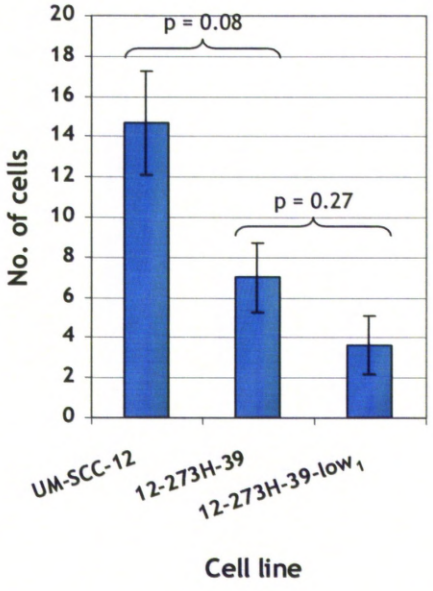

Figure 3.35: Mutant p53-expressing cells do not seem to display increased invasiveness. 50,000 cells were seeded into invasion chambers and allowed to migrate through the membrane towards a serum gradient for 30 hours. The number of cells that passed through the membrane was counted. The histograms represent the mean of three replicates, the error bars represent standard error of mean. Statistical analysis was performed using Student's t-Test.

3.12. Expression of p53-273H alters gene expression

Following the finding that mutant p53-expressing cells display increased motility, gene expression profiles of the highly motile 12-273H-39 cells and parental UM-SCC-12 cells were studied using exon array analysis to investigate the gene expression changes of cells expressing the GOF contact mutant of p53 compared to the parental p53-null cells. Only 12-273H-39 cells (and not 12-175H-20 cells) were included in this analysis due to limited resources and because these cells displayed the most distinct increased motility phenotype.

RNA was extracted from UM-SCC-12 cells and 12-273H-39 cells in triplicate. Following RNA extraction, it is important to assess the quality of the RNA before proceeding to evaluate gene expression. Since mRNA comprises only 1-3% of total RNA it is not easily detectable. Ribosomal RNA, on the other hand, comprises >80% of total RNA, with the majority being 28S and 18S ribosomal RNA (rRNA). These rRNA species appear as two clear bands on agarose gels stained with ethidium bromide (EtBr). Since 28S and 18S rRNA species are derived from the same precursor rRNA, the number of copies of both molecules is the same and the ratio of 28S:18S rRNA relies solely on their size, which is approximately 5 kb and 1.9 kb (in mammals), respectively. The theoretical ratio of 28S:18S is approximately 2.7:1 but a ratio of 2:1 is considered to be indicative of good quality, intact RNA. The ratio of the intensity of these bands can be used for determining the integrity of the extracted RNA due to the fact that these two rRNA species degrade at different rates (495). 28S rRNA is more susceptible to degradation than 18S rRNA, partly due to the presence of 'hidden breaks' in the 28S rRNA molecules. 'Hidden breaks' are actually true breaks in the middle of the 28S rRNA molecules and are called 'hidden' because

under non-denaturing conditions the rRNA molecule is held together by hydrogen bonds between its secondary structure elements.

The ratio of the 28S:18S rRNA in the analysed samples is approximately 2:1 (Figure 3.36) suggesting that the RNA is not degraded. An OD 260/280 ratio is an indication of nucleic acid purity and an ideal value for RNA is 2.0. The ratios obtained for the extracted samples (Table 3.3) are slightly lower (above 1.79), which could be caused by protein or phenol contamination. The OD 260/230 ratio is a secondary indicator of nucleic acid purity. The ratio should be greater than 2.0 and lower ratios may suggest the presence of inorganic contaminants that absorb at 230 nm (guanidine thiocyanate, phenol, EDTA). As shown in Table 3.3, all obtained OD 260/230 ratios were above 2.0, suggesting that the samples are essentially free of inorganic contaminants.

The extracted RNA was deemed suitable for expression analysis, which was performed as described in section 2.18. Cluster analysis of the differentially expressed genes is represented graphically in the form of a heat map (Figure 3.37).

193 genes were found to be differentially regulated in 12-273H-39 cells compared to UM-SCC-12 cells, with 154 genes up-regulated and 39 genes down-regulated more than 2.25-fold (FDR < 0.05; $p < 0.05$). A complete list of differentially regulated genes is presented in Appendix 13. The genes were grouped according to the processes they are involved in and the 10 most significantly affected processes are listed in Figure 3.38.

Table 3.3: Spectrophotometrical quantification of the RNA used for exon arrays. RNA was extracted from the indicated cell lines on three separate occasions (I-III).

	Concentration [µg/µl]	OD 260/280	OD 260/230
UM-SCC-12 I	2.66	1.88	2.23
UM-SCC-12 II	1.45	1.86	2.12
UM-SCC-12 III	1.49	1.79	2.38
12-273H-39 I	2.38	1.84	2.36
12-273H-39 II	1.59	1.82	2.42
12-273H-39 III	1.79	1.88	2.25

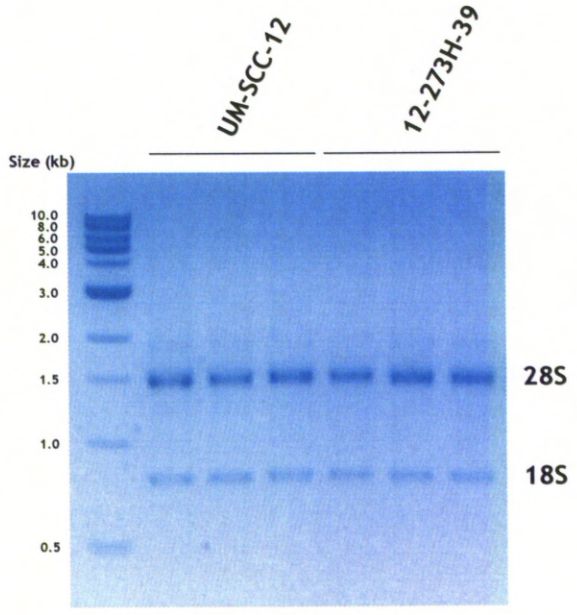

Figure 3.36: RNA used for exon array analysis. RNA was extracted from the indicated cell lines on three separate occasions (I-III). The RNA integrity was tested by running 500 ng of total RNA on a 1% (w/v) agarose gel (with EtBr) and visualised using ultraviolet light. The 28S and 18S RNA bands are indicated.

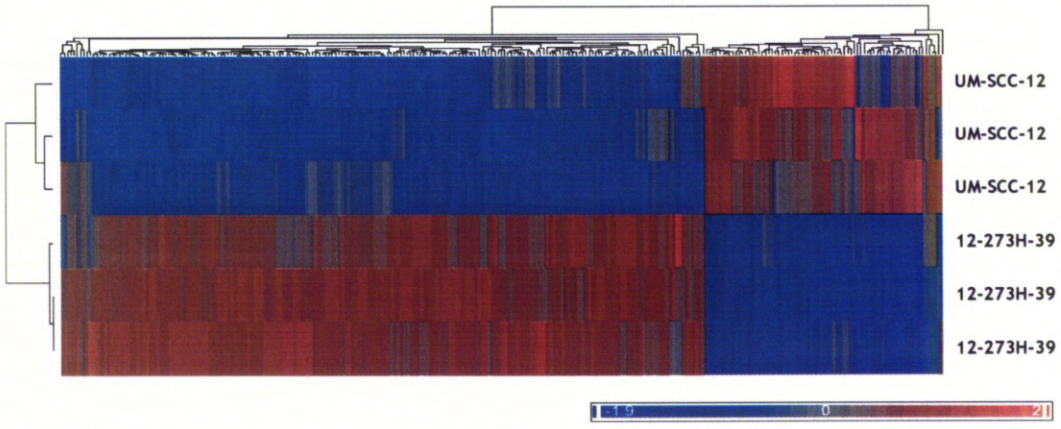

Figure 3.37: Heat map representing the cluster analysis of differentially expressed genes (more than 2.25-fold change) identified using exon microarrays. The heat map was generated by hierarchical clustering of individual genes (each column corresponds to one gene) and samples/cell lines (each row represents a different sample), the cluster relationships are indicated by the tree-like structures adjacent to the map. The genes represented in blue are down-regulated, while the ones represented in red are up-regulated. (Data analysis performed by Dr Bryony Lloyd.)

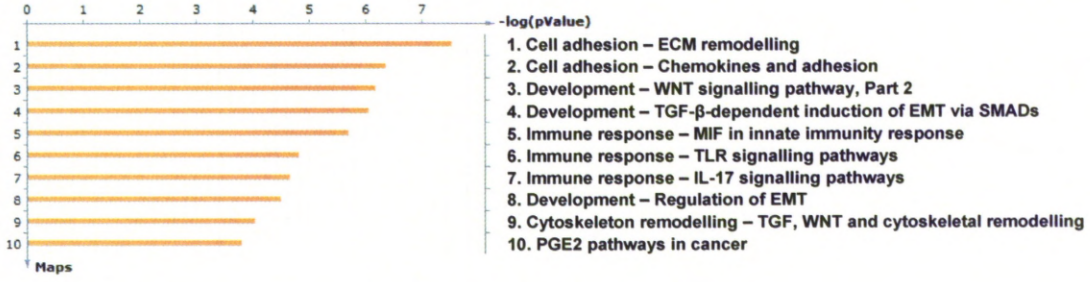

Figure 3.38: The list of 10 processes most significantly affected by the genes differentially expressed in 12-273H-39 cells compared to UM-SCC-12 cells. Pathway analysis was performed using the MetaCore software v. 6.5 (GeneGo, Inc.) based on a proprietary manually created and maintained database of human protein-protein, protein-DNA and protein compound interactions, metabolic and signalling pathways. (Data analysis performed by Dr Bryony Lloyd.)

Interestingly, given the increased migratory potential of 12-273H-39 cells, the most significantly affected pathways are involved in cell adhesion and extracellular matrix (ECM) remodelling, which suggests that the p53-273H mutant may confer the motile phenotype on UM-SCC-12 cells by altering their transcriptome with an emphasis on inducing ECM remodelling programmes. For example, fibronectin, a component of the ECM implicated in cell migration driven by enhanced integrin recycling (see section 1.3.4.3.2.3), was found to be up-regulated 8.4-fold in 12-273H-39 cells.

A number of the identified genes are known to be transcriptional targets of wild-type p53 (including SPRR2A, MFAP5, PTGES, CCND2, OGN, FN1 as well as many others). Based on the transcriptional networks generated from the microarray analysis (Appendix 14) it appears that a number of genes, which were found to be differentially expressed in this study, could be transcriptionally regulated by mutant p53 via other transcription factors, such as Sp1 and NF-κB.

It is noteworthy that Sp1 activates VEGF transcription, hence stimulating angiogenesis (as discussed in section 1.3.2.6). While wild-type p53 is known to repress angiogenesis via binding of p53 to the transcription factor Sp1 (hence inhibiting its ability to bind other promoters such as VEGF), VEGF-A was found to be up-regulated 2.48-fold in the mutant p53 expressing cells compared to p53-null cells, suggesting that the interaction of mutant and wild-type p53 with Sp1 may have opposite outcomes (see section 1.3.4.3.1.2).

3.12.1. Validation of the expression microarray data by qRT-PCR

Following the identification of 193 differentially regulated genes in 12-273H-39 cells, it was important to validate the expression differences obtained from microarray analysis. For this purpose 12 genes were selected from Tables 6.5 and 6.6 (Appendix 13) based on the relative mRNA expression level (normalised to the expression level in the parental UM-SCC-12 cells, further referred to as control expression level) and an analysis (based upon the literature) of their known roles in regulating motility/invasion/metastasis, suggesting that they could be relevant to the observed migratory phenotype of 12-273H-39 cells. A brief summary of the functions of the selected genes is presented in Table 3.4.

qRT-PCR for the selected targets listed in Table 3.4 was performed by members of the Applied Biology team (led by Prof. D. Ross Sibson and Dr Bryony Lloyd, University of Liverpool) using the RNA samples used for microarray analysis to validate the observed differences in gene expression. RNA extracted from 12-175H-20 cells was also included in this analysis to compare the expression levels of the selected genes in cells expressing two different GOF p53 mutants. The experimental setup is described in section 2.19. The relative expression of the 12 selected targets in 12-273H-39 and 12-175H-20 cells compared to UM-SCC-12 cells is presented in Table 3.5, while the normalised expression levels (normalised to histone H3 expression) are presented in Figure 3.39.

Table 3.4: The list of genes selected for validation (by qRT-PCR) of the expression differences obtained from the expression array analysis. The relative expression level (normalised to control expression level) of genes found to be up-regulated are indicated in red, while those of down-regulated genes – in blue.

Gene symbol	Full name	Relative expression	Relevant functions
SPRR2A	Small proline-rich protein 2A	23.13	SPRR2A enhances migration and EMT in wound healing (496)
TLR4	Toll-like receptor 4	14.63	S100A8-SAA3-TLR4 pathway enhances metastasis to the lungs by promoting the accumulation of macrophages and haematopoietic progenitors (497)
S100A8	S100 calcium binding protein A8	10.31	Co-expression of S100A8 and S100A9 is associated with poor tumour differentiation, vessel invasion and node metastasis (498)
C8orf4 / TC1	Chromosome 8 open reading frame 4	10.22	TC1 up-regulates Wnt/β-catenin target genes (MMP7, MMP14, cyclin D1), which are implicated in the aggressive biological behaviour of cancers; enhances Matrigel invasiveness (499)
FN1	Fibronectin 1	8.40	Fibronectin is involved in cell adhesion and migration processes during embryogenesis, wound healing, angiogenesis and metastasis; it promotes cell invasion through increased association with integrins and expression of MMPs (500)
PTGES / PIG12	Prostaglandin E synthase	8.12	PTGES is implicated in cancer metastasis by increasing proliferation, migration and invasiveness of cancer cells (501)
TIMP2	TIMP metallopeptidase inhibitor 2	7.92	Tissue inhibitor of MMP2, prevents protease activity in tissues undergoing ECM remodelling; implicated in tissue invasion and metastasis (502)
TSPAN1	Tetraspanin 1	5.82	Tetraspanin-integrin interaction contributes to increased migration and invasiveness of SCCHN cells (503)
MMP2	Matrix metalloproteinase 2	2.94	MMP2 degrades type IV collagen, the major structural component of basement membranes; it is implicated in migration and invasiveness (504)
CCND2	Cyclin D2	-10.94	Cyclin D2 forms a complex with CDK4 or CDK6, necessary for G1-S transition; it is up-regulated in senescent cells and may contribute to the induction/maintenance of the non-proliferative state (505)
OGN	Osteoglycin	-8.51	High osteoglycin expression contributes to decreased potential for both migration and invasion and decreased metastatic potential (506)
NPNT / POEM	Nephronectin	-6.90	Nephronectin is an ECM protein, the expression of which increases cell adhesion and decreases cell migration and invasion; loss of nephronectin is associated with tumour progression (507)

As shown in Table 3.5 and Figure 3.39 the obtained microarray data have been validated for all the selected genes by qRT-PCR. All of the selected genes found to be up-regulated in 12-273H-39 cells relative to UM-SCC-12 cells in the microarray study have also been found up-regulated by qRT-PCR. Similarly, the genes found to be down-regulated in the microarray analysis were also down-regulated in the qRT-PCR validation study. This suggests that the microarray data is reliable and confirms the observed differences in gene expression.

Note, however, that there is a difference in the scale of the relative expression data obtained from microarray analysis (Table 3.4) and qRT-PCR validation (Table 3.5). The observed differences are due to a difference in the dynamic range of the microarray and qRT-PCR. Dynamic range defines the range of the initial mRNA concentrations, over which accurate expression levels can be determined. Most commercially available microarray platforms have a dynamic range of 3-4 orders of magnitude while real-time PCR can achieve a dynamic range of up to 8 orders of magnitude (508). Consequently, the larger dynamic range of real-time PCR assays provides them with a superior detection sensitivity while the gene expression changes determined using microarray technology are underestimated in the extreme parts of the range (changes > 10 or < -5) (509).

Table 3.5: The relative expression levels (determined by qRT-PCR) of the selected genes in 12-273H-39 and 12-175H-20 cells (normalised to the control expression levels). The relative expression of genes found to be up-regulated is indicated in red, while those of down-regulated genes – in blue. (Data provided by Dr Bryony Lloyd.)

Gene symbol	Relative expression	
	12-273H-39	12-175H-20
SPRR2A	30.6	219.3
TLR4	54.1	1.1
S100A8	83.2	450.4
C8orf4	157.7	15.5
FN1	38.3	3.0
PTGES	428.8	23.4
TIMP2	21.1	2.0
TSPAN1	37.8	21.8
MMP2	8.8	1.8
CCND2	-4.5	-4.6
OGN	-1.6	-1.7
NPNT	-2.3	-4.7

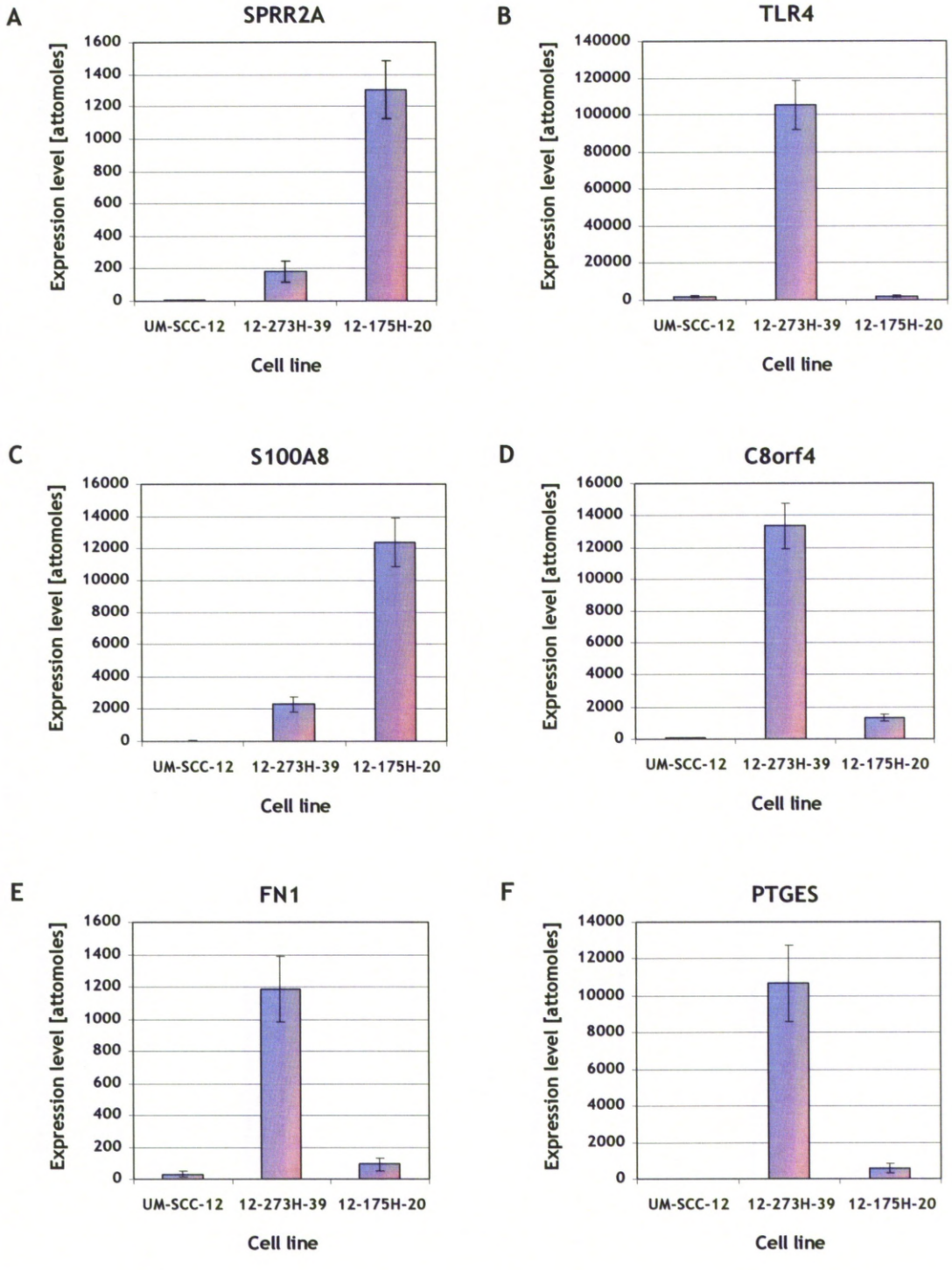

Figure 3.39: Expression levels of the indicated genes in UM-SCC-12, 12-273H-39 and 12-175H-20 cells. qRT-PCR was performed on RNA extracted from the indicated cells lines. The histograms show mean of the average expression levels (normalised to histone H3 expression) in three replicate RNA samples (see section 2.19.4 for details), the error bars represent standard error of mean. (Data provided by Dr Bryony Lloyd.)

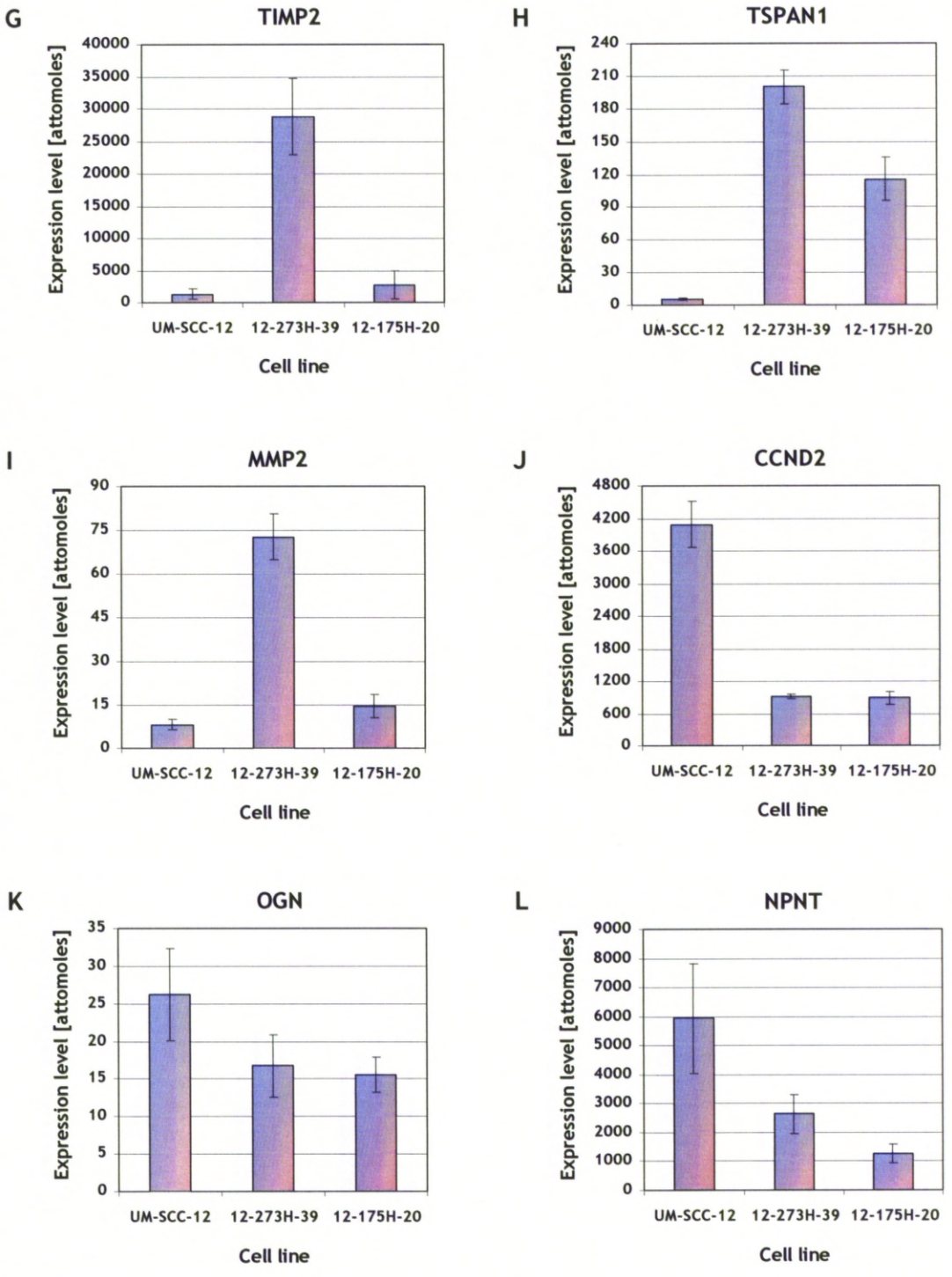

Figure 3.39 (cont.): Expression levels of the indicated genes in UM-SCC-12, 12-273H-39 and 12-175H-20 cells. qRT-PCR was performed on RNA extracted from the indicated cells lines. The histograms show mean of the average expression levels (normalised to histone H3 expression) in three replicate RNA samples (see section 2.19.4 for details), the error bars represent standard error of mean. (Data provided by Dr Bryony Lloyd.)

The qRT-PCR analysis of the selected genes also allowed for comparison of the expression levels of the cell lines expressing two different GOF p53 mutants – p53-273H and p53-175H. Some genes (including TLR4, C8orf4, FN1, PTGES, TIMP2 and MMP2) have been found to be up-regulated only, or much more significantly, in 12-273H-39 cells. Given the fact that these cells display much higher motility than 12-175H-20 cells, these genes might be functionally important in mediating the motile phenotype. TSPAN1 was up-regulated in both cell lines but up-regulation in 12-273H-39 cells was higher. Two of the analysed genes (SPRR2A and S100A8) were up-regulated much more significantly in 12-175H-20 cells than in 12-273H-39 cells. Down-regulation of CCND2, OGN and NPMT was similar in both cell lines.

A number of the validated genes will be selected for functional examination to determine their possible contribution to the observed migratory phenotype of 12-273H-39 cells. The best candidates for functional studies include genes, which are more highly up-regulated in 12-273H-39 cells (displaying dramatically increased migratory potential) compared to 12-175H-20 cells (displaying slightly increased migratory potential).

While the microarray analysis revealed up-regulation of many genes involved in regulation of cell adhesion and ECM remodelling, which could explain the increased migratory potential of 12-273H-39 cells, it is important to remember that the cell lines analysed in this study are clones of UM-SCC-12 cells and, therefore, the possibility of the observed differences being a result of clonal variation cannot be underestimated. Moreover, it should also be mentioned that 12-273H-39 cells and 12-175H-20 cells express TAP-tagged p53 mutants and hence any observed difference could also potentially be due to the presence of this tag. To address these issues, UM-SCC-12

cells were transiently transfected with untagged wt p53, p53-175H, p53-273H or the corresponding empty vector and the expression of the 12 selected genes (Table 3.4) was studied by qRT-PCR.

3.12.2. Validation of the observed gene expression changes in UM-SCC-12 cells

In order to address the issue of clonal variation and to exclude the possibility of the TAP-tag at the N-terminus of p53 mutants affecting the gene expression differences observed in 12-273H-39 cells and 12-175H-20 cells, UM-SCC-12 cells were transfected with untagged wt p53, p53-175H, p53-273H or the corresponding empty vector in triplicate using recently optimised nucleofection (Amaxa Nucleofector Technology). RNA was extracted from each individual transfection and the 12 selected genes (Table 3.4) were analysed by qRT-PCR. A small aliquot of cells from each condition was kept for western blot analysis. The experiment was performed once.

Nucleofection of UM-SCC-12 cells with the untagged p53 forms resulted in a comparable level of expression of p53, p53-175H and p53-273H, respectively (Figure 3.40). MDM2 was clearly induced in cells transfected with wt p53. It seems that the MDM2 level was also marginally higher in cells transfected with p53-175H or p53-273H than in those transfected with empty vector, suggesting that these p53 mutants may retain some residual wt p53 transcriptional activity. Similarly, p21 was induced strongly in cells expressing wt p53 and only slightly in those expressing the p53 mutants.

The observed difference in the mobility of the mutant p53 forms compared to wt p53 is most likely due to differences in the SNP at amino acid 72, with wt p53 having 72R and the p53 mutants – 72P (as discussed in section 3.8).

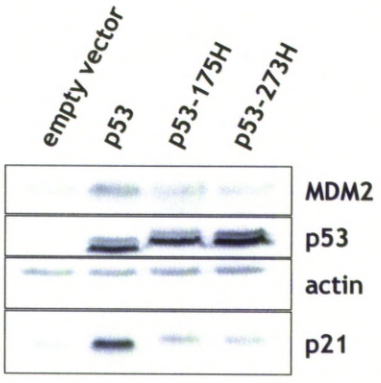

Figure 3.40: Expression levels of the untagged p53 forms in transiently transfected UM-SCC-12 cells. 3×10^6 UM-SCC-12 cells were transfected with 3 µg of wt p53, p53-175H, p53-273H in pCMV-Script or the corresponding empty vector and analysed 24 hours post transfection. The panel shows western blot analysis with the indicated antibodies (DO-1 for p53) from UM-SCC-12 cells transfected with the indicated constructs.

Following RNA extraction from the triplicate transfections, the RNA quality was tested as described previously (section 3.12). Based on the 28S:18S rRNA, OD 260/280 and OD 260/230 ratios of the analysed samples (Table 3.6 and Figure 3.41), the extracted RNA was deemed suitable for qRT-PCR analysis. qRT-PCR was performed by members of the Applied Biology team (led by Prof. D. Ross Sibson and Dr Bryony Lloyd, University of Liverpool) as described previously (section 2.19). The relative expression of the 12 selected targets in UM-SCC-12 cells transfected with wt p53, p53-175H or p53-273H, respectively, compared to UM-SCC-12 cells transfected with the corresponding empty vector is presented in Table 3.7, while the normalised expression levels (normalised to histone H3 expression) are presented in Figure 3.42.

Table 3.6: Spectrophotometrical quantification of the RNA extracted from transiently transfected UM-SCC-12 cells. 3×10^6 UM-SCC-12 cells were transfected with 3 µg of wt p53, p53-175H, p53-273H in pCMV-Script or the corresponding empty vector in triplicate (I-III). RNA was extracted from the transiently transfected cells 24 hours post transfection.

UM-SCC-12 +	Concentration [µg/µl]	OD 260/280	OD 260/230
empty vector I	1.21	1.94	2.36
empty vector II	1.29	2.07	0.97
empty vector III	1.08	1.91	2.39
p53 I	1.30	1.94	2.36
p53 II	1.18	1.93	2.01
p53 III	1.59	1.96	2.23
p53-175H I	1.39	1.67	2.57
p53-175H II	2.01	1.71	2.53
p53-175H III	1.88	1.69	2.47
p53-273H I	1.18	1.65	2.33
p53-273H II	1.57	2.01	2.17
p53-273H III	1.25	1.97	2.69

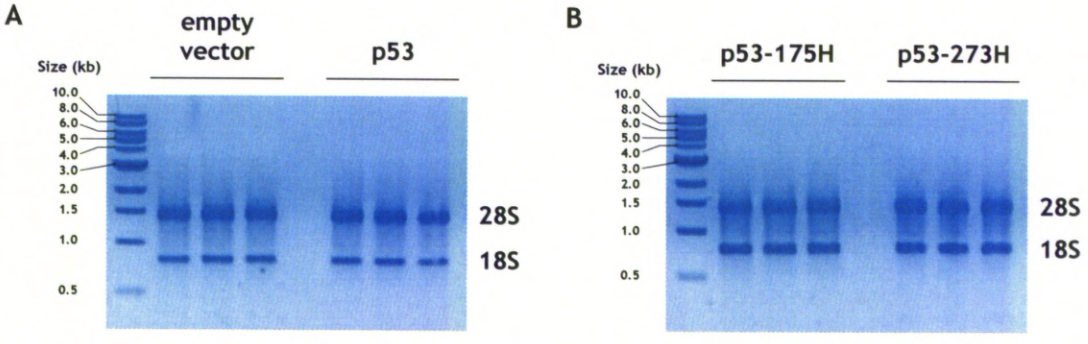

Figure 3.41: RNA extracted from transiently transfected UM-SCC-12 cells. 3×10^6 UM-SCC-12 cells were transfected with 3 µg of wt p53, p53-175H, p53-273H in pCMV-Script or the corresponding empty vector in triplicate. RNA was extracted from the transiently transfected cells 24 hours post transfection. The RNA integrity was tested by running 500 ng of total RNA on a 1% agarose gel (with EtBr) and visualised using ultraviolet light. The 28S and 18S RNA bands are indicated.

As shown in Table 3.7, most of the determined relative gene expression levels of the 12 selected genes in UM-SCC-12 cells transfected with wt p53, p53-175H or p53-273H (normalised to the control expression levels in UM-SCC-12 cells transfected with the corresponding empty vector) were not statistically significantly. The variability of the generated data is well illustrated by the relative expression levels of MMP2 in UM-SCC-12 cells following transfection with wt p53 and p53-175H (Table 3.7). The relative expression levels are equal 1.20 in both cases, yet only the relative expression level in wt p53-expressing UM-SCC-12 cells is statistically significant. This is clearly due to the fact that the variability of the relative expression levels of MMP2 from the triplicate transfections of UM-SCC-12 cells with wt p53 was much lower than that of triplicate transfections of UM-SCC-12 cells with p53-175H, making only the first value statistically significant.

When looking at the average expression levels of each of the 12 selected genes following transfections (Figure 3.42), it is clear that the variation was very high. To determine the source of variation it was necessary to analyse the normalised expression levels (and their variations) for each transfection separately (Appendix 15). In many cases it can be observed that variation for individual transfections was very large (for example for TLR4 expression following p53-273H transfection or FN1 expression following p53 transfection). These variations are derived from the differences between the average expression values determined for the two reverse transcriptions (see Figure 2.2), suggesting that the source of variation lies in the qRT-PCR assays rather than in the actual biological differences.

Table 3.7: The relative expression levels (determined by qRT-PCR) of the selected genes following transfection of UM-SCC-12 cells with wt p53, p53-175H and p53-273H, respectively (normalised to the control expression levels in UM-SCC-12 cells transfected with the corresponding empty vector). The relative expression levels reflecting differences, which were statistically significant ($p < 0.05$ as determined by a Student's t-Test), are shown in red (if up-regulated) or blue (if down-regulated). (Data provided by Dr Bryony Lloyd.)

Gene symbol	Relative expression		
	p53	p53-175H	p53-273H
SPRR2A	-1.12	-1.60	-1.29
TLR4	1.15	1.32	-1.11
S100A8	-1.23	-4.04	-2.69
C8orf4	-3.41	-1.51	1.67
FN1	1.04	-1.38	-1.01
PTGES	1.04	-1.47	-1.30
TIMP2	1.08	-1.40	-1.26
TSPAN1	-1.17	-1.06	1.39
MMP2	1.20	1.20	-1.15
CCND2	1.05	1.14	-1.04
OGN	1.67	1.12	1.59
NPNT	1.10	-1.04	-1.13

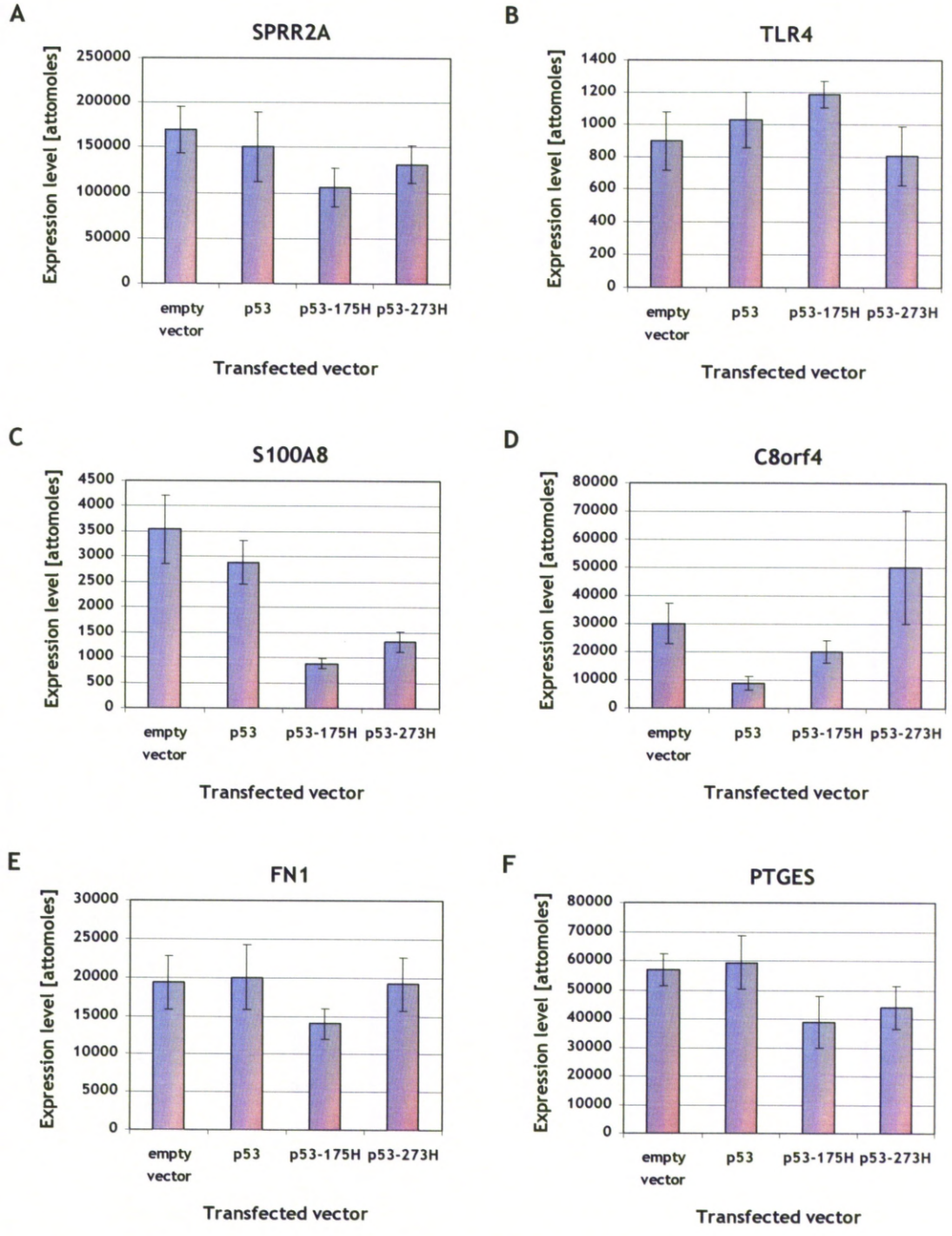

Figure 3.42: Expression levels of the indicated genes in UM-SCC-12 cells following transfection with wt p53, p53-175H, p53-273H or the corresponding empty vector. qRT-PCR was performed on RNA extracted from UM-SCC-12 cells transiently transfected with the indicated vectors. The histograms show mean of the average expression levels (normalised to histone H3 expression) in three replicate RNA samples (see section 2.19.4 for details), the error bars represent standard error of mean. (Data provided by Dr Bryony Lloyd.)

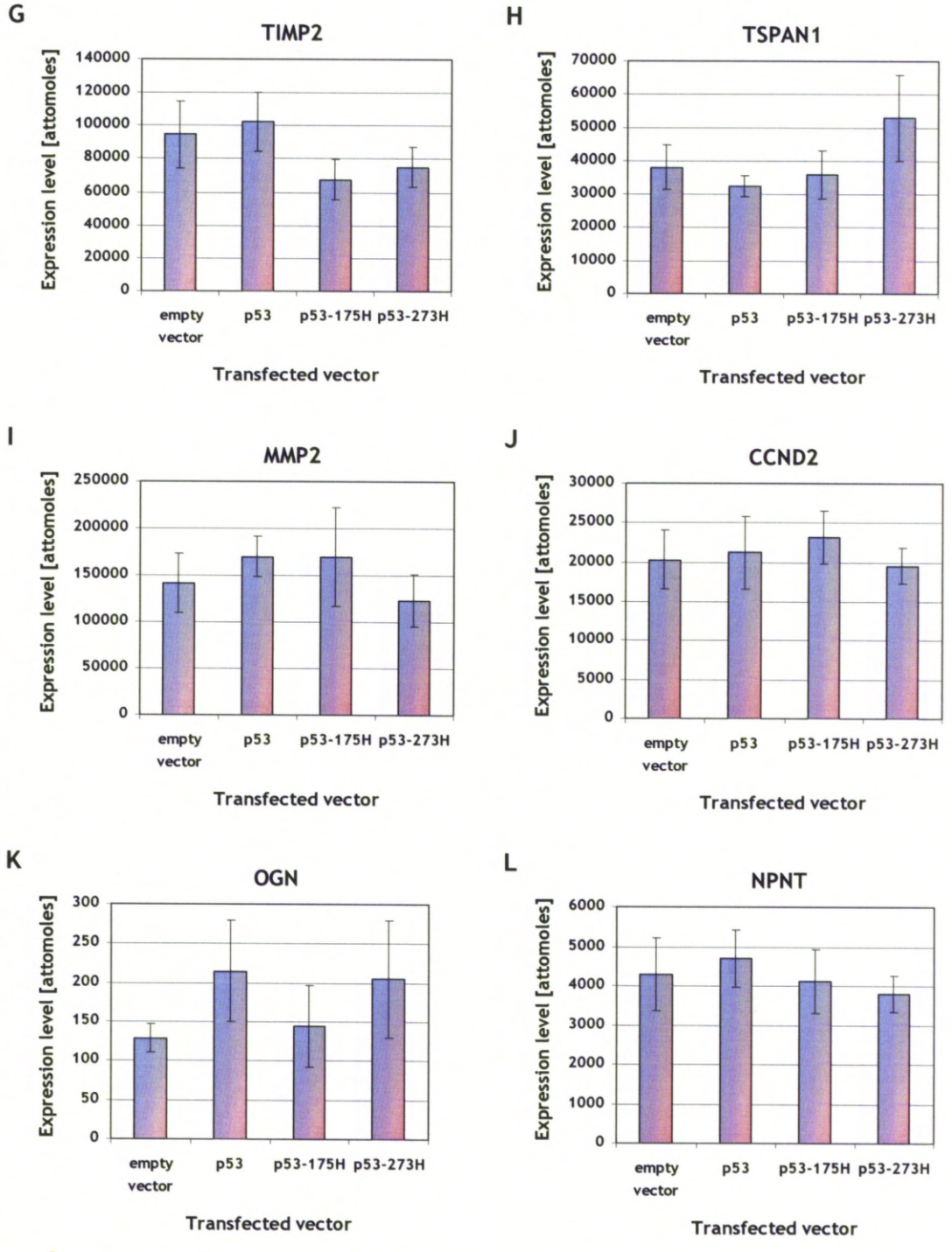

Figure 3.42 (cont.): Expression levels of the indicated genes in UM-SCC-12 cells following transfection with wt p53, p53-175H, p53-273H or the corresponding empty vector. qRT-PCR was performed on RNA extracted from UM-SCC-12 cells transiently transfected with the indicated vectors. The histograms show mean of the average expression levels (normalised to histone H3 expression) in three replicate RNA samples (see section 2.19.4 for details), the error bars represent standard error of mean. (Data provided by Dr Bryony Lloyd.)

There were also some cases, in which the variation for individual transfections was small (such as S100A8 expression following p53-175H transfection or C8orf4 expression following p53-175H transfection). In those instances, any variations observed in Figure 3.42 would most likely be due to biological variation. A possible reason for such variation between the transfection replicates could be operator-based errors.

In the performed nucleofection-based transfections, high toxicity of the procedure was observed (approximately 50% viable cells). Nucleofection is an electroporation-based method, in which specific combinations of electrical pulses permeabilize both the plasma membrane and the nuclear envelope, resulting in DNA transfer directly into the nucleus. The inability of many cells to seal the generated microholes in the plasma membrane is likely the main reason for the high cellular mortality after nucleofection. While nucleofection is a highly cytotoxic transfection technique, it is the only method of the ones tested, with which UM-SCC-12 cells could be successfully transfected (approximately 50% transfection efficiency compared to 1-2% transfection efficiency with other techniques used). It should be possible to increase cell viability through optimisation of this technique, including the nucleofection program and number of cells used.

In conclusion, it will be important to try to eliminate the sources of variation (mostly in the qRT-PCR assays) in future experiments in order to obtain statistically significant differences in gene expression that are a consequence of the expression of the various forms of p53 under study.

3.12.3. Validation of the observed gene expression changes in H1299 cells

In addition to an attempt to validate the gene expression changes obtained from the microarray study in UM-SCC-12 cells to exclude the possibility of clonal variation, a parallel validation was attempted in H1299 cells to determine whether the observed differences are specific to laryngeal squamous cell carcinoma or if they can also be observed in other cells. H1299 cells were transfected with untagged wt p53, p53-175H, p53-273H or the corresponding empty vector (pCMV-Script) in triplicate. RNA was extracted from each individual transfection and the 12 selected genes (Table 3.4) were analysed by qRT-PCR. A small aliquot of cells from each condition was kept for western blot analysis. The experiment was performed once.

Transfection of H1299 cells with the untagged p53 forms resulted in a comparable level of expression of p53, p53-175H and p53-273H, respectively (Figure 3.43). MDM2 was clearly induced in cells transfected with wt p53. A slight increase in MDM2 level was also observed in cells transfected with p53-175H or p53-273H compared to those transfected with empty vector, suggesting that these p53 mutants may retain some residual wt p53 transcriptional activity. p21 induction was observed only in cells expressing wt p53.

The observed difference in the mobility of the mutant p53 forms compared to wt p53 is most likely due to differences in the SNP at amino acid 72, with wt p53 having 72R and the p53 mutants – 72P (as discussed in section 3.8).

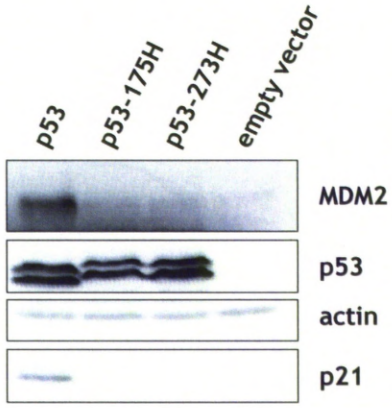

Figure 3.43: Expression levels of the untagged p53 forms in transiently transfected H1299 cells. H1299 cells were transfected with 5 μg of wt p53, p53-175H, p53-273H in pCMV-Script or the corresponding empty vector per 10 cm dish and analysed 24 hours post transfection. The panel shows western blot analysis with the indicated antibodies (DO-1 for p53) from H1299 cells transfected with the indicated constructs.

Following RNA extraction from the triplicate transfections, the RNA quality was tested as described previously (section 3.12). Based on the 28S:18S rRNA, OD 260/280 and OD 260/230 ratios of the analysed samples (Table 3.8 and Figure 3.44), the extracted RNA was deemed suitable for qRT-PCR analysis. qRT-PCR was performed by members of the Applied Biology team (led by Prof. D. Ross Sibson and Dr Bryony Lloyd, University of Liverpool) as described previously (section 2.19). The relative expression of the 12 selected targets in H1299 cells transfected with wt p53, p53-175H or p53-273H, respectively compared to H1299 cells transfected with the corresponding empty vector is presented in Table 3.9, while the normalised expression levels (normalised to histone H3 expression) are presented in Figure 3.45.

Table 3.8: Spectrophotometrical quantification of the RNA extracted from transiently transfected H1299 cells. H1299 cells were transfected with 5 µg of wt p53, p53-175H, p53-273H in pCMV-Script or the corresponding empty vector per 10 cm dish, in triplicate (I-III). RNA was extracted from the transiently transfected cells 24 hours post transfection.

H1299 +	Concentration [µg/µl]	OD 260/280	OD 260/230
empty vector I	2.43	1.73	2.48
empty vector II	1.91	1.75	1.57
empty vector III	2.27	1.70	2.35
p53 I	2.38	1.74	2.21
p53 II	2.20	1.69	2.27
p53 III	2.00	1.69	2.49
p53-175H I	1.95	1.78	1.53
p53-175H II	1.07	1.59	2.45
p53-175H III	2.70	1.74	2.40
p53-273H I	2.22	1.66	2.47
p53-273H II	1.59	1.70	1.69
p53-273H III	2.53	1.72	2.42

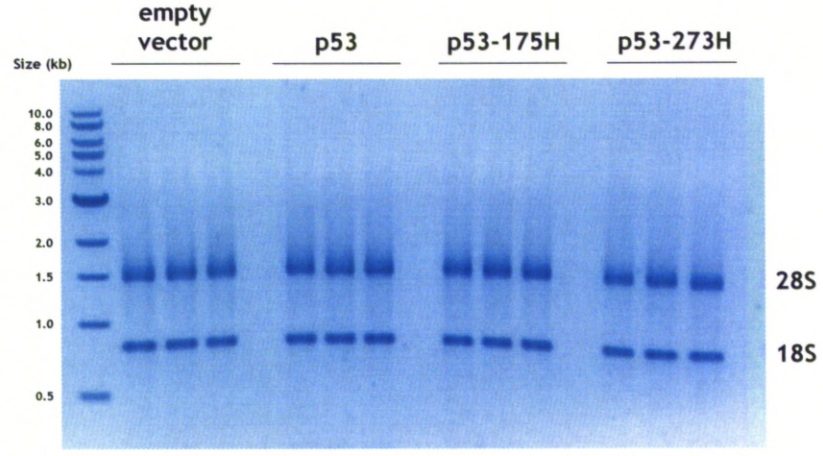

Figure 3.44: RNA extracted from transiently transfected H1299 cells. H1299 cells were transfected with 5 µg of wt p53, p53-175H, p53-273H in pCMV-Script or the corresponding empty vector per 10 cm dish, in triplicate. RNA was extracted from the transiently transfected cells 24 hours post transfection. The RNA integrity was tested by running 500 ng of total RNA on a 1% agarose gel (with EtBr) and visualised using ultraviolet light. The 28S and 18S RNA bands are indicated.

As shown in Table 3.9, most of the determined relative gene expression levels of the 12 selected genes in H1299 cells transfected with wt p53, p53-175H or p53-273H (normalised to the control expression levels in H1299 cells transfected with the corresponding empty vector) were not statistically significantly. When looking at the average expression levels of each of the 12 selected genes following transfections (Figure 3.45), it is clear that the variation was very large, perhaps even larger than in the parallel experiment performed on UM-SCC-12 cells (section 3.12.2). To determine the source of variation it was necessary to analyse the normalised expression levels (and their variations) for each transfection separately (Appendix 16). As observed previously (section 3.12.2), there are cases, in which the variation for individual transfections is very large (for example for FN1 expression following p53 transfection or CCND2 expression following p53-273H transfection). These variations are derived from the differences between the average expression values determined for the two reverse transcriptions (see Figure 2.2), suggesting that the source of variation in these cases lies in the qRT-PCR assays rather than in the actual biological differences.

Table 3.9: The relative expression levels (determined by qRT-PCR) of the selected genes following transfection of H1299 cells with wt p53, p53-175H and p53-273H, respectively (normalised to the control expression levels in UM-SCC-12 cells transfected with the corresponding empty vector). The relative expression levels reflecting differences, which were statistically significant ($p < 0.05$ as determined by a Student's t-Test), are shown in red (if up-regulated) or blue (if down-regulated). (Data provided by Dr Bryony Lloyd.)

Gene	Fold change		
	p53	p53-175H	p53-273H
SPRR2A	1.97	-1.21	2.65
TLR4	2.88	1.10	4.04
S100A8	1.93	-1.10	2.53
C8orf4	1.73	-1.27	1.44
FN1	3.00	1.16	1.14
PTGES	2.11	1.05	1.62
TIMP2	1.11	-1.02	1.03
TSPAN1	1.40	1.04	1.30
MMP2	2.09	-1.25	2.14
CCND2	-1.30	-1.45	-1.63
OGN	1.35	-1.12	1.93
NPNT	2.28	-1.17	-1.03

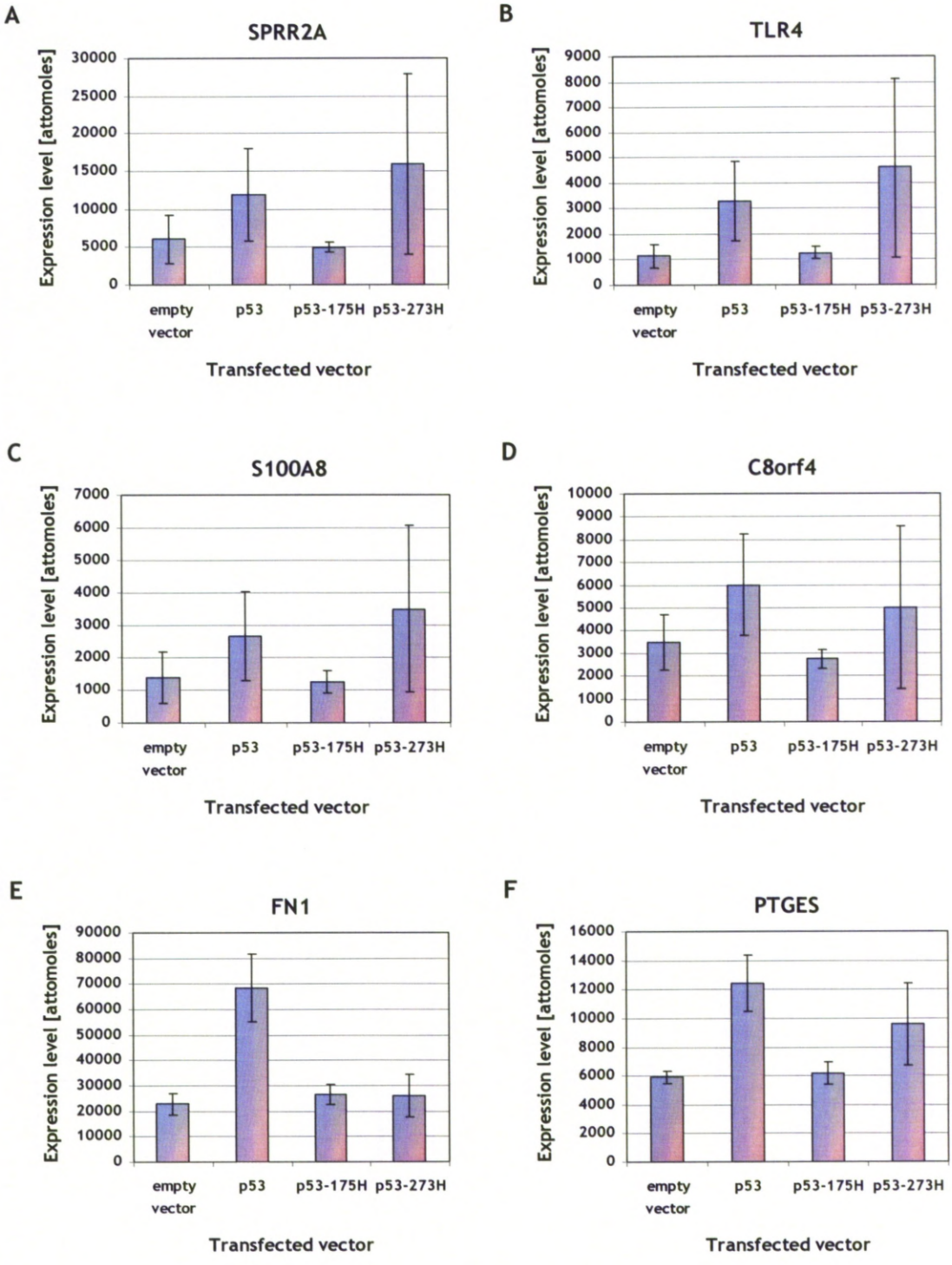

Figure 3.45: Expression levels of the indicated genes in H1299 cells following transfection with wt p53, p53-175H, p53-273H or the corresponding empty vector. qRT-PCR was performed on RNA extracted from H1299 cells transiently transfected with the indicated vectors. The histograms show mean of the average expression levels (normalised to histone H3 expression) in three replicate RNA samples (see section 2.19.4 for details), the error bars represent standard error of mean. (Data provided by Dr Bryony Lloyd.)

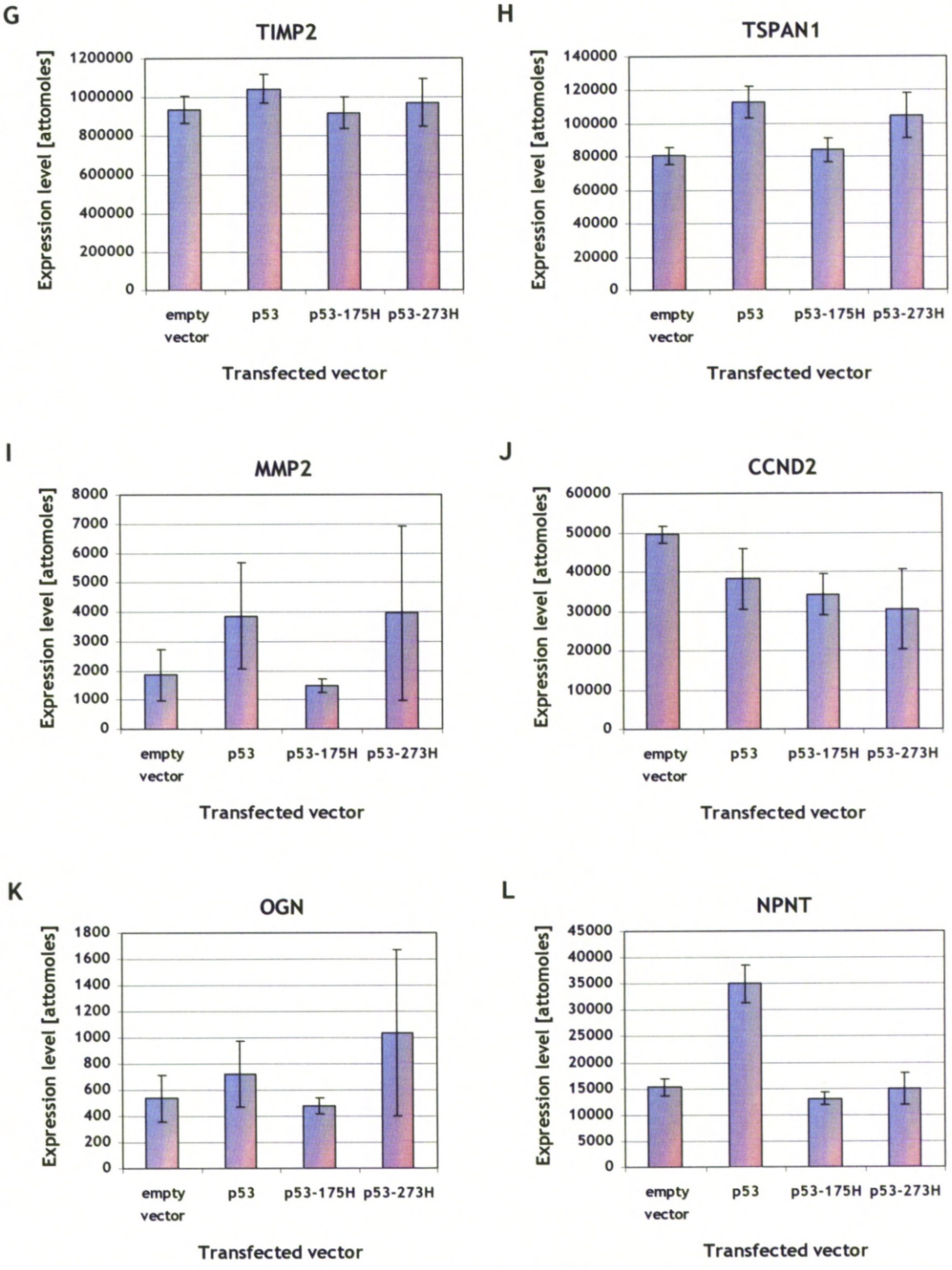

Figure 3.45 (cont.): Expression levels of the indicated genes in H1299 cells following transfection with wt p53, p53-175H, p53-273H or the corresponding empty vector. qRT-PCR was performed on RNA extracted from H1299 cells transiently transfected with the indicated vectors. The histograms show mean of the average expression levels (normalised to histone H3 expression) in three replicate RNA samples (see section 2.19.4 for details), the error bars represent standard error of mean. (Data provided by Dr Bryony Lloyd.)

However, in this experiment the variation for individual transfections was relatively small for most target genes (such as NPNT, PTGES or S100A8 expression in all four transfections). It is therefore most likely that any variations observed in Figure 3.45 are due to biological differences. A possible reason for such variation between the transfection replicates could be operator-based errors.

Compared to nucleofection used in the parallel experiment to transfect UM-SCC-12 cells (see section 3.12.2), GeneJuice transfection was relative non-toxic. GeneJuice, used to transfect H1299 cells, is described by the manufacturer as a proprietary formulation of a non-toxic cellular protein and a small amount of a novel polyamine. Polyamine-DNA complexes (polyplexes) are taken up by the cell through endocytosis. Polyamine-mediated transfection is one of the least toxic transfection methods available. Moreover, GeneJuice transfection can be performed in the presence of serum, which further reduces cytotoxicity and GeneJuice was shown to have the lowest cytotoxicity out of the transfection reagents tested on H1299 cells. Nevertheless, polyamines have been reported to cause membrane permeability (510), which could be the reason for the minimal toxicity observed.

Therefore, in future experiments it will be important to minimise the experimental variability (likely due to operator-based errors), which seems to be the main source of variation in this experiment, in order to more accurately determine the levels of gene expression in response to expression of the various forms of p53 under study.

3.13. Mutant p53 expression sensitises laryngeal cancer cells to ionising radiation

Since radiation therapy is one of the treatment modalities for laryngeal cancer, it was important to determine the impact of mutant p53 expression on the response of cells to ionising radiation.

Clonogenic assays were performed (as described in section 2.23) to investigate the response to γ-radiation of UM-SCC-12 cells, 12-175H-20 cells and 12-273H-39 cells. This experiment was performed once.

UM-SCC-12 (p53-null) cells are relatively radioresistant (Figure 3.46). 12-175H-20 cells are more sensitive to γ-radiation than UM-SCC-12 and 12-273H-39 cells are the most sensitive of all three. Since the studied cell lines are isogenic, the obtained results suggest that mutant p53 expression renders cells sensitive to radiation, with the contact mutation (R273H) having a stronger effect than the structural mutation (R175H). These data are rather unexpected since it is well documented that GOF mutant p53 expression is associated with tumour resistance to ionising radiation (511). On the other hand, a similar effect of p53 mutation has been previously observed in our laboratory, when LSCC cells expressing endogenous homozygous p53 mutations were found to be more sensitive to radiation than cells carrying any other p53 genotype (wt p53, heterozygous mutant p53 or p53-null) (512).

While the mechanistic details of this radiosensitisation remain unclear, the panel of generated isogenic cell lines provides an ideal experimental system for studying the response of LSCC cells to radiation.

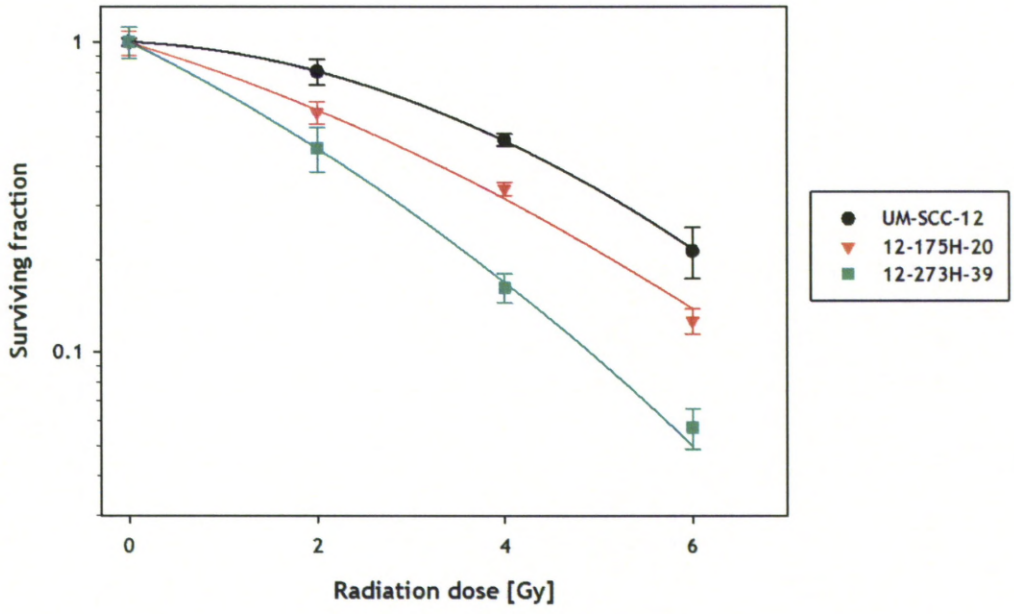

Figure 3.46: Expression of mutant p53 sensitises LSCC cells to ionising radiation. UM-SCC-12 cells, 12-175H-20 cells and 12-273H-39 cells were treated with the indicated doses of γ-irradiation and then seeded at a range of concentrations into 6-well plates and allowed to form colonies for a period of 2 weeks. Clonogenic assays were performed and survival data were fitted to the linear-quadratic equation $y = \exp\left(-\left(a \cdot x + b \cdot x^2\right)\right)$, where y is the surviving fraction and x is the treatment dose; all R^2 values were > 0.81. This experiment was performed once.

Chapter 4

Discussion

4. Discussion

Inactivation of the p53 tumour suppressor pathway, frequently due to missense mutations in the *TP53* gene, is one of the most common genetic alterations in human cancer (134, 139). p53 mutation is consistently associated with poor prognosis and therapeutic response in head and neck cancer (101, 513). It has been suggested that this may be due to an oncogenic gain of function of p53 mutants (reviewed in (514)).

Therefore, the main objective of this project was investigation of the mechanisms and functional consequences of the oncogenic gain of function of mutant p53 in laryngeal cancer cells, which are important preclinical models in the search for new therapies for treatment of laryngeal cancer (463). The two hot-spot mutants chosen for the studies described in this thesis were R175H (a structural mutation affecting p53 folding) and R273H (a contact mutation affecting one of the p53 residues, which make direct contact with DNA) (147). Both of these mutants have been shown to display GOF properties using *in vivo* models (5, 6) and have been documented to occur in laryngeal cancer (139).

Such p53 mutants exert their GOF properties by modifying cells through altered transcriptional activity or novel protein-protein interactions (411, 515). Therefore, the mechanism of action of the GOF p53 mutants discussed above was investigated by identifying the mutant p53 interacting proteins and studying the gene expression changes in cells expressing those p53 mutants. Since many biological functions involve interactions between proteins, identifying the interacting partners of mutant p53 may elucidate, which molecular networks and pathways mutant p53 proteins are involved in, and the identified mutant p53 interacting proteins may represent important new therapeutic targets. The functional consequences of GOF p53

mutations in laryngeal cancer were studied with respect to cellular motility, invasiveness and response to ionising radiation (a common treatment modality for laryngeal cancer).

To permit purification of p53 containing protein complexes for future identification of mutant p53 interacting proteins, cDNAs of wt and the two GOF mutants (R175H and R273H) were cloned into TAP-tag vectors. The constructs were then tested for expression and transcriptional activity in a p53-null background (H1299, a non-small cell lung carcinoma cell line). H1299 cells were chosen for these studies because they lack p53 expression, grow relatively rapidly (doubling in less than 24 hours) and are readily transfectable.

Expression of different p53 forms (wt, R175H or R273H) from a TAP-tag vector resulted in the expression of proteins of apparent molecular weight of 57 kDa, which is in accordance with the predicted size of TAP-tagged p53 – the apparent molecular weight of untagged p53 is 50 kDa and the theoretical molecular weight of the TAP-tag is 8 kDa. Both p53 mutants lack wt transcriptional activity as tested in a luciferase p53 transcriptional activity assay (using a RGC p53 binding element upstream of a p53 consensus binding sequence; see section 3.2). Furthermore, the two p53 mutants studied inhibited the wt p53 transcriptional activity in a dose-dependent manner (Figures 3.10 and 3.11), likely through hetero-oligomerisation of the wt and mutant forms of the protein (a dominant-negative effect) (411). Dominant-negative effects of the p53 mutants on wt p53-activated transcription from the RGC were also reported by others (516). The dominant-negative effect of the structural p53-175H mutant on wt p53 transcriptional activity was found to be stronger than that of the contact p53-273H mutant (Figures 3.10A and 3.11A). This phenomenon was also reported by others (392). It can be explained by the fact that the structural mutants

upon hetero-oligomerization with wt p53 are capable of shifting wt p53 into a mutant conformation while hetero-oligomers of contact mutants with wt p53 may retain some wt transcriptional activity. This is also supported by the fact that in a group of 37 patients with SCCHN the presence of the contact mutation (in 13 patients) is associated with LOH in 100% of cases while the structural mutation (in 24 patients) is associated with LOH in only in 50% of cases ($p = 0.0034$) (394).

Expression of wt p53 from a TAP-tag vector resulted in p53 that activates transcription from RGC, but which produces slightly lower levels of activity compared to the untagged wt p53 (Figure 3.12). It was observed that TAP-tagged wt p53 also reduces the activity of the untagged protein, thus acting as a partial dominant-negative in this system (Figure 3.13). This is likely due to hetero-oligomerisation of the tagged and untagged proteins. Therefore, TAP-tagged wt p53 retains reduced transcriptional activity and can reduce the activity of untagged wt p53 when the two proteins are co-expressed. Since all of the TAP-tagged proteins were to be introduced into p53-null cells, the partial inhibition the untagged wt p53 by the TAP-tagged protein would not be observed. Finally, this dominant-negative effect should not be of major concern unless the TAP-tag fusion prevents functionally critical proteins from associating with p53. Ultimately, the obtained results can be validated by using cDNAs that lack the fusions.

In order to study the interacting partners of the chosen GOF p53 mutants in laryngeal cancer cells, stable cell lines of a functionally p53-null LSCC cell line (UM-SCC-12) have been generated to express the TAP-tagged mutant forms of p53 (Figure 3.17). The approach of generating cell clones with a stable expression of the TAP-tagged p53 forms was taken because a transient expression system was not

feasible due to extremely low transfection efficiency of UM-SCC-12 (typically 1-2%, see Figure 3.15).

One cell clone that stably expresses a TAP-tagged R175H mutant of p53 (12-175H-20) and two cell clones with stable expression of the R273H mutant of p53 (12-273H-39 and 12-273H-41) were generated. It is important to note that in the first attempt to generate mutant p53 expressing LSCC cells, 12-175H-20 was the only positive clone obtained displaying mutant p53 expression and it was one of the most slowly growing ones, which may suggest that the expression of TAP-tagged p53-175H has some inhibitory effects on cell growth. In the second attempt to establish cell clones expressing p53-273H, a clone 12-273H-39 (expressing a high level of p53-273H) was also one of the slower growing cell clones, while another clone 12-273H-41 (expressing a low level of p53-273H comparable to the level of mutant p53 expression in tumour-derived laryngeal cancer cell lines) was established earlier during the selection process because it was growing faster. This further supports the conclusion that these p53 mutants may exhibit some growth inhibitory properties.

Attempts to produce similar clones expressing TAP-tagged wt p53 were unsuccessful in spite of performing the process of cloning and selection twice and selecting a large number of colonies for expansion. Many cell clones were lost during the expansion because they failed to grow (exhibiting signs of senescence or cell cycle arrest) and eventually died. The fast growing clones, on the other hand, showed no p53 expression. Given the potent growth inhibitory effects of wt p53 it could be expected that the cells would not tolerate p53 expression and therefore the failure of these attempts is not surprising. A similar situation was reported in a recent study of the GOF p53 mutants (454). The authors clearly stated that wt p53 was not used in the

analysis because its expression resulted in cell-cycle arrest or apoptosis. Moreover, the authors speculated that obtaining wt p53-expressing cells would likely suggest that these cells had undergone additional alterations allowing them to tolerate wt p53 expression.

Although isogenic cell lines expressing mutant and wt p53 forms would certainly be a valuable system for studying the novel functions of p53 mutants, which are distinct from those of the wt protein, the lack of a wt p53-expressing cell line can be dealt with in validation studies on transiently transfected cells.

Using a simplified TAP-tag purification system (streptavidin affinity purification) in combination with mass spectroscopy, a number of mutant p53 interacting proteins have been identified in lysates from p53-175H and p53-273H mutant expressing LSCC clones (Table 3.2). The identified proteins are discussed in the following section.

Comparing lysates prepared from p53-175H and p53-273H mutant expressing LSCC clones, HSP70 was identified only in the p53-175H-containing complexes. The interaction of HSP70 and p53-175H was also confirmed by immunoprecipitation to be specific and selective for this p53 mutant. Since p53-175H is a structural mutant it seems likely that p53-175H is bound by HSP70 (an inducible chaperone stabilising existing proteins against aggregation and mediating the folding of newly translated proteins) because it is misfolded. Importantly, HSP70 was reported to bind preferentially to conformational p53 mutants (517). The binding sites in p53 for HSP70 have been mapped to hydrophobic secondary structures (especially β-strands) in the central DNA binding domain (518). It has been suggested that these high affinity binding sites are cryptic in wt p53 and become exposed upon p53 mutation, which alters the tertiary structure of the protein causing it to adopt a 'mutant'

conformation. The functional consequences of this interaction are not fully understood but it has been proposed that HSP70 forms a complex with HSP90 and Hdj in an attempt to restore its native conformation (519). However, the inherent instability of conformational p53 mutants is suggested to result in the formation of stalled chaperone-mutant p53 complexes and stabilisation of mutant p53 by molecular chaperones (519).

HSC70, identified by mass spectroscopy in p53-175H-containing complexes, is a constitutive chaperone belonging to the heat shock protein 70 family. HSC70 also assists in appropriate folding of proteins and has 85% sequence identity to HSP70. In the context of conformational p53 mutants, the molecular basis and functional consequences of the interaction between HSC70 and p53-175H are likely to be similar to those described above for HSP70.

BAG2, identified also in p53-175H-containing complexes, is a co-chaperone with high affinity for the ATPase domain of HSC70/HSP70 (492). BAG2 was reported to inhibit the activity of CHIP, a chaperone-associated ubiquitin ligase, which marks misfolded proteins presented by HSC70/HSP70 for proteasomal degradation (493, 520). The presence of BAG2 in the isolated complexes containing p53-175H suggests that BAG2 may contribute to stabilisation of this p53 mutant by inhibiting its proteasomal degradation. The interaction of BAG2 and p53-175H has not been reported previously. It is possible that BAG2 was purified with p53-175H because of its interaction with HSC70/HSP70. The specificity of the BAG2/p53-175H interaction remains to be validated. In the present study it was not possible to accomplish this due to the lack in our laboratory of an anti-BAG2 antibody, which could be used for western blotting to determine whether BAG2 was present in protein complexes isolated from p53-175H expressing cell clone by immunoprecipitation.

Tmod3 was identified in both p53-175H and p53-273H-containing complexes. Tmod3 functions as a negative regulator of cell migration (521). It regulates actin polymerisation by capping the ends of actin filaments and sequestering monomeric actin (522). The interaction of Tmod3 with any p53 forms has not been reported previously. Tmod3 was also not detected by western blotting in the immunoprecipitated complexes containing wt and the two mutant forms of p53, respectively. There are a few possible explanations for this finding. First of all, a possibility exists that Tmod3 bound to the streptavidin sepharose rather than to p53 mutants and was eluted non-specifically from the beads. Secondly, Tmod3 might have been purified with TAP-tagged mutant p53-containing complexes because it might bind to the TAP-tag itself. This would explain why it was not identified in the immunoprecipitated complexes purified using untagged p53 versions as bait. Moreover, it is possible that the antibody used for immunoprecipitation blocks the interaction site of mutant p53 and Tmod3. Finally, the interaction might be weak and the antibody used for western blotting might be not strong enough to detect a possibly small amount of Tmod3 in the purified complexes.

In the first purification of p53-175H-containing complexes MDM2 was identified in the calmodulin eluate containing p53-175H by western blotting (Figure 3.18B). It is important to note, however, that a large proportion (10%) of the final calmodulin eluate was probed with an anti-MDM2 antibody, which can detect very small amounts of MDM2. Interestingly, MDM2 was not identified in the mutant p53-containing complexes by mass spectroscopy. This likely suggests that the interaction of mutant p53 with MDM2 is relatively weak and the amount of MDM2 present in the purified complexes was below the threshold of detection by the mass spectrometer. The fact that both of the studied p53 mutants are bound by MDM2 to some extent is also

supported by the presence of MDM2 in the immunoprecipitated complexes containing p53-175H and p53-273H, which was detected by western blotting.

None of the remaining proteins identified in the mutant p53-containing complexes (but not present in the control sample) was previously reported to interact with wt or mutant p53. It will be important to determine whether these selectively or specifically interact with mutant p53 and also if they do, what the functional consequences of these interactions are. p53 GOF mutants have been linked with poor prognosis and thus novel GOF mutant interacting proteins may represent important new therapeutic targets.

Mutant p53 has been linked with reduced survival and highly metastatic tumours (513). GOF p53 mutants have also been shown to stimulate metastasis in mouse models (395, 523). Since cell motility and invasiveness *in vitro* are often used as surrogate indicators of metastatic potential, the migratory potential and invasiveness of GOF mutant p53 expressing cells were studied.

Boyden chamber motility assays were used initially to investigate the migratory potential of the studied cells. Although one of the GOF mutant p53-expressing cell lines (12-273H-39) displayed 8-fold increased motility compared to the parental UM-SCC-12 cells, 12-273H-null cells exhibited the highest migratory potential in this system with 50-fold higher motility compared to the parental UM-SCC-12 cells (Figure 3.29). 12-273H-null cells went through the cloning and selection process but showed no detectable p53-273H expression. These cells displayed a morphology typical of EMT with elongated, spindle-shaped cells and numerous philopodia (see Appendix 10), which could explain why they were able to migrate through the membrane pores. 12-273H-null cells survived the selection process, which means they express the G418-resistance gene, but show no detectable mutant p53 expression

suggesting that the observed phenotype is likely due to clonal selection from a heterogeneous population of cells. The increased motility of these cells in the Boyden chamber motility assay is a good example why the possibility of clonal variation should never be underestimated.

Overall the studied cell lines were not very motile as determined using the Boyden chamber motility assay when compared to other lines that have been examined in our research laboratory (287). Out of 15,000 cells seeded into the chambers only between 11 and 1,274 cells (less than 8.5%) migrated through the membranes. In contrast with H1299 cells out of 15,000 cells seeded typically 1,500 cells were found to migrate through the membrane (287). These data suggest that this might not be an ideal system to study the migratory potential of these cells. The cells studied in this project are squamous cell carcinoma cells. These cancers arise from epithelial cells forming protective cell layers that line the skin and internal cavities (110). Squamous cells are often flattened and scale-like (from Latin *squama* meaning 'scale'). Due to the flattened morphology of squamous cells and the fact that they usually line surfaces it is possible that these cells have a greater potential to move on flat surfaces (such as the surfaces of a tissue culture dish) rather than in 3D space. The Boyden chamber motility assay measures the ability of cells to migrate through pores in a membrane, which might represent three-dimensional migration. Additionally, it was observed as part of a different experiment (clonogenic assays, section 3.13) that the plating efficiency (see section 2.23) of UM-SCC-12 cells is very low (~9.5%) and even lower for p53-175H and p53-273H-expressing cells (~5.9% and ~3.8%, respectively) and that the cell lines require a considerable time to adhere to the surface of the dish. All of these factors could also contribute to the low numbers of cells migrating through the Boyden chamber membranes.

Therefore, another approach was used to study the motility of these cells – live imaging of cell migration. Interestingly, in this assay 12-273H-null cells behaved almost identically to UM-SCC-12 cells

All the mutant p53-expressing cells (12-175H-20, 12-273H-39 and 12-273H-41 cells) displayed increased motility (as determined by total distance travelled or speed) compared to the parental UM-SCC-12 cells (Figure 3.31A and D). The increase in motility of p53-273H-expressing cells was more significant than that of 12-175H-20 cells. The movement of 12-273H-39 and 12-273H-41 cells was similarly disorganised (as determined by directionality) as that of the parental UM-SCC-12 cells while the migration of 12-175H-20 cells was more organised (higher directionality). Interestingly, a recently published study has also investigated the motility of cells (H1299) expressing the same p53 mutations studied in this project (p53-175H and p53-273H) using similar techniques to the ones described here (live cell imaging and tracking of individual cells) (454). These mutants were reported to promote random cell migration (in terms of decrease in directionality) and disorganised lamellipodia. However, no difference in speed of the mutant p53-expressing cells was observed compared to their parental p53-null cells (H1299), which is in contrast to the results presented here. The authors of the study further propose that the random migration of the mutant p53-expressing cells may be associated with their inability to correctly establish an axis of polarity. The reasons for the differences in the reported results may stem from different cell lines used for studying the effects of the GOF mutants and the differences in their intrinsic motility and directionality of movement. H1299, used in the published article, are non-small cell lung carcinoma cells, which are intrinsically less motile on 2D surfaces (data not shown) than the UM-SCC-12 cells used in this project. The movement of H1299 cells also appears to be more organised

(directionality of ~0.7) compared to the movement of UM-SCC-12 cells, which is intrinsically more random (directionality ~0.2). Moreover, the p53 polymorphism at amino acid 72 could have also contributed to the differences in the obtained results (the mutants used in the published study expressed the codon 72R polymorphism while the mutants used in this project are all codon 72P). p53 polymorphism at codon 72 was reported to be an intragenic modifier of mutant p53 behaviour (412). One of the mechanisms, through which p53 mutants might exert their GOF properties, is binding to and inhibition of the functions of p53-family proteins, p73 and/or p63 (as discussed in section 1.3.4.3.1.1). It was further shown that p53 polymorphism at codon 72R strongly influences the ability of mutant p53 to interact with and inhibit p73 function, but has no influence on the binding of mutant p53 to wt p53 (412). Consequently, 72R conformational p53 mutants were found to be more effective in suppressing p73-dependent apoptosis in cultured cells (412). Additionally, it was observed that in squamous cell carcinomas of the head and neck heterozygous for the p53 polymorphism at codon 72 and displaying p73 expression, it is the 72R allele that is preferentially mutated (in 26 cancers heterozygous for p53 polymorphism at codon 72, the mutated allele was R in 21 cases and P in 5 cases) (412). Furthermore, it was shown that p53-72R mutants are capable of inhibiting chemotherapy-induced apoptosis more efficiently than p53-72P mutants and in a group of SCCHN patients those with tumour-specific expression of the mutant 72R allele had both a decreased response to cisplatin chemotherapy and reduced overall survival compared to those with p53-72P expression (413). Altogether these data suggest that codon 72 polymorphism influences the biological behaviour of p53 mutants, at least in certain types of cancer.

In order to test whether the observed differences in motility of the established mutant p53-expressing clones are due to mutant p53 expression or whether they can be attributed to clonal variation, down-regulation of mutant p53 expression by RNAi was attempted in the highly motile 12-273H-39 cells. However, due to poor transfection efficiency of 12-273H-39 cells, down-regulation of mutant p53 expression (based on western blot analysis) was questionable and therefore the corresponding motility results (although difference in motility was statistically significant 36-48 hours post transfection with siRNA) could not be analysed with confidence (Figure 3.32).

In order to achieve satisfactory down-regulation of mutant p53 expression in 12-273H-39 cells, cell lines with stably reduced mutant p53 levels have been generated (Figure 3.33). The motility of two clones with significantly reduced p53-273H level was analysed and both cell lines displayed significantly reduced motility compared to parental 12-273H-39 cells (Figure 3.34). The data presented here suggest that the increased motility of 12-273H-39 cells is due to mutant p53 expression. However, the motility of the remaining clones expressing reduced levels of p53-273H as well as the motility of the control clones still need to be analysed before the possibility of clonal variation can be excluded and the observed increase in migratory potential of cells contributed unequivocally to mutant p53 expression.

Since mutant p53-expressing laryngeal cancer cells exhibited increased motility (section 3.9 and 3.10), further studies were performed to determine whether the mutant p53-expressing cells displayed increased invasiveness *in vitro*, another surrogate indicator of metastatic potential. Boyden chamber invasion assays were used for this purpose. As previously discussed, Boyden chambers are not an ideal system for studying the LSCC cells used in this project. However, it was expected that

the thin layer of Matrigel that the invasion chambers are coated with should facilitate cell adhesion. Indeed, it appeared as if the cells had adhered to the Matrigel within an hour from the time of seeding as determined microscopically (data not shown). Migration of cells through the Matrigel-coated membranes was also encouraged by the presence of a serum gradient. Moreover, this was the only invasion assay performed routinely and readily available in our laboratory and thus it was decided to attempt analysis of invasion using this system in the first instance despite the anticipated limitations.

Although the variation of the obtained results was very high and none of the resulting differences was statistically significant, 12-273H-39 cells seemed to be less invasive than the parental UM-SCC-12 cells. While this difference is not statistically significant, such reduction of the ability of 12-273H-39 cells to degrade Matrigel could theoretically be explained by a significant up-regulation of fibronectin in these cells (Table 6.5). Fibronectin is a component of ECM and hence the increased production of ECM by 12-273H-39 cells might hinder Matrigel degradation and contribute to the observed reduction in the invasive potential of these cells. However, the increased production of fibronectin may at the same time contribute to the increased motility of these mutant p53-expressing cells on 2D surfaces since fibronectin was significantly up-regulated in the highly motile 12-273H-39 cells and relatively unchanged in the much less motile 12-175H-20 cells (Figure 3.39E). Clearly, the importance of other contributing factors should also not be underestimated.

A recent study reported that fibronectin expression induces autocrine up-regulation of MMP-9, resulting in increased invasiveness of A431 cells (500). While 12-273H-39 cells display increased fibronectin expression, MMP-9 expression was

not up-regulated, which could potentially explain the lack of increased invasiveness of these cells. However, it is more likely that the Boyden chamber invasion assay is simply inappropriate for studying migration or invasiveness of these cells.

The reduced invasiveness of 12-273H-39 cells also seems to be in conflict with the previously mentioned study of GOF p53 mutants (454). Polyclonal populations of mutant p53-expressing H1299 and RPE (retinal pigment epithelial) cells displayed increased invasiveness as determined by their ability to migrate into a Matrigel plug towards a serum and EGF gradient. The first reason for this discrepancy may be the clear differences in the experimental procedures used to study invasiveness of cells. In the study described above cells migrated towards EGF (and serum) gradient. The use of EGF as chemoattractant is clearly biased towards cells displaying increased EGFR expression. Moreover, EGF binding to EGFR triggers receptor internalisation and initiates a signalling cascade through Ras-Raf and PI3K-AKT, resulting in a mitogenic response (128). Therefore, inclusion of EGF in this assay is a clear limitation since EGF might stimulate proliferation of cells, which could be an unnecessary confounding variable.

Another possible reason for the discrepancy in the reported results may lie in the low efficiency with which UM-SCC-12 cells (and any derivatives thereof) migrate through the Boyden chamber membranes and this factor may conceal the actual potential of these cells to degrade Matrigel. It will be important to use a different experimental system, such as invasion into Matrigel plugs, to reliably determine the invasive potential of these mutant p53-expressing cells.

The mechanisms through which GOF p53 mutants promote invasiveness and metastatic potential of tumours are still not entirely understood. Recent reports indicate that mutant p53 increases TGFβ-dependent metastatic potential of cancer

cells via inhibition of p63 function (457) and also promotes invasion through increased integrin (α5β1) and EGFR recycling, which is also linked with suppression of transcriptionally active p63 (454).

p63 is a p53 homologue. Structurally, it contains three functional domains: transactivation, DNA binding and oligomerisation domain. There are many different isoforms of p63, which can be divided into two main groups, which are a result of transcription from two alternative promoters: the TAp63 isoforms, containing a fully function N-terminal TA domain, and the ΔNp63 isoforms, which lack the N-terminal TA domain (524, 525). While the functions of p63 are not entirely understood (partly due to the large number of different isoforms), TAp63 is known to play a critical role in epithelial development and was also suggested to have some functions similar to p53 such as regulation of apoptosis or senescence (526). More recently, p63 (TAp63 and ΔNp63) was suggested to play a role in regulation of cell adhesion and cell survival, with p63 down-regulation resulting in cell detachment and apoptosis (527). Importantly, TAp63 was also suggested to suppress metastasis (528). The short ΔNp63 isoform is a dominant-negative inhibitor of TAp63 and other p53 family members (due to hetero-oligomerization) (526). ΔNp63 was reported to suppress both the extrinsic and the intrinsic apoptotic pathways (see section 1.3.2.2) (529). Moreover, overexpression of the ΔNp63α isoform resulted in sustained proliferation and suppression of oncogene-induced senescence *in vivo*, suggesting that ΔNp63 might function as an oncogene (530).

Importantly, the laryngeal cancer cells studied in this project appear to express predominantly the ΔNp63 isoform (lacking the N-terminal transactivation domain) and little (if any) TAp63, which is a common situation in head and cancer (531). Therefore, suppression of TAp63 function is unlikely to underlie the increased

motility of 12-273H-39 cells and the p53-273H GOF mutant appears to act via an alternative pathway in LSCC cells.

Following the motility and invasion analysis of the mutant p53-expressing cells, gene expression profiles of the highly motile 12-273H-39 cells and parental UM-SCC-12 cells were studied using exon array analysis to investigate the gene expression changes of cells expressing the GOF contact mutant of p53. The expression analysis revealed 154 genes up-regulated and 39 genes down-regulated in the p53-273H-expressing cells. The pathways most significantly affected by the differentially expressed genes are involved in cell adhesion and ECM remodelling (Figure 3.38). Considering the increased migratory potential of 12-273H-39 cells this suggests that p53-273H mutant may confer a motile phenotype on UM-SCC-12 cells by altering their transcriptome with an emphasis on inducing ECM remodelling programmes.

A number of the identified genes are known to be transcriptional targets of wt p53 (including SPRR2A, MFAP5, PTGES, CCND2, OGN and FN1). Based on the transcriptional networks generated from the microarray analysis (Appendix 14) it appears that a number of genes, which were found to be differentially expressed in this study, could be transcriptionally regulated by mutant p53 via other transcription factors, such as Sp1 and NF-κB.

Wild-type p53 is known to bind to transcription factor Sp1, resulting in the inhibition of the ability of Sp1 to bind other promoters (such as VEGF) and this is one of the mechanisms of p53-mediated transcriptional repression (532). However, VEGF-A was found to be up-regulated 2.48-fold in the mutant p53 expressing cells compared to p53-null cells, suggesting that p53-273H might cooperate with Sp1 in induction of Sp1-regulated genes. This would mean that the interaction of mutant and

wild-type p53 with Sp1 may have opposite outcomes. Indeed, mutant p53 has been reported to interact with Sp1 and increase transcription from Sp1-responsive promoters (415).

Based on the generated transcriptional networks p53-273H also seems to affect the expression of a number of NF-κB-responsive genes. This finding is supported by a number of studies, which have reported induction of NF-κB gene expression by tumour-derived p53 mutants (533, 534). Similarly to Sp1, the regulation of NF-κB responsive genes by wt and mutant p53 proteins seems to yield opposite outcomes with wt p53 antagonizing the transactivating effect of NF-κB (535) and mutant p53 stimulating it (534). NF-κB activation results in increased expression of downstream targets, such as MMP9 (535) or BCRP (536), which are associated with increased invasiveness and multi-drug resistance, respectively. Given that the processes controlled by NF-κB are known to include inflammation, transformation, proliferation, angiogenesis, invasion, metastasis, chemoresistance and radioresistance, activation of NF-κB-responsive genes by mutant p53 could provide a plausible mechanistic basis for some or all of its oncogenic gain-of-function effects.

While the results obtained from the microarray analysis of gene expression in p53-null and p53-273H-expressing LSCC cells have been validated by qRT-PCR, it is important to remember that the studied cells (12-273H-39) are a clonal derivative of UM-SCC-12 and hence there is a chance that the observed gene expression changes are due to clonal variation. To address the issue of clonal variation as well as discount any of the observed results being due to the presence of TAP-tag at the N-terminus of p53 mutants, H1299 and UM-SCC-12 cells were transiently transfected with either untagged wt or the two GOF p53 mutants. qRT-PCR of the selected targets was, however, inconclusive due to high experimental variation. Therefore, it will be

important to minimise the experimental variability in order to determine whether the observed differences in gene expression are a consequence of the expression of the various forms of p53 under study.

Moreover, in future experiments a number of the genes validated by qRT-PCR will be selected for functional examination to determine their possible contribution to the observed migratory phenotype of 12-273H-39 cells. The best candidates for functional studies include genes, which are more highly up-regulated in 12-273H-39 cells (displaying dramatically increased migratory potential) compared to 12-175H-20 cells (displaying slightly increased migratory potential), although threshold effects might also complicate this simplistic interpretation.

GOF p53 mutants are widely known to be associated with tumour resistance to treatment (401, 402). Therefore, the response of mutant p53-expressing cells to ionising radiation (IR) has also been studied. Radiotherapy is the basis of treatment for LSCC and p53 is vital for activating the responses to a number of cellular stresses including DNA damage. Therefore, it comes as no surprise that tumour response to radiation therapy relies on the p53 pathway (537). It has been reported that p53-mediated apoptosis is crucial in the sensitivity of tumours to radiation therapy, as wt p53 suppression or p53 inactivation through mutation results in radioresistance (538). However, more recent studies suggest that other p53-regulated processes (such as cell-cycle arrest or senescence) may also contribute to radiation sensitivity mediated by wt p53 (512).

Interestingly, the expression of mutant p53 was shown to sensitise p53-null LSCC cells to IR with p53-273H having a stronger effect than p53-175H (Figure 3.46). It can be speculated that these p53 mutants retain some residual wt p53 activity and are able to induce p53-mediated apoptosis to some extent. p53-273H is a contact mutant

retaining native p53 folding, which may make it more capable of binding and transactivating p53-responsive apoptotic genes than p53-175H, a structural mutant with its DNA binding domain significantly distorted. A similar effect of p53 mutation has been previously observed in our laboratory, when LSCC cells expressing endogenous homozygous p53 mutations were found to be more sensitive to radiation than cells carrying any other p53 genotype (wt p53, heterozygous mutant p53 or p53-null) (512).

However, these results are in contrast to other studies reporting increased radioresistance of mutant p53-expressing tumours and cells *in vitro* (539, 540). It has been suggested that this radioresistance is mediated via stimulation of Gal-3 (an anti-apoptotic molecule transcriptionally repressed by wt p53) expression by GOF p53 mutants in thyroid cancer (540). Gal-3 overexpression was reported in most thyroid cancer cell lines studied, particularly those expressing the R273H mutant of p53 (540). Since Gal-3 up-regulation was not observed in p53-273H-expressing cells in the current study, it seems likely that the malignancies of the head and neck constitute a completely separate group of tumours and the GOF p53 mutants exert their oncogenic properties via alternative mechanisms in this cancer type. These results warrant further study of the mechanisms of radiosensitivity mediated by these two GOF p53 mutants in LSCC cells.

4.1. Future work

The work presented in this thesis identified several new lines of investigation relating to mutant p53 gain-of-function. First of all, HSP70/HSC70 were shown to preferentially interact with the structural mutant p53-175H. In future studies it will be important to determine the functional consequences of these interactions, which can

be studied with the help of HSP70/HSC70 inhibitors. It will also be interesting to study the role of BAG2 in mutant p53-HSP70 complexes. Moreover, it will be important to determine whether the remaining proteins identified in the mutant p53-containing complexes (none of which was reported to interact with wt or mutant p53 previously) selectively or specifically interact with mutant p53. Since p53 GOF mutants are frequently associated with poor prognosis, novel mutant p53 binding partners may represent important new therapeutic targets.

Since mutant p53 has been linked with reduced survival and highly metastatic tumours (513), cell motility and invasiveness (surrogate indicators of metastatic potential) of the mutant p53 expressing cells were studied *in vitro*. While the stable clones expressing p53-175H or p53-273H displayed increased motility, the possibility of the observed phenotype being due to clonal variation could not be excluded. Stable knock-down of p53-273H resulted in reduced motility in two clones tested so far. In order to unequivocally determine whether the increased motility of mutant p53 expressing cells is due to mutant p53 expression, it will be important to test the motility of the remaining knock-down clones and the established control clones.

Exon array analysis revealed a number of differentially expressed genes in the highly motile 12-273H-39 cells compared to the parental p53-null cells. Importantly, the pathways most significantly affected by the differentially expressed genes are involved in cell adhesion and ECM remodelling. The results of the microarray analysis were successfully validated by qRT-PCR. However, it is important to remember that the mutant p53 expressing cells under study are a cell clone and, therefore, the possibility of the obtained results being due to clonal variation also needs to be considered. To address this issue, validation of selected targets was attempted by qRT-PCR in cells (H1299 and UM-SCC-12) following a transient

transfection with wt or mutant p53 forms. While the internal experimental variation was too high to obtain statistically significant data (Figure 3.39 and 3.42), it is also clear that generally there were no significant differences in expression of the studied targets. This may be due to high toxicity of transfection, resulting in highly stressed cells. Therefore, transient transfection of cells with p53 forms does not seem a feasible approach to studying differences in gene expression. Instead, polyclonal populations of cells expressing mutant p53 forms may be established to enable the investigation of gene expression changes in mutant p53 expressing cells. In this way, clonal variation would not be a problem and cells would be allowed sufficient time to recover from the stress of transfection.

Finally, some of the targets identified to be differentially expressed in the mutant p53 expressing polyclonal populations can then be selected for further study. So far, fibronectin, reported to stimulate invasiveness and metastatic potential of cancer cells, seems to be an ideal candidate for future functional studies. The contribution of fibronectin to the increased migratory potential of 12-273H-39 cells could be studied by RNAi and live cell imaging. Identifying targets, through which mutant p53 promotes motility and invasiveness, will be crucial for developing novel targeted therapies. Moreover, it will be important to determine whether any of the differentially expressed genes are direct transcriptional targets of p53 mutants. This could be achieved using chromatin immunoprecipitation (ChIP), which may be performed using TAP-tagged p53 forms and the optimised (highly efficient) TAP-tag purification procedure.

Although the current study failed to demonstrate a role for mutant p53 in stimulating invasiveness (perhaps due to a lack of appropriate experimental system), there is convincing evidence that p53 mutants are involved in the process of invasion

(311). To address this issue, invasion of the mutant p53 expressing laryngeal cancer cells into extracellular matrices (Matrigel or Collagen I) could be investigated (without the use of Boyden chambers). This could be achieved in a number of ways, for example by overlaying seeded cells with Matrigel/Collagen I and applying a chemoattractant above the matrix to stimulate invasion. The cells, which invaded into the matrix, can then be stained with a fluorescent dye (such as Fluorescein or Calcein AM) and the number of invading cells quantified using confocal microscopy.

Finally, the most biologically relevant assay for studying invasion and metastasis are mouse models. In this study mutant p53 expressing cells were also engineered to express a fluorescent protein, mCherry (when attempting to achieve a stable knock-down of mutant p53, the vectors encoding the p53 and scrambled short hairpins also encoded mCherry – see section 2.4.10). These cells could either be used in mouse xenograft models or could be surgically implanted into murine laryngeal tissues. Due to fluorescent labelling of these cells, tumour development and metastasis formation could be monitored using fluorescence *in vivo* imaging systems, without the need to sacrifice animals prematurely (hence reducing the number of animals needed). Additionally, the use of fluorescent cells would make identifying micrometastases following dissection much easier.

Chapter 5

Conclusion

5. Conclusion

Gain-of-function p53 mutants are associated with poor prognosis and therapeutic response in head and neck cancer (101, 513, 541). GOF p53 mutants likely act through altered transcriptional activity and/or novel protein-protein interactions but the molecular details of the mechanisms involved are still not entirely understood. Therefore, the aim of this project was to characterise the mechanisms of mutant p53 GOF in laryngeal cancer by studying protein interactions of p53 mutants and gene expression profiles of cells expressing either of two GOF mutants representing two distinct mutational classes: structural (R175H) and contact (R273H).

Cell clones of a functionally p53-null (truncated) LSCC cell line with stable expression of either TAP-tagged R175H or R273H mutant of p53 have been generated. A number of proteins have been purified and identified in the mutant p53 containing protein complexes in LSCC cells. One of these, HSP70 has been confirmed by immunoprecipitation to selectively interact with the p53-175H mutant, which may play a role in its stabilisation. It will be important to determine whether the remaining identified proteins selectively and/or specifically interact with mutant p53 and what the functional consequences of these interactions are.

Motility analysis of the generated cell clones revealed that p53-273H-expressing cells and to a smaller extent p53-175H-expressing cells display increased motility, which could explain the increased tumorigenic and metastatic potential of tumours harbouring p53 GOF mutants. A stable knock-down of the mutant p53 in 12-273H-39 cells has been shown to reduce the motility of cells suggesting that p53-273H contributes to increased migratory potential of these cells and that this is not a consequence of clonal selection and variation. Interestingly however, those cells did

not exhibit increased invasiveness *in vitro* although the assays used for this latter were based upon Boyden chambers and these may not be appropriate for the squamous cell lines studied here as analysis of cell motility in Boyden chambers suggests (see section 3.9.1).

Analysis of gene expression in p53-273H-expressing vs. p53-null laryngeal cancer cells revealed multiple genes that are differentially regulated in cells expressing the R273H mutant of p53. Importantly, the most significantly affected pathways included cell adhesion and ECM remodelling. Given the increased motility of these cells altered expression of cell adhesion and ECM remodelling regulating genes provides a plausible mechanism for the gain of function of this p53 mutant. In the light of recent studies suggesting that mutant p53 GOF may be achieved, at least in part, through inhibition of the tumour-suppressive effects of TAp63, it is important to note that the laryngeal cancer cells studied in this project appear to express predominantly the ΔNp63 isoform (suggested to have oncogenic functions) (525). This suggests that p63 inhibition by the p53-273H mutant is not central to its gain of oncogenic function in LSCC cells. Analysis of the transcriptional networks generated on the basis of the expression data also suggests that this p53 mutant might modulate transcription through other transcription factors, such as Sp1 and NF-κB.

Unexpectedly, mutant p53 expression seemed to sensitise laryngeal cancer cells to ionising radiation. The fact that tumour-derived mutant p53-expressing laryngeal cancer cells studied in our laboratory also exhibited increased radiosensitivity, suggests that the results presented here are not an artefact and require further study to gain insight into the mechanism of radiosensitivity of mutant p53-expressing LSCC cells.

In conclusion, the studies described here have identified several new lines of investigation connecting mutant p53 with critical pathways involved in the regulation of cell survival (HSP70) and in cell motility (FN1, TIMP2 and others), one of the key determinants of metastatic potential. These results together with increased radiosensitivity of mutant p53-expressing cells also suggest that in LSCC cells p53 GOF mutants may act via different pathways than those previously identified in other cancers and moreover it appears there may be differences in the modes of action of structural and DNA-contact mutants. Functional analysis of these pathways should provide insights into the mechanisms of action of two classes of p53 GOF mutants in LSCC and may lead also to the identification of novel therapeutic targets.

Chapter 6

Appendices

Appendix 1

Table 6.1: The list of genes differentially regulated in UM-SCC-12/high p53-273H, which were selected for qRT-PCR validation. Histone H3 was chosen as a housekeeping reference. The conditions used for amplification of the indicated targets for standard preparation and for qRT-PCR are indicated. (Primer design and optimisation of reaction conditions were performed by Dr Bryony Lloyd.)

Gene	Primer ID	Primer sequence	Hot start		Denature		Anneal and extend		No. of cycles
			Temperature	Time	Temperature	Time	Temperature	Time	
Cyclin D2	CCND2-F	ACCGCGGAGAAGCTGTGCATTT	95°C	3 min	95°C	30 s	65°C	45 s	40
	CCND2-R	ACAGCTGCCAGGTTCCACTTCAA							
Osteoglycin	OGN-F	TTACTGCGCACACCCTGCCAAA	95°C	3 min	95°C	30 s	65°C	45 s	40
	OGN-R	TAAACTAGTGGCCTGCTGACTGTGG							
Nephronectin	NPNT-F	GGCACAAGGTGACGGGGCTG	95°C	3 min	95°C	30 s	60°C	30 s	40
	NPNT-R	GCTCCGTGGGCACCGTGTTT							
Small proline-rich protein 2A	SPPR2A-F	ACCTCAGCAGTGCCAGCAGAAATA	95°C	3 min	95°C	30 s	64°C	30 s	40
	SPPR2A-R	AAGATGAAGGTGGAGCTGTGGAACGA							
Toll-like receptor 4	TLR4-F	ATGCTGCCGTTTTATCACGGAGGT	95°C	3 min	95°C	30 s	64°C	30 s	40
	TLR4-R	AAGCTCAGGTCCAGGTTCTTGGTT							
Matrix metallopeptidase 2	MMP2-F	ACTGCAAGTTCCCCTTCTTGT	95°C	3 min	95°C	30 s	57°C	30 s	40
	MMP2-R	CGTACTTGCCATCCTTCTCAA							
Tetraspanin 1	TSPAN1-F	ATGCAGTTTGTCAACGTGGGCT	95°C	3 min	95°C	30 s	50°C	30 s	46
	TSPAN1-R	ATGAAGAAGAACGTCACGAGGGCA							
S100 calcium binding protein A8	S100A8-F	ATCATGTTGACCGAGCTGGAGAAAGC	95°C	3 min	95°C	30 s	65°C	45 s	40
	S100A8-R	ACTGAGGACACTCGGTCTCTAGCAAT							
Chromosome 8 open reading frame 4	C8orf4-F	AAAGCGAAGCCACCAAGCCATCAT	95°C	3 min	95°C	30 s	50°C	30 s	40
	C8orf4-R	AGATGTTGCCCACGGCTTTCTT							
Fibronectin 1	FN1-F	ACATGGTTTTAGGCGGACCACACC	95°C	3 min	95°C	30 s	50°C	30 s	40
	FN1-R	ACATCTTCCCTGGGGATGTGACCA							
Prostaglandin E synthase	PTGES-F	TTCCCTTGCCGTTGGCTTTGGA	95°C	3 min	95°C	30 s	50°C	30 s	40
	PTGES-R	TGCCCTTTGGAGGGACTCAAACCT							
TIMP metallopeptidase inhibitor 2	TIMP2-F	TTCTGGCATCAGGCACCTGGATT	95°C	3 min	95°C	30 s	60°C	30 s	40
	TIMP2-R	ATGCTTAGCTGGCGTCACATGCA							
Histone H3	H3-F	CCACTGAACTTCTGATTCGC	95°C	3 min	95°C	30 s	64°C	30 s	40
	H3-R	GCGTGCTAGCTGGATGTCTT							

Appendix 2

The results of sequencing of p53 in pCMV-Script. The following primers were used for sequencing:

- CMVfor (5'-CGC AAA TGG GCG GTA GGC GTG-3') – available from Eurofins MWG Operon,
- p53.601-620 (5'-TTG CGT GTG GAG TAT TTG GA-3') – designed specifically for sequencing.

The obtained sequences were aligned to the reference sequence of p53 (accession number: NM_000546) using the AlignX® Module of Vector NTI Advance™ 11 (Invitrogen).

```
                    1                                                                 65
   p53 cDNA     (1) ----------------------------------------------------------------
     CMVfor     (1) TTAGCAGAGCTGGTTTAGTGAACCGTCAGATCCGCTAGCGATTACGCCAAGCTCGAAATTAACCC
p53.601-620     (1) ----------------------------------------------------------------

                   66                                                                130
   p53 cDNA     (1) ----------------------------------------------------------------A
     CMVfor    (66) TCACTAAAGGGAACAAAAGCTGGAGCTCCACCGCGGTGGCGGCCGCTCTAGCCCGGGCGGATCCA
p53.601-620     (1) ----------------------------------------------------------------

                  131                                                               195
   p53 cDNA     (2) TGGAGGAGCCGCAGTCAGATCCTAGCGTCGAGCCCCCTCTGAGTCAGGAAACATTTTCAGACCTA
     CMVfor   (131) TGGAGGAGCCGCAGTCAGATCCTAGCGTCGAGCCCCCTCTGAGTCAGGAAACATTTTCAGACCTA
p53.601-620     (1) ----------------------------------------------------------------

                  196                                                               260
   p53 cDNA    (67) TGGAAACTACTTCCTGAAAACAACGTTCTGTCCCCCTTGCCGTCCCAAGCAATGGATGATTTGAT
     CMVfor   (196) TGGAAACTACTTCCTGAAAACAACGTTCTGTCCCCCTTGCCGTCCCAAGCAATGGATGATTTGAT
p53.601-620     (1) ----------------------------------------------------------------

                  261                                                               325
   p53 cDNA   (132) GCTGTCCCCGGACGATATTGAACAATGGTTCACTGAAGACCCAGGTCCAGATGAAGCTCCCAGAA
     CMVfor   (261) GCTGTCCCCGGACGATATTGAACAATGGTTCACTGAAGACCCAGGTCCAGATGAAGCTCCCAGAA
p53.601-620     (1) ----------------------------------------------------------------
                                  SNP
                  326             72R                                               390
   p53 cDNA   (197) TGCCAGAGGCTGCTCCCCCCGTGGCCCCTGCACCAGCAGCTCCTACACCGGCGGCCCCTGCACCA
     CMVfor   (326) TGCCAGAGGCTGCTCCCCGCGTGGCCCCTGCACCAGCAGCTCCTACACCGGCGGCCCCTGCACCA
p53.601-620     (1) ----------------------------------------------------------------

                  391                                                               455
   p53 cDNA   (262) GCCCCCTCCTGGCCCCTGTCATCTTCTGTCCCTTCCCAGAAAACCTACCAGGGCAGCTACGGTTT
     CMVfor   (391) GCCCCCTCCTGGCCCCTGTCATCTTCTGTCCCTTCCCAGAAAACCTACCAGGGCAGCTACGGTTT
p53.601-620     (1) ----------------------------------------------------------------

                  456                                                               520
   p53 cDNA   (327) CCGTCTGGGCTTCTTGCATTCTGGGACAGCCAAGTCTGTGACTTGCACGTACTCCCCTGCCCTCA
     CMVfor   (456) CCGTCTGGGCTTCTTGCATTCTGGGACAGCCAAGTCTGTGACTTGCACGTACTCCCCTGCCCTCA
p53.601-620     (1) ----------------------------------------------------------------
```

```
                                                                  silent
                    521                                           mutation  585
   p53 cDNA   (392) ACAAGATGTTTTGCCAACTGGCCAAGACCTGCCCTGTGCAGCTGTGGGTTGATTCCACACCCCCG
     CMVfor   (521) ACAAGATGTTTTGCCAACTGGCCAAGACCTGCCCTGTGCAGCTGTGGGTTGATTCAACACCCCCG
p53.601-620     (1) ------------------------------------------------------------

                    586                                                       650
   p53 cDNA   (457) CCCGGCACCCGCGTCCGCGCCATGGCCATCTACAAGCAGTCACAGCACATGACGGAGGTTGTGAG
     CMVfor   (586) CCCGGCACCCGCGTCCGCGCCATGGCCATCTACAAGCAGTCACAGCACATGACGGAGGTTGTGAG
p53.601-620     (1) ------------------------------------------------------------

                    651                                                       715
   p53 cDNA   (522) GCGCTGCCCCCACCATGAGCGCTGCTCAGATAGCGATGGTCTGGCCCCTCCTCAGCATCTTATCC
     CMVfor   (651) GCGCTGCCCCCACCATGAGCGCTGCTCAGATAGCGATGGTCTGGCCCCTCCTCAGCATCTTATCC
p53.601-620     (1) ------------------------------------------------------------

                    716                                                       780
   p53 cDNA   (587) GAGTGGAAGGAAATTTGCGTGTGGAGTATTTGGATGACAGAAACACTTTTCGACATAGTGTGGTG
     CMVfor   (716) GAGTGGAAGGAAATTTGCGTGTGGAGTATTTGGATGACAGAAACACTTTTCGACATAGTGTGGTG
p53.601-620     (1) ----------------------------------------------TCG--ATAGTGTGGTG

                    781                                                       845
   p53 cDNA   (652) GTGCCCTATGAGCCGCCTGAGGTTGGCTCTGACTGTACCACCATCCACTACAACTACATGTGTAA
     CMVfor   (781) GTGCCCTATGAGCCGCCTGAGGTTGGCTCTGACTGTACCACCATCCACTACAACTACATGTGTAA
p53.601-620    (15) GTGCCCTATGAGCCGCCTGAGGTTGGCTCTGACTGTACCACCATCCACTACAACTACATGTGTAA

                    846                                                       910
   p53 cDNA   (717) CAGTTCCTGCATGGGCGGCATGAACCGGAGGCCCATCCTCACCATCATCACACTGGAAGACTCCA
     CMVfor   (846) CAGTTCCTGCATGGGCGGCATGAACCGGAGGCCCATCCTCACCATCATCACACTGGAAGACTCCA
p53.601-620    (80) CAGTTCCTGCATGGGCGGCATGAACCGGAGGCCCATCCTCACCATCATCACACTGGAAGACTCCA

                    911                                                       975
   p53 cDNA   (782) GTGGTAATCTACTGGGACGGAACAGCTTTGAGGTGCGTGTTTGTGCCTGTCCTGGGAGAGACCGG
     CMVfor   (911) GTGGTAATCTACTGGGACGGAACAGCTTTGAGGTGCGTGTTTGTGCCTGTCCTGGGAGAGACCGG
p53.601-620   (145) GTGGTAATCTACTGGGACGGAACAGCTTTGAGGTGCGTGTTTGTGCCTGTCCTGGGAGAGACCGG

                    976                                                      1040
   p53 cDNA   (847) CGCACAGAGGAAGAGAATCTCCGCAAGAAAGGGGAGCCTCACCACGAGCTGCCCCCAGGGAGCAC
     CMVfor   (976) CGCACAGAGGAAGAGAATCTCCGCAAGAAAGGGGAGCCTCACCACGAGCTGCCCCCAGGGAGCAC
p53.601-620   (210) CGCACAGAGGAAGAGAATCTCCGCAAGAAAGGGGAGCCTCACCACGAGCTGCCCCCAGGGAGCAC

                   1041                                                      1105
   p53 cDNA   (912) TAAGCGAGCACTGCCCAACAACACCAGCTCCTCTCCCCAGCCAAAGAAGAAACCACTGGATGGAG
     CMVfor  (1041) TAAGCGAGCACTGCCCA----------------------------------------------
p53.601-620   (275) TAAGCGAGCACTGCCCAACAACACCAGCTCCTCTCCCCAGCCAAAGAAGAAACCACTGGATGGAG

                   1106                                                      1170
   p53 cDNA   (977) AATATTTCACCCTTCAGATCCGTGGGCGTGAGCGCTTCGAGATGTTCCGAGAGCTGAATGAGGCC
     CMVfor  (1058) ------------------------------------------------------------
p53.601-620   (340) AATATTTCACCCTTCAGATCCGTGGGCGTGAGCGCTTCGAGATGTTCCGAGAGCTGAATGAGGCC

                   1171                                                      1235
   p53 cDNA  (1042) TTGGAACTCAAGGATGCCCAGGCTGGGAAGGAGCCAGGGGGGAGCAGGGCTCACTCCAGCCACCT
     CMVfor  (1058) ------------------------------------------------------------
p53.601-620   (405) TTGGAACTCAAGGATGCCCAGGCTGGGAAGGAGCCAGGGGGGAGCAGGGCTCACTCCAGCCACCT

                   1236                                                      1300
   p53 cDNA  (1107) GAAGTCCAAAAAGGGTCAGTCTACCTCCCGCCATAAAAAACTCATGTTCAAGACAGAAGGGCCTG
     CMVfor  (1058) ------------------------------------------------------------
p53.601-620   (470) GAAGTCCAAAAAGGGTCAGTCTACCTCCCGCCATAAAAAACTCATGTTCAAGACAGAAGGGCCTG

                   1301                                                      1365
   p53 cDNA  (1172) ACTCAGACTGA-----------------------------------------------------
     CMVfor  (1058) ------------------------------------------------------------
p53.601-620   (535) ACTCAGACTGAGAATTCGATATCAAGCTTATCGATACCGTCGACCTCGAGGGGGGGCCCGGTACC

                   1366                                                      1430
   p53 cDNA  (1183) ------------------------------------------------------------
     CMVfor  (1058) ------------------------------------------------------------
p53.601-620   (600) AGGTAAGTGTACCCAATTCGCCCTATAGTGAGTCGTATTACAATTCACTCGATCGCCCTTCCCAA

                   1431                                                      1495
   p53 cDNA  (1183) ------------------------------------------------------------
     CMVfor  (1058) ------------------------------------------------------------
p53.601-620   (665) CAGTTGCGCAGCCTGAATGGCGAATGGAGATCCAATTTTTAAGTGTATAATGTGTTAAACTACTG
```

```
                  1496                                                                1560
   p53 cDNA  (1183) ------------------------------------------------------------------
     CMVfor  (1058) ------------------------------------------------------------------
p53.601-620   (730) ATTCTAATTGTTTGTGTATTTTAGATTCACAGTCCCAAGGCTCATTTCAGGCCCCTCAGTCCTCA

                  1561                                                                1625
   p53 cDNA  (1183) ------------------------------------------------------------------
     CMVfor  (1058) ------------------------------------------------------------------
p53.601-620   (795) CAGTCTGTTCATGATCATAATCAGCCATACCACATTTGTAGAGGTTTTACTTGCTTTAAAAAACC

                  1626                                                                1690
   p53 cDNA  (1183) ------------------------------------------------------------------
     CMVfor  (1058) ------------------------------------------------------------------
p53.601-620   (860) TCCCACACCTCCCCCTGAACCTGAAACATAAAATGAATGCAATTGTTGTTGTTAACTTGTTTATT

                  1691                                                                1755
   p53 cDNA  (1183) ------------------------------------------------------------------
     CMVfor  (1058) ------------------------------------------------------------------
p53.601-620   (925) GCAGCTTATAATGGTTACAAATAAAGCAATAGCATCACAAATTTCACAAATAAAGCATTTTTTTC

                  1756                          1792
   p53 cDNA  (1183) ------------------------------------
     CMVfor  (1058) ------------------------------------
p53.601-620   (990) ACTGCATTCTAGTTGTGGTTTGTCCAAACTCATCAAT
```

Appendix 3

The results of sequencing of p53 in pNTAP-B. The following primers were used for sequencing:

- CMVfor (5'-CGC AAA TGG GCG GTA GGC GTG-3') – available from Eurofins MWG Operon,
- p53.601-620 (5'-TTG CGT GTG GAG TAT TTG GA-3') – designed specifically for sequencing.

The obtained sequences were aligned to the reference sequence of p53 (accession number: NM_000546) using the AlignX® Module of Vector NTI Advance™ 11 (Invitrogen).

```
                    1                                                        65
   p53 cDNA     (1) ------------------------------------------------------------
     CMVfor     (1) TATAGCAGAGCTGGTTTAGTGAACCGTCAGATCCGCTAGCGATTACGCCAAGCTCGAAATTAACC
p53.601-620     (1) ------------------------------------------------------------

                    66                                                      130
   p53 cDNA     (1) ------------------------------------------------------------
     CMVfor    (66) CTCACTAAAGGGAACAAAAGCTGGAGCTCCACCGCGGTGGCGGCCGCCACCATGAAGCGACGATG
p53.601-620     (1) ------------------------------------------------------------

                    131                         CBP                         195
   p53 cDNA     (1) ------------------------------------------------------------
     CMVfor   (131) GAAAAAGAATTTCATAGCCGTCTCAGCAGCCAACCGCTTTAAGAAAATCTCATCCTCCGGGGCAC
p53.601-620     (1) ------------------------------------------------------------

                    196                                                     260
   p53 cDNA     (1) ------------------------------------------------------------
     CMVfor   (196) TTGGAAGCGGTAGCGGTACCATGGACGAGAAGACCACCGGCTGGCGGGGCGGCCACGTGGTGGAG
p53.601-620     (1) ------------------------------------------------------------

                    261                         SBP                         325
   p53 cDNA     (1) ------------------------------------------------------------
     CMVfor   (261) GGCCTGGCCGGCGAGCTGGAGCAGCTGCGGGCCAGGCTGGAGCACCACCCTCAGGGCCAGCGGGA
p53.601-620     (1) ------------------------------------------------------------

                    326                                                     390
   p53 cDNA     (1) ----------------------------------------ATGGAGGAGCCGCAGTCAGATCCTA
     CMVfor   (326) GCCCTCCGGCGGCTGCAAGCTGGGCTGCCCGGGCGGATCCATGGAGGAGCCGCAGTCAGATCCTA
p53.601-620     (1) ------------------------------------------------------------

                    391                                                     455
   p53 cDNA    (26) GCGTCGAGCCCCCTCTGAGTCAGGAAACATTTTCAGACCTATGGAAACTACTTCCTGAAAACAAC
     CMVfor   (391) GCGTCGAGCCCCCTCTGAGTCAGGAAACATTTTCAGACCTATGGAAACTACTTCCTGAAAACAAC
p53.601-620     (1) ------------------------------------------------------------

                    456                                                     520
   p53 cDNA    (91) GTTCTGTCCCCCTTGCCGTCCCAAGCAATGGATGATTTGATGCTGTCCCCGGACGATATTGAACA
     CMVfor   (456) GTTCTGTCCCCCTTGCCGTCCCAAGCAATGGATGATTTGATGCTGTCCCCGGACGATATTGAACA
p53.601-620     (1) ------------------------------------------------------------
```

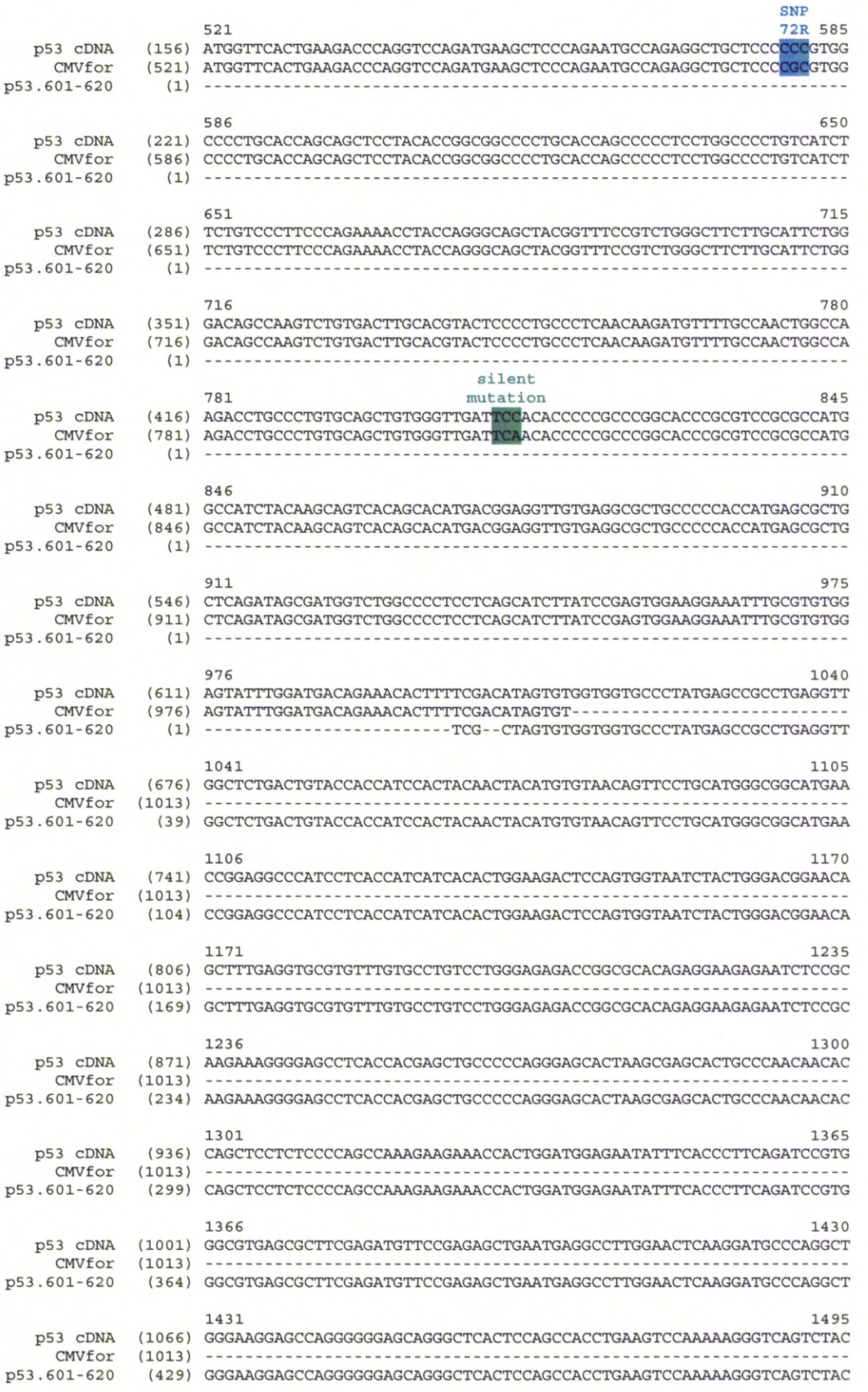
SNP
72R
silent
mutation
p53 cDNA
CMVfor
p53.601-620

```
                1496                                                                1560
   p53 cDNA  (1131) CTCCCGCCATAAAAAACTCATGTTCAAGACAGAAGGGCCTGACTCAGACTGA-------------
     CMVfor  (1013) ------------------------------------------------------------------
p53.601-620   (494) CTCCCGCCATAAAAAACTCATGTTCAAGACAGAAGGGCCTGACTCAGACTGAGAATTCGATATCA

                1561                                                                1625
   p53 cDNA  (1183) ------------------------------------------------------------------
     CMVfor  (1013) ------------------------------------------------------------------
p53.601-620   (559) AGCTTATCGATACCGTCGACCTCGAGGGGGGGCCCGGTACCTTAATTAATTAAGGTACCAGGTAA

                1626                                                                1690
   p53 cDNA  (1183) ------------------------------------------------------------------
     CMVfor  (1013) ------------------------------------------------------------------
p53.601-620   (624) GTGTACCCAATTCGCCCTATAGTGAGTCGTATTACAATTCACTCGATCGCCCTTCCCAACAGTTG

                1691                                                                1755
   p53 cDNA  (1183) ------------------------------------------------------------------
     CMVfor  (1013) ------------------------------------------------------------------
p53.601-620   (689) CGCAGCCTGAATGGCGAATGGAGATCCAATTTTTAAGTGTATAATGTGTTAAACTACTGATTCTA

                1756                                                                1820
   p53 cDNA  (1183) ------------------------------------------------------------------
     CMVfor  (1013) ------------------------------------------------------------------
p53.601-620   (754) ATTGTTTGTGTATTTTAGATTCACAGTCCCAAGGCTCATTTCAGGCCCCTCAGTCCTCACAGTCT

                1821                                                                1885
   p53 cDNA  (1183) ------------------------------------------------------------------
     CMVfor  (1013) ------------------------------------------------------------------
p53.601-620   (819) GTTCATGATCATAATCAGCCATACCACATTTGTAGAGGTTTTACTTGCTTTAAAAAACCTCCCAC

                1886                                                                1950
   p53 cDNA  (1183) ------------------------------------------------------------------
     CMVfor  (1013) ------------------------------------------------------------------
p53.601-620   (884) ACCTCCCCCTGAACCTGAAACATAAAATGAATGCAATTGTTGTTGTTAACTTGTTTATTGCAGCT

                1951                                                                2015
   p53 cDNA  (1183) ------------------------------------------------------------------
     CMVfor  (1013) ------------------------------------------------------------------
p53.601-620   (949) TATAATGGTTACAAATAAAGCAATAGCATCACAAATTTCACAAATAAAGCATTTTTTCACTGCAT

                2016                            2051
   p53 cDNA  (1183) -----------------------------------
     CMVfor  (1013) -----------------------------------
p53.601-620  (1014) TCTAGTTGTGGTTTGTCCAAACTCATCATGTATCTA
```

Appendix 4

The results of sequencing of p53-175H in pCB6+. The following primers were used for sequencing:

- CMVfor (5'-CGC AAA TGG GCG GTA GGC GTG-3') – available from Eurofins MWG Operon,
- p53.601-620 (5'-TTG CGT GTG GAG TAT TTG GA-3') – designed specifically for sequencing.

The obtained sequences were aligned to the reference sequence of p53 (accession number: NM_000546) using the AlignX® Module of Vector NTI Advance™ 11 (Invitrogen).

```
                    1                                                        65
   p53 cDNA     (1) ------------------------------------------------------------
     CMVfor     (1) ATAGCAGAGCTCGTTTAGTGAACCGTCAGAATTAATTCAGATCTGAATTCGAGCTCGCCCGGGGA
p53.601-620     (1) ------------------------------------------------------------

                    66                                                      130
   p53 cDNA     (1) ------------------------------------------------------------
     CMVfor    (66) TCCCGCTAGAGCCACCGTCCAGGGAGCAGGTAGCTGCTGGGCTCCGGGGACACTTTGCGTTCGGG
p53.601-620     (1) ------------------------------------------------------------

                   131                                                      195
   p53 cDNA     (1) ------------------------------------------------------------
     CMVfor   (131) CTGGGAGCGTGCTTTCCACGACGGTGACACGCTTCCCTGGATTGGCAGCCAGACTGCCTTCCGGG
p53.601-620     (1) ------------------------------------------------------------

                   196                                                      260
   p53 cDNA     (1) --------ATGGAGGAGCCGCAGTCAGATCCTAGCGTCGAGCCCCCTCTGAGTCAGGAAACATTT
     CMVfor   (196) TCACTGCCATGGAGGAGCCGCAGTCAGATCCTAGCGTCGAGCCCCCTCTGAGTCAGGAAACATTT
p53.601-620     (1) ------------------------------------------------------------

                   261                                                      325
   p53 cDNA    (58) TCAGACCTATGGAAACTACTTCCTGAAAACAACGTTCTGTCCCCCTTGCCGTCCCAAGCAATGGA
     CMVfor   (261) TCAGACCTATGGAAACTACTTCCTGAAAACAACGTTCTGTCCCCCTTGCCGTCCCAAGCAATGGA
p53.601-620     (1) ------------------------------------------------------------

                   326                                                      390
   p53 cDNA   (123) TGATTTGATGCTGTCCCCGGACGATATTGAACAATGGTTCACTGAAGACCCAGGTCCAGATGAAG
     CMVfor   (326) TGATTTGATGCTGTCCCCGGACGATATTGAACAATGGTTCACTGAAGACCCAGGTCCAGATGAAG
p53.601-620     (1) ------------------------------------------------------------
                                       SNP
                   391                 72P                                  455
   p53 cDNA   (188) CTCCCAGAATGCCAGAGGCTGCTCCCCCCGTGGCCCCTGCACCAGCAGCTCCTACACCGGCGGCC
     CMVfor   (391) CTCCCAGAATGCCAGAGGCTGCTCCCCCCGTGGCCCCTGCACCAGCAGCTCCTACACCGGCGGCC
p53.601-620     (1) ------------------------------------------------------------

                   456                                                      520
   p53 cDNA   (253) CCTGCACCAGCCCCCTCCTGGCCCCTGTCATCTTCTGTCCCTTCCCAGAAAACCTACCAGGGCAG
     CMVfor   (456) CCTGCACCAGCCCCCTCCTGGCCCCTGTCATCTTCTGTCCCTTCCCAGAAAACCTACCAGGGCAG
p53.601-620     (1) ------------------------------------------------------------
```

```
                    521                                                                585
   p53 cDNA    (318) CTACGGTTTCCGTCTGGGCTTCTTGCATTCTGGGACAGCCAAGTCTGTGACTTGCACGTACTCCC
     CMVfor    (521) CTACGGTTTCCGTCTGGGCTTCTTGCATTCTGGGACAGCCAAGTCTGTGACTTGCACGTACTCCC
p53.601-620      (1) ------------------------------------------------------------------

                    586                                                                650
   p53 cDNA    (383) CTGCCCTCAACAAGATGTTTTGCCAACTGGCCAAGACCTGCCCTGTGCAGCTGTGGGTTGATTCC
     CMVfor    (586) CTGCCCTCAACAAGATGTTTTGCCAACTGGCCAAGACCTGCCCTGTGCAGCTGTGGGTTGATTCC
p53.601-620      (1) ------------------------------------------------------------------

                    651                                                                715
   p53 cDNA    (448) ACACCCCCGCCCGGCACCCGCGTCCGCGCCATGGCCATCTACAAGCAGTCACAGCACATGACGGA
     CMVfor    (651) ACACCCCCGCCCGGCACCCGCGTCCGCGCCATGGCCATCTACAAGCAGTCACAGCACATGACGGA
p53.601-620      (1) ------------------------------------------------------------------

                    716       R175H                                                    780
   p53 cDNA    (513) GGTTGTGAGGCGCTGCCCCCACCATGAGCGCTGCTCAGATAGCGATGGTCTGGCCCCTCCTCAGC
     CMVfor    (716) GGTTGTGAGGCACTGCCCCCACCATGAGCGCTGCTCAGATAGCGATGGTCTGGCCCCTCCTCAGC
p53.601-620      (1) ------------------------------------------------------------------

                    781                                                                845
   p53 cDNA    (578) ATCTTATCCGAGTGGAAGGAAATTTGCGTGTGGAGTATTTGGATGACAGAAACACTTTTCGACAT
     CMVfor    (781) ATCTTATCCGAGTGGAAGGAAATTTGCGTGTGGAGTATTTGGATGACAGAAACACTTTTCGACAT
p53.601-620      (1) ----------------------------------------------------------------AAT

                    846                                                                910
   p53 cDNA    (643) AGTGTGGTGGTGCCCTATGAGCCGCCTGAGGTTGGCTCTGACTGTACCACCATCCACTACAACTA
     CMVfor    (846) AGTGTGGTGGTGCCCTATGAGCCGCCTGAGGTTGGCTCTGACTGTACCACCATCCACTACAACTA
p53.601-620      (4) AGTGTGGTGGTGCCCTATGAGCCGCCTGAGGTTGGCTCTGACTGTACCACCATCCACTACAACTA

                    911                                                                975
   p53 cDNA    (708) CATGTGTAACAGTTCCTGCATGGGCGGCATGAACCGGAGGCCCATCCTCACCATCATCACACTGG
     CMVfor    (911) CATGTGTAACAGTTCCTGCATGGGCGGCATGAACCGGAGGCCCATCCTCACCATCATCACACTGG
p53.601-620     (69) CATGTGTAACAGTTCCTGCATGGGCGGCATGAACCGGAGGCCCATCCTCACCATCATCACACTGG

                    976                                                               1040
   p53 cDNA    (773) AAGACTCCAGTGGTAATCTACTGGGACGGAACAGCTTTGAGGTGCGTGTTTGTGCCTGTCCTGGG
     CMVfor    (976) A-GACTCCAGTGGTA-TCTACTGGA----------------------------------------
p53.601-620    (134) AAGACTCCAGTGGTAATCTACTGGGACGGAACAGCTTTGAGGTGCGTGTTTGTGCCTGTCCTGGG

                   1041                                                               1105
   p53 cDNA    (838) AGAGACCGGCGCACAGAGGAAGAGAATCTCCGCAAGAAAGGGGAGCCTCACCACGAGCTGCCCCC
     CMVfor    (999) ------------------------------------------------------------------
p53.601-620    (199) AGAGACCGGCGCACAGAGGAAGAGAATCTCCGCAAGAAAGGGGAGCCTCACCACGAGCTGCCCCC

                   1106                                                               1170
   p53 cDNA    (903) AGGGAGCACTAAGCGAGCACTGCCCAACAACACCAGCTCCTCTCCCCAGCCAAAGAAGAAACCAC
     CMVfor    (999) ------------------------------------------------------------------
p53.601-620    (264) AGGGAGCACTAAGCGAGCACTGCCCAACAACACCAGCTCCTCTCCCCAGCCAAAGAAGAAACCAC

                   1171                                                               1235
   p53 cDNA    (968) TGGATGGAGAATATTTCACCCTTCAGATCCGTGGGCGTGAGCGCTTCGAGATGTTCCGAGAGCTG
     CMVfor    (999) ------------------------------------------------------------------
p53.601-620    (329) TGGATGGAGAATATTTCACCCTTCAGATCCGTGGGCGTGAGCGCTTCGAGATGTTCCGAGAGCTG

                   1236                                                               1300
   p53 cDNA   (1033) AATGAGGCCTTGGAACTCAAGGATGCCCAGGCTGGGAAGGAGCCAGGGGGGAGCAGGGCTCACTC
     CMVfor    (999) ------------------------------------------------------------------
p53.601-620    (394) AATGAGGCCTTGGAACTCAAGGATGCCCAGGCTGGGAAGGAGCCAGGGGGGAGCAGGGCTCACTC

                   1301                                                               1365
   p53 cDNA   (1098) CAGCCACCTGAAGTCCAAAAAGGGTCAGTCTACCTCCCGCCATAAAAAACTCATGTTCAAGACAG
     CMVfor    (999) ------------------------------------------------------------------
p53.601-620    (459) CAGCCACCTGAAGTCCAAAAAGGGTCAGTCTACCTCCCGCCATAAAAAACTCATGTTCAAGACAG

                   1366                                                               1430
   p53 cDNA   (1163) AAGGGCCTGACTCAGACTGA--------------------------------------------------
     CMVfor    (999) ------------------------------------------------------------------
p53.601-620    (524) AAGGGCCTGACTCAGACTGACATTCTCCACTTCTTGTTCCCCACTGACAGCCTCCCACCCCCATC

                   1431                                                               1495
   p53 cDNA   (1183) ------------------------------------------------------------------
     CMVfor    (999) ------------------------------------------------------------------
p53.601-620    (589) TCTCCCTCCCCTGCCATTTTGGGTTTTGGGTCTTTGAACCCTTGCTTGCAATAGGTGTGCGTCAG
```

```
                    1496                                                                1560
   p53 cDNA  (1183) ------------------------------------------------------------------------
     CMVfor   (999) ------------------------------------------------------------------------
p53.601-620   (654) AAGCACCCAGGACTTCCATTTGCTTTGTCCCGGGGCTCCACTGAACAAGTTGGCCTGCACTGGTG

                    1561                                                                1625
   p53 cDNA  (1183) ------------------------------------------------------------------------
     CMVfor   (999) ------------------------------------------------------------------------
p53.601-620   (719) TTTTGTTGTGGGGAGGAGGATGGGGAGTAGGACATACCAGCTTAGATTTTAAGGTTTTTACTGTG

                    1626                                                                1690
   p53 cDNA  (1183) ------------------------------------------------------------------------
     CMVfor   (999) ------------------------------------------------------------------------
p53.601-620   (784) AGGGATGTTTGGGAGATGTAAGAAATGTTCTTGCAGTTAAGGGTTAGTTTACAATCAGCCACATT

                    1691
   p53 cDNA  (1183) --------
     CMVfor   (999) --------
p53.601-620   (849) CTACGTAG
```

Appendix 5

The results of sequencing of p53-175H in pCR2.1. The following primers were used for sequencing:

- M13 uni (-21) (5'-TGT AAA ACG ACG GCC AGT-3') – available from Eurofins MWG Operon,
- M13 rev (-29) (5'-CAG GAA ACA GCT ATG ACC-3') – available from Eurofins MWG Operon.

The obtained sequences were aligned to the reference sequence of p53 (accession number: NM_000546) for M13 uni (-21) or to the reverse complement (rc) of this sequence for M13 rev (-29) using the AlignX® Module of Vector NTI Advance™ 11 (Invitrogen).

```
                      1                                                    64
     p53 cDNA     (1) ------------------------------------------------------------
M13 uni (-20)     (1) TAGGGCGATTGGGCCCTCTAGATGCATGCTCGAGCGGCCGCCAGTGTGATGGATATCTGCAGAA

                     65                                                   128
     p53 cDNA     (1) ------------------ATGGAGGAGCCGCAGTCAGATCCTAGCGTCGAGCCCCCTCTGAGTC
M13 uni (-20)    (65) TTCGGCTTGAGAGGATCCATGGAGGAGCCGCAGTCAGATCCTAGCGTCGAGCCCCCTCTGAGTC

                    129                                                   192
     p53 cDNA     (47) AGGAAACATTTTCAGACCTATGGAAACTACTTCCTGAAAACAACGTTCTGTCCCCCTTGCCGTC
M13 uni (-20)    (129) AGGAAACATTTTCAGACCTATGGAAACTACTTCCTGAAAACAACGTTCTGTCCCCCTTGCCGTC

                    193                                                   256
     p53 cDNA    (111) CCAAGCAATGGATGATTTGATGCTGTCCCCGGACGATATTGAACAATGGTTCACTGAAGACCCA
M13 uni (-20)    (193) CCAAGCAATGGATGATTTGATGCTGTCCCCGGACGATATTGAACAATGGTTCACTGAAGACCCA
                                                      SNP
                    257                               72P                 320
     p53 cDNA    (175) GGTCCAGATGAAGCTCCCAGAATGCCAGAGGCTGCTCCCCCCGTGGCCCCTGCACCAGCAGCTC
M13 uni (-20)    (257) GGTCCAGATGAAGCTCCCAGAATGCCAGAGGCTGCTCCCCCCGTGGCCCCTGCACCAGCAGCTC

                    321                                                   384
     p53 cDNA    (239) CTACACCGGCGGCCCCTGCACCAGCCCCCTCCTGGCCCCTGTCATCTTCTGTCCCTTCCCAGAA
M13 uni (-20)    (321) CTACACCGGCGGCCCCTGCACCAGCCCCCTCCTGGCCCCTGTCATCTTCTGTCCCTTCCCAGAA

                    385                                                   448
     p53 cDNA    (303) AACCTACCAGGGCAGCTACGGTTTCCGTCTGGGCTTCTTGCATTCTGGGACAGCCAAGTCTGTG
M13 uni (-20)    (385) AACCTACCAGGGCAGCTACGGTTTCCGTCTGGGCTTCTTGCATTCTGGGACAGCCAAGTCTGTG

                    449                                                   512
     p53 cDNA    (367) ACTTGCACGTACTCCCCTGCCCTCAACAAGATGTTTTGCCAACTGGCCAAGACCTGCCCTGTGC
M13 uni (-20)    (449) ACTTGCACGTACTCCCCTGCCCTCAACAAGATGTTTTGCCAACTGGCCAAGACCTGCCCTGTGC

                    513                                                   576
     p53 cDNA    (431) AGCTGTGGGTTGATTCCACACCCCCGCCCGGCACCCGCGTCCGCGCCATGGCCATCTACAAGCA
M13 uni (-20)    (513) AGCTGTGGGTTGATTCCACACCCCCGCCCGGCACCCGCGTCCGCGCCATGGCCATCTACAAGCA
                                        SNP
                    577                 R175H                             640
     p53 cDNA    (495) GTCACAGCACATGACGGAGGTTGTGAGGCGCTGCCCCCACCATGAGCGCTGCTCAGATAGCGAT
M13 uni (-20)    (577) GTCACAGCACATGACGGAGGTTGTGAGGCACTGCCCCCACCATGAGCGCTGCTCAGATAGCGAT
```

```
                    641                                                                 704
     p53 cDNA     (559) GGTCTGGCCCCTCCTCAGCATCTTATCCGAGTGGAAGGAAATTTGCGTGTGGAGTATTTGGATG
M13 uni (-20)     (641) GGTCTGGCCCCTCCTCAGCATCTTATCCGAGTGGAAGGAAATTTGCGTGTGGAGTATTTGGATG

                    705                                                                 768
     p53 cDNA     (623) ACAGAAACACTTTTCGACATAGTGTGGTGGTGCCCTATGAGCCGCCTGAGGTTGGCTCTGACTG
M13 uni (-20)     (705) ACAGAAACACTTTTCGACATAGTGTGGTGGTGCCCTATGAGCCGCCTGAGGTTGGCTCTGACTG

                    769                                                                 832
     p53 cDNA     (687) TACCACCATCCACTACAACTACATGTGTAACAGTTCCTGCATGGGCGGCATGAACCGGAGGCCC
M13 uni (-20)     (769) TACCACCATCCACTACAACTACATGTGTAACAGTTCCTGCATGGGCGGCATGAACCGGAGGCCC

                    833                                                                 896
     p53 cDNA     (751) ATCCTCACCATCATCACACTGGAAGACTCCAGTGGTAATCTACTGGGACGGAACAGCTTTGAGG
M13 uni (-20)     (833) ATCCTCACCATCATCACACTGGAAGACTCCAGTGGTAATCTACTGGGACGGAACAGCTTTGAGG

                    897                                                                 960
     p53 cDNA     (815) TGCGTGTTTGTGCCTGTCCTGGGAGAGACCGGCGCACAGAGGAAGAGAATCTCCGCAAGAAAGG
M13 uni (-20)     (897) TGCGTGTTTGTGCCTGTCCTGGGAGAGACCGGCGCACAGAGGAAGAGAATCTCCGCAAGAAAGG

                    961                                                                1024
     p53 cDNA     (879) GGAGCCTCACCACGAGCTGCCCCCAGGGAGCACTAAGCGAGCACTGCCCAACAACACCAGCTCC
M13 uni (-20)     (961) G-AGCCTCACCACGAGCTGCCCCCAGGGAGCACTAAGCGAGCACTGCCCAACA-CACCAGCTCC

                   1025                                                                1088
     p53 cDNA     (943) TCTCCCCAGCCAAAGAAGAAACCACTGGATGGAGAATATTTCACCCTTCAGATCCGTGGGCGTG
M13 uni (-20)    (1023) TCTCCC-AGCCAAAGA-GAAACCACTG-----------------------------------

                   1089                                                                1152
     p53 cDNA     (1007) AGCGCTTCGAGATGTTCCGAGAGCTGAATGAGGCCTTGGAACTCAAGGATGCCCAGGCTGGGAA
M13 uni (-20)    (1048) ------------------------------------------------------------

                   1153                                                                1216
     p53 cDNA     (1071) GGAGCCAGGGGGGAGCAGGGCTCACTCCAGCCACCTGAAGTCCAAAAAGGGTCAGTCTACCTCC
M13 uni (-20)    (1048) ------------------------------------------------------------

                   1217                                  1264
     p53 cDNA     (1135) CGCCATAAAAAACTCATGTTCAAGACAGAAGGGCCTGACTCAGACTGA
M13 uni (-20)    (1048) ----------------------------------------------
```

```
                      1                                                          64
  p53 cDNA rc       (1) ----------------------------------------------------------TCAGTCTGAGTC
M13 rev (-29)       (1) CGGATCACTAGTAACGGCCGCCAGTGTGCTGGAATTCGGCTTGAGAGAATTCTCAGTCTGAGTC

                     65                                                          128
  p53 cDNA rc      (13) AGGCCCTTCTGTCTTGAACATGAGTTTTTTATGGCGGGAGGTAGACTGACCCTTTTTGGACTTC
M13 rev (-29)      (65) AGGCCCTTCTGTCTTGAACATGAGTTTTTTATGGCGGGAGGTAGACTGACCCTTTTTGGACTTC

                    129                                                          192
  p53 cDNA rc      (77) AGGTGGCTGGAGTGAGCCCTGCTCCCCCCTGGCTCCTTCCCAGCCTGGGCATCCTTGAGTTCCA
M13 rev (-29)     (129) AGGTGGCTGGAGTGAGCCCTGCTCCCCCCTGGCTCCTTCCCAGCCTGGGCATCCTTGAGTTCCA

                    193                                                          256
  p53 cDNA rc     (141) AGGCCTCATTCAGCTCTCGGAACATCTCGAAGCGCTCACGCCCACGGATCTGAAGGGTGAAATA
M13 rev (-29)     (193) AGGCCTCATTCAGCTCTCGGAACATCTCGAAGCGCTCACGCCCACGGATCTGAAGGGTGAAATA

                    257                                                          320
  p53 cDNA rc     (205) TTCTCCATCCAGTGGTTTCTTCTTTGGCTGGGGAGAGGAGCTGGTGTTGTTGGGCAGTGCTCGC
M13 rev (-29)     (257) TTCTCCATCCAGTGGTTTCTTCTTTGGCTGGGGAGAGGAGCTGGTGTTGTTGGGCAGTGCTCGC

                    321                                                          384
  p53 cDNA rc     (269) TTAGTGCTCCCTGGGGGCAGCTCGTGGTGAGGCTCCCCTTTCTTGCGGAGATTCTCTTCCTCTG
M13 rev (-29)     (321) TTAGTGCTCCCTGGGGGCAGCTCGTGGTGAGGCTCCCCTTTCTTGCGGAGATTCTCTTCCTCTG

                    385                                                          448
  p53 cDNA rc     (333) TGCGCCGGTCTCTCCCAGGACAGGCACAAACACGCACCTCAAAGCTGTTCCGTCCCAGTAGATT
M13 rev (-29)     (385) TGCGCCGGTCTCTCCCAGGACAGGCACAAACACGCACCTCAAAGCTGTTCCGTCCCAGTAGATT

                    449                                                          512
  p53 cDNA rc     (397) ACCACTGGAGTCTTCCAGTGTGATGATGGTGAGGATGGGCCTCCGGTTCATGCCGCCCATGCAG
M13 rev (-29)     (449) ACCACTGGAGTCTTCCAGTGTGATGATGGTGAGGATGGGCCTCCGGTTCATGCCGCCCATGCAG

                    513                                                          576
  p53 cDNA rc     (461) GAACTGTTACACATGTAGTTGTAGTGGATGGTGGTACAGTCAGAGCCAACCTCAGGCGGCTCAT
M13 rev (-29)     (513) GAACTGTTACACATGTAGTTGTAGTGGATGGTGGTACAGTCAGAGCCAACCTCAGGCGGCTCAT
```

```
                      577                                                                 640
  p53 cDNA rc    (525) AGGGCACCACCACACTATGTCGAAAAGTGTTTCTGTCATCCAAATACTCCACACGCAAATTTCC
M13 rev (-29)    (577) AGGGCACCACCACACTATGTCGAAAAGTGTTTCTGTCATCCAAATACTCCACACGCAAATTTCC

                      641                                                                 704
  p53 cDNA rc    (589) TTCCACTCGGATAAGATGCTGAGGAGGGGCCAGACCATCGCTATCTGAGCAGCGCTCATGGTGG
M13 rev (-29)    (641) TTCCACTCGGATAAGATGCTGAGGAGGGGCCAGACCATCGCTATCTGAGCAGCGCTCATGGTGG

                      705 R175H                                                           768
  p53 cDNA rc    (653) GGGCAGCGCCTCACAACCTCCGTCATGTGCTGTGACTGCTTGTAGATGGCCATGGCGCGGACGC
M13 rev (-29)    (705) GGGCAGTGCCTCACAACCTCCGTCATGTGCTGTGACTGCTTGTAGATGGCCATGGCGCGGACGC

                      769                                                                 832
  p53 cDNA rc    (717) GGGTGCCGGGCGGGGGTGTGGAATCAACCCACAGCTGCACAGGGCAGGTCTTGGCCAGTTGGCA
M13 rev (-29)    (769) GGGTGCCGGGCGGGGGTGTGGAATCAACCCACAGCTGCACAGGGCAGGTCTTGGCCAGTTGGCA

                      833                                                                 896
  p53 cDNA rc    (781) AAACATCTTGTTGAGGGCAGGGGAGTACGTGCAAGTCACAGACTTGGCTGTCCCAGAATGCAAG
M13 rev (-29)    (833) AAACATCTTGTTGAGGGCAGGGGAGTACGTGCAAGTCACAGACTTGGCTGTCCCAGAATGCAAG

                      897                                                                 960
  p53 cDNA rc    (845) AAGCCCAGACGGAAACCGTAGCTGCCCTGGTAGGTTTTCTGGGAAGGGACAGAAGATGACAGGG
M13 rev (-29)    (897) AAGCCCAGACGGAAACCGTAGCTGCCCTGGTAG------------------------------

                      961                                                                1024
  p53 cDNA rc    (909) GCCAGGAGGGGGCTGGTGCAGGGGCCGCCGGTGTAGGAGCTGCTGGTGCAGGGGCCACGGGGGG
M13 rev (-29)    (930) ------------------------------------------------------------------

                     1025                                                                1088
  p53 cDNA rc    (973) AGCAGCCTCTGGCATTCTGGGAGCTTCATCTGGACCTGGGTCTTCAGTGAACCATTGTTCAATA
M13 rev (-29)    (930) ------------------------------------------------------------------

                     1089                                                                1152
  p53 cDNA rc   (1037) TCGTCCGGGGACAGCATCAAATCATCCATTGCTTGGGACGGCAAGGGGGACAGAACGTTGTTTT
M13 rev (-29)    (930) ------------------------------------------------------------------

                     1153                                                                1216
  p53 cDNA rc   (1101) CAGGAAGTAGTTTCCATAGGTCTGAAAATGTTTCCTGACTCAGAGGGGGCTCGACGCTAGGATC
M13 rev (-29)    (930) ------------------------------------------------------------------

                     1217          1234
  p53 cDNA rc   (1165) TGACTGCGGCTCCTCCAT
M13 rev (-29)    (930) ------------------
```

Appendix 6

The results of sequencing of p53-175H in pNTAP-B. The following primers were used for sequencing:

- CMVfor (5'-CGC AAA TGG GCG GTA GGC GTG-3') – available from Eurofins MWG Operon,
- p53.601-620 (5'-TTG CGT GTG GAG TAT TTG GA-3') – designed specifically for sequencing.

The obtained sequences were aligned to the reference sequence of p53 (accession number: NM_000546) using the AlignX® Module of Vector NTI Advance™ 11 (Invitrogen).

```
                    1                                                        65
   p53 cDNA     (1) ------------------------------------------------------------
     CMVfor     (1) ATAGCAGAGCTGGTTTAGTGACCGTCAGATCCGCTAGCGATTACGCCAAGCTCGAAATTAACCCT
p53.601-620     (1) ------------------------------------------------------------

                   66                                                       130
   p53 cDNA     (1) ------------------------------------------------------------
     CMVfor    (66) CACTAAAGGGAACAAAAGCTGGAGCTCCACCGCGGTGGCGGCCGCCACCATGAAGCGACCGATGGA
p53.601-620     (1) ------------------------------------------------------------

                  131                          CBP                       195
   p53 cDNA     (1) ------------------------------------------------------------
     CMVfor   (131) AAAAGAATTTCATAGCCGTCTCAGCAGCCAACCGCTTTAAGAAAATCTCATCCTCCGGGGCACTT
p53.601-620     (1) ------------------------------------------------------------

                  196                                                       260
   p53 cDNA     (1) ------------------------------------------------------------
     CMVfor   (196) GGAAGCGGTAGCGGTACCATGGACGAGAAGACCACCGGCTGGCGGGGCGGCCACGTGGTGGAGGG
p53.601-620     (1) ------------------------------------------------------------

                  261                          SBP                       325
   p53 cDNA     (1) ------------------------------------------------------------
     CMVfor   (261) CCTGGCCGGCGAGCTGGAGCAGCTGCGGGCCAGGCTGGAGCACCACCCTCAGGGCCAGCGGGAGC
p53.601-620     (1) ------------------------------------------------------------

                  326                                                       390
   p53 cDNA     (1) ----------------------------------------ATGGAGGAGCCGCAGTCAGATCCTAGC
     CMVfor   (326) CCTCCGGCGGCTGCAAGCTGGGCTGCCCGGGCGGATCCATGGAGGAGCCGCAGTCAGATCCTAGC
p53.601-620     (1) ------------------------------------------------------------

                  391                                                       455
   p53 cDNA    (28) GTCGAGCCCCCTCTGAGTCAGGAAACATTTTCAGACCTATGGAAACTACTTCCTGAAAACAACGT
     CMVfor   (391) GTCGAGCCCCCTCTGAGTCAGGAAACATTTTCAGACCTATGGAAACTACTTCCTGAAAACAACGT
p53.601-620     (1) ------------------------------------------------------------

                  456                                                       520
   p53 cDNA    (93) TCTGTCCCCCTTGCCGTCCCAAGCAATGGATGATTTGATGCTGTCCCCGGACGATATTGAACAAT
     CMVfor   (456) TCTGTCCCCCTTGCCGTCCCAAGCAATGGATGATTTGATGCTGTCCCCGGACGATATTGAACAAT
p53.601-620     (1) ------------------------------------------------------------
```

```
                                                                                                SNP
                                                                                                72P
                        521                                                                             585
   p53 cDNA    (158) GGTTCACTGAAGACCCAGGTCCAGATGAAGCTCCCAGAATGCCAGAGGCTGCTCCCCCCGTGGCC
     CMVfor    (521) GGTTCACTGAAGACCCAGGTCCAGATGAAGCTCCCAGAATGCCAGAGGCTGCTCCCCCCGTGGCC
p53.601-620      (1) ------------------------------------------------------------------

                        586                                                                             650
   p53 cDNA    (223) CCTGCACCAGCAGCTCCTACACCGGCGGCCCCTGCACCAGCCCCCTCCTGGCCCCTGTCATCTTC
     CMVfor    (586) CCTGCACCAGCAGCTCCTACACCGGCGGCCCCTGCACCAGCCCCCTCCTGGCCCCTGTCATCTTC
p53.601-620      (1) ------------------------------------------------------------------

                        651                                                                             715
   p53 cDNA    (288) TGTCCCTTCCCAGAAAACCTACCAGGGCAGCTACGGTTTCCGTCTGGGCTTCTTGCATTCTGGGA
     CMVfor    (651) TGTCCCTTCCCAGAAAACCTACCAGGGCAGCTACGGTTTCCGTCTGGGCTTCTTGCATTCTGGGA
p53.601-620      (1) ------------------------------------------------------------------

                        716                                                                             780
   p53 cDNA    (353) CAGCCAAGTCTGTGACTTGCACGTACTCCCCTGCCCTCAACAAGATGTTTTGCCAACTGGCCAAG
     CMVfor    (716) CAGCCAAGTCTGTGACTTGCACGTACTCCCCTGCCCTCAACAAGATGTTTTGCCAACTGGCCAAG
p53.601-620      (1) ------------------------------------------------------------------

                        781                                                                             845
   p53 cDNA    (418) ACCTGCCCTGTGCAGCTGTGGGTTGATTCCACACCCCCGCCCGGCACCCGCGTCCGCGCCATGGC
     CMVfor    (781) ACCTGCCCTGTGCAGCTGTGGGTTGATTCCACACCCCCGCCCGGCACCCGCGTCCGCGCCATGGC
p53.601-620      (1) ------------------------------------------------------------------

                        846                                                R175H        910
   p53 cDNA    (483) CATCTACAAGCAGTCACAGCACATGACGGAGGTTGTGAGGCGCTGCCCCCACCATGAGCGCTGCT
     CMVfor    (846) CATCTACAAGCAGTCACAGCACATGACGGAGGTTGTGAGGCACTGCCCCCACCATGAGCGCTGCT
p53.601-620      (1) ------------------------------------------------------------------

                        911                                                                             975
   p53 cDNA    (548) CAGATAGCGATGGTCTGGCCCCTCCTCAGCATCTTATCCGAGTGGAAGGAAATTTGCGTGTGGAG
     CMVfor    (911) CAGATAGCGATGGTCTGGCCCCTCCTCAGCATCTTATCCGAGTGGAAGG----------------
p53.601-620      (1) ------------------------------------------------------------------

                        976                                                                            1040
   p53 cDNA    (613) TATTTGGATGACAGAAACACTTTTCGACATAGTGTGGTGGTGCCCTATGAGCCGCCTGAGGTTGG
     CMVfor    (960) ------------------------------------------------------------------
p53.601-620      (1) ----------------------TCGC--TAGTGTGGTGGTGCCCTATGAGCCGCCTGAGGTTGG

                       1041                                                                            1105
   p53 cDNA    (678) CTCTGACTGTACCACCATCCACTACAACTACATGTGTAACAGTTCCTGCATGGGCGGCATGAACC
     CMVfor    (960) ------------------------------------------------------------------
p53.601-620     (41) CTCTGACTGTACCACCATCCACTACAACTACATGTGTAACAGTTCCTGCATGGGCGGCATGAACC

                       1106                                                                            1170
   p53 cDNA    (743) GGAGGCCCATCCTCACCATCATCACACTGGAAGACTCCAGTGGTAATCTACTGGGACGGAACAGC
     CMVfor    (960) ------------------------------------------------------------------
p53.601-620    (106) GGAGGCCCATCCTCACCATCATCACACTGGAAGACTCCAGTGGTAATCTACTGGGACGGAACAGC

                       1171                                                                            1235
   p53 cDNA    (808) TTTGAGGTGCGTGTTTGTGCCTGTCCTGGGAGAGACCGGCGCACAGAGGAAGAGAATCTCCGCAA
     CMVfor    (960) ------------------------------------------------------------------
p53.601-620    (171) TTTGAGGTGCGTGTTTGTGCCTGTCCTGGGAGAGACCGGCGCACAGAGGAAGAGAATCTCCGCAA

                       1236                                                                            1300
   p53 cDNA    (873) GAAAGGGGAGCCTCACCACGAGCTGCCCCCAGGGAGCACTAAGCGAGCACTGCCCAACAACACCA
     CMVfor    (960) ------------------------------------------------------------------
p53.601-620    (236) GAAAGGGGAGCCTCACCACGAGCTGCCCCCAGGGAGCACTAAGCGAGCACTGCCCAACAACACCA

                       1301                                                                            1365
   p53 cDNA    (938) GCTCCTCTCCCCAGCCAAAGAAGAAACCACTGGATGGAGAATATTTCACCCTTCAGATCCGTGGG
     CMVfor    (960) ------------------------------------------------------------------
p53.601-620    (301) GCTCCTCTCCCCAGCCAAAGAAGAAACCACTGGATGGAGAATATTTCACCCTTCAGATCCGTGGG

                       1366                                                                            1430
   p53 cDNA   (1003) CGTGAGCGCTTCGAGATGTTCCGAGAGCTGAATGAGGCCTTGGAACTCAAGGATGCCCAGGCTGG
     CMVfor    (960) ------------------------------------------------------------------
p53.601-620    (366) CGTGAGCGCTTCGAGATGTTCCGAGAGCTGAATGAGGCCTTGGAACTCAAGGATGCCCAGGCTGG

                       1431                                                                            1495
   p53 cDNA   (1068) GAAGGAGCCAGGGGGGAGCAGGGCTCACTCCAGCCACCTGAAGTCCAAAAAGGGTCAGTCTACCT
     CMVfor    (960) ------------------------------------------------------------------
p53.601-620    (431) GAAGGAGCCAGGGGGGAGCAGGGCTCACTCCAGCCACCTGAAGTCCAAAAAGGGTCAGTCTACCT
```

```
                    1496                                                                1560
   p53 cDNA  (1133) CCCGCCATAAAAAACTCATGTTCAAGACAGAAGGGCCTGACTCAGACTGA---------------
     CMVfor   (960) ------------------------------------------------------------------
p53.601-620   (496) CCCGCCATAAAAAACTCATGTTCAAGACAGAAGGGCCTGACTCAGACTGAGAATTCGATATCAAG

                    1561                                                                1625
   p53 cDNA  (1183) ------------------------------------------------------------------
     CMVfor   (960) ------------------------------------------------------------------
p53.601-620   (561) CTTATCGATACCGTCGACCTCGAGGGGGGGCCCGGTACCTTAATTAATTAAGGTACCAGGTAAGT

                    1626                                                                1690
   p53 cDNA  (1183) ------------------------------------------------------------------
     CMVfor   (960) ------------------------------------------------------------------
p53.601-620   (626) GTACCCAATTCGCCCTATAGTGAGTCGTATTACAATTCACTCGATCGCCCTTCCCAACAGTTGCG

                    1691                                                                1755
   p53 cDNA  (1183) ------------------------------------------------------------------
     CMVfor   (960) ------------------------------------------------------------------
p53.601-620   (691) CAGCCTGAATGGCGAATGGAGATCCAATTTTTAAGTGTATAATGTGTTAAACTACTGATTCTAAT

                    1756                                                                1820
   p53 cDNA  (1183) ------------------------------------------------------------------
     CMVfor   (960) ------------------------------------------------------------------
p53.601-620   (756) TGTTTGTGTATTTTAGATTCACAGTCCCAAGGCTCATTTCAGGCCCCTCAGTCCTCACAGTCTGT

                    1821                                                                1885
   p53 cDNA  (1183) ------------------------------------------------------------------
     CMVfor   (960) ------------------------------------------------------------------
p53.601-620   (821) TCATGATCATAATCAGCCATACCACATTTGTAGAGGTTTTACTTGCTTTAAAAAACCTCCCACAC

                    1886                                                                1950
   p53 cDNA  (1183) ------------------------------------------------------------------
     CMVfor   (960) ------------------------------------------------------------------
p53.601-620   (886) CTCCCCCTGAACCTGAAACATAAAATGAATGCAATTGTTGTTGTTAACTTGTTTATTGCAGCTTA

                    1951                                                                2015
   p53 cDNA  (1183) ------------------------------------------------------------------
     CMVfor   (960) ------------------------------------------------------------------
p53.601-620   (951) TAATGGTTACAAATAAAGCAATAGCATCACAAATTTCACAAATAAAGCATTTTTTTCACTGCATT

                    2016                          2050
   p53 cDNA  (1183) ------------------------------
     CMVfor   (960) ------------------------------
p53.601-620  (1016) CTAGTTGTGGTTTGTCCAAACTCATCAATGTATCT
```

Appendix 7

The results of sequencing of p53-273H in pET24a(+).The following primers were used for sequencing:

- T7 (5'-TAA TAC GAC TCA CTA TAG GG-3') – available from Eurofins MWG Operon,
- p53.601-620 (5'-TTG CGT GTG GAG TAT TTG GA-3') – designed specifically for sequencing.

The obtained sequences were aligned to the reference sequence of p53 (accession number: NM_000546) using the AlignX® Module of Vector NTI Advance™ 11 (Invitrogen).

```
                    1                                                    65
   p53 cDNA     (1) ------------------------------------ATGGAGGAGCCGCAGTCAGATCCTAG
         T7     (1) TAGAATAATTTTGTTTAACTTTAAGAAGGAGATATACATATGGAGGAGCCGCAGTCAGATCCTAG
p53.601-620     (1) ------------------------------------------------------------

                   66                                                   130
   p53 cDNA    (27) CGTCGAGCCCCCTCTGAGTCAGGAAACATTTTCAGACCTATGGAAACTACTTCCTGAAAACAACG
         T7    (66) CGTCGAGCCCCCTCTGAGTCAGGAAACATTTTCAGACCTATGGAAACTACTTCCTGAAAACAACG
p53.601-620     (1) ------------------------------------------------------------

                  131                                                   195
   p53 cDNA    (92) TTCTGTCCCCCTTGCCGTCCCAAGCAATGGATGATTTGATGCTGTCCCCGGACGATATTGAACAA
         T7   (131) TTCTGTCCCCCTTGCCGTCCCAAGCAATGGATGATTTGATGCTGTCCCCGGACGATATTGAACAA
p53.601-620     (1) ------------------------------------------------------------
                                                                  SNP
                  196                                              72P  260
   p53 cDNA   (157) TGGTTCACTGAAGACCCAGGTCCAGATGAAGCTCCCAGAATGCCAGAGGCTGCTCCCCCCGTGGC
         T7   (196) TGGTTCACTGAAGACCCAGGTCCAGATGAAGCTCCCAGAATGCCAGAGGCTGCTCCCCCCGTGGC
p53.601-620     (1) ------------------------------------------------------------

                  261                                                   325
   p53 cDNA   (222) CCCTGCACCAGCAGCTCCTACACCGGCGGCCCCTGCACCAGCCCCCTCCTGGCCCCTGTCATCTT
         T7   (261) CCCTGCACCAGCAGCTCCTACACCGGCGGCCCCTGCACCAGCCCCCTCCTGGCCCCTGTCATCTT
p53.601-620     (1) ------------------------------------------------------------

                  326                                                   390
   p53 cDNA   (287) CTGTCCCTTCCCAGAAAACCTACCAGGGCAGCTACGGTTTCCGTCTGGGCTTCTTGCATTCTGGG
         T7   (326) CTGTCCCTTCCCAGAAAACCTACCAGGGCAGCTACGGTTTCCGTCTGGGCTTCTTGCATTCTGGG
p53.601-620     (1) ------------------------------------------------------------

                  391                                                   455
   p53 cDNA   (352) ACAGCCAAGTCTGTGACTTGCACGTACTCCCCTGCCCTCAACAAGATGTTTTGCCAACTGGCCAA
         T7   (391) ACAGCCAAGTCTGTGACTTGCACGTACTCCCCTGCCCTCAACAAGATGTTTTGCCAACTGGCCAA
p53.601-620     (1) ------------------------------------------------------------

                  456                                                   520
   p53 cDNA   (417) GACCTGCCCTGTGCAGCTGTGGGTTGATTCCACACCCCCGCCCGGCACCCGCGTCCGCGCCATGG
         T7   (456) GACCTGCCCTGTGCAGCTGTGGGTTGATTCCACACCCCCGCCCGGCACCCGCGTCCGCGCCATGG
p53.601-620     (1) ------------------------------------------------------------
```

```
                    521                                                                 585
   p53 cDNA    (482) CCATCTACAAGCAGTCACAGCACATGACGGAGGTTGTGAGGCGCTGCCCCCACCATGAGCGCTGC
         T7    (521) CCATCTACAAGCAGTCACAGCACATGACGGAGGTTGTGAGGCGCTGCCCCCACCATGAGCGCTGC
p53.601-620      (1) ------------------------------------------------------------

                    586                                                                 650
   p53 cDNA    (547) TCAGATAGCGATGGTCTGGCCCCTCCTCAGCATCTTATCCGAGTGGAAGGAAATTTGCGTGTGGA
         T7    (586) TCAGATAGCGATGGTCTGGCCCCTCCTCAGCATCTTATCCGAGTGGAAGGAAATTTGCGTGTGGA
p53.601-620      (1) ------------------------------------------------------------

                    651                                                                 715
   p53 cDNA    (612) GTATTTGGATGACAGAAACACTTTTCGACATAGTGTGGTGGTGCCCTATGAGCCGCCTGAGGTTG
         T7    (651) GTATTTGGATGACAGAAACACTTTTCGACATAGTGTGGTGGTGCCCTATGAGCCGCCTGAGGTTG
p53.601-620      (1) ------------------------CGAC-TAGTGTGGTGGTGCCCTATGAGCCGCCTGAGGTTG

                    716                                                                 780
   p53 cDNA    (677) GCTCTGACTGTACCACCATCCACTACAACTACATGTGTAACAGTTCCTGCATGGGCGGCATGAAC
         T7    (716) GCTCTGACTGTACCACCATCCACTACAACTACATGTGTAACAGTTCCTGCATGGGCGGCATGAAC
p53.601-620     (40) GCTCTGACTGTACCACCATCCACTACAACTACATGTGTAACAGTTCCTGCATGGGCGGCATGAAC

                    781                                                                 845
   p53 cDNA    (742) CGGAGGCCCATCCTCACCATCATCACACTGGAAGACTCCAGTGGTAATCTACTGGGACGGAACAG
         T7    (781) CGGAGGCCCATCCTCACCATCATCACACTGGAAGACTCCAGTGGTAATCTACTGGGACGGAACAG
p53.601-620   (105) CGGAGGCCCATCCTCACCATCATCACACTGGAAGACTCCAGTGGTAATCTACTGGGACGGAACAG

                    846       R273H                                                     910
   p53 cDNA    (807) CTTTGAGGTGCGTGTTTGTGCCTGTCCTGGGAGAGACCGGCGCACAGAGGAAGAGAATCTCCGCA
         T7    (846) CTTTGAGGTGCATGTTTGTGCCTGTCCTGGGAGAGACCGGCGCACAGAGGAAGAGAATCTCCGCA
p53.601-620   (170) CTTTGAGGTGCATGTTTGTGCCTGTCCTGGGAGAGACCGGCGCACAGAGGAAGAGAATCTCCGCA

                    911                                                                 975
   p53 cDNA    (872) AGAAAGGGGAGCCTCACCACGAGCTGCCCCCAGGGAGCACTAAGCGAGCACTGCCCAACAACACC
         T7    (911) AGAAAGGGGAGCCTCACCACGAGCTGCCCCCAGGGAGCACTAAGCGAGCACTGCCCAACAACACC
p53.601-620   (235) AGAAAGGGGAGCCTCACCACGAGCTGCCCCCAGGGAGCACTAAGCGAGCACTGCCCAACAACACC

                    976                                                                1040
   p53 cDNA    (937) AGCTCCTCTCCCCAGCCAAAGAAGAAACCACTGGATGGAGAATATTTCACCCTTCAGATCCGTGG
         T7    (976) AGCTCCTCTCCC-AGCCAAAGAAGAAACCACTG------------------------------
p53.601-620   (300) AGCTCCTCTCCCCAGCCAAAGAAGAAACCACTGGATGGAGAATATTTCACCCTTCAGATCCGTGG

                    1041                                                               1105
   p53 cDNA   (1002) GCGTGAGCGCTTCGAGATGTTCCGAGAGCTGAATGAGGCCTTGGAACTCAAGGATGCCCAGGCTG
         T7   (1008) ------------------------------------------------------------
p53.601-620   (365) GCGTGAGCGCTTCGAGATGTTCCGAGAGCTGAATGAGGCCTTGGAACTCAAGGATGCCCAGGCTG

                    1106                                                               1170
   p53 cDNA   (1067) GGAAGGAGCCAGGGGGGAGCAGGGCTCACTCCAGCCACCTGAAGTCCAAAAAGGGTCAGTCTACC
         T7   (1008) ------------------------------------------------------------
p53.601-620   (430) GGAAGGAGCCAGGGGGGAGCAGGGCTCACTCCAGCCACCTGAAGTCCAAAAAGGGTCAGTCTACC

                    1171                                                               1235
   p53 cDNA   (1132) TCCCGCCATAAAAAACTCATGTTCAAGACAGAAGGGCCTGACTCAGACTGA--------------
         T7   (1008) ------------------------------------------------------------
p53.601-620   (495) TCCCGCCATAAAAAACTCATGTTCAAGACAGAAGGGCCTGACTCAGACTGAATTCGAGCTCCGTC

                    1236                                                               1300
   p53 cDNA   (1183) ------------------------------------------------------------
         T7   (1008) ------------------------------------------------------------
p53.601-620   (560) GACAAGCTTGCGGCCGCACTCGAGCACCACCACCACCACCACTGAGATCCGGCTGCTAACAAAGC

                    1301                                                               1365
   p53 cDNA   (1183) ------------------------------------------------------------
         T7   (1008) ------------------------------------------------------------
p53.601-620   (625) CCGAAAGGAAGCTGAGTTGGCTGCTGCCACCGCTGAGCAATAACTAGCATAACCCCTTGGGGCCT

                    1366                                                               1430
   p53 cDNA   (1183) ------------------------------------------------------------
         T7   (1008) ------------------------------------------------------------
p53.601-620   (690) CTAAACGGGTCTTGAGGGGTTTTTTGCTGAAAGGAGGAACTATATCCGGATTGGCGAATGGGACG

                    1431                                                               1495
   p53 cDNA   (1183) ------------------------------------------------------------
         T7   (1008) ------------------------------------------------------------
p53.601-620   (755) CGCCCTGTAGCGGCGCATTAAGCGCGGCGGGTGTGGTGGTTACGCGCAGCGTGACCGCTACACTT
```

```
                    1496                                                                1560
   p53 cDNA  (1183) ------------------------------------------------------------------
         T7  (1008) ------------------------------------------------------------------
p53.601-620   (820) GCCAGCGCCCTAGCGCCCGCTCCTTTCGCTTTCTTCCCTTCCTTTCTCGCCACGTTCGCCGGCTT

                    1561                                                                1625
   p53 cDNA  (1183) ------------------------------------------------------------------
         T7  (1008) ------------------------------------------------------------------
p53.601-620   (885) TCCCCGTCAAGCTCTAAATCGGGGGCTCCCTTTAGGGTTCCGATTTAGTGCTTTACGGCACCTCG

                    1626                                                        1683
   p53 cDNA  (1183) ----------------------------------------------------------
         T7  (1008) ----------------------------------------------------------
p53.601-620   (950) ACCCCAAAAACTTGATTAGGGTGATGGTTCACGTAGTGGGCCATCGCCCTGATAGACG
```

Appendix 8

The results of sequencing of p53-273H in pNTAP-B. The following primers were used for sequencing:

- CMVfor (5'-CGC AAA TGG GCG GTA GGC GTG-3') – available from Eurofins MWG Operon,
- p53.601-620 (5'-TTG CGT GTG GAG TAT TTG GA-3') – designed specifically for sequencing.

The obtained sequences were aligned to the reference sequence of p53 (accession number: NM_000546) using the AlignX® Module of Vector NTI Advance™ 11 (Invitrogen).

```
                  1                                                          65
   p53 cDNA     (1) ------------------------------------------------------------
     CMVfor     (1) TATAGCAGAGCTGGTTTAGTGAACCGTCAGATCCGCTAGCGATTACGCCAAGCTCGAAATTAACC
p53.601-620     (1) ------------------------------------------------------------

                  66                                                        130
   p53 cDNA     (1) ------------------------------------------------------------
     CMVfor    (66) CTCACTAAAGGGAACAAAAGCTGGAGCTCCACCGCGGTGGCGGCCGCCACCATGAAGCGACGATG
p53.601-620     (1) ------------------------------------------------------------

                 131                          CBP                           195
   p53 cDNA     (1) ------------------------------------------------------------
     CMVfor   (131) GAAAAAGAATTTCATAGCCGTCTCAGCAGCCAACCGCTTTAAGAAAATCTCATCCTCCGGGGCAC
p53.601-620     (1) ------------------------------------------------------------

                 196                                                        260
   p53 cDNA     (1) ------------------------------------------------------------
     CMVfor   (196) TTGGAAGCGGTAGCGGTACCATGGACGAGAAGACCACCGGCTGGCGGGGCGGCCACGTGGTGGAG
p53.601-620     (1) ------------------------------------------------------------

                 261                          SBP                           325
   p53 cDNA     (1) ------------------------------------------------------------
     CMVfor   (261) GGCCTGGCCGGCGAGCTGGAGCAGCTGCGGGCCAGGCTGGAGCACCACCCTCAGGGCCAGCGGGA
p53.601-620     (1) ------------------------------------------------------------

                 326                                                        390
   p53 cDNA     (1) ----------------------------------------ATGGAGGAGCCGCAGTCAGATCCTA
     CMVfor   (326) GCCCTCCGGCGGCTGCAAGCTGGGCTGCCCGGGCGGATCTATGGAGGAGCCGCAGTCAGATCCTA
p53.601-620     (1) ------------------------------------------------------------

                 391                                                        455
   p53 cDNA    (26) GCGTCGAGCCCCCTCTGAGTCAGGAAACATTTTCAGACCTATGGAAACTACTTCCTGAAAACAAC
     CMVfor   (391) GCGTCGAGCCCCCTCTGAGTCAGGAAACATTTTCAGACCTATGGAAACTACTTCCTGAAAACAAC
p53.601-620     (1) ------------------------------------------------------------

                 456                                                        520
   p53 cDNA    (91) GTTCTGTCCCCCTTGCCGTCCCAAGCAATGGATGATTTGATGCTGTCCCCGGACGATATTGAACA
     CMVfor   (456) GTTCTGTCCCCCTTGCCGTCCCAAGCAATGGATGATTTGATGCTGTCCCCGGACGATATTGAACA
p53.601-620     (1) ------------------------------------------------------------
```

```
                                                                                                                SNP
                                521                                                                        72P 585
   p53 cDNA    (156) ATGGTTCACTGAAGACCCAGGTCCAGATGAAGCTCCCAGAATGCCAGAGGCTGCTCCCCCCGTGG
     CMVfor    (521) ATGGTTCACTGAAGACCCAGGTCCAGATGAAGCTCCCAGAATGCCAGAGGCTGCTCCCCCCGTGG
p53.601-620      (1) ------------------------------------------------------------------

                                586                                                                        650
   p53 cDNA    (221) CCCCTGCACCAGCAGCTCCTACACCGGCGGCCCCTGCACCAGCCCCCTCCTGGCCCCTGTCATCT
     CMVfor    (586) CCCCTGCACCAGCAGCTCCTACACCGGCGGCCCCTGCACCAGCCCCCTCCTGGCCCCTGTCATCT
p53.601-620      (1) ------------------------------------------------------------------

                                651                                                                        715
   p53 cDNA    (286) TCTGTCCCTTCCCAGAAAACCTACCAGGGCAGCTACGGTTTCCGTCTGGGCTTCTTGCATTCTGG
     CMVfor    (651) TCTGTCCCTTCCCAGAAAACCTACCAGGGCAGCTACGGTTTCCGTCTGGGCTTCTTGCATTCTGG
p53.601-620      (1) ------------------------------------------------------------------

                                716                                                                        780
   p53 cDNA    (351) GACAGCCAAGTCTGTGACTTGCACGTACTCCCCTGCCCTCAACAAGATGTTTTGCCAACTGGCCA
     CMVfor    (716) GACAGCCAAGTCTGTGACTTGCACGTACTCCCCTGCCCTCAACAAGATGTTTTGCCAACTGGCCA
p53.601-620      (1) ------------------------------------------------------------------

                                781                                                                        845
   p53 cDNA    (416) AGACCTGCCCTGTGCAGCTGTGGGTTGATTCCACACCCCCGCCCGGCACCCGCGTCCGCGCCATG
     CMVfor    (781) AGACCTGCCCTGTGCAGCTGTGGGTTGATTCCACACCCCCGCCCGGCACCCGCGTCCGCGCCATG
p53.601-620      (1) ------------------------------------------------------------------

                                846                                                                        910
   p53 cDNA    (481) GCCATCTACAAGCAGTCACAGCACATGACGGAGGTTGTGAGGCGCTGCCCCCACCATGAGCGCTG
     CMVfor    (846) GCCATCTACAAGCAGTCACAGCACATGACGGAGGTTGTGAGGCGCTGCCCCCACCATGAGCGCTG
p53.601-620      (1) ------------------------------------------------------------------

                                911                                                                        975
   p53 cDNA    (546) CTCAGATAGCGATGGTCTGGCCCCTCCTCAGCATCTTATCCGAGTGGAAGGAAATTTGCGTGTGG
     CMVfor    (911) CTCAGATAGCGATGGTCTGGCCCCTCCTCAGCATCTTATCCGAGTGGAAGGAAATTTGCGTGTGG
p53.601-620      (1) ------------------------------------------------------------------

                                976                                                                       1040
   p53 cDNA    (611) AGTATTTGGATGACAGAAACACTTTTCGACATAGTGTGGTGGTGCCCTATGAGCCGCCTGAGGTT
     CMVfor    (976) AG--------------------------------------------------------------
p53.601-620      (1) ----------------------------CTAGTGTGGTGGTGCCCTATGAGCCGCCTGAGGTT

                               1041                                                                       1105
   p53 cDNA    (676) GGCTCTGACTGTACCACCATCCACTACAACTACATGTGTAACAGTTCCTGCATGGGCGGCATGAA
     CMVfor    (978) ------------------------------------------------------------------
p53.601-620     (36) GGCTCTGACTGTACCACCATCCACTACAACTACATGTGTAACAGTTCCTGCATGGGCGGCATGAA

                               1106                                                                       1170
   p53 cDNA    (741) CCGGAGGCCCATCCTCACCATCATCACACTGGAAGACTCCAGTGGTAATCTACTGGGACGGAACA
     CMVfor    (978) ------------------------------------------------------------------
p53.601-620    (101) CCGGAGGCCCATCCTCACCATCATCACACTGGAAGACTCCAGTGGTAATCTACTGGGACGGAACA

                               1171      R273H                                                            1235
   p53 cDNA    (806) GCTTTGAGGTGCGTGTTTGTGCCTGTCCTGGGAGAGACCGGCGCACAGAGGAAGAGAATCTCCGC
     CMVfor    (978) ------------------------------------------------------------------
p53.601-620    (166) GCTTTGAGGTGCATGTTTGTGCCTGTCCTGGGAGAGACCGGCGCACAGAGGAAGAGAATCTCCGC

                               1236                                                                       1300
   p53 cDNA    (871) AAGAAAGGGGAGCCTCACCACGAGCTGCCCCCAGGGAGCACTAAGCGAGCACTGCCCAACAACAC
     CMVfor    (978) ------------------------------------------------------------------
p53.601-620    (231) AAGAAAGGGGAGCCTCACCACGAGCTGCCCCCAGGGAGCACTAAGCGAGCACTGCCCAACAACAC

                               1301                                                                       1365
   p53 cDNA    (936) CAGCTCCTCTCCCCAGCCAAAGAAGAAACCACTGGATGGAGAATATTTCACCCTTCAGATCCGTG
     CMVfor    (978) ------------------------------------------------------------------
p53.601-620    (296) CAGCTCCTCTCCCCAGCCAAAGAAGAAACCACTGGATGGAGAATATTTCACCCTTCAGATCCGTG

                               1366                                                                       1430
   p53 cDNA   (1001) GGCGTGAGCGCTTCGAGATGTTCCGAGAGCTGAATGAGGCCTTGGAACTCAAGGATGCCCAGGCT
     CMVfor    (978) ------------------------------------------------------------------
p53.601-620    (361) GGCGTGAGCGCTTCGAGATGTTCCGAGAGCTGAATGAGGCCTTGGAACTCAAGGATGCCCAGGCT

                               1431                                                                       1495
   p53 cDNA   (1066) GGGAAGGAGCCAGGGGGGAGCAGGGCTCACTCCAGCCACCTGAAGTCCAAAAAGGGTCAGTCTAC
     CMVfor    (978) ------------------------------------------------------------------
p53.601-620    (426) GGGAAGGAGCCAGGGGGGAGCAGGGCTCACTCCAGCCACCTGAAGTCCAAAAAGGGTCAGTCTAC
```

```
                    1496                                                                1560
   p53 cDNA  (1131) CTCCCGCCATAAAAAACTCATGTTCAAGACAGAAGGGCCTGACTCAGACTGA------------
     CMVfor   (978) ------------------------------------------------------------
p53.601-620   (491) CTCCCGCCATAAAAAACTCATGTTCAAGACAGAAGGGCCTGACTCAGACTGAATTCGATATCAAG

                    1561                                                                1625
   p53 cDNA  (1183) ------------------------------------------------------------
     CMVfor   (978) ------------------------------------------------------------
p53.601-620   (556) CTTATCGATACCGTCGACCTCGAGGGGGGGCCCGGTACCTTAATTAATTAAGGTACCAGGTAAGT

                    1626                                                                1690
   p53 cDNA  (1183) ------------------------------------------------------------
     CMVfor   (978) ------------------------------------------------------------
p53.601-620   (621) GTACCCAATTCGCCCTATAGTGAGTCGTATTACAATTCACTCGATCGCCCTTCCCAACAGTTGCG

                    1691                                                                1755
   p53 cDNA  (1183) ------------------------------------------------------------
     CMVfor   (978) ------------------------------------------------------------
p53.601-620   (686) CAGCCTGAATGGCGAATGGAGATCCAATTTTTAAGTGTATAATGTGTTAAACTACTGATTCTAAT

                    1756                                                                1820
   p53 cDNA  (1183) ------------------------------------------------------------
     CMVfor   (978) ------------------------------------------------------------
p53.601-620   (751) TGTTTGTGTATTTTAGATTCACAGTCCCAAGGCTCATTTCAGGCCCCTCAGTCCTCACAGTCTGT

                    1821                                                                1885
   p53 cDNA  (1183) ------------------------------------------------------------
     CMVfor   (978) ------------------------------------------------------------
p53.601-620   (816) TCATGATCATAATCAGCCATACCACATTTGTAGAGGTTTTACTTGCTTTAAAAAACCTCCCACAC

                    1886                                                                1950
   p53 cDNA  (1183) ------------------------------------------------------------
     CMVfor   (978) ------------------------------------------------------------
p53.601-620   (881) CTCCCCCTGAACCTGAAACATAAAATGAATGCAATTGTTGTTGTTAACTTGTTTATTGCAGCTTA

                    1951                                                                2015
   p53 cDNA  (1183) ------------------------------------------------------------
     CMVfor   (978) ------------------------------------------------------------
p53.601-620   (946) TAATGGTTACAAATAAAGCAATAGCATCACAAATTTCACAAATAAAGCATTTTTTTCACTGCATT

                    2016                2039
   p53 cDNA  (1183) ----------------------
     CMVfor   (978) ----------------------
p53.601-620  (1011) CTAGTTGTGGTTTGTCCAAACTCA
```

Appendix 9

Table 6.2: The list of proteins identified in the streptavidin eluate fraction purified from UM-SCC-12 cells.

Symbol	Full name	No. of peptides	Coverage
MYH9	Myosin-9	69	32.30%
ACTG	Actin, cytoplasmic 2	45	54.93%
ACTB	Actin, cytoplasmic 1	43	54.93%
MYO1C	Myosin-1C	23	25.39%
CLH1	Clathrin heavy chain 1	15	13.07%
MYO1B	Myosin-1B	17	13.38%
LIMA1	LIM domain and actin-binding protein 1	8	14.76%
TBA1B	Tubulin alpha-1B chain	8	28.82%
TBA1C	Tubulin alpha-1C chain	8	28.95%
BASP1	Brain acid soluble protein 1	10	46.26%
CALM	Calmodulin	10	39.60%
PYC	Pyruvate carboxylase, mitochondrial	7	11.04%
ANXA2	Annexin A2	10	28.61%
TPM4	Tropomyosin alpha-4 chain	8	27.82%
DREB	Drebrin	9	15.87%
MYL6	Myosin light polypeptide 6	6	45.70%
TBB5	Tubulin beta chain	6	18.02%
TBB2C	Tubulin beta-2C chain	6	17.98%
TBB2B	Tubulin beta-2B chain	5	15.28%
TBB2A	Tubulin beta-2A chain	5	15.28%
TBB3	Tubulin beta-3 chain	5	12.00%
TBB4	Tubulin beta-4 chain	4	13.96%
TPM3	Tropomyosin alpha-3 chain	5	16.55%
HSP7C	Heat shock cognate 71 kDa protein	3	6.97%
EF1A3	Putative elongation factor 1-alpha-like 3	3	11.04%
EF1A1	Elongation factor 1-alpha-1	3	11.04%
EF1A2	Elongation factor 1-alpha-2	2	5.83%
RLA2	60S acidic ribosomal protein P2	3	59.13%
NPM	Nucleophosmin	3	16.33%
CALL3	Calmodulin-like protein 3	2	18.79%
HSPB1	Heat shock protein beta-1	2	16.10%
MRLC3	Myosin regulatory light chain MRLC3	2	18.13%
MRLC2	Myosin regulatory light chain MRLC2	2	18.02%
PLAK	Junction plakoglobin	2	5.10%
TPM3L	Putative tropomyosin alpha-3 chain-like protein	4	6.73%
GNAI2	Guanine nucleotide-binding protein G(i) alpha-2 subunit	2	7.32%
GNAI1	Guanine nucleotide-binding protein G(i) alpha-1 subunit	1	3.67%
GNAI3	Guanine nucleotide-binding protein G(k) subunit alpha	1	3.67%
CAPZB	F-actin-capping protein subunit beta	2	14.08%
G3P	Glyceraldehyde-3-phosphate dehydrogenase	2	8.36%
GBB2	Guanine nucleotide-binding protein G(I)/G(S)/G(T) subunit beta-2	1	5.59%
ACTBL	Beta-actin-like protein 2	6	19.15%
AHNK	Neuroblast differentiation-associated protein AHNAK	1	0.54%
PP1G	Serine/threonine-protein phosphatase PP1-gamma catalytic subunit	1	5.26%
PP1B	Serine/threonine-protein phosphatase PP1-beta catalytic subunit	1	5.20%
PP1A	Serine/threonine-protein phosphatase PP1-alpha catalytic subunit	1	5.15%
COF1	Cofilin-1	1	10.24%
COF2	Cofilin-2	1	10.24%
RLA1	60S acidic ribosomal protein P1	1	14.04%
MYH10	Myosin-10	10	6.58%
ANXA1	Annexin A1	1	4.62%
YBOX1	Nuclease-sensitive element-binding protein 1	1	5.86%
CAV1	Caveolin-1	1	11.80%
RL12	60S ribosomal protein L12	1	9.09%
RL7A	60S ribosomal protein L7a	1	9.02%
RL32	60S ribosomal protein L32	1	9.63%

Table 6.2 (cont.): The list of proteins identified in the streptavidin eluate fraction purified from UM-SCC-12 cells.

Symbol	Full name	No. of peptides	Coverage
RS5	40S ribosomal protein S5	1	7.35%
RL7	60S ribosomal protein L7	1	7.66%
COR1C	Coronin-1C	1	3.38%
GBG12	Guanine nucleotide-binding protein G(I)/G(S)/G(O) subunit gamma-12	1	22.22%
RL6	60S ribosomal protein L6	1	5.21%
RL21	60S ribosomal protein L21	1	9.38%
PRP19	Pre-mRNA-processing factor 19	1	2.38%
RL8	60S ribosomal protein L8	1	6.23%
CAZA1	F-actin-capping protein subunit alpha-1	1	5.59%
ACTC	Actin, alpha cardiac muscle 1	11	17.77%
ACTS	Actin, alpha skeletal muscle	11	17.77%
ACTA	Actin, aortic smooth muscle	7	14.85%
ACTH	Actin, gamma-enteric smooth muscle	7	14.89%
ATPB	ATP synthase subunit beta, mitochondrial	1	3.02%
UBIQ	Ubiquitin	1	21.05%

Note: Not all the identified peptides could be unequivocally assigned to one protein due to high sequence similarity of many proteins. Those ambiguous cases are shaded with the same colour.

Table 6.3: The list of proteins identified in the streptavidin eluate fraction purified from 12-175H-20 cells.

Symbol	Full name	No. of peptides	Coverage
MYH9	Myosin-9	118	41.12%
HSP71	Heat shock 70 kDa protein 1	38	51.79%
HSP7C	Heat shock cognate 71 kDa protein	43	46.13%
ACTB	Actin, cytoplasmic 1	45	55.20%
MYO1C	Myosin-1C	22	26.17%
TBB5	Tubulin beta chain	18	41.89%
P53	Cellular tumour antigen p53	21	41.48%
TBA1B	Tubulin alpha-1B chain	17	42.57%
CALM	Calmodulin	15	79.19%
MYO1B	Myosin-1B	21	13.64%
BASP1	Brain acid soluble protein 1	12	46.26%
MYL6	Myosin light polypeptide 6	13	45.70%
MYH10	Myosin-10	16	10.68%
BAG2	BAG family molecular chaperone regulator 2	7	30.33%
CLH1	Clathrin heavy chain 1	8	6.39%
TPM3	Tropomyosin alpha-3 chain	5	16.55%
MRLC3	Myosin regulatory light chain MRLC3	8	35.09%
MRLC2	Myosin regulatory light chain MRLC2	8	34.88%
ANXA2	Annexin A2	7	14.45%
DREB	Drebrin	4	10.63%
LIMA1	LIM domain and actin-binding protein 1	3	6.46%
TPM4	Tropomyosin alpha-4 chain	7	15.32%
HSPB1	Heat shock protein beta-1	3	26.34%
TPM3L	Putative tropomyosin alpha-3 chain-like protein	4	6.73%
TMOD3	Tropomodulin-3	2	12.22%
COF1	Cofilin-1	2	18.67%
COF2	Cofilin-2	1	10.24%
TBB2C	Tubulin beta-2C chain	17	35.73%
ACTG	Actin, cytoplasmic 2	44	55.20%
MYLK2	Myosin light chain kinase 2, skeletal/cardiac muscle	1	1.85%
ACTC	Actin, alpha cardiac muscle 1	9	17.77%
ACTS	Actin, alpha skeletal muscle	9	17.77%
ACTA	Actin, aortic smooth muscle	6	14.85%
ACTH	Actin, gamma-enteric smooth muscle	6	14.89%
PYC	Pyruvate carboxylase, mitochondrial	1	1.87%
MYO6	Myosin-VI	1	1.16%
YBOX1	Nuclease-sensitive element-binding protein 1	1	5.86%

Note: Not all the identified peptides could be unequivocally assigned to one protein due to high sequence similarity of many proteins. Those ambiguous cases are shaded with the same colour. The proteins present only in the test sample and not in the control are shown in red.

Table 6.4: The list of proteins identified in the streptavidin eluate fraction purified from 12-273H-39 cells.

Symbol	Full name	No. of peptides	Coverage
MYH9	Myosin-9	163	45.51%
MYH10	Myosin-10	51	26.01%
ACTB	Actin, cytoplasmic 1	52	47.47%
P53	Cellular tumour antigen p53	37	57.51%
MYO1C	Myosin-1C	20	21.07%
MYO1B	Myosin-1B	14	12.85%
CALM	Calmodulin	18	45.64%
MYL6	Myosin light polypeptide 6	15	52.98%
DREB	Drebrin	11	16.02%
LIMA1	LIM domain and actin-binding protein 1	7	11.73%
TPM4	Tropomyosin alpha-4 chain	8	23.79%
TBA3E	Tubulin alpha-3E chain	5	13.56%
TBA3C	Tubulin alpha-3C/D chain	5	13.56%
TBA1B	Tubulin alpha-1B chain	4	10.20%
TBA1A	Tubulin alpha-1A chain	4	10.20%
TPM3	Tropomyosin alpha-3 chain	7	22.54%
ML12B	Myosin regulatory light chain 12B	9	33.72%
ML12A	Myosin regulatory light chain 12A	9	33.92%
BASP1	Brain acid soluble protein 1	6	35.68%
K2C1	Keratin, type II cytoskeletal 1	4	7.14%
ANXA2	Annexin A2	4	14.75%
AXA2L	Putative annexin A2-like protein	3	10.62%
ALBU	Serum albumin	3	7.88%
TBB5	Tubulin beta chain	4	9.46%
TBB2C	Tubulin beta-2C chain	4	9.44%
TBB2B	Tubulin beta-2B chain	4	9.44%
TBB2A	Tubulin beta-2A chain	4	9.44%
TBB3	Tubulin beta-3 chain	4	9.33%
MYO6	Myosin-VI	2	2.01%
NPM	Nucleophosmin	2	11.56%
TPM3L	Putative tropomyosin alpha-3 chain-like protein	5	13.90%
K1C10	Keratin, type I cytoskeletal 10	2	3.94%
COR1C	Coronin-1C	2	8.65%
CD59	CD59 glycoprotein	2	20.31%
MYLK2	Myosin light chain kinase 2, skeletal/cardiac muscle	2	1.85%
K22E	Keratin, type II cytoskeletal 2 epidermal	3	5.63%
K2C6A	Keratin, type II cytoskeletal 6A	2	3.90%
K2C75	Keratin, type II cytoskeletal 75	1	2.18%
K2C5	Keratin, type II cytoskeletal 5	2	3.73%
K2C6C	Keratin, type II cytoskeletal 6C	2	3.90%
K2C6B	Keratin, type II cytoskeletal 6B	2	3.90%
K2C79	Keratin, type II cytoskeletal 79	1	2.24%
TMOD3	Tropomodulin-3	1	3.41%
ACTG	Actin, cytoplasmic 2	49	47.20%
H12	Histone H1.2	1	7.51%
ACTC	Actin, alpha cardiac muscle 1	13	14.32%
ACTS	Actin, alpha skeletal muscle	13	14.32%
ACTA	Actin, aortic smooth muscle	9	11.41%
ACTH	Actin, gamma-enteric smooth muscle	9	11.44%

Note: Not all the identified peptides could be unequivocally assigned to one protein due to high sequence similarity of many proteins. Those ambiguous cases are shaded with the same colour. The proteins present only in the test sample and not in the control are shown in red.

Appendix 10

Live cell imaging was performed on UM-SCC-12, 12-175H-20, 12-273H-39, 12-273H-41 and 12-273H-null cells. The cells were imaged for 14.4 hours with a time-lapse of 3 min. Movies were generated from the recorded images at 15 frames/sec. See the attached CD for representative movies.

Appendix 11

12-273H-39 cells were transfected with scrambled siRNA, siRNA for p53, Lipofectamine alone or left untreated. The cells were imaged for 12 hours (24-36 hours post treatment and 36-48 hours post treatment) with a time lapse of 3 min. Movies were generated from the recorded images at 15 frames/sec. See the attached CD for representative movies.

Appendix 12

Live cell imaging was performed on UM-SCC-12, 12-273H-39, 12-273H-39-low$_1$ and 12-273H-39-low$_3$ cells. The cells were imaged for 12 hours with a time-lapse of 3 min. Movies were generated from the recorded images at 15 frames/sec. See the attached CD for representative movies.

Appendix 13

Table 6.5: The list of genes, which were found to be up-regulated in 12-273H-39 cells compared to UM-SCC-12 cells. Statistical analysis was performed using Student's t-Test. (Data analysis performed by Dr Bryony Lloyd.)

Gene symbol	Full name	Relative expression	p value
TP53	tumour protein p53	65.4	0.000006
SPRR2A	small proline-rich protein 2A	23.1	0.0013
TLR4	toll-like receptor 4	14.6	0.00019
MFAP5	microfibrillar associated protein 5	12.0	0.0051
C3	complement component 3	11.6	0.00049
CLDN4	claudin 4	10.5	0.007
S100A8	S100 calcium binding protein A8	10.3	0.00012
C8orf4	chromosome 8 open reading frame 4	10.2	0.000026
FN1	fibronectin 1	8.4	0.017
PTGES	prostaglandin E synthase	8.1	0.000005
TIMP2	TIMP metallopeptidase inhibitor 2	7.9	0.0058
EVI2B	ecotropic viral integration site 2B	7.6	0.00046
TGM3	transglutaminase 3	7.4	0.0243
NCF2	neutrophil cytosolic factor 2	7.3	0.00076
GDF15	growth differentiation factor 15	7.2	0.0018
IL24	interleukin 24	7.1	0.026
KLRC3	killer cell lectin-like receptor subfamily C, member 3	6.9	0.000098
SDR16C5	short chain dehydrogenase/reductase family 16C, member 5	6.6	0.000075
LCN2	lipocalin 2	6.5	0.0025
RAET1L	retinoic acid early transcript 1L	6.0	0.0028
SAA1	serum amyloid A1	6.0	0.0024
ULBP1	UL16 binding protein 1	5.9	0.0032
TSPAN1	tetraspanin 1	5.8	0.00073
SLC16A3	solute carrier family 16, member 3 (monocarboxylic acid transporter 4)	5.6	0.00068
CLDN1	claudin 1	5.6	0.041
SCEL	sciellin	5.5	0.000067
TSPAN8	tetraspanin 8	5.5	0.0066
PLA2G16	phospholipase A2, group XVI	5.5	0.0028
SLC2A3	solute carrier family 2 (facilitated glucose transporter)	5.3	0.0061
GFPT2	glutamine-fructose-6-phosphate transaminase 2	5.0	0.0035
TNFRSF9	tumour necrosis factor receptor superfamily, member 9	4.9	0.015
BIRC3	baculoviral IAP repeat-containing 3	4.8	0.016
IFIT2	interferon-induced protein with tetratricopeptide repeats 2	4.8	0.00093
TSPAN18	tetraspanin 18	4.7	0.00018
CXCL1	chemokine (C-X-C motif) ligand 1 (melanoma growth stimulating activity, alpha)	4.7	0.0073
TFP1	tissue factor pathway inhibitor (lipoprotein-associated coagulation inhibitor)	4.6	0.0051
ACAA2	acetyl-Coenzyme A acyltransferase 2	4.5	0.013
CYP1B1	cytochrome P450, family 1, subfamily B, polypeptide 1	4.4	0.0056
STEAP1	six transmembrane epithelial antigen of the prostate 1	4.4	0.0015
SLPI	secretory leukocyte peptidase inhibitor	4.4	0.010
PTGS2	prostaglandin-endoperoxide synthase 2 (prostaglandin G/H synthase and cyclooxygenase)	4.3	0.00052
SPRY2	sprouty homolog 2 (Drosophila)	4.1	0.0018
ZNF114	zinc finger protein 114	4.0	0.000005

Table 6.5 (cont.): The list of genes, which were found to be up-regulated in 12-273H-39 cells compared to UM-SCC-12 cells. Statistical analysis was performed using Student's t-Test. (Data analysis performed by Dr Bryony Lloyd.)

Gene symbol	Full name	Relative expression	p value
LOX	lysyl oxidase	4.0	0.0022
IL8	interleukin 8	4.0	0.0066
PROS1	protein S (alpha)	3.9	0.0028
GCNT3	glucosaminyl (N-acetyl) transferase 3, mucin type	3.9	0.0039
PLAU	plasminogen activator, urokinase	3.9	0.011
SPRR2D	small proline-rich protein 2D	3.9	0.0022
DNER	delta/notch-like EGF repeat containing	3.9	0.011
RGS2	regulator of G-protein signalling 2, 24kDa	3.8	0.00061
CLDN7	claudin 7	3.8	0.027
GPR110	G protein-coupled receptor 110	3.7	0.017
DLX5	distal-less homeobox 5	3.7	0.0046
LIPH	lipase, member H	3.7	0.00017
LAPTM5	lysosomal protein transmembrane 5	3.7	0.000030
EPAS1	endothelial PAS domain protein 1	3.6	0.013
SPRR3	small proline-rich protein 3	3.5	0.0020
PI3	peptidase inhibitor 3, skin-derived	3.5	0.0022
GNG2	guanine nucleotide binding protein (G protein), gamma 2	3.5	0.00041
IGFBP7	insulin-like growth factor binding protein 7	3.5	0.000017
ANKRD22	ankyrin repeat domain 22	3.5	0.011
EHF	ets homologous factor	3.4	0.0067
PAG1	phosphoprotein associated with glycosphingolipid microdomains 1	3.4	0.010
PDZD2	PDZ domain containing 2	3.4	0.00034
ABCA12	ATP-binding cassette, sub-family A (ABC1), member 12	3.4	0.000029
IGFL1	IGF-like family member 1	3.4	0.0014
SAMD9L	sterile alpha motif domain containing 9-like	3.3	0.0041
DDX58	DEAD (Asp-Glu-Ala-Asp) box polypeptide 58	3.3	0.0044
IL1F9	interleukin 1 family, member 9	3.3	0.0014
MAP3K5	mitogen-activated protein kinase kinase kinase 5	3.3	0.00025
RBM47	RNA binding motif protein 47	3.2	0.0050
DNAH6	dynein, axonemal, heavy chain 6	3.2	0.0025
GPR126	G protein-coupled receptor 126	3.1	0.021
FAM49A	family with sequence similarity 49, member A	3.1	0.0014
DUSP10	dual specificity phosphatase 10	3.1	0.0017
ALDH1A1	aldehyde dehydrogenase 1 family, member A1	3.0	0.0042
NRP2	neuropilin 2	3.0	0.0031
RBKS	ribokinase	3.0	0.00065
IRAK2	interleukin-1 receptor-associated kinase 2	3.0	0.0013
ATP6V0D2	ATPase, H^+ transporting, lysosomal 38kDa, V0 subunit d2	3.0	0.00015
RASSF5	Ras association (RalGDS/AF-6) domain family member 5	3.0	0.000619
MMP2	matrix metallopeptidase 2 (gelatinase A, 72kDa gelatinase, 72kDa type IV collagenase)	2.9	0.00050
GPR1	G protein-coupled receptor 1	2.9	0.020
TXNIP	thioredoxin interacting protein	2.9	0.0085
SPRR1B	small proline-rich protein 1B (cornifin)	2.9	0.0040
ABLIM3	actin binding LIM protein family, member 3	2.9	0.0040
TIMP3	TIMP metallopeptidase inhibitor 3	2.9	0.0011
SLFN5	schlafen family member 5	2.9	0.00095
CXCL2	chemokine (C-X-C motif) ligand 2	2.8	0.020
RNF146	ring finger protein 146	2.8	0.0030

Table 6.5 (cont.): The list of genes, which were found to be up-regulated in 12-273H-39 cells compared to UM-SCC-12 cells. Statistical analysis was performed using Student's t-Test. (Data analysis performed by Dr Bryony Lloyd.)

Gene symbol	Full name	Relative expression	p value
LY96	lymphocyte antigen 96	2.8	0.0087
ECM1	extracellular matrix protein 1	2.8	0.0010
C5orf41	chromosome 5 open reading frame 41	2.8	0.0067
GPR110	G protein-coupled receptor 110	2.8	0.0091
CCL20	chemokine (C-C motif) ligand 20	2.8	0.000032
GJB4	gap junction protein, beta 4, 30.3kDa	2.8	0.0073
RASA4	RAS p21 protein activator 4	2.8	0.00050
TMEM159	transmembrane protein 159	2.7	0.0052
TSPAN2	tetraspanin 2	2.7	0.0054
SAT1	spermidine/spermine N1-acetyltransferase 1	2.7	0.0012
PTAFR	platelet-activating factor receptor	2.7	0.035
LGALS3	lectin, galactoside-binding, soluble, 3	2.7	0.00044
SLC1A1	solute carrier family 1 (neuronal/epithelial high affinity glutamate transporter, system Xag), member 1	2.7	0.0057
SPARC	secreted protein, acidic, cysteine-rich (osteonectin)	2.7	0.023
FRK	fyn-related kinase	2.7	0.023
PLXNA2	plexin A2	2.6	0.017
MR1	major histocompatibility complex, class I-related	2.6	0.00067
CYP39A1	cytochrome P450, family 39, subfamily A, polypeptide 1	2.6	0.0015
MMP28	matrix metallopeptidase 28	2.6	0.00018
TMEM47	transmembrane protein 47	2.6	0.0033
SERPINB1	serpin peptidase inhibitor, clade B (ovalbumin), member 1	2.5	0.019
MARCH3	membrane-associated ring finger (C3HC4) 3	2.5	0.0061
HEY1	hairy/enhancer-of-split related with YRPW motif 1	2.5	0.0014
VEGFA	vascular endothelial growth factor A	2.5	0.0037
NPL	N-acetylneuraminate pyruvate lyase (dihydrodipicolinate synthase)	2.5	0.012
EVI2A	ecotropic viral integration site 2A	2.5	0.0028
MT1X	metallothionein 1X	2.5	0.0032
ANKRD42	ankyrin repeat domain 42	2.5	0.0016
KRT86	keratin 86	2.5	0.0026
ERRFI1	ERBB receptor feedback inhibitor 1	2.4	0.0030
CBWD3	COBW domain containing 3	2.4	0.051
ID2	inhibitor of DNA binding 2, dominant negative helix-loop-helix protein	2.4	0.013
MMP1	matrix metallopeptidase 1 (interstitial collagenase)	2.4	0.0027
CITED2	Cbp/p300-interacting transactivator, with Glu/Asp-rich carboxy-terminal domain, 2	2.4	0.0014
AGAP11	ankyrin repeat and GTPase domain Arf GTPase activating protein 11	2.4	0.0022
DAB2	disabled homolog 2, mitogen-responsive phosphoprotein (Drosophila)	2.4	0.019
MERTK	c-mer proto-oncogene tyrosine kinase	2.4	0.025
GSDMC	gasdermin C	2.4	0.00033
TRIB2	tribbles homolog 2 (Drosophila)	2.4	0.0016
GPNMB	glycoprotein (transmembrane) nmb	2.4	0.030
MYEOV	myeloma overexpressed (in a subset of t(11;14) positive multiple myelomas)	2.4	0.0066
IFIT1	interferon-induced protein with tetratricopeptide repeats	2.4	0.030

Table 6.5 (cont.): The list of genes, which were found to be up-regulated in 12-273H-39 cells compared to UM-SCC-12 cells. Statistical analysis was performed using Student's t-Test. (Data analysis performed by Dr Bryony Lloyd.)

Gene symbol	Full name	Relative expression	p value
C9orf70	chromosome 9 open reading frame 70	2.4	0.00039
RHBDL2	rhomboid, veinlet-like 2 (Drosophila)	2.4	0.000067
DOCK4	dedicator of cytokinesis 4	2.4	0.0026
SAA1	serum amyloid A1	2.4	0.041
MCTP1	multiple C2 domains, transmembrane 1	2.4	0.0010
RWDD2A	RWD domain containing 2A	2.4	0.0048
RPL41	ribosomal protein L41	2.4	0.012
CA13	carbonic anhydrase XIII	2.3	0.0026
SEMA3B	sema domain, immunoglobulin domain (Ig), short basic domain, secreted, (semaphorin) 3B	2.3	0.00022
LPAR3	lysophosphatidic acid receptor 3	2.3	0.0018
DUSP1	dual specificity phosphatase 1	2.3	0.0015
HLA-B	major histocompatibility complex, class I, B	2.3	0.0045
C15orf52	chromosome 15 open reading frame 52	2.3	0.0010
ENC1	ectodermal-neural cortex (with BTB-like domain)	2.3	0.038
CAPG	capping protein (actin filament), gelsolin-like	2.3	0.00031
STK10	serine/threonine kinase 10	2.3	0.0023
LIF	leukaemia inhibitory factor (cholinergic differentiation factor)	2.3	0.026
NOV	nephroblastoma overexpressed gene	2.3	0.00028
TLN2	talin 2	2.3	0.00092
SOD2	superoxide dismutase 2, mitochondrial	2.3	0.0087
ZNF718	zinc finger protein 718	2.3	0.0035

Table 6.6: The list of genes, which were found to be down-regulated in 12-273H-39 cells compared to UM-SCC-12 cells. Statistical analysis was performed using Student's t-Test. (Data analysis performed by Dr Bryony Lloyd.)

Gene symbol	Full name	Relative expression	p value
LPAR1	lysophosphatidic acid receptor 1	-2.3	0.0011
NOS1	nitric oxide synthase 1 (neuronal)	-2.3	0.0021
PRR5L	proline rich 5 like	-2.3	0.010
CABLES1	Cdk5 and Abl enzyme substrate 1	-2.4	0.041
LEF1	lymphoid enhancer-binding factor 1	-2.4	0.030
PPP4R4	protein phosphatase 4, regulatory subunit 4	-2.5	0.0039
MTMR10	myotubularin related protein 10	-2.5	0.00035
OBP2B	odorant binding protein 2B	-2.6	0.038
NMT2	N-myristoyltransferase 2	-2.6	0.0046
CCDC3	coiled-coil domain containing 3	-2.6	0.0055
FLRT2	fibronectin leucine rich transmembrane protein 2	-2.6	0.00085
ACSM2B	acyl-CoA synthetase medium-chain family member 2B	-2.6	0.022
FBN2	fibrillin 2	-2.6	0.0060
SIRPA	signal-regulatory protein alpha	-2.6	0.000030
CNTN1	contactin 1	-2.7	0.0029
HTRA3	HtrA serine peptidase 3	-2.7	0.00047
TAF1A	TATA box binding protein (TBP)-associated factor, RNA polymerase I, A, 48kDa	-2.8	0.0069
RFX7	regulatory factor X, 7	-2.8	0.0045
SLC1A4	solute carrier family 1 (glutamate/neutral amino acid transporter), member 4	-2.8	0.037
LAMA1	laminin, alpha 1	-2.8	0.000045
KMO	kynurenine 3-monooxygenase (kynurenine 3-hydroxylase)	-2.8	0.0066
WNT7B	wingless-type MMTV integration site family, member 7B	-3.0	0.00027
FECH	ferrochelatase (protoporphyria)	-3.0	0.0036
CCBE1	collagen and calcium binding EGF domains 1	-3.0	0.0017
WNT5A	wingless-type MMTV integration site family, member 5A	-3.0	0.0026
FGFR2	fibroblast growth factor receptor 2	-3.1	0.0039
FST	follistatin	-3.2	0.0025
SLC2A5	solute carrier family 2 (facilitated glucose/fructose transporter), member 5	-3.2	0.023
COL12A1	collagen, type XII, alpha 1	-3.4	0.0070
RBMS3	RNA binding motif, single stranded interacting protein 3	-3.8	0.0018
RARB	retinoic acid receptor, beta	-3.9	0.0085
KRT14	keratin 14	-4.1	0.0086
CYP24A1	cytochrome P450, family 24, subfamily A, polypeptide 1	-5.1	0.014
SERPINF1	serpin peptidase inhibitor, clade F (alpha-2 antiplasmin, pigment epithelium derived factor), member 1	-5.2	0.0026
OLR1	oxidized low density lipoprotein (lectin-like) receptor 1	-5.8	0.017
PART1	prostate androgen-regulated transcript 1	-6.0	0.0080
NPNT	nephronectin	-6.9	0.0034
OGN	osteoglycin	-8.5	0.000010
CCND2	cyclin D2	-10.9	0.000028

Appendix 14

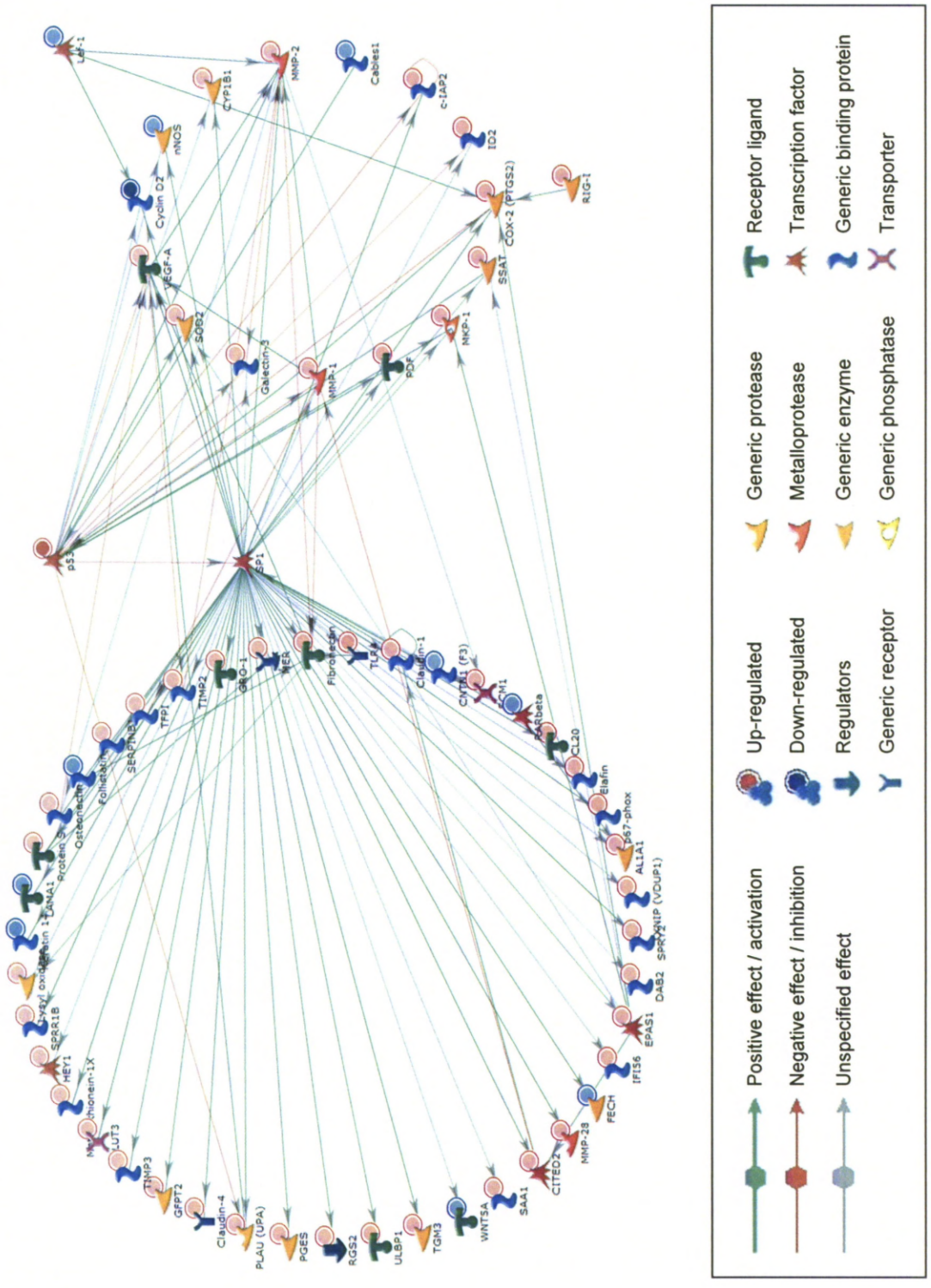

Figure 6.1: A model of network of transcriptional regulation by p53-273H via Sp1 $\left(p = 7.86 \times 10^{-158}\right)$. p value was calculated using a formula for hypergeometric distribution. (Data analysis performed by Dr Bryony Lloyd.)

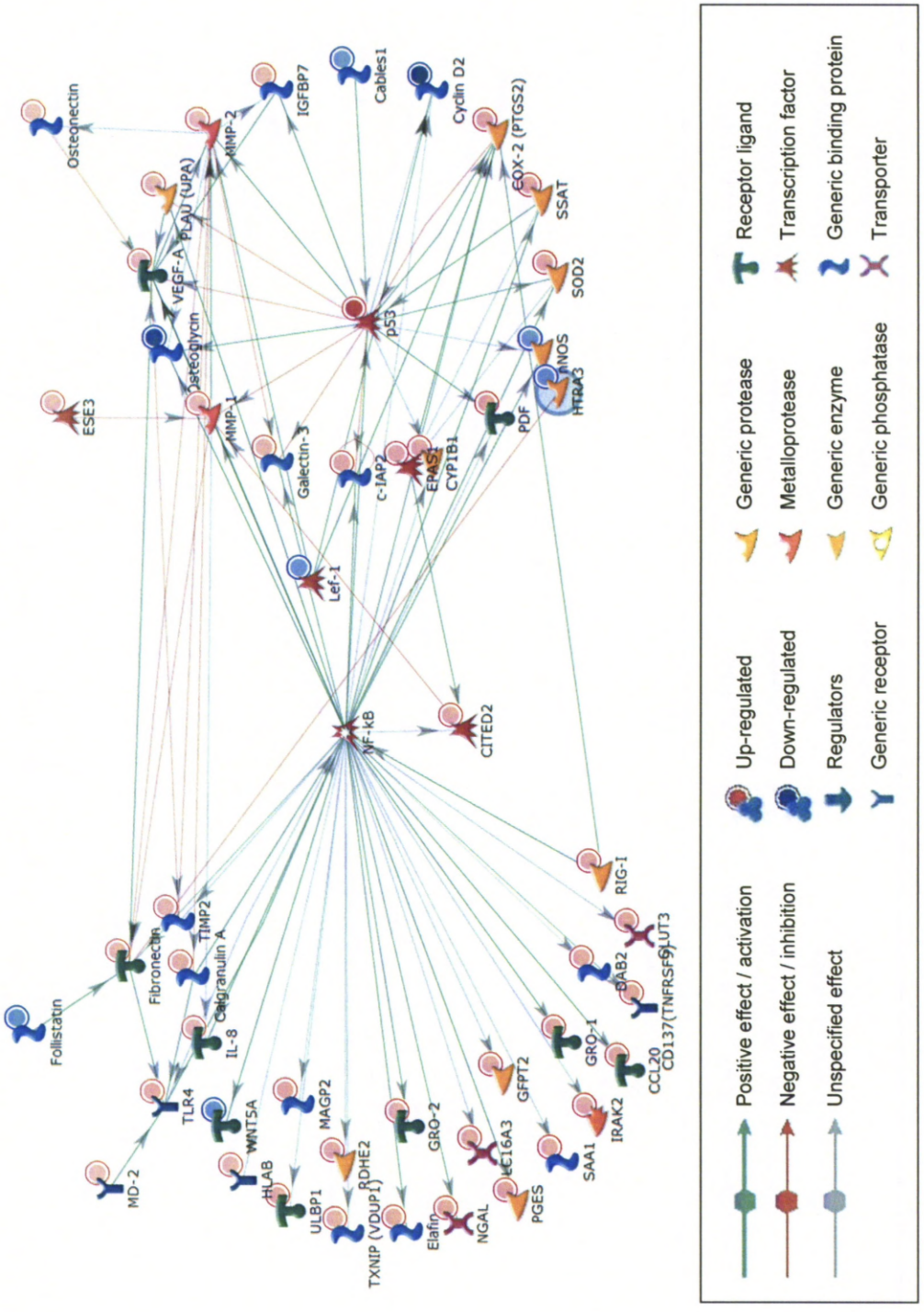

Figure 6.2: A model of network of transcriptional regulation by p53-273H via NF-κB $\left(p = 2.36 \times 10^{-218}\right)$. p value was calculated using a formula for hypergeometric distribution. (Data analysis performed by Dr Bryony Lloyd.)

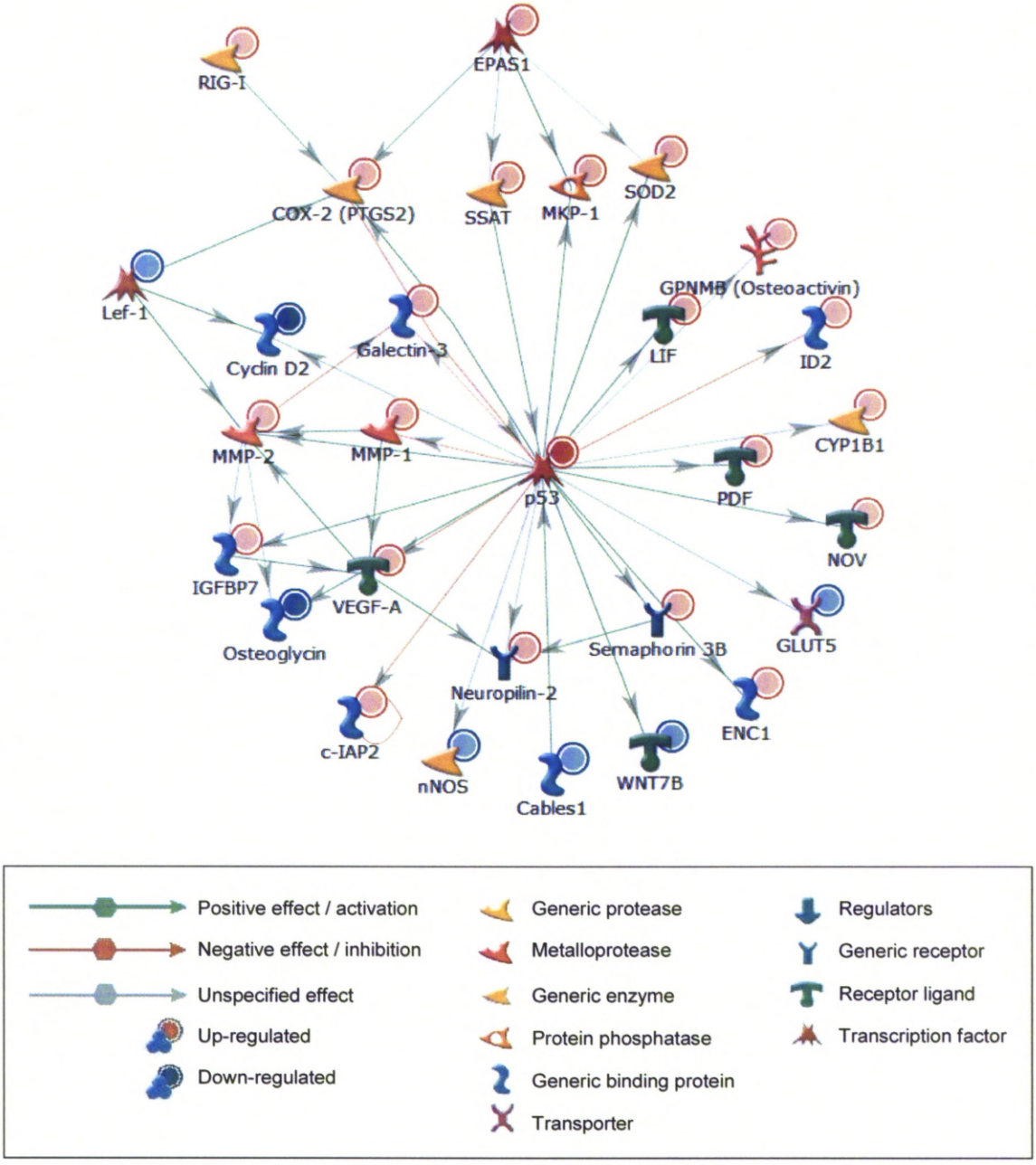

Figure 6.3: A model of network of transcriptional regulation by p53-273H $\left(p = 8.17 \times 10^{-75}\right)$. p value was calculated using a formula for hypergeometric distribution. (Data analysis performed by Dr Bryony Lloyd.)

Appendix 15

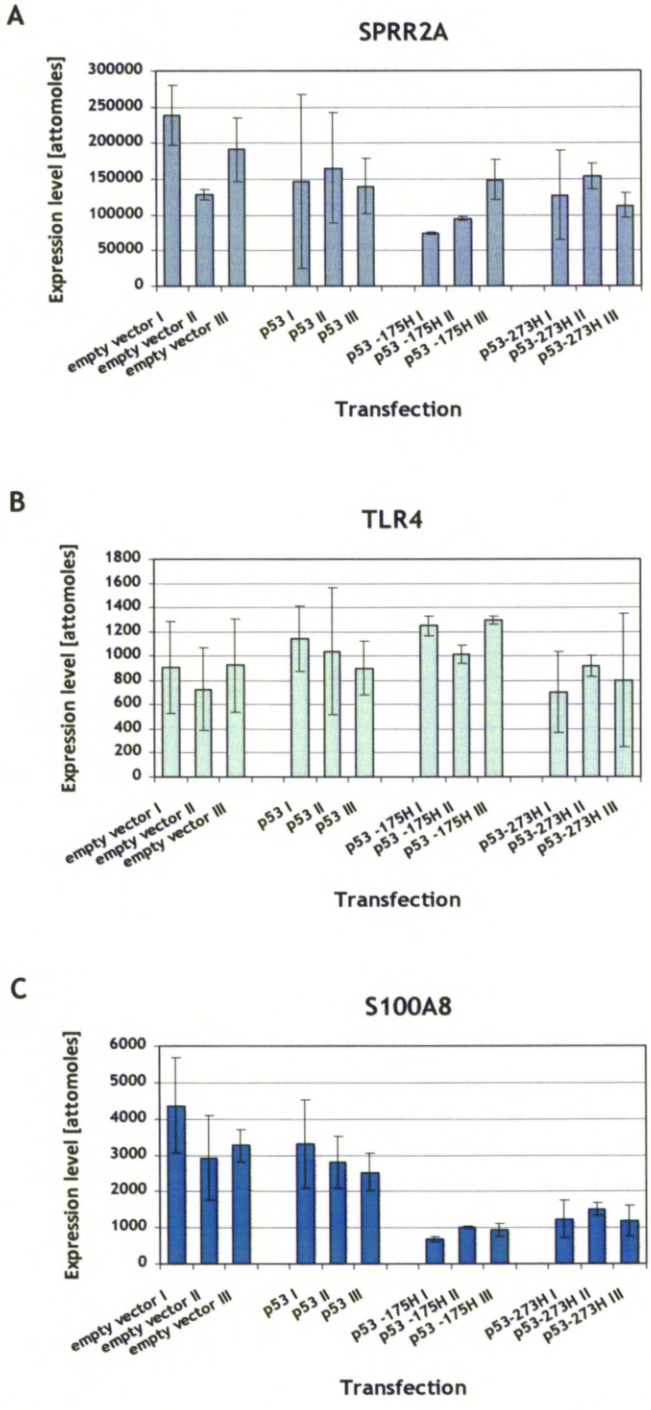

Figure 6.4: Expression levels of the indicated genes in the individual transfections of UM-SCC-12 cells. qRT-PCR was performed on RNA extracted from UM-SCC-12 cells transiently transfected in triplicate with the indicated vectors. The histograms show mean of the average expression levels (normalised to histone H3 expression) from two reverse transcription reactions performed from RNA samples for each transfection (see Figure 2.2), the error bars represent standard deviation. (Data provided by Dr Bryony Lloyd.)

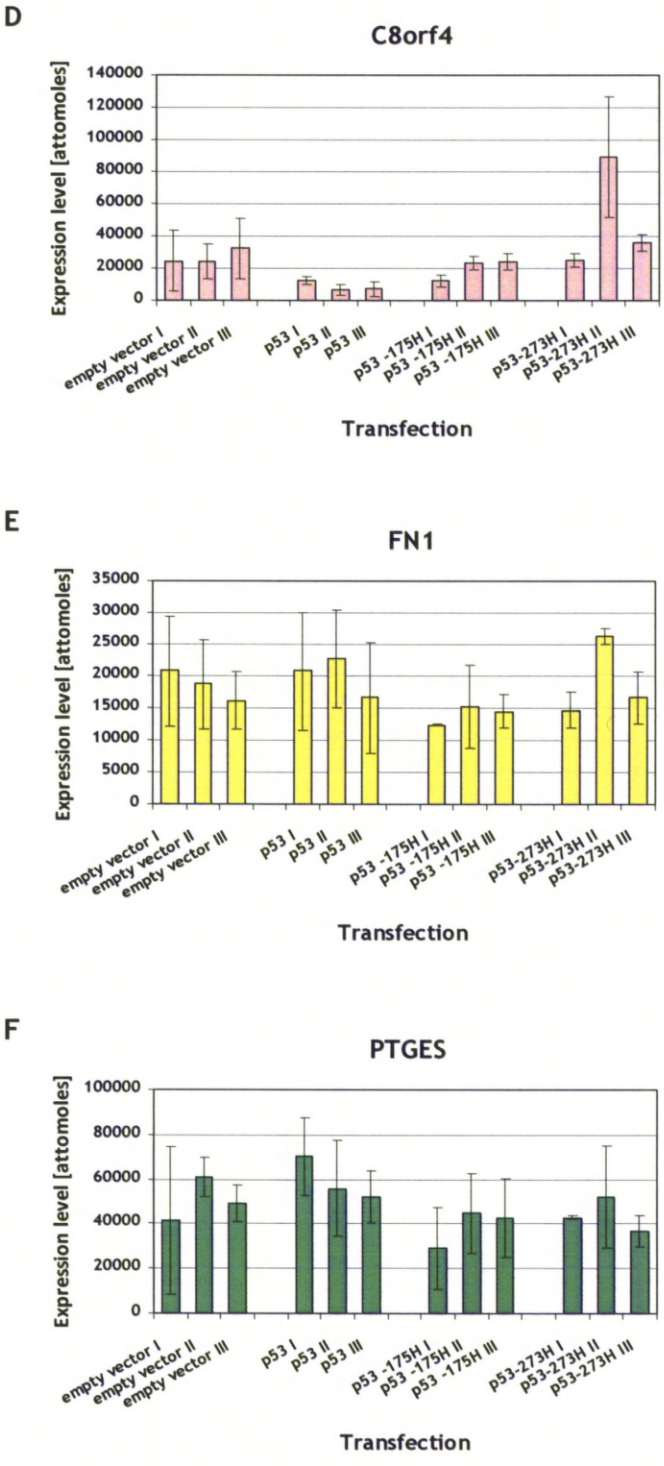

Figure 6.4 (cont.): Expression levels of the indicated genes in the individual transfections of UM-SCC-12 cells. qRT-PCR was performed on RNA extracted from UM-SCC-12 cells transiently transfected in triplicate with the indicated vectors. The histograms show mean of the average expression levels (normalised to histone H3 expression) from two reverse transcription reactions performed from RNA samples for each transfection (see Figure 2.2), the error bars represent standard deviation. (Data provided by Dr Bryony Lloyd.)

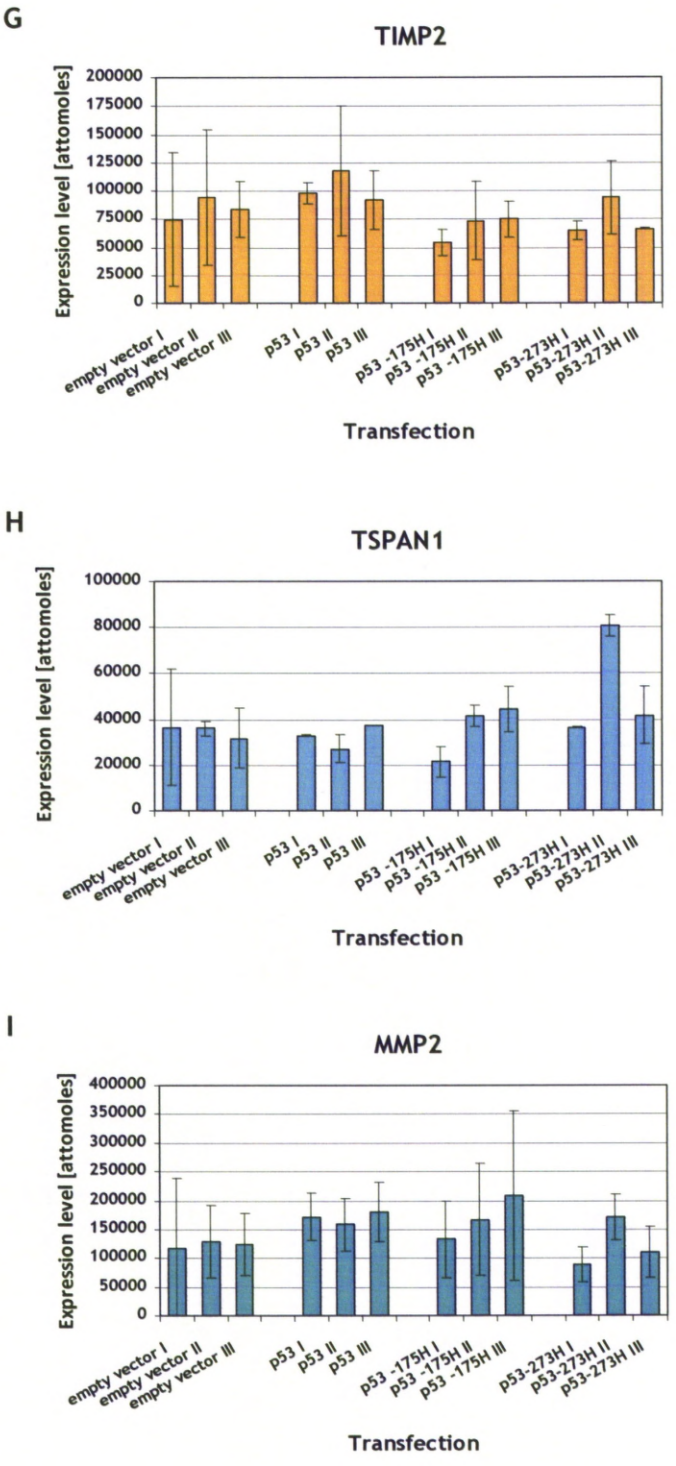

Figure 6.4 (cont.): Expression levels of the indicated genes in the individual transfections of UM-SCC-12 cells. qRT-PCR was performed on RNA extracted from UM-SCC-12 cells transiently transfected in triplicate with the indicated vectors. The histograms show mean of the average expression levels (normalised to histone H3 expression) from two reverse transcription reactions performed from RNA samples for each transfection (see Figure 2.2), the error bars represent standard deviation. (Data provided by Dr Bryony Lloyd.)

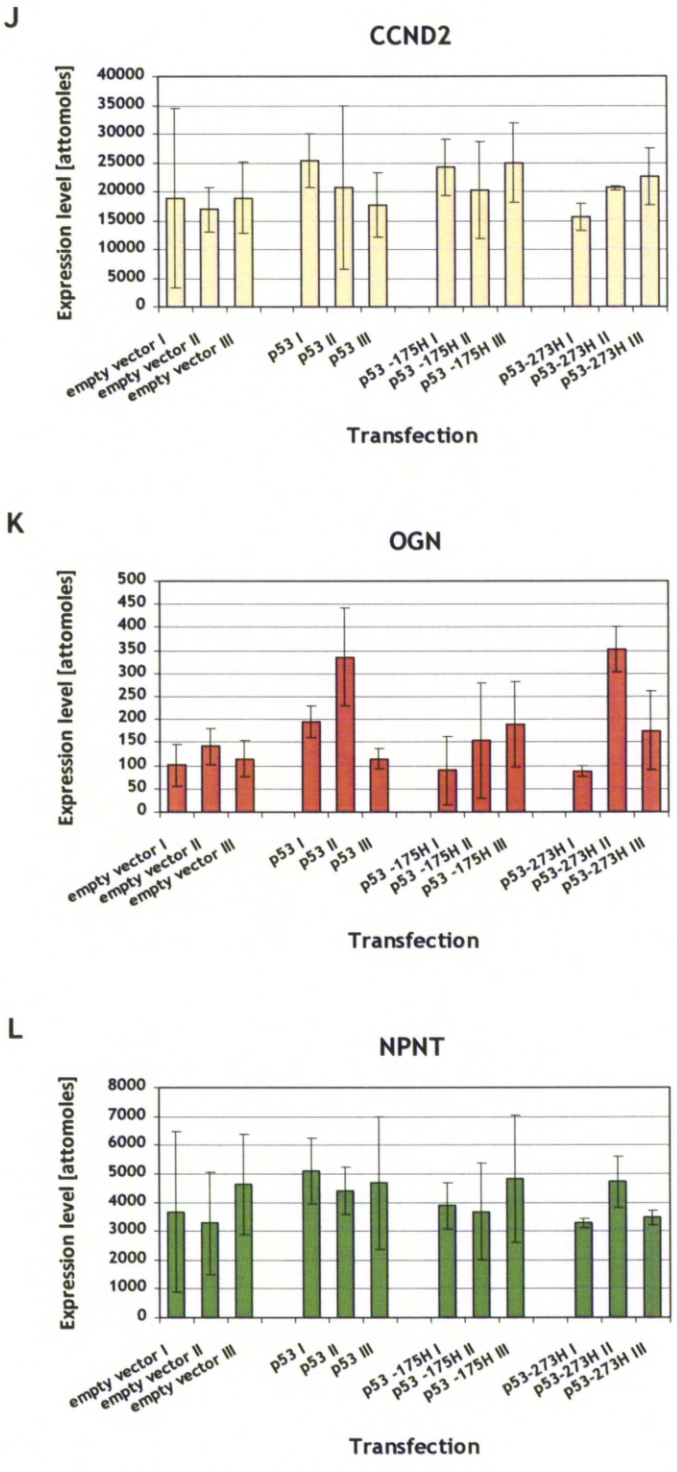

Figure 6.4 (cont.): Expression levels of the indicated genes in the individual transfections of UM-SCC-12 cells. qRT-PCR was performed on RNA extracted from UM-SCC-12 cells transiently transfected in triplicate with the indicated vectors. The histograms show mean of the average expression levels (normalised to histone H3 expression) from two reverse transcription reactions performed from RNA samples for each transfection (see Figure 2.2), the error bars represent standard deviation. (Data provided by Dr Bryony Lloyd.)

Appendix 16

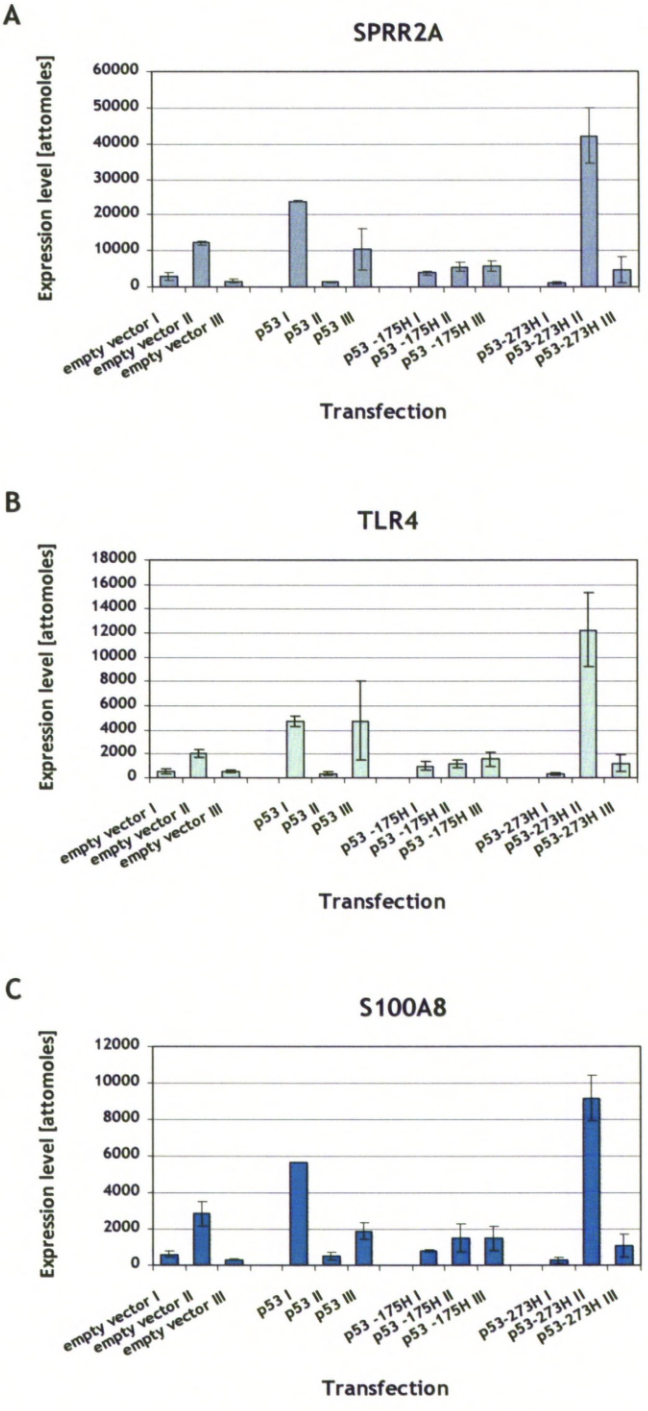

Figure 6.5: Expression levels of the indicated genes in the individual transfections of H1299 cells. qRT-PCR was performed on RNA extracted from H1299 cells transiently transfected in triplicate with the indicated vectors. The histograms show mean of the average expression levels (normalised to histone H3 expression) from two reverse transcription reactions performed from RNA samples for each transfection (see Figure 2.2), the error bars represent standard deviation. (Data provided by Dr Bryony Lloyd.)

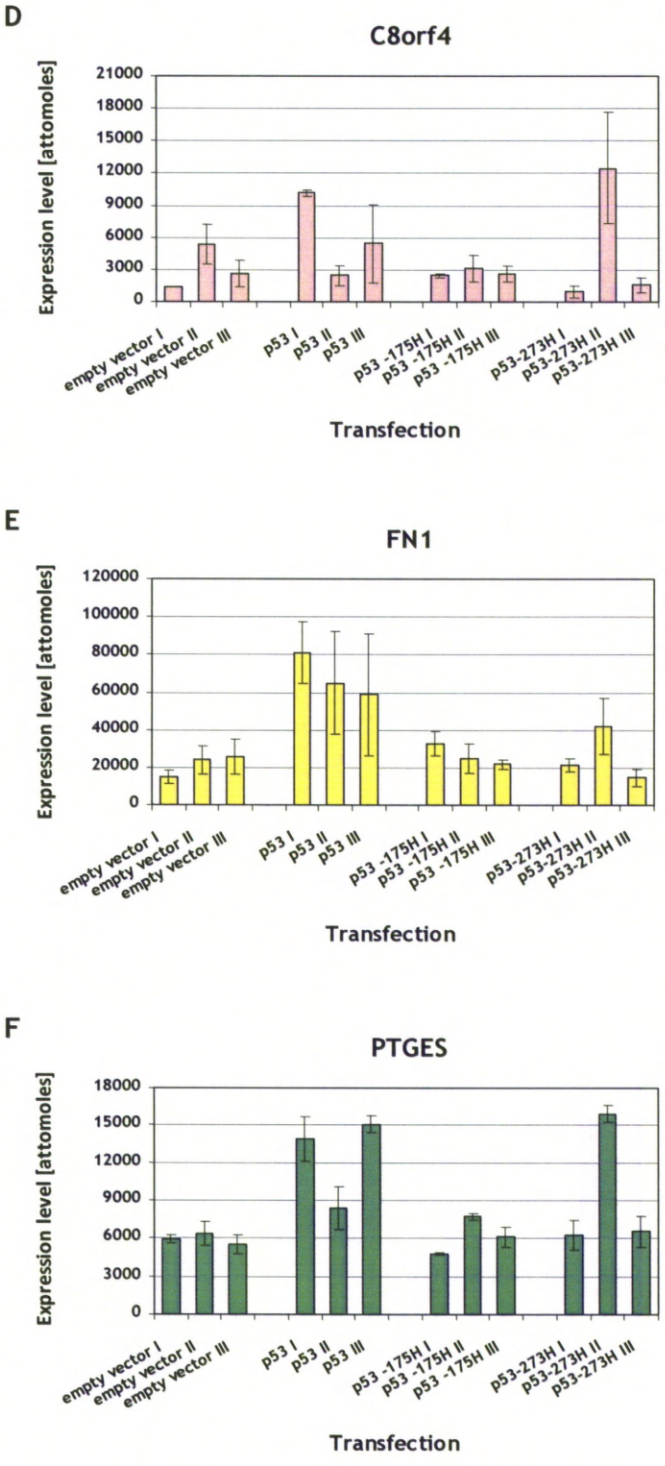

Figure 6.5 (cont.): Expression levels of the indicated genes in the individual transfections of H1299 cells. qRT-PCR was performed on RNA extracted from H1299 cells transiently transfected in triplicate with the indicated vectors. The histograms show mean of the average expression levels (normalised to histone H3 expression) from two reverse transcription reactions performed from RNA samples for each transfection (see Figure 2.2), the error bars represent standard deviation. (Data provided by Dr Bryony Lloyd.)

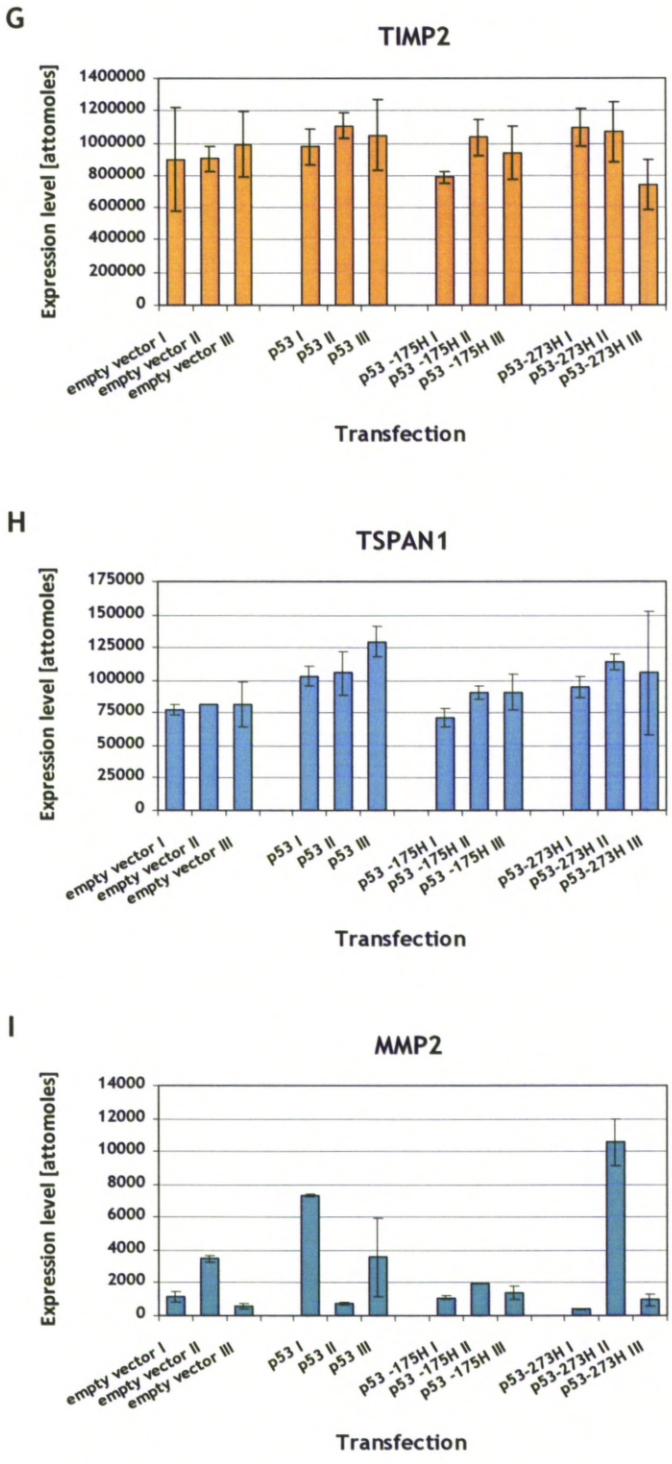

Figure 6.5 (cont.): Expression levels of the indicated genes in the individual transfections of H1299 cells. qRT-PCR was performed on RNA extracted from H1299 cells transiently transfected in triplicate with the indicated vectors. The histograms show mean of the average expression levels (normalised to histone H3 expression) from two reverse transcription reactions performed from RNA samples for each transfection (see Figure 2.2), the error bars represent standard deviation. (Data provided by Dr Bryony Lloyd.)

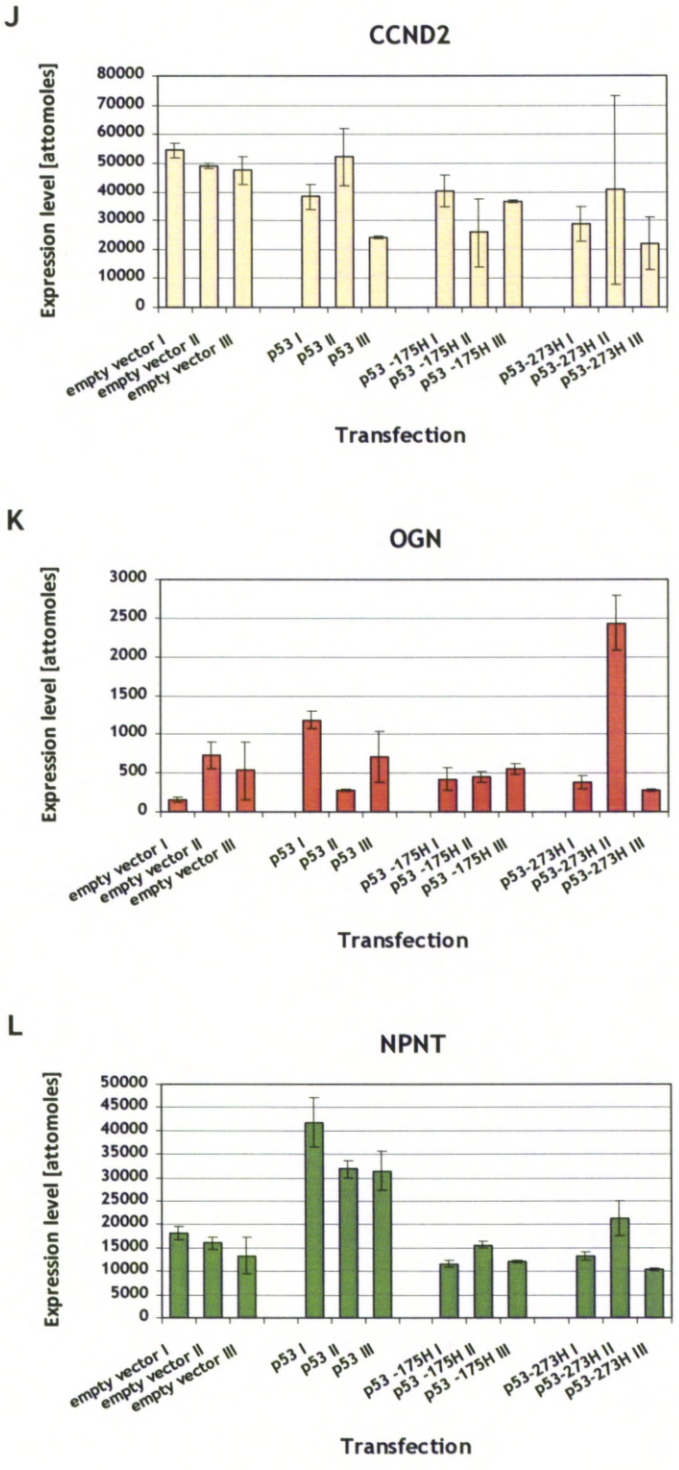

Figure 6.5 (cont.): Expression levels of the indicated genes in the individual transfections of H1299 cells. qRT-PCR was performed on RNA extracted from H1299 cells transiently transfected in triplicate with the indicated vectors. The histograms show mean of the average expression levels (normalised to histone H3 expression) from two reverse transcription reactions performed from RNA samples for each transfection (see Figure 2.2), the error bars represent standard deviation. (Data provided by Dr Bryony Lloyd.)

References

References

1. Hanahan, D. and Weinberg, R.A. (2000). The hallmarks of cancer. *Cell* **100**(1): 57-70.

2. Gibbs, W.W. (2003). Untangling the roots of cancer. *Sci Am* **289**(1): 56-65.

3. Vogelstein, B. and Kinzler, K.W. (2004). Cancer genes and the pathways they control. *Nat Med* **10**(8): 789-99.

4. Sun, W. and Yang, J. (2010). Functional mechanisms for human tumor suppressors. *J Cancer* **1**: 136-40.

5. Lang, G.A., Iwakuma, T., Suh, Y.A., Liu, G., Rao, V.A., Parant, J.M., Valentin-Vega, Y.A., Terzian, T., Caldwell, L.C., Strong, L.C., El-Naggar, A.K. and Lozano, G. (2004). Gain of function of a p53 hot spot mutation in a mouse model of Li-Fraumeni syndrome. *Cell* **119**(6): 861-72.

6. Olive, K.P., Tuveson, D.A., Ruhe, Z.C., Yin, B., Willis, N.A., Bronson, R.T., Crowley, D. and Jacks, T. (2004). Mutant p53 gain of function in two mouse models of Li-Fraumeni syndrome. *Cell* **119**(6): 847-60.

7. Sigal, A. and Rotter, V. (2000). Oncogenic mutations of the p53 tumor suppressor: the demons of the guardian of the genome. *Cancer Res* **60**(24): 6788-93.

8. Nelson, D.L. and Cox, M.M. (2004). Lehninger Principles of Biochemistry, p. 966-978. W. H. Freeman, New York.

9. Vogelstein, B. and Kinzler, K.W. (1993). The multistep nature of cancer. *Trends Genet* **9**(4): 138-41.

10. Ravindranath, Y. (2003). Recent advances in pediatric acute lymphoblastic and myeloid leukemia. *Curr Opin Oncol* **15**(1): 23-35.

11. Kroemer, G. and Pouyssegur, J. (2008). Tumor cell metabolism: cancer's Achilles' heel. *Cancer Cell* **13**(6): 472-82.

12. Hanahan, D. and Weinberg, R.A. (2011). Hallmarks of cancer: the next generation. *Cell* **144**(5): 646-74.

13. Balkwill, F., Charles, K.A. and Mantovani, A. (2005). Smoldering and polarized inflammation in the initiation and promotion of malignant disease. *Cancer Cell* 7(3): 211-7.

14. Dvorak, H.F. (1986). Tumors: wounds that do not heal. Similarities between tumor stroma generation and wound healing. *N Engl J Med* **315**(26): 1650-9.

15. Mantovani, A., Allavena, P., Sica, A. and Balkwill, F. (2008). Cancer-related inflammation. *Nature* **454**(7203): 436-44.

16. Luo, J., Solimini, N.L. and Elledge, S.J. (2009). Principles of cancer therapy: oncogene and non-oncogene addiction. *Cell* **136**(5): 823-37.

17. Batsakis, J.G. (1979). Tumors of the head and neck: clinical and pathological considerations. Williams & Wilkins, Baltimore.

18. Boyle, P. and Levin, B. (2008). "World Cancer Report". I. Press, Lyon.

19. Schlecht, N.F. (2005). Prognostic value of human papillomavirus in the survival of head and neck cancer patients: an overview of the evidence. *Oncol Rep* **14**(5): 1239-47.

20. Cooper, J.S., Pajak, T.F., Rubin, P., Tupchong, L., Brady, L.W., Leibel, S.A., Laramore, G.E., Marcial, V.A., Davis, L.W., Cox, J.D. and et al. (1989). Second malignancies in patients who have head and neck cancer: incidence, effect on survival and implications based on the RTOG experience. *Int J Radiat Oncol Biol Phys* **17**(3): 449-56.

21. Döbrőssy, L. (2005). Epidemiology of head and neck cancer: magnitude of the problem. *Cancer Metastasis Rev* **24**(1): 9-17.

22. IARC (1996). Cancer in the European Union in 1990. IARC, Lyon.

23. Stewart, B.W. and Kleihues, P. (2003). "World Cancer Report". I. Press, Lyon.

24. Bray, F., Sankila, R., Ferlay, J. and Parkin, D.M. (2002). Estimates of cancer incidence and mortality in Europe in 1995. *Eur J Cancer* **38**(1): 99-166.

25. Cancer Research UK. Available at: http://info.cancerresearchuk.org/cancerstats/types/larynx/incidence/index.htm. Accessed February 14, 2011.

26. Sturgis, E.M. and Cinciripini, P.M. (2007). Trends in head and neck cancer incidence in relation to smoking prevalence: an emerging epidemic of human papillomavirus-associated cancers? *Cancer* **110**(7): 1429-35.

27. Sherman, C.D., Jr. (1990). Cancer of the head and neck. IN *Manual of Clinical Oncology*. UICC, Springer.

28. Bosch, F.X., Ritter, D., Enders, C., Flechtenmacher, C., Abel, U., Dietz, A., Hergenhahn, M. and Weidauer, H. (2004). Head and neck tumor sites differ in prevalence and spectrum of p53 alterations but these have limited prognostic value. *Int J Cancer* **111**(4): 530-8.

29. Radiation Medical Group, Inc. Available at: http://www.rmg.md/cancers/head-neck/index.htm. Accessed February 14, 2011.

30. Brennan, J.A., Boyle, J.O., Koch, W.M., Goodman, S.N., Hruban, R.H., Eby, Y.J., Couch, M.J., Forastiere, A.A. and Sidransky, D. (1995). Association between cigarette smoking and mutation of the p53 gene in squamous-cell carcinoma of the head and neck. *N Engl J Med* **332**(11): 712-7.

31. Lewin, F., Norell, S.E., Johansson, H., Gustavsson, P., Wennerberg, J., Biorklund, A. and Rutqvist, L.E. (1998). Smoking tobacco, oral snuff, and alcohol in the etiology of squamous cell carcinoma of the head and neck: a population-based case-referent study in Sweden. *Cancer* **82**(7): 1367-75.

32. Mork, J., Lie, A.K., Glattre, E., Hallmans, G., Jellum, E., Koskela, P., Moller, B., Pukkala, E., Schiller, J.T., Youngman, L., Lehtinen, M. and Dillner, J. (2001). Human papillomavirus infection as a risk factor for squamous-cell carcinoma of the head and neck. *N Engl J Med* **344**(15): 1125-31.

33. Estève, J., Riboli, E., Péquignot, G., Terracini, B., Merletti, F., Crosignani, P., Ascunce, N., Zubiri, L., Blanchet, F., Raymond, L., Repetto, F. and Tuyns, A.J. (1996). Diet and cancers of the larynx and hypopharynx: the IARC multi-center study in southwestern Europe. *Cancer Causes Control* **7**(2): 240-52.

34. Gustavsson, P., Jakobsson, R., Johansson, H., Lewin, F., Norell, S. and Rutkvist, L.E. (1998). Occupational exposures and squamous cell carcinoma of the oral cavity, pharynx, larynx, and oesophagus: a case-control study in Sweden. *Occup Environ Med* **55**(6): 393-400.

35. Zheng, T.Z., Boyle, P., Hu, H.F., Duan, J., Jian, P.J., Ma, D.Q., Shui, L.P., Niu, S.R., Scully, C. and MacMahon, B. (1990). Dentition, oral hygiene, and risk of oral cancer: a case-control study in Beijing, People's Republic of China. *Cancer Causes Control* **1**(3): 235-41.

36. Elwood, J.M., Pearson, J.C., Skippen, D.H. and Jackson, S.M. (1984). Alcohol, smoking, social and occupational factors in the aetiology of cancer of the oral cavity, pharynx and larynx. *Int J Cancer* **34**(5): 603-12.

37. Mackillop, W.J., Zhang-Salomons, J., Boyd, C.J. and Groome, P.A. (2000). Associations between community income and cancer incidence in Canada and the United States. *Cancer* **89**(4): 901-12.

38. Maier, H., Dietz, A., Gewelke, U., Heller, W.D. and Weidauer, H. (1992). Tobacco and alcohol and the risk of head and neck cancer. *Clin Investig* **70**(3-4): 320-7.

39. Carbone, D. (1992). Smoking and cancer. *Am J Med* **93**(1A): 13S-17S.

40. WHO (2003). "The World Health Report – Shaping the Future", p. 91-95.

41. Tuyns, A.J., Esteve, J., Raymond, L., Berrino, F., Benhamou, E., Blanchet, F., Boffetta, P., Crosignani, P., del Moral, A., Lehmann, W. and et al. (1988). Cancer of the larynx/hypopharynx, tobacco and alcohol: IARC international case-control study

in Turin and Varese (Italy), Zaragoza and Navarra (Spain), Geneva (Switzerland) and Calvados (France). *Int J Cancer* **41**(4): 483-91.

42. Yu, G.P., Ostroff, J.S., Zhang, Z.F., Tang, J. and Schantz, S.P. (1997). Smoking history and cancer patient survival: a hospital cancer registry study. *Cancer Detect Prev* **21**(6): 497-509.

43. Spitz, M.R., Fueger, J.J., Goepfert, H., Hong, W.K. and Newell, G.R. (1988). Squamous cell carcinoma of the upper aerodigestive tract. A case comparison analysis. *Cancer* **61**(1): 203-8.

44. Boffetta, P., Hecht, S., Gray, N., Gupta, P. and Straif, K. (2008). Smokeless tobacco and cancer. *Lancet Oncol* **9**(7): 667-75.

45. Stockwell, H.G. and Lyman, G.H. (1986). Impact of smoking and smokeless tobacco on the risk of cancer of the head and neck. *Head Neck Surg* **9**(2): 104-10.

46. Attner, P., Du, J., Nasman, A., Hammarstedt, L., Ramqvist, T., Lindholm, J., Marklund, L., Dalianis, T. and Munck-Wikland, E. (2010). The role of human papillomavirus in the increased incidence of base of tongue cancer. *Int J Cancer* **126**(12): 2879-84.

47. IARC Working Group on the Evaluation of Carcinogenic Risks to Humans (1995). Human papillomaviruses, *IARC Monogr Eval Carcinog Risks Hum* **64**: 1-378. IARC, Lyon.

48. Syrjänen, K., Syrjänen, S., Lamberg, M., Pyrhönen, S. and Nuutinen, J. (1983). Morphological and immunohistochemical evidence suggesting human papillomavirus (HPV) involvement in oral squamous cell carcinogenesis. *Int J Oral Surg* **12**(6): 418-24.

49. Gillison, M.L., Koch, W.M., Capone, R.B., Spafford, M., Westra, W.H., Wu, L., Zahurak, M.L., Daniel, R.W., Viglione, M., Symer, D.E., Shah, K.V. and Sidransky, D. (2000). Evidence for a causal association between human papillomavirus and a subset of head and neck cancers. *J Natl Cancer Inst* **92**(9): 709-20.

50. McKaig, R.G., Baric, R.S. and Olshan, A.F. (1998). Human papillomavirus and head and neck cancer: epidemiology and molecular biology. *Head Neck* **20**(3): 250-65.

51. Dayyani, F., Etzel, C.J., Liu, M., Ho, C.H., Lippman, S.M. and Tsao, A.S. (2010). Meta-analysis of the impact of human papillomavirus (HPV) on cancer risk and overall survival in head and neck squamous cell carcinomas (HNSCC). *Head Neck Oncol* **2**: 15.

52. Kreimer, A.R., Clifford, G.M., Boyle, P. and Franceschi, S. (2005). Human papillomavirus types in head and neck squamous cell carcinomas worldwide: a systematic review. *Cancer Epidemiol Biomarkers Prev* **14**(2): 467-75.

53. Snow, A.N. and Laudadio, J. (2010). Human papillomavirus detection in head and neck squamous cell carcinomas. *Adv Anat Pathol* **17**(6): 394-403.

54. Torrente, M.C., Rodrigo, J.P., Haigentz, M., Jr., Dikkers, F.G., Rinaldo, A., Takes, R.P., Olofsson, J. and Ferlito, A. (2011). Human papillomavirus infections in laryngeal cancer. *Head Neck* **33**(4): 581-6.

55. Kim, L., King, T. and Agulnik, M. (2010). Head and neck cancer: changing epidemiology and public health implications. *Oncology (Williston Park)* **24**(10): 915-9, 924.

56. Cohen, M.A., Weinstein, G.S., O'Malley, B.W., Jr., Feldman, M. and Quon, H. (2011). Transoral robotic surgery and human papillomavirus status: Oncologic results. *Head Neck* **33**(4): 573-80.

57. Gungor, A., Cincik, H., Baloglu, H., Cekin, E., Dogru, S. and Dursun, E. (2007). Human papilloma virus prevalence in laryngeal squamous cell carcinoma. *J Laryngol Otol* **121**(8): 772-4.

58. Liu, B., Lu, Z., Wang, P., Basang, Z. and Rao, X. (2010). Prevalence of high-risk human papillomavirus types (HPV-16, HPV-18) and their physical status in primary laryngeal squamous cell carcinoma. *Neoplasma* **57**(6): 594-600.

59. Morshed, K. (2010). Association between human papillomavirus infection and laryngeal squamous cell carcinoma. *J Med Virol* **82**(6): 1017-23.

60. Ha, P.K., Pai, S.I., Westra, W.H., Gillison, M.L., Tong, B.C., Sidransky, D. and Califano, J.A. (2002). Real-time quantitative PCR demonstrates low prevalence of human papillomavirus type 16 in premalignant and malignant lesions of the oral cavity. *Clin Cancer Res* **8**(5): 1203-9.

61. van Houten, V.M., Snijders, P.J., van den Brekel, M.W., Kummer, J.A., Meijer, C.J., van Leeuwen, B., Denkers, F., Smeele, L.E., Snow, G.B. and Brakenhoff, R.H. (2001). Biological evidence that human papillomaviruses are etiologically involved in a subgroup of head and neck squamous cell carcinomas. *Int J Cancer* **93**(2): 232-5.

62. Khleif, S.N., DeGregori, J., Yee, C.L., Otterson, G.A., Kaye, F.J., Nevins, J.R. and Howley, P.M. (1996). Inhibition of cyclin D-CDK4/CDK6 activity is associated with an E2F-mediated induction of cyclin kinase inhibitor activity. *Proc Natl Acad Sci U S A* **93**(9): 4350-4.

63. Smeets, S.J., Hesselink, A.T., Speel, E.J., Haesevoets, A., Snijders, P.J., Pawlita, M., Meijer, C.J., Braakhuis, B.J., Leemans, C.R. and Brakenhoff, R.H. (2007). A novel algorithm for reliable detection of human papillomavirus in paraffin embedded head and neck cancer specimen. *Int J Cancer* **121**(11): 2465-72.

64. Baumann, J.L., Cohen, S., Evjen, A.N., Law, J.H., Vadivelu, S., Attia, A., Schindler, J.S., Chung, C.H., Wirth, P.S., Meijer, C.J., Snijders, P.J., Yarbrough, W.G. and Slebos, R.J. (2009). Human papillomavirus in early laryngeal carcinoma. *Laryngoscope* **119**(8): 1531-7.

65. Laco, J., Slaninka, I., Jirasek, M., Celakovsky, P., Vosmikova, H. and Ryska, A. (2008). High-risk human papillomavirus infection and p16INK4a protein expression in laryngeal lesions. *Pathol Res Pract* **204**(8): 545-52.

66. Weinberger, P.M., Yu, Z., Haffty, B.G., Kowalski, D., Harigopal, M., Brandsma, J., Sasaki, C., Joe, J., Camp, R.L., Rimm, D.L. and Psyrri, A. (2006). Molecular classification identifies a subset of human papillomavirus-associated oropharyngeal cancers with favorable prognosis. *J Clin Oncol* **24**(5): 736-47.

67. Hobbs, C.G., Sterne, J.A., Bailey, M., Heyderman, R.S., Birchall, M.A. and Thomas, S.J. (2006). Human papillomavirus and head and neck cancer: a systematic review and meta-analysis. *Clin Otolaryngol* **31**(4): 259-66.

68. Klozar, J., Kratochvil, V., Salakova, M., Smahelova, J., Vesela, E., Hamsikova, E., Betka, J. and Tachezy, R. (2008). HPV status and regional metastasis in the prognosis of oral and oropharyngeal cancer. *Eur Arch Otorhinolaryngol* **265 Suppl 1**: S75-82.

69. Smith, E.M., Wang, D., Kim, Y., Rubenstein, L.M., Lee, J.H., Haugen, T.H. and Turek, L.P. (2008). P16INK4a expression, human papillomavirus, and survival in head and neck cancer. *Oral Oncol* **44**(2): 133-42.

70. Fakhry, C., Westra, W.H., Li, S., Cmelak, A., Ridge, J.A., Pinto, H., Forastiere, A. and Gillison, M.L. (2008). Improved survival of patients with human papillomavirus-positive head and neck squamous cell carcinoma in a prospective clinical trial. *J Natl Cancer Inst* **100**(4): 261-9.

71. Worden, F.P., Kumar, B., Lee, J.S., Wolf, G.T., Cordell, K.G., Taylor, J.M., Urba, S.G., Eisbruch, A., Teknos, T.N., Chepeha, D.B., Prince, M.E., Tsien, C.I., D'Silva, N.J., Yang, K., Kurnit, D.M., Mason, H.L., Miller, T.H., Wallace, N.E., Bradford, C.R. and Carey, T.E. (2008). Chemoselection as a strategy for organ preservation in advanced oropharynx cancer: response and survival positively associated with HPV16 copy number. *J Clin Oncol* **26**(19): 3138-46.

72. Lucenteforte, E., Garavello, W., Bosetti, C. and La Vecchia, C. (2009). Dietary factors and oral and pharyngeal cancer risk. *Oral Oncol* **45**(6): 461-7.

73. Franco, E.L., Kowalski, L.P., Oliveira, B.V., Curado, M.P., Pereira, R.N., Silva, M.E., Fava, A.S. and Torloni, H. (1989). Risk factors for oral cancer in Brazil: a case-control study. *Int J Cancer* **43**(6): 992-1000.

74. Kasum, C.M., Jacobs, D.R., Jr., Nicodemus, K. and Folsom, A.R. (2002). Dietary risk factors for upper aerodigestive tract cancers. *Int J Cancer* **99**(2): 267-72.

75. Zheng, T., Boyle, P., Willett, W.C., Hu, H., Dan, J., Evstifeeva, T.V., Niu, S. and MacMahon, B. (1993). A case-control study of oral cancer in Beijing, People's Republic of China. Associations with nutrient intakes, foods and food groups. *Eur J Cancer B Oral Oncol* **29B**(1): 45-55.

76. Zheng, W., Blot, W.J., Shu, X.O., Diamond, E.L., Gao, Y.T., Ji, B.T. and Fraumeni, J.F., Jr. (1992). Risk factors for oral and pharyngeal cancer in Shanghai, with emphasis on diet. *Cancer Epidemiol Biomarkers Prev* **1**(6): 441-8.

77. De Stefani, E., Boffetta, P., Ronco, A.L., Correa, P., Oreggia, F., Deneo-Pellegrini, H., Mendilaharsu, M. and Leiva, J. (2005). Dietary patterns and risk of cancer of the oral cavity and pharynx in Uruguay. *Nutr Cancer* **51**(2): 132-9.

78. Franceschi, S., Favero, A., Conti, E., Talamini, R., Volpe, R., Negri, E., Barzan, L. and La Vecchia, C. (1999). Food groups, oils and butter, and cancer of the oral cavity and pharynx. *Br J Cancer* **80**(3-4): 614-20.

79. Talamini, R., Vaccarella, S., Barbone, F., Tavani, A., La Vecchia, C., Herrero, R., Muñoz, N. and Franceschi, S. (2000). Oral hygiene, dentition, sexual habits and risk of oral cancer. *Br J Cancer* **83**(9): 1238-42.

80. Marques, L.A., Eluf-Neto, J., Figueiredo, R.A., Góis-Filho, J.F., Kowalski, L.P., Carvalho, M.B., Abrahão, M. and Wünsch-Filho, V. (2008). Oral health, hygiene practices and oral cancer. *Rev Saude Publica* **42**(3): 471-9.

81. Homann, N., Tillonen, J., Rintamaki, H., Salaspuro, M., Lindqvist, C. and Meurman, J.H. (2001). Poor dental status increases acetaldehyde production from ethanol in saliva: a possible link to increased oral cancer risk among heavy drinkers. *Oral Oncol* **37**(2): 153-8.

82. Maier, H. and Tisch, M. (1999). Occupation and cancer of the head-neck area. *HNO* **47**(12): 1025-37.

83. IARC (1990). Cancer: Causes, Occurrence and Control. IARC Press, Lyon.

84. Bánóczy, J., Gintner, Z. and Dombi, C. (2001). Tobacco use and oral leukoplakia. *J Dent Educ* **65**(4): 322-7.

85. Brockstein, B. and Masters, G. (eds.) (2004). Head and Neck Cancer. IN *Cancer Treatment and Research*, S. T. Rosen (series ed.). Kluwer Academic Publishers, Dordrecht.

86. Priante, A.V., Castilho, E.C. and Kowalski, L.P. (2011). Second Primary Tumors in Patients with Head and Neck Cancer. *Curr Oncol Rep* **13**(2): 132-7.

87. Slaughter, D.P., Southwick, H.W. and Smejkal, W. (1953). Field cancerization in oral stratified squamous epithelium; clinical implications of multicentric origin. *Cancer* **6**(5): 963-8.

88. Allegra, E., Baudi, F., La Boria, A., Fagiani, F., Garozzo, A. and Costanzo, F.S. (2009). Multiple head and neck tumours and their genetic relationship. *Acta Otorhinolaryngol Ital* **29**(5): 237-41.

89. Bedi, G.C., Westra, W.H., Gabrielson, E., Koch, W. and Sidransky, D. (1996). Multiple head and neck tumors: evidence for a common clonal origin. *Cancer Res* **56**(11): 2484-7.

90. Tabor, M.P., Brakenhoff, R.H., Ruijter-Schippers, H.J., Van Der Wal, J.E., Snow, G.B., Leemans, C.R. and Braakhuis, B.J. (2002). Multiple head and neck tumors frequently originate from a single preneoplastic lesion. *Am J Pathol* **161**(3): 1051-60.

91. Scholes, A.G., Woolgar, J.A., Boyle, M.A., Brown, J.S., Vaughan, E.D., Hart, C.A., Jones, A.S. and Field, J.K. (1998). Synchronous oral carcinomas: independent or common clonal origin? *Cancer Res* **58**(9): 2003-6.

92. Leibel, S.A., Scott, C.B., Mohiuddin, M., Marcial, V.A., Coia, L.R., Davis, L.W. and Fuks, Z. (1991). The effect of local-regional control on distant metastatic dissemination in carcinoma of the head and neck: results of an analysis from the RTOG head and neck database. *Int J Radiat Oncol Biol Phys* **21**(3): 549-56.

93. Calhoun, K.H., Fulmer, P., Weiss, R. and Hokanson, J.A. (1994). Distant metastases from head and neck squamous cell carcinomas. *Laryngoscope* **104**(10): 1199-205.

94. Ghosh, S.K., Roland, N.J., Kumar, A., Tandon, S., Lancaster, J.L., Jackson, S.R., Jones, A., Lewis Jones, H., Hanlon, R. and Jones, T.M. (2009). Detection of synchronous lung tumors in patients presenting with squamous cell carcinoma of the head and neck. *Head Neck* **31**(12): 1563-70.

95. Osman, I., Sherman, E., Singh, B., Venkatraman, E., Zelefsky, M., Bosl, G., Scher, H., Shah, J., Shaha, A., Kraus, D., Cordon-Cardo, C. and Pfister, D.G. (2002). Alteration of p53 pathway in squamous cell carcinoma of the head and neck: impact on treatment outcome in patients treated with larynx preservation intent. *J Clin Oncol* **20**(13): 2980-7.

96. Hegde, P.U., Brenski, A.C., Caldarelli, D.D., Hutchinson, J., Panje, W.R., Wood, N.B., Leurgans, S., Preisler, H.D., Taylor, S.G.t., Caldarelli, L. and Coon, J.S. (1998). Tumor angiogenesis and p53 mutations: prognosis in head and neck cancer. *Arch Otolaryngol Head Neck Surg* **124**(1): 80-5.

97. Freier, K., Bosch, F.X., Flechtenmacher, C., Devens, F., Benner, A., Lichter, P., Joos, S. and Hofele, C. (2003). Distinct site-specific oncoprotein overexpression in head and neck squamous cell carcinoma: a tissue microarray analysis. *Anticancer Res* **23**(5A): 3971-7.

98. Vaidya, A.M., Petruzzelli, G.J., Clark, J. and Emami, B. (2001). Patterns of spread in recurrent head and neck squamous cell carcinoma. *Otolaryngol Head Neck Surg* **125**(4): 393-6.

99. Kumar, B., Cordell, K.G., Lee, J.S., Worden, F.P., Prince, M.E., Tran, H.H., Wolf, G.T., Urba, S.G., Chepeha, D.B., Teknos, T.N., Eisbruch, A., Tsien, C.I., Taylor, J.M., D'Silva, N.J., Yang, K., Kurnit, D.M., Bauer, J.A., Bradford, C.R. and Carey, T.E. (2008). EGFR, p16, HPV Titer, Bcl-xL and p53, sex, and smoking as indicators

of response to therapy and survival in oropharyngeal cancer. *J Clin Oncol* **26**(19): 3128-37.

100. McNeil, C. (2000). HPV in oropharyngeal cancers: new data inspire hope for vaccines. *J Natl Cancer Inst* **92**(9): 680-1.

101. Poeta, M.L., Manola, J., Goldwasser, M.A., Forastiere, A., Benoit, N., Califano, J.A., Ridge, J.A., Goodwin, J., Kenady, D., Saunders, J., Westra, W., Sidransky, D. and Koch, W.M. (2007). TP53 mutations and survival in squamous-cell carcinoma of the head and neck. *N Engl J Med* **357**(25): 2552-61.

102. Blons, H. and Laurent-Puig, P. (2003). TP53 and head and neck neoplasms. *Hum Mutat* **21**(3): 252-7.

103. Singer, B. and Essigmann, J.M. (1991). Site-specific mutagenesis: retrospective and prospective. *Carcinogenesis* **12**(6): 949-55.

104. Olivier, M., Eeles, R., Hollstein, M., Khan, M.A., Harris, C.C. and Hainaut, P. (2002). The IARC TP53 database: new online mutation analysis and recommendations to users. *Hum Mutat* **19**(6): 607-14.

105. Zhou, H., Zhu, L.X., Li, K. and Hei, T.K. (1999). Radon, tobacco-specific nitrosamine and mutagenesis in mammalian cells. *Mutat Res* **430**(1): 145-53.

106. Boyle, J.O., Hakim, J., Koch, W., van der Riet, P., Hruban, R.H., Roa, R.A., Correo, R., Eby, Y.J., Ruppert, J.M. and Sidransky, D. (1993). The incidence of p53 mutations increases with progression of head and neck cancer. *Cancer Res* **53**(19): 4477-80.

107. Hainaut, P., Soussi, T., Shomer, B., Hollstein, M., Greenblatt, M., Hovig, E., Harris, C.C. and Montesano, R. (1997). Database of p53 gene somatic mutations in human tumors and cell lines: updated compilation and future prospects. *Nucleic Acids Res* **25**(1): 151-7.

108. Tandon, S., Tudur-Smith, C., Riley, R.D., Boyd, M.T. and Jones, T.M. (2010). A systematic review of p53 as a prognostic factor of survival in squamous cell carcinoma of the four main anatomical subsites of the head and neck. *Cancer Epidemiol Biomarkers Prev* **19**(2): 574-87.

109. Park, H.W., Song, S.Y., Lee, T.J., Jeong, D. and Lee, T.Y. (2007). Abrogation of the p16-retinoblastoma-cyclin D1 pathway in head and neck squamous cell carcinomas. *Oncol Rep* **18**(1): 267-72.

110. Weinberg, R.A. (2007). The Biology of Cancer. Garland Science, Taylor & Francis Group, LLC, New York.

111. Kamb, A., Gruis, N.A., Weaver-Feldhaus, J., Liu, Q., Harshman, K., Tavtigian, S.V., Stockert, E., Day, R.S., 3rd, Johnson, B.E. and Skolnick, M.H. (1994). A cell cycle regulator potentially involved in genesis of many tumor types. *Science* **264**(5157): 436-40.

112. Kumar, R.V., Kadkol, S.S., Daniel, R., Shenoy, A.M. and Shah, K.V. (2003). Human papillomavirus, p53 and cyclin D1 expression in oropharyngeal carcinoma. *Int J Oral Maxillofac Surg* **32**(5): 539-43.

113. Michalides, R.J., van Veelen, N.M., Kristel, P.M., Hart, A.A., Loftus, B.M., Hilgers, F.J. and Balm, A.J. (1997). Overexpression of cyclin D1 indicates a poor prognosis in squamous cell carcinoma of the head and neck. *Arch Otolaryngol Head Neck Surg* **123**(5): 497-502.

114. Pignataro, L., Pruneri, G., Carboni, N., Capaccio, P., Cesana, B.M., Neri, A. and Buffa, R. (1998). Clinical relevance of cyclin D1 protein overexpression in laryngeal squamous cell carcinoma. *J Clin Oncol* **16**(9): 3069-77.

115. Miracca, E.C., Kowalski, L.P. and Nagai, M.A. (1999). High prevalence of p16 genetic alterations in head and neck tumours. *Br J Cancer* **81**(4): 677-83.

116. Reed, A.L., Califano, J., Cairns, P., Westra, W.H., Jones, R.M., Koch, W., Ahrendt, S., Eby, Y., Sewell, D., Nawroz, H., Bartek, J. and Sidransky, D. (1996). High frequency of p16 (CDKN2/MTS-1/INK4A) inactivation in head and neck squamous cell carcinoma. *Cancer Res* **56**(16): 3630-3.

117. Psyrri, A. and DiMaio, D. (2008). Human papillomavirus in cervical and head-and-neck cancer. *Nat Clin Pract Oncol* **5**(1): 24-31.

118. Fallai, C., Perrone, F., Licitra, L., Pilotti, S., Locati, L., Bossi, P., Orlandi, E., Palazzi, M. and Olmi, P. (2009). Oropharyngeal squamous cell carcinoma treated with radiotherapy or radiochemotherapy: prognostic role of TP53 and HPV status. *Int J Radiat Oncol Biol Phys* **75**(4): 1053-9.

119. Hubbert, N.L., Sedman, S.A. and Schiller, J.T. (1992). Human papillomavirus type 16 E6 increases the degradation rate of p53 in human keratinocytes. *J Virol* **66**(10): 6237-41.

120. Klingelhutz, A.J., Foster, S.A. and McDougall, J.K. (1996). Telomerase activation by the E6 gene product of human papillomavirus type 16. *Nature* **380**(6569): 79-82.

121. Liu, X., Dakic, A., Zhang, Y., Dai, Y., Chen, R. and Schlegel, R. (2009). HPV E6 protein interacts physically and functionally with the cellular telomerase complex. *Proc Natl Acad Sci U S A* **106**(44): 18780-5.

122. Mao, L., El-Naggar, A.K., Fan, Y.H., Lee, J.S., Lippman, S.M., Kayser, S., Lotan, R. and Hong, W.K. (1996). Telomerase activity in head and neck squamous cell carcinoma and adjacent tissues. *Cancer Res* **56**(24): 5600-4.

123. Boyer, S.N., Wazer, D.E. and Band, V. (1996). E7 protein of human papilloma virus-16 induces degradation of retinoblastoma protein through the ubiquitin-proteasome pathway. *Cancer Res* **56**(20): 4620-4.

124. Zhang, H.S., Postigo, A.A. and Dean, D.C. (1999). Active transcriptional repression by the Rb-E2F complex mediates G1 arrest triggered by p16INK4a, TGFbeta, and contact inhibition. *Cell* **97**(1): 53-61.

125. Klussmann, J.P., Gultekin, E., Weissenborn, S.J., Wieland, U., Dries, V., Dienes, H.P., Eckel, H.E., Pfister, H.J. and Fuchs, P.G. (2003). Expression of p16 protein identifies a distinct entity of tonsillar carcinomas associated with human papillomavirus. *Am J Pathol* **162**(3): 747-53.

126. Ozanne, B., Richards, C.S., Hendler, F., Burns, D. and Gusterson, B. (1986). Over-expression of the EGF receptor is a hallmark of squamous cell carcinomas. *J Pathol* **149**(1): 9-14.

127. Grandis, J.R. and Tweardy, D.J. (1993). Elevated levels of transforming growth factor alpha and epidermal growth factor receptor messenger RNA are early markers of carcinogenesis in head and neck cancer. *Cancer Res* **53**(15): 3579-84.

128. Herbst, R.S. (2004). Review of epidermal growth factor receptor biology. *Int J Radiat Oncol Biol Phys* **59**(2 Suppl): 21-6.

129. Lin, S.Y., Makino, K., Xia, W., Matin, A., Wen, Y., Kwong, K.Y., Bourguignon, L. and Hung, M.C. (2001). Nuclear localization of EGF receptor and its potential new role as a transcription factor. *Nat Cell Biol* **3**(9): 802-8.

130. Pinto, C., Barone, C.A., Girolomoni, G., Russi, E.G., Carlo Merlano, M., Ferrari, D. and Maiello, E. (2011). Management of Skin Toxicity Associated with Cetuximab Treatment in Combination with Chemotherapy or Radiotherapy. *Oncologist* **16**(2): 228-38.

131. Numico, G., Silvestris, N. and Grazioso Russi, E. (2011). Advances in EGFR-directed therapy in head and neck cancer. *Front Biosci (Schol Ed)* **3**: 454-66.

132. Raza, S., Kornblum, N., Kancharla, V.P., Baig, M.A., Singh, A.B. and Kalavar, M. (2011). Emerging Therapies in the Treatment of Locally Advanced Squamous Cell Cancers of Head and Neck. *Recent Pat Anticancer Drug Discov* **6**(2): 246-57.

133. Leemans, C.R., Braakhuis, B.J. and Brakenhoff, R.H. (2011). The molecular biology of head and neck cancer. *Nat Rev Cancer* **11**(1): 9-22.

134. Vogelstein, B., Lane, D. and Levine, A.J. (2000). Surfing the p53 network. *Nature* **408**(6810): 307-10.

135. Lane, D.P. and Crawford, L.V. (1979). T antigen is bound to a host protein in SV40-transformed cells. *Nature* **278**(5701): 261-3.

136. Rotter, V., Abutbul, H. and Wolf, D. (1983). The presence of p53 transformation-related protein in Ab-MuLV transformed cells is required for their development into lethal tumors in mice. *Int J Cancer* **31**(3): 315-20.

137. Levine, A.J. (1989). The p53 tumor suppressor gene and gene product. *Princess Takamatsu Symp* **20**: 221-30.

138. Nigro, J.M., Baker, S.J., Preisinger, A.C., Jessup, J.M., Hostetter, R., Cleary, K., Bigner, S.H., Davidson, N., Baylin, S., Devilee, P. and et al. (1989). Mutations in the p53 gene occur in diverse human tumour types. *Nature* **342**(6250): 705-8.

139. Petitjean, A., Mathe, E., Kato, S., Ishioka, C., Tavtigian, S.V., Hainaut, P. and Olivier, M. (2007). Impact of mutant p53 functional properties on TP53 mutation patterns and tumor phenotype: lessons from recent developments in the IARC TP53 database (version R15). *Hum Mutat* **28**(6): 622-9.

140. Schmieg, F.I. and Simmons, D.T. (1988). Characterization of the in vitro interaction between SV40 T antigen and p53: mapping the p53 binding site. *Virology* **164**(1): 132-40.

141. Unger, T., Nau, M.M., Segal, S. and Minna, J.D. (1992). p53: a transdominant regulator of transcription whose function is ablated by mutations occurring in human cancer. *EMBO J* **11**(4): 1383-90.

142. Horikoshi, N., Usheva, A., Chen, J., Levine, A.J., Weinmann, R. and Shenk, T. (1995). Two domains of p53 interact with the TATA-binding protein, and the adenovirus 13S E1A protein disrupts the association, relieving p53-mediated transcriptional repression. *Mol Cell Biol* **15**(1): 227-34.

143. Lu, H. and Levine, A.J. (1995). Human TAFII31 protein is a transcriptional coactivator of the p53 protein. *Proc Natl Acad Sci U S A* **92**(11): 5154-8.

144. Xiao, H., Pearson, A., Coulombe, B., Truant, R., Zhang, S., Regier, J.L., Triezenberg, S.J., Reinberg, D., Flores, O., Ingles, C.J. and et al. (1994). Binding of basal transcription factor TFIIH to the acidic activation domains of VP16 and p53. *Mol Cell Biol* **14**(10): 7013-24.

145. Lin, J., Wu, X., Chen, J., Chang, A. and Levine, A.J. (1994). Functions of the p53 protein in growth regulation and tumor suppression. *Cold Spring Harb Symp Quant Biol* **59**: 215-23.

146. Bargonetti, J., Manfredi, J.J., Chen, X., Marshak, D.R. and Prives, C. (1993). A proteolytic fragment from the central region of p53 has marked sequence-specific DNA-binding activity when generated from wild-type but not from oncogenic mutant p53 protein. *Genes Dev* 7(12B): 2565-74.

147. Cho, Y., Gorina, S., Jeffrey, P.D. and Pavletich, N.P. (1994). Crystal structure of a p53 tumor suppressor-DNA complex: understanding tumorigenic mutations. *Science* **265**(5170): 346-55.

148. Pavletich, N.P., Chambers, K.A. and Pabo, C.O. (1993). The DNA-binding domain of p53 contains the four conserved regions and the major mutation hot spots. *Genes Dev* 7(12B): 2556-64.

149. Lee, W., Harvey, T.S., Yin, Y., Yau, P., Litchfield, D. and Arrowsmith, C.H. (1994). Solution structure of the tetrameric minimum transforming domain of p53. *Nat Struct Biol* **1**(12): 877-90.

150. Jeffrey, P.D., Gorina, S. and Pavletich, N.P. (1995). Crystal structure of the tetramerization domain of the p53 tumor suppressor at 1.7 angstroms. *Science* **267**(5203): 1498-502.

151. Wang, Y., Reed, M., Wang, P., Stenger, J.E., Mayr, G., Anderson, M.E., Schwedes, J.F. and Tegtmeyer, P. (1993). p53 domains: identification and characterization of two autonomous DNA-binding regions. *Genes Dev* **7**(12B): 2575-86.

152. Lee, S., Elenbaas, B., Levine, A. and Griffith, J. (1995). p53 and its 14 kDa C-terminal domain recognize primary DNA damage in the form of insertion/deletion mismatches. *Cell* **81**(7): 1013-20.

153. Brain, R. and Jenkins, J.R. (1994). Human p53 directs DNA strand reassociation and is photolabelled by 8-azido ATP. *Oncogene* **9**(6): 1775-80.

154. Malecka, K.A., Ho, W.C. and Marmorstein, R. (2009). Crystal structure of a p53 core tetramer bound to DNA. *Oncogene* **28**(3): 325-33.

155. Laptenko, O. and Prives, C. (2006). Transcriptional regulation by p53: one protein, many possibilities. *Cell Death Differ* **13**(6): 951-61.

156. El-Deiry, W.S., Kern, S.E., Pietenpol, J.A., Kinzler, K.W. and Vogelstein, B. (1992). Definition of a consensus binding site for p53. *Nat Genet* **1**(1): 45-9.

157. Riley, T., Sontag, E., Chen, P. and Levine, A. (2008). Transcriptional control of human p53-regulated genes. *Nat Rev Mol Cell Biol* **9**(5): 402-12.

158. Pal, S., Datta, K. and Mukhopadhyay, D. (2001). Central role of p53 on regulation of vascular permeability factor/vascular endothelial growth factor (VPF/VEGF) expression in mammary carcinoma. *Cancer Res* **61**(18): 6952-7.

159. Ueba, T., Nosaka, T., Takahashi, J.A., Shibata, F., Florkiewicz, R.Z., Vogelstein, B., Oda, Y., Kikuchi, H. and Hatanaka, M. (1994). Transcriptional regulation of basic fibroblast growth factor gene by p53 in human glioblastoma and hepatocellular carcinoma cells. *Proc Natl Acad Sci U S A* **91**(19): 9009-13.

160. Subbaramaiah, K., Altorki, N., Chung, W.J., Mestre, J.R., Sampat, A. and Dannenberg, A.J. (1999). Inhibition of cyclooxygenase-2 gene expression by p53. *J Biol Chem* **274**(16): 10911-5.

161. Murphy, M., Ahn, J., Walker, K.K., Hoffman, W.H., Evans, R.M., Levine, A.J. and George, D.L. (1999). Transcriptional repression by wild-type p53 utilizes histone deacetylases, mediated by interaction with mSin3a. *Genes Dev* **13**(19): 2490-501.

162. Koumenis, C., Alarcon, R., Hammond, E., Sutphin, P., Hoffman, W., Murphy, M., Derr, J., Taya, Y., Lowe, S.W., Kastan, M. and Giaccia, A. (2001). Regulation of p53 by hypoxia: dissociation of transcriptional repression and apoptosis from p53-dependent transactivation. *Mol Cell Biol* **21**(4): 1297-310.

163. Vousden, K.H. and Lane, D.P. (2007). p53 in health and disease. *Nat Rev Mol Cell Biol* **8**(4): 275-83.

164. Zhao, R., Gish, K., Murphy, M., Yin, Y., Notterman, D., Hoffman, W.H., Tom, E., Mack, D.H. and Levine, A.J. (2000). Analysis of p53-regulated gene expression patterns using oligonucleotide arrays. *Genes Dev* **14**(8): 981-93.

165. Kannan, K., Amariglio, N., Rechavi, G., Jakob-Hirsch, J., Kela, I., Kaminski, N., Getz, G., Domany, E. and Givol, D. (2001). DNA microarrays identification of primary and secondary target genes regulated by p53. *Oncogene* **20**(18): 2225-34.

166. Frebourg, T., Kassel, J., Lam, K.T., Gryka, M.A., Barbier, N., Andersen, T.I., Borresen, A.L. and Friend, S.H. (1992). Germ-line mutations of the p53 tumor suppressor gene in patients with high risk for cancer inactivate the p53 protein. *Proc Natl Acad Sci U S A* **89**(14): 6413-7.

167. Abbas, T. and Dutta, A. (2009). p21 in cancer: intricate networks and multiple activities. *Nat Rev Cancer* **9**(6): 400-14.

168. Pines, J. and Hunter, T. (1991). Cyclin-dependent kinases: a new cell cycle motif? *Trends Cell Biol* **1**(5): 117-21.

169. Marx, J. (1993). How p53 suppresses cell growth. *Science* **262**(5140): 1644-5.

170. Xiong, Y. and Beach, D. (1991). Population explosion in the cyclin family. *Curr Biol* **1**(6): 362-4.

171. Xiong, Y., Hannon, G.J., Zhang, H., Casso, D., Kobayashi, R. and Beach, D. (1993). p21 is a universal inhibitor of cyclin kinases. *Nature* **366**(6456): 701-4.

172. Waga, S., Hannon, G.J., Beach, D. and Stillman, B. (1994). The p21 inhibitor of cyclin-dependent kinases controls DNA replication by interaction with PCNA. *Nature* **369**(6481): 574-8.

173. Waldman, T., Kinzler, K.W. and Vogelstein, B. (1995). p21 is necessary for the p53-mediated G1 arrest in human cancer cells. *Cancer Res* **55**(22): 5187-90.

174. Marx, J. (1994). New link found between p53 and DNA repair. *Science* **266**(5189): 1321-2.

175. Zhan, Q., Antinore, M.J., Wang, X.W., Carrier, F., Smith, M.L., Harris, C.C. and Fornace, A.J., Jr. (1999). Association with Cdc2 and inhibition of Cdc2/Cyclin B1 kinase activity by the p53-regulated protein Gadd45. *Oncogene* **18**(18): 2892-900.

176. Mhawech, P. (2005). 14-3-3 proteins - an update. *Cell Res* **15**(4): 228-36.

177. Chan, T.A., Hermeking, H., Lengauer, C., Kinzler, K.W. and Vogelstein, B. (1999). 14-3-3Sigma is required to prevent mitotic catastrophe after DNA damage. *Nature* **401**(6753): 616-20.

178. Heald, R., McLoughlin, M. and McKeon, F. (1993). Human wee1 maintains mitotic timing by protecting the nucleus from cytoplasmically activated Cdc2 kinase. *Cell* **74**(3): 463-74.

179. Jin, P., Hardy, S. and Morgan, D.O. (1998). Nuclear localization of cyclin B1 controls mitotic entry after DNA damage. *J Cell Biol* **141**(4): 875-85.

180. Ohki, R., Nemoto, J., Murasawa, H., Oda, E., Inazawa, J., Tanaka, N. and Taniguchi, T. (2000). Reprimo, a new candidate mediator of the p53-mediated cell cycle arrest at the G2 phase. *J Biol Chem* **275**(30): 22627-30.

181. El-Deiry, W.S. (1998). Regulation of p53 downstream genes. *Semin Cancer Biol* **8**(5): 345-57.

182. Bates, S. and Vousden, K.H. (1999). Mechanisms of p53-mediated apoptosis. *Cell Mol Life Sci* **55**(1): 28-37.

183. Yu, J. and Zhang, L. (2005). The transcriptional targets of p53 in apoptosis control. *Biochem Biophys Res Commun* **331**(3): 851-8.

184. Haupt, S., Berger, M., Goldberg, Z. and Haupt, Y. (2003). Apoptosis - the p53 network. *J Cell Sci* **116**(Pt 20): 4077-85.

185. Cohen, G.M. (1997). Caspases: the executioners of apoptosis. *Biochem J* **326 (Pt 1)**: 1-16.

186. Ashkenazi, A. and Dixit, V.M. (1998). Death receptors: signaling and modulation. *Science* **281**(5381): 1305-8.

187. Kroemer, G. (2003). Mitochondrial control of apoptosis: an introduction. *Biochem Biophys Res Commun* **304**(3): 433-5.

188. Li, P., Nijhawan, D., Budihardjo, I., Srinivasula, S.M., Ahmad, M., Alnemri, E.S. and Wang, X. (1997). Cytochrome c and dATP-dependent formation of Apaf-1/caspase-9 complex initiates an apoptotic protease cascade. *Cell* **91**(4): 479-89.

189. Polyak, K., Xia, Y., Zweier, J.L., Kinzler, K.W. and Vogelstein, B. (1997). A model for p53-induced apoptosis. *Nature* **389**(6648): 300-5.

190. Thorburn, A. (2004). Death receptor-induced cell killing. *Cell Signal* **16**(2): 139-44.

191. Nagata, S. and Golstein, P. (1995). The Fas death factor. *Science* **267**(5203): 1449-56.

192. Owen-Schaub, L.B., Zhang, W., Cusack, J.C., Angelo, L.S., Santee, S.M., Fujiwara, T., Roth, J.A., Deisseroth, A.B., Zhang, W.W., Kruzel, E. and et al. (1995). Wild-type human p53 and a temperature-sensitive mutant induce Fas/APO-1 expression. *Mol Cell Biol* **15**(6): 3032-40.

193. Bennett, M., Macdonald, K., Chan, S.W., Luzio, J.P., Simari, R. and Weissberg, P. (1998). Cell surface trafficking of Fas: a rapid mechanism of p53-mediated apoptosis. *Science* **282**(5387): 290-3.

194. Fukazawa, T., Fujiwara, T., Morimoto, Y., Shao, J., Nishizaki, M., Kadowaki, Y., Hizuta, A., Owen-Schaub, L.B., Roth, J.A. and Tanaka, N. (1999). Differential involvement of the CD95 (Fas/APO-1) receptor/ligand system on apoptosis induced by the wild-type p53 gene transfer in human cancer cells. *Oncogene* **18**(13): 2189-99.

195. Wu, G.S., Burns, T.F., McDonald, E.R., 3rd, Jiang, W., Meng, R., Krantz, I.D., Kao, G., Gan, D.D., Zhou, J.Y., Muschel, R., Hamilton, S.R., Spinner, N.B., Markowitz, S., Wu, G. and el-Deiry, W.S. (1997). KILLER/DR5 is a DNA damage-inducible p53-regulated death receptor gene. *Nat Genet* **17**(2): 141-3.

196. Pitti, R.M., Marsters, S.A., Ruppert, S., Donahue, C.J., Moore, A. and Ashkenazi, A. (1996). Induction of apoptosis by Apo-2 ligand, a new member of the tumor necrosis factor cytokine family. *J Biol Chem* **271**(22): 12687-90.

197. Lin, Y., Ma, W. and Benchimol, S. (2000). Pidd, a new death-domain-containing protein, is induced by p53 and promotes apoptosis. *Nat Genet* **26**(1): 122-7.

198. Berube, C., Boucher, L.M., Ma, W., Wakeham, A., Salmena, L., Hakem, R., Yeh, W.C., Mak, T.W. and Benchimol, S. (2005). Apoptosis caused by p53-induced protein with death domain (PIDD) depends on the death adapter protein RAIDD. *Proc Natl Acad Sci U S A* **102**(40): 14314-20.

199. Miyashita, T. and Reed, J.C. (1995). Tumor suppressor p53 is a direct transcriptional activator of the human bax gene. *Cell* **80**(2): 293-9.

200. Oltvai, Z.N., Milliman, C.L. and Korsmeyer, S.J. (1993). Bcl-2 heterodimerizes in vivo with a conserved homolog, Bax, that accelerates programmed cell death. *Cell* **74**(4): 609-19.

201. Knudson, C.M., Tung, K.S., Tourtellotte, W.G., Brown, G.A. and Korsmeyer, S.J. (1995). Bax-deficient mice with lymphoid hyperplasia and male germ cell death. *Science* **270**(5233): 96-9.

202. Strasser, A., Harris, A.W., Huang, D.C., Krammer, P.H. and Cory, S. (1995). Bcl-2 and Fas/APO-1 regulate distinct pathways to lymphocyte apoptosis. *EMBO J* **14**(24): 6136-47.

203. Oda, E., Ohki, R., Murasawa, H., Nemoto, J., Shibue, T., Yamashita, T., Tokino, T., Taniguchi, T. and Tanaka, N. (2000). Noxa, a BH3-only member of the Bcl-2 family and candidate mediator of p53-induced apoptosis. *Science* **288**(5468): 1053-8.

204. Nakano, K. and Vousden, K.H. (2001). PUMA, a novel proapoptotic gene, is induced by p53. *Mol Cell* **7**(3): 683-94.

205. Oda, K., Arakawa, H., Tanaka, T., Matsuda, K., Tanikawa, C., Mori, T., Nishimori, H., Tamai, K., Tokino, T., Nakamura, Y. and Taya, Y. (2000). p53AIP1, a potential mediator of p53-dependent apoptosis, and its regulation by Ser-46-phosphorylated p53. *Cell* **102**(6): 849-62.

206. Robles, A.I., Bemmels, N.A., Foraker, A.B. and Harris, C.C. (2001). APAF-1 is a transcriptional target of p53 in DNA damage-induced apoptosis. *Cancer Res* **61**(18): 6660-4.

207. MacLachlan, T.K. and El-Deiry, W.S. (2002). Apoptotic threshold is lowered by p53 transactivation of caspase-6. *Proc Natl Acad Sci U S A* **99**(14): 9492-7.

208. Budhram-Mahadeo, V., Morris, P.J., Smith, M.D., Midgley, C.A., Boxer, L.M. and Latchman, D.S. (1999). p53 suppresses the activation of the Bcl-2 promoter by the Brn-3a POU family transcription factor. *J Biol Chem* **274**(21): 15237-44.

209. Miyashita, T., Krajewski, S., Krajewska, M., Wang, H.G., Lin, H.K., Liebermann, D.A., Hoffman, B. and Reed, J.C. (1994). Tumor suppressor p53 is a regulator of bcl-2 and bax gene expression in vitro and in vivo. *Oncogene* **9**(6): 1799-805.

210. Miyashita, T., Harigai, M., Hanada, M. and Reed, J.C. (1994). Identification of a p53-dependent negative response element in the bcl-2 gene. *Cancer Res* **54**(12): 3131-5.

211. Tomita, Y., Marchenko, N., Erster, S., Nemajerova, A., Dehner, A., Klein, C., Pan, H., Kessler, H., Pancoska, P. and Moll, U.M. (2006). WT p53, but not tumor-derived mutants, bind to Bcl2 via the DNA binding domain and induce mitochondrial permeabilization. *J Biol Chem* **281**(13): 8600-6.

212. Yamaoka, A., Kuwabara, I., Frigeri, L.G. and Liu, F.T. (1995). A human lectin, galectin-3 (epsilon bp/Mac-2), stimulates superoxide production by neutrophils. *J Immunol* **154**(7): 3479-87.

213. Rao, P.V., Krishna, C.M. and Zigler, J.S., Jr. (1992). Identification and characterization of the enzymatic activity of zeta-crystallin from guinea pig lens. A novel NADPH:quinone oxidoreductase. *J Biol Chem* **267**(1): 96-102.

214. Rienhoff, H.Y., Jr., Huang, J.H., Li, X.X. and Liao, W.S. (1990). Molecular and cellular biology of serum amyloid A. *Mol Biol Med* **7**(3): 287-98.

215. Hayward, D.C., Delaney, S.J., Campbell, H.D., Ghysen, A., Benzer, S., Kasprzak, A.B., Cotsell, J.N., Young, I.G. and Miklos, G.L. (1993). The sluggish-A gene of Drosophila melanogaster is expressed in the nervous system and encodes proline oxidase, a mitochondrial enzyme involved in glutamate biosynthesis. *Proc Natl Acad Sci U S A* **90**(7): 2979-83.

216. Lehar, S.M., Nacht, M., Jacks, T., Vater, C.A., Chittenden, T. and Guild, B.C. (1996). Identification and cloning of EI24, a gene induced by p53 in etoposide-treated cells. *Oncogene* **12**(6): 1181-7.

217. Liu, B., Chen, Y. and St Clair, D.K. (2008). ROS and p53: a versatile partnership. *Free Radic Biol Med* **44**(8): 1529-35.

218. Budanov, A.V., Sablina, A.A., Feinstein, E., Koonin, E.V. and Chumakov, P.M. (2004). Regeneration of peroxiredoxins by p53-regulated sestrins, homologs of bacterial AhpD. *Science* **304**(5670): 596-600.

219. Tan, M., Li, S., Swaroop, M., Guan, K., Oberley, L.W. and Sun, Y. (1999). Transcriptional activation of the human glutathione peroxidase promoter by p53. *J Biol Chem* **274**(17): 12061-6.

220. Tomko, R.J., Jr., Bansal, P. and Lazo, J.S. (2006). Airing out an antioxidant role for the tumor suppressor p53. *Mol Interv* **6**(1): 23-5, 2.

221. Vlatković, N., Crawford, K., Rubbi, C.P. and Boyd, M.T. (2011). Tissue-specific therapeutic targeting of p53 in cancer: one size does not fit all. *Curr Pharm Des* **17**(6): 618-30.

222. Vousden, K.H. and Prives, C. (2009). Blinded by the Light: The Growing Complexity of p53. *Cell* **137**(3): 413-31.

223. Komarov, P.G., Komarova, E.A., Kondratov, R.V., Christov-Tselkov, K., Coon, J.S., Chernov, M.V. and Gudkov, A.V. (1999). A chemical inhibitor of p53 that protects mice from the side effects of cancer therapy. *Science* **285**(5434): 1733-7.

224. Schwieger, A., Bauer, L., Hanusch, J., Sers, C., Schafer, R. and Bauer, G. (2001). *ras* oncogene expression determines sensitivity for intercellular induction of apoptosis. *Carcinogenesis* **22**(9): 1385-92.

225. Vousden, K.H. (2000). p53: death star. *Cell* **103**(5): 691-4.

226. Attardi, L.D., Reczek, E.E., Cosmas, C., Demicco, E.G., McCurrach, M.E., Lowe, S.W. and Jacks, T. (2000). PERP, an apoptosis-associated target of p53, is a novel member of the PMP-22/gas3 family. *Genes Dev* **14**(6): 704-18.

227. Relaix, F., Wei, X., Li, W., Pan, J., Lin, Y., Bowtell, D.D., Sassoon, D.A. and Wu, X. (2000). Pw1/Peg3 is a potential cell death mediator and cooperates with Siah1a in p53-mediated apoptosis. *Proc Natl Acad Sci U S A* **97**(5): 2105-10.

228. Chen, X., Ko, L.J., Jayaraman, L. and Prives, C. (1996). p53 levels, functional domains, and DNA damage determine the extent of the apoptotic response of tumor cells. *Genes Dev* **10**(19): 2438-51.

229. Thornborrow, E.C. and Manfredi, J.J. (1999). One mechanism for cell type-specific regulation of the bax promoter by the tumor suppressor p53 is dictated by the p53 response element. *J Biol Chem* **274**(47): 33747-56.

230. Espinosa, J.M. and Emerson, B.M. (2001). Transcriptional regulation by p53 through intrinsic DNA/chromatin binding and site-directed cofactor recruitment. *Mol Cell* **8**(1): 57-69.

231. Shikama, N., Lee, C.W., France, S., Delavaine, L., Lyon, J., Krstic-Demonacos, M. and La Thangue, N.B. (1999). A novel cofactor for p300 that regulates the p53 response. *Mol Cell* **4**(3): 365-76.

232. Samuels-Lev, Y., O'Connor, D.J., Bergamaschi, D., Trigiante, G., Hsieh, J.K., Zhong, S., Campargue, I., Naumovski, L., Crook, T. and Lu, X. (2001). ASPP proteins specifically stimulate the apoptotic function of p53. *Mol Cell* **8**(4): 781-94.

233. Flores, E.R., Tsai, K.Y., Crowley, D., Sengupta, S., Yang, A., McKeon, F. and Jacks, T. (2002). p63 and p73 are required for p53-dependent apoptosis in response to DNA damage. *Nature* **416**(6880): 560-4.

234. Wynford-Thomas, D. (1996). Telomeres, p53 and cellular senescence. *Oncol Res* **8**(10-11): 387-98.

235. Lowe, S.W., Cepero, E. and Evan, G. (2004). Intrinsic tumour suppression. *Nature* **432**(7015): 307-15.

236. Campisi, J. (2000). Cancer, aging and cellular senescence. *In Vivo* **14**(1): 183-8.

237. Chiu, C.P. and Harley, C.B. (1997). Replicative senescence and cell immortality: the role of telomeres and telomerase. *Proc Soc Exp Biol Med* **214**(2): 99-106.

238. Campisi, J. (2001). Cellular senescence as a tumor-suppressor mechanism. *Trends Cell Biol* **11**(11): S27-31.

239. Bringold, F. and Serrano, M. (2000). Tumor suppressors and oncogenes in cellular senescence. *Exp Gerontol* **35**(3): 317-29.

240. Groth, A., Weber, J.D., Willumsen, B.M., Sherr, C.J. and Roussel, M.F. (2000). Oncogenic Ras induces p19ARF and growth arrest in mouse embryo fibroblasts lacking p21Cip1 and p27Kip1 without activating cyclin D-dependent kinases. *J Biol Chem* **275**(35): 27473-80.

241. Sherr, C.J. and Weber, J.D. (2000). The ARF/p53 pathway. *Curr Opin Genet Dev* **10**(1): 94-9.

242. Ferbeyre, G., de Stanchina, E., Querido, E., Baptiste, N., Prives, C. and Lowe, S.W. (2000). PML is induced by oncogenic ras and promotes premature senescence. *Genes Dev* **14**(16): 2015-27.

243. Pearson, M., Carbone, R., Sebastiani, C., Cioce, M., Fagioli, M., Saito, S., Higashimoto, Y., Appella, E., Minucci, S., Pandolfi, P.P. and Pelicci, P.G. (2000). PML regulates p53 acetylation and premature senescence induced by oncogenic Ras. *Nature* **406**(6792): 207-10.

244. Burkhart, B.A., Alcorta, D.A., Chiao, C., Isaacs, J.S. and Barrett, J.C. (1999). Two posttranscriptional pathways that regulate p21(Cip1/Waf1/Sdi1) are identified by HPV16-E6 interaction and correlate with life span and cellular senescence. *Exp Cell Res* **247**(1): 168-75.

245. Wahl, G.M., Linke, S.P., Paulson, T.G. and Huang, L.C. (1997). Maintaining genetic stability through TP53 mediated checkpoint control. *Cancer Surv* **29**: 183-219.

246. Linke, S.P., Clarkin, K.C., Di Leonardo, A., Tsou, A. and Wahl, G.M. (1996). A reversible, p53-dependent G0/G1 cell cycle arrest induced by ribonucleotide depletion in the absence of detectable DNA damage. *Genes Dev* **10**(8): 934-47.

247. Longhese, M.P., Mantiero, D. and Clerici, M. (2006). The cellular response to chromosome breakage. *Mol Microbiol* **60**(5): 1099-108.

248. Tanaka, H., Arakawa, H., Yamaguchi, T., Shiraishi, K., Fukuda, S., Matsui, K., Takei, Y. and Nakamura, Y. (2000). A ribonucleotide reductase gene involved in a p53-dependent cell-cycle checkpoint for DNA damage. *Nature* **404**(6773): 42-9.

249. Lane, D.P. (1992). p53, guardian of the genome. *Nature* **358**(6381): 15-6.

250. Adimoolam, S. and Ford, J.M. (2002). p53 and DNA damage-inducible expression of the xeroderma pigmentosum group C gene. *Proc Natl Acad Sci U S A* **99**(20): 12985-90.

251. Hwang, B.J., Ford, J.M., Hanawalt, P.C. and Chu, G. (1999). Expression of the p48 xeroderma pigmentosum gene is p53-dependent and is involved in global genomic repair. *Proc Natl Acad Sci U S A* **96**(2): 424-8.

252. Sugasawa, K., Ng, J.M., Masutani, C., Iwai, S., van der Spek, P.J., Eker, A.P., Hanaoka, F., Bootsma, D. and Hoeijmakers, J.H. (1998). Xeroderma pigmentosum group C protein complex is the initiator of global genome nucleotide excision repair. *Mol Cell* **2**(2): 223-32.

253. Volker, M., Mone, M.J., Karmakar, P., van Hoffen, A., Schul, W., Vermeulen, W., Hoeijmakers, J.H., van Driel, R., van Zeeland, A.A. and Mullenders, L.H. (2001). Sequential assembly of the nucleotide excision repair factors *in vivo*. *Mol Cell* **8**(1): 213-24.

254. Stoimenov, I. and Helleday, T. (2009). PCNA on the crossroad of cancer. *Biochem Soc Trans* **37**(Pt 3): 605-13.

255. Xu, J. and Morris, G.F. (1999). p53-mediated regulation of proliferating cell nuclear antigen expression in cells exposed to ionizing radiation. *Mol Cell Biol* **19**(1): 12-20.

256. Li, R., Waga, S., Hannon, G.J., Beach, D. and Stillman, B. (1994). Differential effects by the p21 CDK inhibitor on PCNA-dependent DNA replication and repair. *Nature* **371**(6497): 534-7.

257. Flores-Rozas, H., Kelman, Z., Dean, F.B., Pan, Z.Q., Harper, J.W., Elledge, S.J., O'Donnell, M. and Hurwitz, J. (1994). Cdk-interacting protein 1 directly binds with proliferating cell nuclear antigen and inhibits DNA replication catalyzed by the DNA polymerase delta holoenzyme. *Proc Natl Acad Sci U S A* **91**(18): 8655-9.

258. Smith, M.L., Chen, I.T., Zhan, Q., Bae, I., Chen, C.Y., Gilmer, T.M., Kastan, M.B., O'Connor, P.M. and Fornace, A.J., Jr. (1994). Interaction of the p53-regulated protein Gadd45 with proliferating cell nuclear antigen. *Science* **266**(5189): 1376-80.

259. Scherer, S.J., Maier, S.M., Seifert, M., Hanselmann, R.G., Zang, K.D., Muller-Hermelink, H.K., Angel, P., Welter, C. and Schartl, M. (2000). p53 and c-Jun functionally synergize in the regulation of the DNA repair gene hMSH2 in response to UV. *J Biol Chem* **275**(48): 37469-73.

260. Lamers, M.H., Perrakis, A., Enzlin, J.H., Winterwerp, H.H., de Wind, N. and Sixma, T.K. (2000). The crystal structure of DNA mismatch repair protein MutS binding to a G x T mismatch. *Nature* **407**(6805): 711-7.

261. Flores-Rozas, H., Clark, D. and Kolodner, R.D. (2000). Proliferating cell nuclear antigen and Msh2p-Msh6p interact to form an active mispair recognition complex. *Nat Genet* **26**(3): 375-8.

262. Fukasawa, K., Choi, T., Kuriyama, R., Rulong, S. and Vande Woude, G.F. (1996). Abnormal centrosome amplification in the absence of p53. *Science* **271**(5256): 1744-7.

263. Bailly, E. and Bornens, M. (1992). Cell biology. Centrosome and cell division. *Nature* **355**(6358): 300-1.

264. Donehower, L.A., Harvey, M., Slagle, B.L., McArthur, M.J., Montgomery, C.A., Jr., Butel, J.S. and Bradley, A. (1992). Mice deficient for p53 are developmentally normal but susceptible to spontaneous tumours. *Nature* **356**(6366): 215-21.

265. Takahashi, Y., Bucana, C.D., Cleary, K.R. and Ellis, L.M. (1998). p53, vessel count, and vascular endothelial growth factor expression in human colon cancer. *Int J Cancer* **79**(1): 34-8.

266. Gasparini, G., Weidner, N., Bevilacqua, P., Maluta, S., Dalla Palma, P., Caffo, O., Barbareschi, M., Boracchi, P., Marubini, E. and Pozza, F. (1994). Tumor microvessel density, p53 expression, tumor size, and peritumoral lymphatic vessel invasion are relevant prognostic markers in node-negative breast carcinoma. *J Clin Oncol* **12**(3): 454-66.

267. Teodoro, J.G., Evans, S.K. and Green, M.R. (2007). Inhibition of tumor angiogenesis by p53: a new role for the guardian of the genome. *J Mol Med* **85**(11): 1175-86.

268. Pugh, C.W. and Ratcliffe, P.J. (2003). Regulation of angiogenesis by hypoxia: role of the HIF system. *Nat Med* **9**(6): 677-84.

269. Forsythe, J.A., Jiang, B.H., Iyer, N.V., Agani, F., Leung, S.W., Koos, R.D. and Semenza, G.L. (1996). Activation of vascular endothelial growth factor gene transcription by hypoxia-inducible factor 1. *Mol Cell Biol* **16**(9): 4604-13.

270. Ravi, R., Mookerjee, B., Bhujwalla, Z.M., Sutter, C.H., Artemov, D., Zeng, Q., Dillehay, L.E., Madan, A., Semenza, G.L. and Bedi, A. (2000). Regulation of tumor angiogenesis by p53-induced degradation of hypoxia-inducible factor 1alpha. *Genes Dev* **14**(1): 34-44.

271. Sherif, Z.A., Nakai, S., Pirollo, K.F., Rait, A. and Chang, E.H. (2001). Downmodulation of bFGF-binding protein expression following restoration of p53 function. *Cancer Gene Ther* **8**(10): 771-82.

272. Zou, Z., Gao, C., Nagaich, A.K., Connell, T., Saito, S., Moul, J.W., Seth, P., Appella, E. and Srivastava, S. (2000). p53 regulates the expression of the tumor suppressor gene maspin. *J Biol Chem* **275**(9): 6051-4.

273. Teodoro, J.G., Parker, A.E., Zhu, X. and Green, M.R. (2006). p53-mediated inhibition of angiogenesis through up-regulation of a collagen prolyl hydroxylase. *Science* **313**(5789): 968-71.

274. Dameron, K.M., Volpert, O.V., Tainsky, M.A. and Bouck, N. (1994). Control of angiogenesis in fibroblasts by p53 regulation of thrombospondin-1. *Science* **265**(5178): 1582-4.

275. Nishimori, H., Shiratsuchi, T., Urano, T., Kimura, Y., Kiyono, K., Tatsumi, K., Yoshida, S., Ono, M., Kuwano, M., Nakamura, Y. and Tokino, T. (1997). A novel brain-specific p53-target gene, BAI1, containing thrombospondin type 1 repeats inhibits experimental angiogenesis. *Oncogene* **15**(18): 2145-50.

276. Nor, J.E., Mitra, R.S., Sutorik, M.M., Mooney, D.J., Castle, V.P. and Polverini, P.J. (2000). Thrombospondin-1 induces endothelial cell apoptosis and inhibits angiogenesis by activating the caspase death pathway. *J Vasc Res* **37**(3): 209-18.

277. Kaur, B., Brat, D.J., Devi, N.S. and Van Meir, E.G. (2005). Vasculostatin, a proteolytic fragment of brain angiogenesis inhibitor 1, is an antiangiogenic and antitumorigenic factor. *Oncogene* **24**(22): 3632-42.

278. Folkman, J., Long, D.M., Jr. and Becker, F.F. (1963). Growth and metastasis of tumor in organ culture. *Cancer* **16**: 453-67.

279. Kern, A., Taubert, H., Scheele, J., Rudroff, C., Mothes, H., Kappler, M., Bartel, F. and Richter, K.K. (2002). Association of p53 mutations, microvessel density and neoangiogenesis in pairs of colorectal cancers and corresponding liver metastases. *Int J Oncol* **21**(2): 243-9.

280. Navone, N.M., Troncoso, P., Pisters, L.L., Goodrow, T.L., Palmer, J.L., Nichols, W.W., von Eschenbach, A.C. and Conti, C.J. (1993). p53 protein accumulation and gene mutation in the progression of human prostate carcinoma. *J Natl Cancer Inst* **85**(20): 1657-69.

281. Bolós, V., Peinado, H., Pérez-Moreno, M.A., Fraga, M.F., Esteller, M. and Cano, A. (2003). The transcription factor Slug represses E-cadherin expression and induces epithelial to mesenchymal transitions: a comparison with Snail and E47 repressors. *J Cell Sci* **116**(Pt 3): 499-511.

282. Shih, J.Y., Tsai, M.F., Chang, T.H., Chang, Y.L., Yuan, A., Yu, C.J., Lin, S.B., Liou, G.Y., Lee, M.L., Chen, J.J., Hong, T.M., Yang, S.C., Su, J.L., Lee, Y.C. and Yang, P.C. (2005). Transcription repressor slug promotes carcinoma invasion and predicts outcome of patients with lung adenocarcinoma. *Clin Cancer Res* **11**(22): 8070-8.

283. Thiery, J.P., Acloque, H., Huang, R.Y. and Nieto, M.A. (2009). Epithelial-mesenchymal transitions in development and disease. *Cell* **139**(5): 871-90.

284. Chang, C.J., Chao, C.H., Xia, W., Yang, J.Y., Xiong, Y., Li, C.W., Yu, W.H., Rehman, S.K., Hsu, J.L., Lee, H.H., Liu, M., Chen, C.T., Yu, D. and Hung, M.C. (2011). p53 regulates epithelial-mesenchymal transition and stem cell properties through modulating miRNAs. *Nat Cell Biol* **13**(3): 317-23.

285. Shiota, M., Izumi, H., Onitsuka, T., Miyamoto, N., Kashiwagi, E., Kidani, A., Hirano, G., Takahashi, M., Naito, S. and Kohno, K. (2008). Twist and p53 reciprocally regulate target genes via direct interaction. *Oncogene* **27**(42): 5543-53.

286. Wang, S.P., Wang, W.L., Chang, Y.L., Wu, C.T., Chao, Y.C., Kao, S.H., Yuan, A., Lin, C.W., Yang, S.C., Chan, W.K., Li, K.C., Hong, T.M. and Yang, P.C. (2009). p53 controls cancer cell invasion by inducing the MDM2-mediated degradation of Slug. *Nat Cell Biol* **11**(6): 694-704.

287. Polański, R., Warburton, H.E., Ray-Sinha, A., Devling, T., Pakuła, H., Rubbi, C.P., Vlatković, N. and Boyd, M.T. (2010). MDM2 promotes cell motility and invasiveness through a RING-finger independent mechanism. *FEBS Lett* **584**(22): 4695-702.

288. Yang, J.Y., Zong, C.S., Xia, W., Wei, Y., Ali-Seyed, M., Li, Z., Broglio, K., Berry, D.A. and Hung, M.C. (2006). MDM2 promotes cell motility and invasiveness by regulating E-cadherin degradation. *Mol Cell Biol* **26**(19): 7269-82.

289. Kim, T., Veronese, A., Pichiorri, F., Lee, T.J., Jeon, Y.J., Volinia, S., Pineau, P., Marchio, A., Palatini, J., Suh, S.S., Alder, H., Liu, C.G., Dejean, A. and Croce, C.M. (2011). p53 regulates epithelial-mesenchymal transition through microRNAs targeting ZEB1 and ZEB2. *J Exp Med* **208**(5): 875-83.

290. Chen, W.T. (1989). Proteolytic activity of specialized surface protrusions formed at rosette contact sites of transformed cells. *J Exp Zool* **251**(2): 167-85.

291. Davies, W.A. and Stossel, T.P. (1977). Peripheral hyaline blebs (podosomes) of macrophages. *J Cell Biol* **75**(3): 941-55.

292. Mukhopadhyay, U.K., Eves, R., Jia, L., Mooney, P. and Mak, A.S. (2009). p53 suppresses Src-induced podosome and rosette formation and cellular invasiveness through the upregulation of caldesmon. *Mol Cell Biol* **29**(11): 3088-98.

293. Eves, R., Webb, B.A., Zhou, S. and Mak, A.S. (2006). Caldesmon is an integral component of podosomes in smooth muscle cells. *J Cell Sci* **119**(Pt 9): 1691-702.

294. Quintavalle, M., Elia, L., Condorelli, G. and Courtneidge, S.A. (2010). MicroRNA control of podosome formation in vascular smooth muscle cells in vivo and in vitro. *J Cell Biol* **189**(1): 13-22.

295. Sablina, A.A., Chumakov, P.M. and Kopnin, B.P. (2003). Tumor suppressor p53 and its homologue p73alpha affect cell migration. *J Biol Chem* **278**(30): 27362-71.

296. Iotsova, V. and Stehelin, D. (1996). Down-regulation of fibronectin gene expression by the p53 tumor suppressor protein. *Cell Growth Differ* **7**(5): 629-34.

297. Comer, K.A., Dennis, P.A., Armstrong, L., Catino, J.J., Kastan, M.B. and Kumar, C.C. (1998). Human smooth muscle alpha-actin gene is a transcriptional target of the p53 tumor suppressor protein. *Oncogene* **16**(10): 1299-308.

298. Nobes, C.D. and Hall, A. (1995). Rho, rac, and cdc42 GTPases regulate the assembly of multimolecular focal complexes associated with actin stress fibers, lamellipodia, and filopodia. *Cell* **81**(1): 53-62.

299. Gaggioli, C., Hooper, S., Hidalgo-Carcedo, C., Grosse, R., Marshall, J.F., Harrington, K. and Sahai, E. (2007). Fibroblast-led collective invasion of carcinoma cells with differing roles for RhoGTPases in leading and following cells. *Nat Cell Biol* **9**(12): 1392-400.

300. Ridley, A.J., Paterson, H.F., Johnston, C.L., Diekmann, D. and Hall, A. (1992). The small GTP-binding protein rac regulates growth factor-induced membrane ruffling. *Cell* **70**(3): 401-10.

301. Ridley, A.J. and Hall, A. (1992). The small GTP-binding protein rho regulates the assembly of focal adhesions and actin stress fibers in response to growth factors. *Cell* **70**(3): 389-99.

302. Sahai, E. and Marshall, C.J. (2003). Differing modes of tumour cell invasion have distinct requirements for Rho/ROCK signalling and extracellular proteolysis. *Nat Cell Biol* **5**(8): 711-9.

303. Peterson, J., Zheng, Y., Bender, L., Myers, A., Cerione, R. and Bender, A. (1994). Interactions between the bud emergence proteins Bem1p and Bem2p and Rho-type GTPases in yeast. *J Cell Biol* **127**(5): 1395-406.

304. Sanz-Moreno, V. and Marshall, C.J. (2009). Rho-GTPase signaling drives melanoma cell plasticity. *Cell Cycle* **8**(10): 1484-7.

305. Stambolic, V., MacPherson, D., Sas, D., Lin, Y., Snow, B., Jang, Y., Benchimol, S. and Mak, T.W. (2001). Regulation of PTEN transcription by p53. *Mol Cell* **8**(2): 317-25.

306. Maehama, T. and Dixon, J.E. (1998). The tumor suppressor, PTEN/MMAC1, dephosphorylates the lipid second messenger, phosphatidylinositol 3,4,5-trisphosphate. *J Biol Chem* **273**(22): 13375-8.

307. Stambolic, V., Suzuki, A., de la Pompa, J.L., Brothers, G.M., Mirtsos, C., Sasaki, T., Ruland, J., Penninger, J.M., Siderovski, D.P. and Mak, T.W. (1998). Negative regulation of PKB/Akt-dependent cell survival by the tumor suppressor PTEN. *Cell* **95**(1): 29-39.

308. Han, J., Luby-Phelps, K., Das, B., Shu, X., Xia, Y., Mosteller, R.D., Krishna, U.M., Falck, J.R., White, M.A. and Broek, D. (1998). Role of substrates and products of PI 3-kinase in regulating activation of Rac-related guanosine triphosphatases by Vav. *Science* **279**(5350): 558-60.

309. del Peso, L., Hernandez-Alcoceba, R., Embade, N., Carnero, A., Esteve, P., Paje, C. and Lacal, J.C. (1997). Rho proteins induce metastatic properties *in vivo*. *Oncogene* **15**(25): 3047-57.

310. Gadéa, G., Lapasset, L., Gauthier-Rouvière, C. and Roux, P. (2002). Regulation of Cdc42-mediated morphological effects: a novel function for p53. *EMBO J* **21**(10): 2373-82.

311. Muller, P.A., Vousden, K.H. and Norman, J.C. (2011). p53 and its mutants in tumor cell migration and invasion. *J Cell Biol* **192**(2): 209-18.

312. Guo, F. and Zheng, Y. (2004). Rho family GTPases cooperate with p53 deletion to promote primary mouse embryonic fibroblast cell invasion. *Oncogene* **23**(33): 5577-85.

313. Pinner, S. and Sahai, E. (2008). Imaging amoeboid cancer cell motility in vivo. *J Microsc* **231**(3): 441-5.

314. Lefort, K., Mandinova, A., Ostano, P., Kolev, V., Calpini, V., Kolfschoten, I., Devgan, V., Lieb, J., Raffoul, W., Hohl, D., Neel, V., Garlick, J., Chiorino, G. and Dotto, G.P. (2007). Notch1 is a p53 target gene involved in human keratinocyte tumor suppression through negative regulation of ROCK1/2 and MRCKalpha kinases. *Genes Dev* **21**(5): 562-77.

315. Ongusaha, P.P., Kim, H.G., Boswell, S.A., Ridley, A.J., Der, C.J., Dotto, G.P., Kim, Y.B., Aaronson, S.A. and Lee, S.W. (2006). RhoE is a pro-survival p53 target gene that inhibits ROCK I-mediated apoptosis in response to genotoxic stress. *Curr Biol* **16**(24): 2466-72.

316. Goh, L.L. and Manser, E. (2010). The RhoA GEF Syx is a target of Rnd3 and regulated via a Raf1-like ubiquitin-related domain. *PLoS One* **5**(8): e12409.

317. Wennerberg, K., Forget, M.A., Ellerbroek, S.M., Arthur, W.T., Burridge, K., Settleman, J., Der, C.J. and Hansen, S.H. (2003). Rnd proteins function as RhoA antagonists by activating p190 RhoGAP. *Curr Biol* **13**(13): 1106-15.

318. Woods, D.B. and Vousden, K.H. (2001). Regulation of p53 function. *Exp Cell Res* **264**(1): 56-66.

319. Reich, N.C., Oren, M. and Levine, A.J. (1983). Two distinct mechanisms regulate the levels of a cellular tumor antigen, p53. *Mol Cell Biol* **3**(12): 2143-50.

320. Finlay, C.A., Hinds, P.W., Tan, T.H., Eliyahu, D., Oren, M. and Levine, A.J. (1988). Activating mutations for transformation by p53 produce a gene product that forms an hsc70-p53 complex with an altered half-life. *Mol Cell Biol* **8**(2): 531-9.

321. Marine, J.C., Francoz, S., Maetens, M., Wahl, G., Toledo, F. and Lozano, G. (2006). Keeping p53 in check: essential and synergistic functions of Mdm2 and Mdm4. *Cell Death Differ* **13**(6): 927-34.

322. Jones, S.N., Roe, A.E., Donehower, L.A. and Bradley, A. (1995). Rescue of embryonic lethality in Mdm2-deficient mice by absence of p53. *Nature* **378**(6553): 206-8.

323. Parant, J., Chavez-Reyes, A., Little, N.A., Yan, W., Reinke, V., Jochemsen, A.G. and Lozano, G. (2001). Rescue of embryonic lethality in Mdm4-null mice by loss of Trp53 suggests a nonoverlapping pathway with MDM2 to regulate p53. *Nat Genet* **29**(1): 92-5.

324. Montes de Oca Luna, R., Wagner, D.S. and Lozano, G. (1995). Rescue of early embryonic lethality in mdm2-deficient mice by deletion of p53. *Nature* **378**(6553): 203-6.

325. Haupt, Y., Maya, R., Kazaz, A. and Oren, M. (1997). Mdm2 promotes the rapid degradation of p53. *Nature* **387**(6630): 296-9.

326. Kubbutat, M.H., Jones, S.N. and Vousden, K.H. (1997). Regulation of p53 stability by Mdm2. *Nature* **387**(6630): 299-303.

327. Lai, Z., Ferry, K.V., Diamond, M.A., Wee, K.E., Kim, Y.B., Ma, J., Yang, T., Benfield, P.A., Copeland, R.A. and Auger, K.R. (2001). Human mdm2 mediates multiple mono-ubiquitination of p53 by a mechanism requiring enzyme isomerization. *J Biol Chem* **276**(33): 31357-67.

328. Shi, D., Pop, M.S., Kulikov, R., Love, I.M., Kung, A.L. and Grossman, S.R. (2009). CBP and p300 are cytoplasmic E4 polyubiquitin ligases for p53. *Proc Natl Acad Sci U S A* **106**(38): 16275-80.

329. Zhu, Q., Yao, J., Wani, G., Wani, M.A. and Wani, A.A. (2001). Mdm2 mutant defective in binding p300 promotes ubiquitination but not degradation of p53: evidence for the role of p300 in integrating ubiquitination and proteolysis. *J Biol Chem* **276**(32): 29695-701.

330. Okamoto, K., Taya, Y. and Nakagama, H. (2009). Mdmx enhances p53 ubiquitination by altering the substrate preference of the Mdm2 ubiquitin ligase. *FEBS Lett* **583**(17): 2710-4.

331. Wu, X., Bayle, J.H., Olson, D. and Levine, A.J. (1993). The p53-mdm-2 autoregulatory feedback loop. *Genes Dev* **7**(7A): 1126-32.

332. Barak, Y., Juven, T., Haffner, R. and Oren, M. (1993). mdm2 expression is induced by wild type p53 activity. *EMBO J* **12**(2): 461-8.

333. Fang, S., Jensen, J.P., Ludwig, R.L., Vousden, K.H. and Weissman, A.M. (2000). Mdm2 is a RING finger-dependent ubiquitin protein ligase for itself and p53. *J Biol Chem* **275**(12): 8945-51.

334. Brady, M., Vlatkovic, N. and Boyd, M.T. (2005). Regulation of p53 and MDM2 activity by MTBP. *Mol Cell Biol* **25**(2): 545-53.

335. Chan, D.W., Son, S.C., Block, W., Ye, R., Khanna, K.K., Wold, M.S., Douglas, P., Goodarzi, A.A., Pelley, J., Taya, Y., Lavin, M.F. and Lees-Miller, S.P. (2000). Purification and characterization of ATM from human placenta. A manganese-dependent, wortmannin-sensitive serine/threonine protein kinase. *J Biol Chem* **275**(11): 7803-10.

336. Canman, C.E., Lim, D.S., Cimprich, K.A., Taya, Y., Tamai, K., Sakaguchi, K., Appella, E., Kastan, M.B. and Siliciano, J.D. (1998). Activation of the ATM kinase by ionizing radiation and phosphorylation of p53. *Science* **281**(5383): 1677-9.

337. Shieh, S.Y., Ahn, J., Tamai, K., Taya, Y. and Prives, C. (2000). The human homologs of checkpoint kinases Chk1 and Cds1 (Chk2) phosphorylate p53 at multiple DNA damage-inducible sites. *Genes Dev* **14**(3): 289-300.

338. Chehab, N.H., Malikzay, A., Appel, M. and Halazonetis, T.D. (2000). Chk2/hCds1 functions as a DNA damage checkpoint in G(1) by stabilizing p53. *Genes Dev* **14**(3): 278-88.

339. Hirao, A., Kong, Y.Y., Matsuoka, S., Wakeham, A., Ruland, J., Yoshida, H., Liu, D., Elledge, S.J. and Mak, T.W. (2000). DNA damage-induced activation of p53 by the checkpoint kinase Chk2. *Science* **287**(5459): 1824-7.

340. Chehab, N.H., Malikzay, A., Stavridi, E.S. and Halazonetis, T.D. (1999). Phosphorylation of Ser-20 mediates stabilization of human p53 in response to DNA damage. *Proc Natl Acad Sci U S A* **96**(24): 13777-82.

341. Hammond, E.M. and Giaccia, A.J. (2004). The role of ATM and ATR in the cellular response to hypoxia and re-oxygenation. *DNA Repair (Amst)* **3**(8-9): 1117-22.

342. Tibbetts, R.S., Brumbaugh, K.M., Williams, J.M., Sarkaria, J.N., Cliby, W.A., Shieh, S.Y., Taya, Y., Prives, C. and Abraham, R.T. (1999). A role for ATR in the DNA damage-induced phosphorylation of p53. *Genes Dev* **13**(2): 152-7.

343. Das, K.C. and Dashnamoorthy, R. (2004). Hyperoxia activates the ATR-Chk1 pathway and phosphorylates p53 at multiple sites. *Am J Physiol Lung Cell Mol Physiol* **286**(1): L87-97.

344. Shieh, S.Y., Ikeda, M., Taya, Y. and Prives, C. (1997). DNA damage-induced phosphorylation of p53 alleviates inhibition by MDM2. *Cell* **91**(3): 325-34.

345. Agrawal, A., Yang, J., Murphy, R.F. and Agrawal, D.K. (2006). Regulation of the p14ARF-Mdm2-p53 pathway: an overview in breast cancer. *Exp Mol Pathol* **81**(2): 115-22.

346. Moll, U.M. and Petrenko, O. (2003). The MDM2-p53 interaction. *Mol Cancer Res* **1**(14): 1001-8.

347. Weber, J.D., Taylor, L.J., Roussel, M.F., Sherr, C.J. and Bar-Sagi, D. (1999). Nucleolar Arf sequesters Mdm2 and activates p53. *Nat Cell Biol* **1**(1): 20-6.

348. Oliner, J.D., Pietenpol, J.A., Thiagalingam, S., Gyuris, J., Kinzler, K.W. and Vogelstein, B. (1993). Oncoprotein MDM2 conceals the activation domain of tumour suppressor p53. *Nature* **362**(6423): 857-60.

349. Ito, A., Lai, C.H., Zhao, X., Saito, S., Hamilton, M.H., Appella, E. and Yao, T.P. (2001). p300/CBP-mediated p53 acetylation is commonly induced by p53-activating agents and inhibited by MDM2. *EMBO J* **20**(6): 1331-40.

350. Shvarts, A., Steegenga, W.T., Riteco, N., van Laar, T., Dekker, P., Bazuine, M., van Ham, R.C., van der Houven van Oordt, W., Hateboer, G., van der Eb, A.J. and Jochemsen, A.G. (1996). MDMX: a novel p53-binding protein with some functional properties of MDM2. *EMBO J* **15**(19): 5349-57.

351. Xiong, S., Van Pelt, C.S., Elizondo-Fraire, A.C., Liu, G. and Lozano, G. (2006). Synergistic roles of Mdm2 and Mdm4 for p53 inhibition in central nervous system development. *Proc Natl Acad Sci U S A* **103**(9): 3226-31.

352. Sabbatini, P. and McCormick, F. (2002). MDMX inhibits the p300/CBP-mediated acetylation of p53. *DNA Cell Biol* **21**(7): 519-25.

353. Prives, C. and Hall, P.A. (1999). The p53 pathway. *J Pathol* **187**(1): 112-26.

354. Takenaka, I., Morin, F., Seizinger, B.R. and Kley, N. (1995). Regulation of the sequence-specific DNA binding function of p53 by protein kinase C and protein phosphatases. *J Biol Chem* **270**(10): 5405-11.

355. Hupp, T.R. and Lane, D.P. (1994). Allosteric activation of latent p53 tetramers. *Curr Biol* **4**(10): 865-75.

356. Meek, D.W., Simon, S., Kikkawa, U. and Eckhart, W. (1990). The p53 tumour suppressor protein is phosphorylated at serine 389 by casein kinase II. *EMBO J* **9**(10): 3253-60.

357. Hupp, T.R., Meek, D.W., Midgley, C.A. and Lane, D.P. (1992). Regulation of the specific DNA binding function of p53. *Cell* **71**(5): 875-86.

358. Hao, M., Lowy, A.M., Kapoor, M., Deffie, A., Liu, G. and Lozano, G. (1996). Mutation of phosphoserine 389 affects p53 function in vivo. *J Biol Chem* **271**(46): 29380-5.

359. Gu, W. and Roeder, R.G. (1997). Activation of p53 sequence-specific DNA binding by acetylation of the p53 C-terminal domain. *Cell* **90**(4): 595-606.

360. Joseph, T.W., Zaika, A. and Moll, U.M. (2003). Nuclear and cytoplasmic degradation of endogenous p53 and HDM2 occurs during down-regulation of the p53 response after multiple types of DNA damage. *FASEB J* **17**(12): 1622-30.

361. Louria-Hayon, I., Grossman, T., Sionov, R.V., Alsheich, O., Pandolfi, P.P. and Haupt, Y. (2003). The promyelocytic leukemia protein protects p53 from Mdm2-mediated inhibition and degradation. *J Biol Chem* **278**(35): 33134-41.

362. Kobet, E., Zeng, X., Zhu, Y., Keller, D. and Lu, H. (2000). MDM2 inhibits p300-mediated p53 acetylation and activation by forming a ternary complex with the two proteins. *Proc Natl Acad Sci U S A* **97**(23): 12547-52.

363. Luo, J., Su, F., Chen, D., Shiloh, A. and Gu, W. (2000). Deacetylation of p53 modulates its effect on cell growth and apoptosis. *Nature* **408**(6810): 377-81.

364. Selivanova, G., Kawasaki, T., Ryabchenko, L. and Wiman, K.G. (1998). Reactivation of mutant p53: a new strategy for cancer therapy. *Semin Cancer Biol* **8**(5): 369-78.

365. Vousden, K.H. and Vande Woude, G.F. (2000). The ins and outs of p53. *Nat Cell Biol* **2**(10): E178-80.

366. Shaulsky, G., Goldfinger, N., Ben-Ze'ev, A. and Rotter, V. (1990). Nuclear accumulation of p53 protein is mediated by several nuclear localization signals and plays a role in tumorigenesis. *Mol Cell Biol* **10**(12): 6565-77.

367. Giannakakou, P., Sackett, D.L., Ward, Y., Webster, K.R., Blagosklonny, M.V. and Fojo, T. (2000). p53 is associated with cellular microtubules and is transported to the nucleus by dynein. *Nat Cell Biol* **2**(10): 709-17.

368. Stommel, J.M., Marchenko, N.D., Jimenez, G.S., Moll, U.M., Hope, T.J. and Wahl, G.M. (1999). A leucine-rich nuclear export signal in the p53 tetramerization domain: regulation of subcellular localization and p53 activity by NES masking. *EMBO J* **18**(6): 1660-72.

369. Lohrum, M.A., Woods, D.B., Ludwig, R.L., Balint, E. and Vousden, K.H. (2001). C-terminal ubiquitination of p53 contributes to nuclear export. *Mol Cell Biol* **21**(24): 8521-32.

370. Boyd, S.D., Tsai, K.Y. and Jacks, T. (2000). An intact HDM2 RING-finger domain is required for nuclear exclusion of p53. *Nat Cell Biol* **2**(9): 563-8.

371. Geyer, R.K., Yu, Z.K. and Maki, C.G. (2000). The MDM2 RING-finger domain is required to promote p53 nuclear export. *Nat Cell Biol* **2**(9): 569-73.

372. Moll, U.M., Riou, G. and Levine, A.J. (1992). Two distinct mechanisms alter p53 in breast cancer: mutation and nuclear exclusion. *Proc Natl Acad Sci U S A* **89**(15): 7262-6.

373. Moll, U.M., LaQuaglia, M., Benard, J. and Riou, G. (1995). Wild-type p53 protein undergoes cytoplasmic sequestration in undifferentiated neuroblastomas but not in differentiated tumors. *Proc Natl Acad Sci U S A* **92**(10): 4407-11.

374. O'Brate, A. and Giannakakou, P. (2003). The importance of p53 location: nuclear or cytoplasmic zip code? *Drug Resist Updat* **6**(6): 313-22.

375. Sengupta, S., Vonesch, J.L., Waltzinger, C., Zheng, H. and Wasylyk, B. (2000). Negative cross-talk between p53 and the glucocorticoid receptor and its role in neuroblastoma cells. *EMBO J* **19**(22): 6051-64.

376. Vousden, K.H. and Lu, X. (2002). Live or let die: the cell's response to p53. *Nat Rev Cancer* **2**(8): 594-604.

377. Soussi, T. (2007). p53 alterations in human cancer: more questions than answers. *Oncogene* **26**(15): 2145-56.

378. Sjöblom, T., Jones, S., Wood, L.D., Parsons, D.W., Lin, J., Barber, T.D., Mandelker, D., Leary, R.J., Ptak, J., Silliman, N., Szabo, S., Buckhaults, P., Farrell, C., Meeh, P., Markowitz, S.D., Willis, J., Dawson, D., Willson, J.K., Gazdar, A.F., Hartigan, J., Wu, L., Liu, C., Parmigiani, G., Park, B.H., Bachman, K.E., Papadopoulos, N., Vogelstein, B., Kinzler, K.W. and Velculescu, V.E. (2006). The consensus coding sequences of human breast and colorectal cancers. *Science* **314**(5797): 268-74.

379. Knudson, A.G., Jr. (1971). Mutation and cancer: statistical study of retinoblastoma. *Proc Natl Acad Sci U S A* **68**(4): 820-3.

380. Hussain, S.P. and Harris, C.C. (1998). Molecular epidemiology of human cancer: contribution of mutation spectra studies of tumor suppressor genes. *Cancer Res* **58**(18): 4023-37.

381. Kato, S., Han, S.Y., Liu, W., Otsuka, K., Shibata, H., Kanamaru, R. and Ishioka, C. (2003). Understanding the function-structure and function-mutation relationships of p53 tumor suppressor protein by high-resolution missense mutation analysis. *Proc Natl Acad Sci U S A* **100**(14): 8424-9.

382. Shaulian, E., Zauberman, A., Ginsberg, D. and Oren, M. (1992). Identification of a minimal transforming domain of p53: negative dominance through abrogation of sequence-specific DNA binding. *Mol Cell Biol* **12**(12): 5581-92.

383. Kern, S.E., Pietenpol, J.A., Thiagalingam, S., Seymour, A., Kinzler, K.W. and Vogelstein, B. (1992). Oncogenic forms of p53 inhibit p53-regulated gene expression. *Science* **256**(5058): 827-30.

384. Unger, T., Mietz, J.A., Scheffner, M., Yee, C.L. and Howley, P.M. (1993). Functional domains of wild-type and mutant p53 proteins involved in transcriptional regulation, transdominant inhibition, and transformation suppression. *Mol Cell Biol* **13**(9): 5186-94.

385. Milner, J. and Medcalf, E.A. (1991). Cotranslation of activated mutant p53 with wild type drives the wild-type p53 protein into the mutant conformation. *Cell* **65**(5): 765-74.

386. Greenblatt, M.S., Bennett, W.P., Hollstein, M. and Harris, C.C. (1994). Mutations in the p53 tumor suppressor gene: clues to cancer etiology and molecular pathogenesis. *Cancer Res* **54**(18): 4855-78.

387. Cao, Y., Gao, Q., Wazer, D.E. and Band, V. (1997). Abrogation of wild-type p53-mediated transactivation is insufficient for mutant p53-induced immortalization of normal human mammary epithelial cells. *Cancer Res* **57**(24): 5584-9.

388. Hinds, P.W., Finlay, C.A., Quartin, R.S., Baker, S.J., Fearon, E.R., Vogelstein, B. and Levine, A.J. (1990). Mutant p53 DNA clones from human colon carcinomas cooperate with ras in transforming primary rat cells: a comparison of the "hot spot" mutant phenotypes. *Cell Growth Differ* **1**(12): 571-80.

389. Ory, K., Legros, Y., Auguin, C. and Soussi, T. (1994). Analysis of the most representative tumour-derived p53 mutants reveals that changes in protein conformation are not correlated with loss of transactivation or inhibition of cell proliferation. *EMBO J* **13**(15): 3496-504.

390. Kern, S.E., Kinzler, K.W., Bruskin, A., Jarosz, D., Friedman, P., Prives, C. and Vogelstein, B. (1991). Identification of p53 as a sequence-specific DNA-binding protein. *Science* **252**(5013): 1708-11.

391. Bargonetti, J., Friedman, P.N., Kern, S.E., Vogelstein, B. and Prives, C. (1991). Wild-type but not mutant p53 immunopurified proteins bind to sequences adjacent to the SV40 origin of replication. *Cell* **65**(6): 1083-91.

392. Chène, P. (1998). *In vitro* analysis of the dominant negative effect of p53 mutants. *J Mol Biol* **281**(2): 205-9.

393. Blandino, G., Levine, A.J. and Oren, M. (1999). Mutant p53 gain of function: differential effects of different p53 mutants on resistance of cultured cells to chemotherapy. *Oncogene* **18**(2): 477-85.

394. Erber, R., Conradt, C., Homann, N., Enders, C., Finckh, M., Dietz, A., Weidauer, H. and Bosch, F.X. (1998). TP53 DNA contact mutations are selectively associated with allelic loss and have a strong clinical impact in head and neck cancer. *Oncogene* **16**(13): 1671-9.

395. Liu, G., McDonnell, T.J., Montes de Oca Luna, R., Kapoor, M., Mims, B., El-Naggar, A.K. and Lozano, G. (2000). High metastatic potential in mice inheriting a targeted p53 missense mutation. *Proc Natl Acad Sci U S A* **97**(8): 4174-9.

396. Halevy, O., Michalovitz, D. and Oren, M. (1990). Different tumor-derived p53 mutants exhibit distinct biological activities. *Science* **250**(4977): 113-6.

397. Hsiao, M., Low, J., Dorn, E., Ku, D., Pattengale, P., Yeargin, J. and Haas, M. (1994). Gain-of-function mutations of the p53 gene induce lymphohematopoietic metastatic potential and tissue invasiveness. *Am J Pathol* **145**(3): 702-14.

398. Shaulsky, G., Goldfinger, N. and Rotter, V. (1991). Alterations in tumor development in vivo mediated by expression of wild type or mutant p53 proteins. *Cancer Res* **51**(19): 5232-7.

399. El-Hizawi, S., Lagowski, J.P., Kulesz-Martin, M. and Albor, A. (2002). Induction of gene amplification as a gain-of-function phenotype of mutant p53 proteins. *Cancer Res* **62**(11): 3264-70.

400. Olivier, M., Langerod, A., Carrieri, P., Bergh, J., Klaar, S., Eyfjord, J., Theillet, C., Rodriguez, C., Lidereau, R., Bieche, I., Varley, J., Bignon, Y., Uhrhammer, N., Winqvist, R., Jukkola-Vuorinen, A., Niederacher, D., Kato, S., Ishioka, C., Hainaut, P. and Borresen-Dale, A.L. (2006). The clinical value of somatic TP53 gene mutations in 1,794 patients with breast cancer. *Clin Cancer Res* **12**(4): 1157-67.

401. Aas, T., Borresen, A.L., Geisler, S., Smith-Sorensen, B., Johnsen, H., Varhaug, J.E., Akslen, L.A. and Lonning, P.E. (1996). Specific P53 mutations are associated with *de novo* resistance to doxorubicin in breast cancer patients. *Nat Med* **2**(7): 811-4.

402. Bergh, J., Norberg, T., Sjogren, S., Lindgren, A. and Holmberg, L. (1995). Complete sequencing of the p53 gene provides prognostic information in breast cancer patients, particularly in relation to adjuvant systemic therapy and radiotherapy. *Nat Med* **1**(10): 1029-34.

403. Pugacheva, E.N., Ivanov, A.V., Kravchenko, J.E., Kopnin, B.P., Levine, A.J. and Chumakov, P.M. (2002). Novel gain of function activity of p53 mutants: activation of the dUTPase gene expression leading to resistance to 5-fluorouracil. *Oncogene* **21**(30): 4595-600.

404. Bristow, R.G., Peacock, J., Jang, A., Kim, J., Hill, R.P. and Benchimol, S. (2003). Resistance to DNA-damaging agents is discordant from experimental metastatic capacity in MEF ras-transformants-expressing gain of function MTp53. *Oncogene* **22**(19): 2960-6.

405. Cadwell, C. and Zambetti, G.P. (2001). The effects of wild-type p53 tumor suppressor activity and mutant p53 gain-of-function on cell growth. *Gene* **277**(1-2): 15-30.

406. Gaiddon, C., Lokshin, M., Ahn, J., Zhang, T. and Prives, C. (2001). A subset of tumor-derived mutant forms of p53 down-regulate p63 and p73 through a direct interaction with the p53 core domain. *Mol Cell Biol* **21**(5): 1874-87.

407. Strano, S., Munarriz, E., Rossi, M., Cristofanelli, B., Shaul, Y., Castagnoli, L., Levine, A.J., Sacchi, A., Cesareni, G., Oren, M. and Blandino, G. (2000). Physical and functional interaction between p53 mutants and different isoforms of p73. *J Biol Chem* **275**(38): 29503-12.

408. Davison, T.S., Vagner, C., Kaghad, M., Ayed, A., Caput, D. and Arrowsmith, C.H. (1999). p73 and p63 are homotetramers capable of weak heterotypic interactions with each other but not with p53. *J Biol Chem* **274**(26): 18709-14.

409. Yuan, Z.M., Shioya, H., Ishiko, T., Sun, X., Gu, J., Huang, Y.Y., Lu, H., Kharbanda, S., Weichselbaum, R. and Kufe, D. (1999). p73 is regulated by tyrosine kinase c-Abl in the apoptotic response to DNA damage. *Nature* **399**(6738): 814-7.

410. Irwin, M.S., Kondo, K., Marin, M.C., Cheng, L.S., Hahn, W.C. and Kaelin, W.G., Jr. (2003). Chemosensitivity linked to p73 function. *Cancer Cell* **3**(4): 403-10.

411. Sigal, A. and Rotter, V. (2005). The Oncogenic Activity of p53 Mutants. IN *Protein Reviews: The p53 Tumor Suppressor Pathway and Cancer*, G. P. Zambetti (ed.), **Vol. 2**, p. 199-223. Springer US, New York.

412. Marin, M.C., Jost, C.A., Brooks, L.A., Irwin, M.S., O'Nions, J., Tidy, J.A., James, N., McGregor, J.M., Harwood, C.A., Yulug, I.G., Vousden, K.H., Allday, M.J., Gusterson, B., Ikawa, S., Hinds, P.W., Crook, T. and Kaelin, W.G., Jr. (2000). A common polymorphism acts as an intragenic modifier of mutant p53 behaviour. *Nat Genet* **25**(1): 47-54.

413. Bergamaschi, D., Gasco, M., Hiller, L., Sullivan, A., Syed, N., Trigiante, G., Yulug, I., Merlano, M., Numico, G., Comino, A., Attard, M., Reelfs, O., Gusterson, B., Bell, A.K., Heath, V., Tavassoli, M., Farrell, P.J., Smith, P., Lu, X. and Crook, T. (2003). p53 polymorphism influences response in cancer chemotherapy via modulation of p73-dependent apoptosis. *Cancer Cell* **3**(4): 387-402.

414. Kim, E. and Deppert, W. (2007). Interactions of mutant p53 with DNA: guilt by association. *Oncogene* **26**(15): 2185-90.

415. Chicas, A., Molina, P. and Bargonetti, J. (2000). Mutant p53 forms a complex with Sp1 on HIV-LTR DNA. *Biochem Biophys Res Commun* **279**(2): 383-90.

416. Sampath, J., Sun, D., Kidd, V.J., Grenet, J., Gandhi, A., Shapiro, L.H., Wang, Q., Zambetti, G.P. and Schuetz, J.D. (2001). Mutant p53 cooperates with ETS and selectively up-regulates human MDR1 not MRP1. *J Biol Chem* **276**(42): 39359-67.

417. Di Agostino, S., Strano, S., Emiliozzi, V., Zerbini, V., Mottolese, M., Sacchi, A., Blandino, G. and Piaggio, G. (2006). Gain of function of mutant p53: the mutant p53/NF-Y protein complex reveals an aberrant transcriptional mechanism of cell cycle regulation. *Cancer Cell* **10**(3): 191-202.

418. Chin, K.V., Ueda, K., Pastan, I. and Gottesman, M.M. (1992). Modulation of activity of the promoter of the human MDR1 gene by Ras and p53. *Science* **255**(5043): 459-62.

419. Kim, E., Günther, W., Yoshizato, K., Meissner, H., Zapf, S., Nüsing, R.M., Yamamoto, H., Van Meir, E.G., Deppert, W. and Giese, A. (2003). Tumor suppressor p53 inhibits transcriptional activation of invasion gene thromboxane synthase mediated by the proto-oncogenic factor ets-1. *Oncogene* **22**(49): 7716-27.

420. Koutsodontis, G., Vasilaki, E., Chou, W.C., Papakosta, P. and Kardassis, D. (2005). Physical and functional interactions between members of the tumour suppressor p53 and the Sp families of transcription factors: importance for the regulation of genes involved in cell-cycle arrest and apoptosis. *Biochem J* **389**(Pt 2): 443-55.

421. Yang, X., Pater, A. and Tang, S.C. (1999). Cloning and characterization of the human BAG-1 gene promoter: upregulation by tumor-derived p53 mutants. *Oncogene* **18**(32): 4546-53.

422. Deb, S., Jackson, C.T., Subler, M.A. and Martin, D.W. (1992). Modulation of cellular and viral promoters by mutant human p53 proteins found in tumor cells. *J Virol* **66**(10): 6164-70.

423. Frazier, M.W., He, X., Wang, J., Gu, Z., Cleveland, J.L. and Zambetti, G.P. (1998). Activation of c-myc gene expression by tumor-derived p53 mutants requires a discrete C-terminal domain. *Mol Cell Biol* **18**(7): 3735-43.

424. Margulies, L. and Sehgal, P.B. (1993). Modulation of the human interleukin-6 promoter (IL-6) and transcription factor C/EBP beta (NF-IL6) activity by p53 species. *J Biol Chem* **268**(20): 15096-100.

425. Tsutsumi-Ishii, Y., Tadokoro, K., Hanaoka, F. and Tsuchida, N. (1995). Response of heat shock element within the human HSP70 promoter to mutated p53 genes. *Cell Growth Differ* **6**(1): 1-8.

426. Lányi, Á., Deb, D., Seymour, R.C., Ludes-Meyers, J.H., Subler, M.A. and Deb, S. (1998). 'Gain of function' phenotype of tumor-derived mutant p53 requires the oligomerization/nonsequence-specific nucleic acid-binding domain. *Oncogene* **16**(24): 3169-76.

427. Lee, Y.I., Lee, S., Das, G.C., Park, U.S. and Park, S.M. (2000). Activation of the insulin-like growth factor II transcription by aflatoxin B1 induced p53 mutant 249 is caused by activation of transcription complexes; implications for a gain-of-function during the formation of hepatocellular carcinoma. *Oncogene* **19**(33): 3717-26.

428. Weisz, L., Zalcenstein, A., Stambolsky, P., Cohen, Y., Goldfinger, N., Oren, M. and Rotter, V. (2004). Transactivation of the EGR1 gene contributes to mutant p53 gain of function. *Cancer Res* **64**(22): 8318-27.

429. Lin, J., Teresky, A.K. and Levine, A.J. (1995). Two critical hydrophobic amino acids in the N-terminal domain of the p53 protein are required for the gain of function phenotypes of human p53 mutants. *Oncogene* **10**(12): 2387-90.

430. Koga, H. and Deppert, W. (2000). Identification of genomic DNA sequences bound by mutant p53 protein (Gly245-->Ser) in vivo. *Oncogene* **19**(36): 4178-83.

431. Muller, B.F., Paulsen, D. and Deppert, W. (1996). Specific binding of MAR/SAR DNA-elements by mutant p53. *Oncogene* **12**(9): 1941-52.

432. Wang, Y.H. and Griffith, J. (1995). Expanded CTG triplet blocks from the myotonic dystrophy gene create the strongest known natural nucleosome positioning elements. *Genomics* **25**(2): 570-3.

433. Saveliev, A., Everett, C., Sharpe, T., Webster, Z. and Festenstein, R. (2003). DNA triplet repeats mediate heterochromatin-protein-1-sensitive variegated gene silencing. *Nature* **422**(6934): 909-13.

434. Chen, Y., Chen, P.L. and Lee, W.H. (1994). Hot-spot p53 mutants interact specifically with two cellular proteins during progression of the cell cycle. *Mol Cell Biol* **14**(10): 6764-72.

435. Gallagher, W.M., Argentini, M., Sierra, V., Bracco, L., Debussche, L. and Conseiller, E. (1999). MBP1: a novel mutant p53-specific protein partner with oncogenic properties. *Oncogene* **18**(24): 3608-16.

436. Peng, Y., Chen, L., Li, C., Lu, W., Agrawal, S. and Chen, J. (2001). Stabilization of the MDM2 oncoprotein by mutant p53. *J Biol Chem* **276**(9): 6874-8.

437. Midgley, C.A. and Lane, D.P. (1997). p53 protein stability in tumour cells is not determined by mutation but is dependent on Mdm2 binding. *Oncogene* **15**(10): 1179-89.

438. Terzian, T., Suh, Y.A., Iwakuma, T., Post, S.M., Neumann, M., Lang, G.A., Van Pelt, C.S. and Lozano, G. (2008). The inherent instability of mutant p53 is alleviated by Mdm2 or p16INK4a loss. *Genes Dev* **22**(10): 1337-44.

439. Momand, J. and Zambetti, G.P. (1997). Mdm-2: "big brother" of p53. *J Cell Biochem* **64**(3): 343-52.

440. Hinds, P.W., Finlay, C.A., Frey, A.B. and Levine, A.J. (1987). Immunological evidence for the association of p53 with a heat shock protein, hsc70, in p53-plus-ras-transformed cell lines. *Mol Cell Biol* 7(8): 2863-9.

441. Whitesell, L., Sutphin, P.D., Pulcini, E.J., Martinez, J.D. and Cook, P.H. (1998). The physical association of multiple molecular chaperone proteins with mutant p53 is altered by geldanamycin, an hsp90-binding agent. *Mol Cell Biol* **18**(3): 1517-24.

442. Peng, Y., Chen, L., Li, C., Lu, W. and Chen, J. (2001). Inhibition of MDM2 by hsp90 contributes to mutant p53 stabilization. *J Biol Chem* **276**(44): 40583-90.

443. Finlay, C.A. (1993). The mdm-2 oncogene can overcome wild-type p53 suppression of transformed cell growth. *Mol Cell Biol* **13**(1): 301-6.

444. Børresen, A.L., Andersen, T.I., Eyfjörd, J.E., Cornelis, R.S., Thorlacius, S., Borg, A., Johansson, U., Theillet, C., Scherneck, S., Hartman, S. and et al. (1995). TP53 mutations and breast cancer prognosis: particularly poor survival rates for cases with mutations in the zinc-binding domains. *Genes Chromosomes Cancer* **14**(1): 71-5.

445. Wang, X.J., Greenhalgh, D.A., Jiang, A., He, D., Zhong, L., Brinkley, B.R. and Roop, D.R. (1998). Analysis of centrosome abnormalities and angiogenesis in epidermal-targeted p53172H mutant and p53-knockout mice after chemical carcinogenesis: evidence for a gain of function. *Mol Carcinog* **23**(3): 185-92.

446. Gualberto, A., Aldape, K., Kozakiewicz, K. and Tlsty, T.D. (1998). An oncogenic form of p53 confers a dominant, gain-of-function phenotype that disrupts spindle checkpoint control. *Proc Natl Acad Sci U S A* **95**(9): 5166-71.

447. Talos, F., Nemajerova, A., Flores, E.R., Petrenko, O. and Moll, U.M. (2007). p73 suppresses polyploidy and aneuploidy in the absence of functional p53. *Mol Cell* **27**(4): 647-59.

448. Lotem, J. and Sachs, L. (1995). A mutant p53 antagonizes the deregulated c-myc-mediated enhancement of apoptosis and decrease in leukemogenicity. *Proc Natl Acad Sci U S A* **92**(21): 9672-6.

449. Peled, A., Zipori, D. and Rotter, V. (1996). Cooperation between p53-dependent and p53-independent apoptotic pathways in myeloid cells. *Cancer Res* **56**(9): 2148-56.

450. Inoue, R., Asker, C., Klangby, U., Pisa, P. and Wiman, K.G. (1999). Induction of the human ARF protein by serum starvation. *Anticancer Res* **19**(4B): 2939-43.

451. Li, R., Sutphin, P.D., Schwartz, D., Matas, D., Almog, N., Wolkowicz, R., Goldfinger, N., Pei, H., Prokocimer, M. and Rotter, V. (1998). Mutant p53 protein expression interferes with p53-independent apoptotic pathways. *Oncogene* **16**(25): 3269-77.

452. Wong, R.P., Tsang, W.P., Chau, P.Y., Co, N.N., Tsang, T.Y. and Kwok, T.T. (2007). p53-R273H gains new function in induction of drug resistance through down-regulation of procaspase-3. *Mol Cancer Ther* **6**(3): 1054-61.

453. Adamson, E.D. and Mercola, D. (2002). Egr1 transcription factor: multiple roles in prostate tumor cell growth and survival. *Tumour Biol* **23**(2): 93-102.

454. Muller, P.A., Caswell, P.T., Doyle, B., Iwanicki, M.P., Tan, E.H., Karim, S., Lukashchuk, N., Gillespie, D.A., Ludwig, R.L., Gosselin, P., Cromer, A., Brugge, J.S., Sansom, O.J., Norman, J.C. and Vousden, K.H. (2009). Mutant p53 drives invasion by promoting integrin recycling. *Cell* **139**(7): 1327-41.

455. Hingorani, S.R., Wang, L., Multani, A.S., Combs, C., Deramaudt, T.B., Hruban, R.H., Rustgi, A.K., Chang, S. and Tuveson, D.A. (2005). Trp53R172H and KrasG12D cooperate to promote chromosomal instability and widely metastatic pancreatic ductal adenocarcinoma in mice. *Cancer Cell* **7**(5): 469-83.

456. Dong, P., Tada, M., Hamada, J., Nakamura, A., Moriuchi, T. and Sakuragi, N. (2007). p53 dominant-negative mutant R273H promotes invasion and migration of human endometrial cancer HHUA cells. *Clin Exp Metastasis* **24**(6): 471-83.

457. Adorno, M., Cordenonsi, M., Montagner, M., Dupont, S., Wong, C., Hann, B., Solari, A., Bobisse, S., Rondina, M.B., Guzzardo, V., Parenti, A.R., Rosato, A., Bicciato, S., Balmain, A. and Piccolo, S. (2009). A Mutant-p53/Smad complex opposes p63 to empower TGFbeta-induced metastasis. *Cell* **137**(1): 87-98.

458. Derynck, R., Akhurst, R.J. and Balmain, A. (2001). TGF-beta signaling in tumor suppression and cancer progression. *Nat Genet* **29**(2): 117-29.

459. Wrana, J.L. (1998). TGF-beta receptors and signalling mechanisms. *Miner Electrolyte Metab* **24**(2-3): 120-30.

460. Kalo, E., Buganim, Y., Shapira, K.E., Besserglick, H., Goldfinger, N., Weisz, L., Stambolsky, P., Henis, Y.I. and Rotter, V. (2007). Mutant p53 attenuates the SMAD-dependent transforming growth factor beta1 (TGF-beta1) signaling pathway by repressing the expression of TGF-beta receptor type II. *Mol Cell Biol* **27**(23): 8228-42.

461. Caswell, P.T., Chan, M., Lindsay, A.J., McCaffrey, M.W., Boettiger, D. and Norman, J.C. (2008). Rab-coupling protein coordinates recycling of alpha5beta1 integrin and EGFR1 to promote cell migration in 3D microenvironments. *J Cell Biol* **183**(1): 143-55.

462. Bhattacharya, S., Darjatmoko, S.R. and Polans, A.S. (2011). Resveratrol modulates the malignant properties of cutaneous melanoma through changes in the activation and attenuation of the antiapoptotic protooncogenic protein Akt/PKB. *Melanoma Res* **21**(3): 180-7.

463. Lin, C.J., Grandis, J.R., Carey, T.E., Gollin, S.M., Whiteside, T.L., Koch, W.M., Ferris, R.L. and Lai, S.Y. (2007). Head and neck squamous cell carcinoma cell lines: established models and rationale for selection. *Head Neck* **29**(2): 163-88.

464. Birnboim, H.C. and Doly, J. (1979). A rapid alkaline extraction procedure for screening recombinant plasmid DNA. *Nucleic Acids Res* **7**(6): 1513-23.

465. National Center for Biotechnology Information (NCBI) website. Available at: http://blast.ncbi.nlm.nih.gov/Blast.cgi?PAGE_TYPE=BlastSearch&PROG_DEF=blastn&BLAST_PROG_DEF=megaBlast&BLAST_SPEC=blast2seq. Accessed December 2, 2007.

466. Komarova, E.A., Chernov, M.V., Franks, R., Wang, K., Armin, G., Zelnick, C.R., Chin, D.M., Bacus, S.S., Stark, G.R. and Gudkov, A.V. (1997). Transgenic mice

with p53-responsive lacZ: p53 activity varies dramatically during normal development and determines radiation and drug sensitivity in vivo. *EMBO J* **16**(6): 1391-400.

467. Martinez, L.A., Naguibneva, I., Lehrmann, H., Vervisch, A., Tchenio, T., Lozano, G. and Harel-Bellan, A. (2002). Synthetic small inhibiting RNAs: efficient tools to inactivate oncogenic mutations and restore p53 pathways. *Proc Natl Acad Sci U S A* **99**(23): 14849-54.

468. Chevallet, M., Luche, S. and Rabilloud, T. (2006). Silver staining of proteins in polyacrylamide gels. *Nat Protoc* **1**(4): 1852-8.

469. ProMab Biotechnologies' website. Available at: http://www.promab.com/service2.asp. Accessed December 8, 2008.

470. Warburton, H.E., Brady, M., Vlatkovic, N., Linehan, W.M., Parsons, K. and Boyd, M.T. (2005). p53 regulation and function in renal cell carcinoma. *Cancer Res* **65**(15): 6498-503.

471. Mojica, W. and Hawthorn, L. (2010). Normal colon epithelium: a dataset for the analysis of gene expression and alternative splicing events in colon disease. *BMC Genomics* **11**: 5.

472. Affymetrix, Inc. Available at: http://media.affymetrix.com/support/technical/technotes/exon_array_design_technote.pdf. Accessed July 24, 2011.

473. The Paterson Institute for Cancer Research. Available at: http://bioinformatics.picr.man.ac.uk/vice/Welcome.vice. Accessed May 17, 2011.

474. Shaw, E.J., Haylock, B., Husband, D., du Plessis, D., Sibson, D.R., Warnke, P.C. and Walker, C. (2010). Gene expression in oligodendroglial tumors. *Anal Cell Pathol (Amst)* **33**(2): 81-94.

475. Keefe, A.D., Wilson, D.S., Seelig, B. and Szostak, J.W. (2001). One-step purification of recombinant proteins using a nanomolar-affinity streptavidin-binding peptide, the SBP-Tag. *Protein Expr Purif* **23**(3): 440-6.

476. Blumenthal, D.K., Takio, K., Edelman, A.M., Charbonneau, H., Titani, K., Walsh, K.A. and Krebs, E.G. (1985). Identification of the calmodulin-binding domain of skeletal muscle myosin light chain kinase. *Proc Natl Acad Sci U S A* **82**(10): 3187-91.

477. Stofko-Hahn, R.E., Carr, D.W. and Scott, J.D. (1992). A single step purification for recombinant proteins. Characterization of a microtubule associated protein (MAP 2) fragment which associates with the type II cAMP-dependent protein kinase. *FEBS Lett* **302**(3): 274-8.

478. Angers, S. (2008). Proteomic analyses of protein complexes in the Wnt pathway. *Methods Mol Biol* **468**: 223-30.

479. Carey, F.A. (2000). Organic Chemistry. McGraw-Hill Companies, New York.

480. Copple, I.M., Lister, A., Obeng, A.D., Kitteringham, N.R., Jenkins, R.E., Layfield, R., Foster, B.J., Goldring, C.E. and Park, B.K. (2010). Physical and functional interaction of sequestosome 1 with Keap1 regulates the Keap1-Nrf2 cell defense pathway. *J Biol Chem* **285**(22): 16782-8.

481. Shilov, I.V., Seymour, S.L., Patel, A.A., Loboda, A., Tang, W.H., Keating, S.P., Hunter, C.L., Nuwaysir, L.M. and Schaeffer, D.A. (2007). The Paragon Algorithm, a next generation search engine that uses sequence temperature values and feature probabilities to identify peptides from tandem mass spectra. *Mol Cell Proteomics* **6**(9): 1638-55.

482. Franken, N.A., Rodermond, H.M., Stap, J., Haveman, J. and van Bree, C. (2006). Clonogenic assay of cells in vitro. *Nat Protoc* **1**(5): 2315-9.

483. Dale, R.G. (1985). The application of the linear-quadratic dose-effect equation to fractionated and protracted radiotherapy. *Br J Radiol* **58**(690): 515-28.

484. LabLife's website. Available at: http://www.addgene.org/pgvec1?f=v&cmd=showfile&file=searchvec. Accessed April 10, 2011.

485. Schwab, S.R., Shugart, J.A., Horng, T., Malarkannan, S. and Shastri, N. (2004). Unanticipated antigens: translation initiation at CUG with leucine. *PLoS Biol* **2**(11): e366.

486. Chang, C.P., Chen, S.J., Lin, C.H., Wang, T.L. and Wang, C.C. (2010). A single sequence context cannot satisfy all non-AUG initiator codons in yeast. *BMC Microbiol* **10**: 188.

487. Subler, M.A., Martin, D.W. and Deb, S. (1992). Inhibition of viral and cellular promoters by human wild-type p53. *J Virol* **66**(8): 4757-62.

488. Thavathiru, E. and Das, G.M. (2001). Activation of pRL-TK by 12S E1A oncoprotein: drawbacks of using an internal reference reporter in transcription assays. *Biotechniques* **31**(3): 528-30, 532.

489. Docstoc. Available at: http://www.docstoc.com/docs/19876404/Two-step-TAP-Tag-purification. Accessed May 8, 2011.

490. Séraphin, B., Puig, O., Bouveret, E., Rutz, B. and Caspary, F. (2002). Tandem Affinity Purification to Enhance Interacting Protein Identification. IN *Protein-Protein Interactions: A Molecular Cloning Manual*, E. A. Golemis (ed.), 1st ed., p. 313-328. Cold Spring Harbor Laboratory Press, New York.

491. Hartl, F.U., Martin, J. and Neupert, W. (1992). Protein folding in the cell: the role of molecular chaperones Hsp70 and Hsp60. *Annu Rev Biophys Biomol Struct* **21**: 293-322.

492. Takayama, S., Xie, Z. and Reed, J.C. (1999). An evolutionarily conserved family of Hsp70/Hsc70 molecular chaperone regulators. *J Biol Chem* **274**(2): 781-6.

493. Dai, Q., Qian, S.B., Li, H.H., McDonough, H., Borchers, C., Huang, D., Takayama, S., Younger, J.M., Ren, H.Y., Cyr, D.M. and Patterson, C. (2005). Regulation of the cytoplasmic quality control protein degradation pathway by BAG2. *J Biol Chem* **280**(46): 38673-81.

494. Matlashewski, G.J., Tuck, S., Pim, D., Lamb, P., Schneider, J. and Crawford, L.V. (1987). Primary structure polymorphism at amino acid residue 72 of human p53. *Mol Cell Biol* **7**(2): 961-3.

495. Venkov, P.V. and Hadjiolov, A.A. (1969). Differential stability of 28s and 18s rat liver ribosomal ribonucleic acids. *Biochem J* **115**(1): 91-4.

496. Demetris, A.J., Specht, S., Nozaki, I., Lunz, J.G., 3rd, Stolz, D.B., Murase, N. and Wu, T. (2008). Small proline-rich proteins (SPRR) function as SH3 domain ligands, increase resistance to injury and are associated with epithelial-mesenchymal transition (EMT) in cholangiocytes. *J Hepatol* **48**(2): 276-88.

497. Hiratsuka, S., Watanabe, A., Sakurai, Y., Akashi-Takamura, S., Ishibashi, S., Miyake, K., Shibuya, M., Akira, S., Aburatani, H. and Maru, Y. (2008). The S100A8-serum amyloid A3-TLR4 paracrine cascade establishes a pre-metastatic phase. *Nat Cell Biol* **10**(11): 1349-55.

498. Arai, K., Takano, S., Teratani, T., Ito, Y., Yamada, T. and Nozawa, R. (2008). S100A8 and S100A9 overexpression is associated with poor pathological parameters in invasive ductal carcinoma of the breast. *Curr Cancer Drug Targets* **8**(4): 243-52.

499. Kim, B., Koo, H., Yang, S., Bang, S., Jung, Y., Kim, Y., Kim, J., Park, J., Moon, R.T., Song, K. and Lee, I. (2006). TC1(C8orf4) correlates with Wnt/beta-catenin target genes and aggressive biological behavior in gastric cancer. *Clin Cancer Res* **12**(11 Pt 1): 3541-8.

500. Chen, S.H., Lin, C.Y., Lee, L.T., Chang, G.D., Lee, P.P., Hung, C.C., Kao, W.T., Tsai, P.H., Schally, A.V., Hwang, J.J. and Lee, M.T. (2010). Up-regulation of fibronectin and tissue transglutaminase promotes cell invasion involving increased association with integrin and MMP expression in A431 cells. *Anticancer Res* **30**(10): 4177-86.

501. Kamei, D., Murakami, M., Sasaki, Y., Nakatani, Y., Majima, M., Ishikawa, Y., Ishii, T., Uematsu, S., Akira, S., Hara, S. and Kudo, I. (2009). Microsomal prostaglandin E synthase-1 in both cancer cells and hosts contributes to tumour growth, invasion and metastasis. *Biochem J* **425**(2): 361-71.

502. Yao, L., Liu, P., Lu, X. and Liu, F. (2010). Expression of tissue inhibitor of metalloproteinase-2 in nasopharyngeal carcinoma. *Lin Chung Er Bi Yan Hou Tou Jing Wai Ke Za Zhi* **24**(18): 831-3.

503. Huang, Y., Sook-Kim, M. and Ratovitski, E. (2008). Midkine promotes tetraspanin-integrin interaction and induces FAK-Stat1alpha pathway contributing to migration/invasiveness of human head and neck squamous cell carcinoma cells. *Biochem Biophys Res Commun* **377**(2): 474-8.

504. O-Charoenrat, P., Sarkaria, I., Talbot, S.G., Reddy, P., Dao, S., Ngai, I., Shaha, A., Kraus, D., Shah, J., Rusch, V., Ramanathan, Y. and Singh, B. (2008). SCCRO (DCUN1D1) induces extracellular matrix invasion by activating matrix metalloproteinase 2. *Clin Cancer Res* **14**(21): 6780-9.

505. Meyyappan, M., Wong, H., Hull, C. and Riabowol, K.T. (1998). Increased expression of cyclin D2 during multiple states of growth arrest in primary and established cells. *Mol Cell Biol* **18**(6): 3163-72.

506. Cui, X., Song, B., Hou, L., Wei, Z. and Tang, J. (2008). High expression of osteoglycin decreases the metastatic capability of mouse hepatocarcinoma Hca-F cells to lymph nodes. *Acta Biochim Biophys Sin (Shanghai)* **40**(4): 349-55.

507. Kuphal, S., Wallner, S. and Bosserhoff, A.K. (2008). Loss of nephronectin promotes tumor progression in malignant melanoma. *Cancer Sci* **99**(2): 229-33.

508. Wang, Y., Barbacioru, C., Hyland, F., Xiao, W., Hunkapiller, K.L., Blake, J., Chan, F., Gonzalez, C., Zhang, L. and Samaha, R.R. (2006). Large scale real-time PCR validation on gene expression measurements from two commercial long-oligonucleotide microarrays. *BMC Genomics* **7**: 59.

509. Calduch-Giner, J.A., Davey, G., Saera-Vila, A., Houeix, B., Talbot, A., Prunet, P., Cairns, M.T. and Pérez-Sánchez, J. (2010). Use of microarray technology to assess the time course of liver stress response after confinement exposure in gilthead sea bream (Sparus aurata L.). *BMC Genomics* **11**: 193.

510. Prevette, L.E., Mullen, D.G. and Holl, M.M. (2010). Polycation-induced cell membrane permeability does not enhance cellular uptake or expression efficiency of delivered DNA. *Mol Pharm* **7**(3): 870-83.

511. Yamazaki, Y., Chiba, I., Hirai, A., Notani, K., Kashiwazaki, H., Tei, K., Totsuka, Y., Iizuka, T., Kohgo, T. and Fukuda, H. (2003). Radioresistance in oral squamous cell carcinoma with p53 DNA contact mutation. *Am J Clin Oncol* **26**(5): e124-9.

512. Arya, A.K., El-Fert, A., Devling, T., Eccles, R.M., Aslam, M.A., Rubbi, C.P., Vlatkovic, N., Fenwick, J., Lloyd, B.H., Sibson, D.R., Jones, T.M. and Boyd, M.T. (2010). Nutlin-3, the small-molecule inhibitor of MDM2, promotes senescence and radiosensitises laryngeal carcinoma cells harbouring wild-type p53. *Br J Cancer* **103**(2): 186-95.

513. Yamazaki, Y., Chiba, I., Hirai, A., Sugiura, C., Notani, K., Kashiwazaki, H., Tei, K., Totsuka, Y. and Fukuda, H. (2003). Specific p53 mutations predict poor prognosis in oral squamous cell carcinoma. *Oral Oncol* **39**(2): 163-9.

514. Brosh, R. and Rotter, V. (2009). When mutants gain new powers: news from the mutant p53 field. *Nat Rev Cancer* **9**(10): 701-13.

515. Strano, S., Dell'Orso, S., Mongiovi, A.M., Monti, O., Lapi, E., Di Agostino, S., Fontemaggi, G. and Blandino, G. (2007). Mutant p53 proteins: between loss and gain of function. *Head Neck* **29**(5): 488-96.

516. Zhang, W., Shay, J.W. and Deisseroth, A. (1993). Inactive p53 mutants may enhance the transcriptional activity of wild-type p53. *Cancer Res* **53**(20): 4772-5.

517. Stürzbecher, H.W., Chumakov, P., Welch, W.J. and Jenkins, J.R. (1987). Mutant p53 proteins bind hsp 72/73 cellular heat shock-related proteins in SV40-transformed monkey cells. *Oncogene* **1**(2): 201-11.

518. Fourie, A.M., Hupp, T.R., Lane, D.P., Sang, B.C., Barbosa, M.S., Sambrook, J.F. and Gething, M.J. (1997). HSP70 binding sites in the tumor suppressor protein p53. *J Biol Chem* **272**(31): 19471-9.

519. Walerych, D., Olszewski, M.B., Gutkowska, M., Helwak, A., Zylicz, M. and Zylicz, A. (2009). Hsp70 molecular chaperones are required to support p53 tumor suppressor activity under stress conditions. *Oncogene* **28**(48): 4284-94.

520. Arndt, V., Daniel, C., Nastainczyk, W., Alberti, S. and Hohfeld, J. (2005). BAG-2 acts as an inhibitor of the chaperone-associated ubiquitin ligase CHIP. *Mol Biol Cell* **16**(12): 5891-900.

521. Fischer, R.S., Fritz-Six, K.L. and Fowler, V.M. (2003). Pointed-end capping by tropomodulin3 negatively regulates endothelial cell motility. *J Cell Biol* **161**(2): 371-80.

522. Fischer, R.S., Yarmola, E.G., Weber, K.L., Speicher, K.D., Speicher, D.W., Bubb, M.R. and Fowler, V.M. (2006). Tropomodulin 3 binds to actin monomers. *J Biol Chem* **281**(47): 36454-65.

523. Morton, J.P., Timpson, P., Karim, S.A., Ridgway, R.A., Athineos, D., Doyle, B., Jamieson, N.B., Oien, K.A., Lowy, A.M., Brunton, V.G., Frame, M.C., Evans, T.R. and Sansom, O.J. (2010). Mutant p53 drives metastasis and overcomes growth arrest/senescence in pancreatic cancer. *Proc Natl Acad Sci U S A* **107**(1): 246-51.

524. Graziano, V. and De Laurenzi, V. (2011). Role of p63 in cancer development. *Biochim Biophys Acta* **1816**(1): 57-66.

525. Nekulova, M., Holcakova, J., Coates, P. and Vojtesek, B. (2011). The role of p63 in cancer, stem cells and cancer stem cells. *Cell Mol Biol Lett* **16**(2): 296-327.

526. Yang, A., Kaghad, M., Wang, Y., Gillett, E., Fleming, M.D., Dotsch, V., Andrews, N.C., Caput, D. and McKeon, F. (1998). p63, a p53 homolog at 3q27-29, encodes multiple products with transactivating, death-inducing, and dominant-negative activities. *Mol Cell* **2**(3): 305-16.

527. Carroll, D.K., Carroll, J.S., Leong, C.O., Cheng, F., Brown, M., Mills, A.A., Brugge, J.S. and Ellisen, L.W. (2006). p63 regulates an adhesion programme and cell survival in epithelial cells. *Nat Cell Biol* **8**(6): 551-61.

528. Su, X., Chakravarti, D., Cho, M.S., Liu, L., Gi, Y.J., Lin, Y.L., Leung, M.L., El-Naggar, A., Creighton, C.J., Suraokar, M.B., Wistuba, I. and Flores, E.R. (2010). TAp63 suppresses metastasis through coordinate regulation of Dicer and miRNAs. *Nature* **467**(7318): 986-90.

529. Mundt, H.M., Stremmel, W., Melino, G., Krammer, P.H., Schilling, T. and Müller, M. (2010). Dominant negative (DeltaN) p63alpha induces drug resistance in hepatocellular carcinoma by interference with apoptosis signaling pathways. *Biochem Biophys Res Commun* **396**(2): 335-41.

530. Keyes, W.M., Pecoraro, M., Aranda, V., Vernersson-Lindahl, E., Li, W., Vogel, H., Guo, X., Garcia, E.L., Michurina, T.V., Enikolopov, G., Muthuswamy, S.K. and Mills, A.A. (2010). DeltaNp63alpha is an oncogene that targets chromatin remodeler Lsh to drive skin stem cell proliferation and tumorigenesis. *Cell Stem Cell* **8**(2): 164-76.

531. Sniezek, J.C., Matheny, K.E., Westfall, M.D. and Pietenpol, J.A. (2004). Dominant negative p63 isoform expression in head and neck squamous cell carcinoma. *Laryngoscope* **114**(12): 2063-72.

532. Bargonetti, J., Chicas, A., White, D. and Prives, C. (1997). p53 represses Sp1 DNA binding and HIV-LTR directed transcription. *Cell Mol Biol (Noisy-le-grand)* **43**(7): 935-49.

533. Scian, M.J., Stagliano, K.E., Anderson, M.A., Hassan, S., Bowman, M., Miles, M.F., Deb, S.P. and Deb, S. (2005). Tumor-derived p53 mutants induce NF-kappaB2 gene expression. *Mol Cell Biol* **25**(22): 10097-110.

534. Weisz, L., Damalas, A., Liontos, M., Karakaidos, P., Fontemaggi, G., Maor-Aloni, R., Kalis, M., Levrero, M., Strano, S., Gorgoulis, V.G., Rotter, V., Blandino, G. and Oren, M. (2007). Mutant p53 enhances nuclear factor kappaB activation by tumor necrosis factor alpha in cancer cells. *Cancer Res* **67**(6): 2396-401.

535. Liu, J., Zhan, M., Hannay, J.A., Das, P., Bolshakov, S.V., Kotilingam, D., Yu, D., Lazar, A.F., Pollock, R.E. and Lev, D. (2006). Wild-type p53 inhibits nuclear factor-kappaB-induced matrix metalloproteinase-9 promoter activation: implications for soft tissue sarcoma growth and metastasis. *Mol Cancer Res* **4**(11): 803-10.

536. Wang, X., Wu, X., Wang, C., Zhang, W., Ouyang, Y., Yu, Y. and He, Z. (2010). Transcriptional suppression of breast cancer resistance protein (BCRP) by wild-type p53 through the NF-kappaB pathway in MCF-7 cells. *FEBS Lett* **584**(15): 3392-7.

537. Gudkov, A.V. and Komarova, E.A. (2003). The role of p53 in determining sensitivity to radiotherapy. *Nat Rev Cancer* **3**(2): 117-29.

538. Lowe, S.W., Bodis, S., McClatchey, A., Remington, L., Ruley, H.E., Fisher, D.E., Housman, D.E. and Jacks, T. (1994). p53 status and the efficacy of cancer therapy *in vivo*. *Science* **266**(5186): 807-10.

539. Cuddihy, A.R., Jalali, F., Coackley, C. and Bristow, R.G. (2008). WTp53 induction does not override MTp53 chemoresistance and radioresistance due to gain-of-function in lung cancer cells. *Mol Cancer Ther* **7**(4): 980-92.

540. Lavra, L., Ulivieri, A., Rinaldo, C., Dominici, R., Volante, M., Luciani, E., Bartolazzi, A., Frasca, F., Soddu, S. and Sciacchitano, S. (2009). Gal-3 is stimulated by gain-of-function p53 mutations and modulates chemoresistance in anaplastic thyroid carcinomas. *J Pathol* **218**(1): 66-75.

541. Peltonen, J.K., Vahakangas, K.H., Helppi, H.M., Bloigu, R., Paakko, P. and Turpeenniemi-Hujanen, T. (2011). Specific TP53 mutations predict aggressive phenotype in head and neck squamous cell carcinoma: a retrospective archival study. *Head Neck Oncol* **3**: 20.